ELUCIDATING THE ROLE OF UNZIPPED IN THE VISUAL SYSTEM OF *DROSOPHILA*

by

Ece Terzioğlu Kara

M.S., Molecular Biology and Genetics, Bilkent University, 2006

B.S., Biological Sciences and Bioengineering, Sabancı University, 2004

Submitted to the Institute for Graduate Studies in
Science and Engineering in partial fulfilment of
the requirement for the degree of
Doctor of Philosophy

Graduate Program in Molecular Biology and Genetics
Boğaziçi University

2015

To the candles of my life, my families…

ACKNOWLEDGEMENTS

First of all I would like to present my sincere gratitude to my thesis supervisor Assoc. Prof. Arzu Çelik for her support throughout the years that I have spent in Boğaziçi University. Her guidance in the projects, academic writing, and scientific thinking was very valuable and enlightening. She introduced me to the world of neuroscience and *Drosophila,* which I enjoyed very much. I also had the chance to be a part of the team who established the fly lab in Boğaziçi, which has been a privilage.

I would like to acknowledge Prof. Kuyaş Buğra who has followed up my studies from the very beginning and accepted to be in my thesis committee. She gave critical feedback throughout my work and took the time to evaluate it, which I am thankful for. I would also like to thank Prof. Müge Türet who was very supportive throughout my PhD in every possible way. She also accepted to be on my thesis committee and took the time to evaluate my thesis, which I am grateful for. I would like to express my gratitude for Assoc. Prof. Uygar Tazebay and Assoc. Prof. Ferruh Özcan, for accepting to be on my thesis committee and sparing their time to evaluate my thesis. They are both very valuable professors that I have met in my 'Molecular Biology' journey, and I learned a lot from them both scientifically and personally. I would also like to thank Prof. Zehra Sayers who has introduced me to the world of Molecular Biology 15 years ago and supported me in every decision that I made. She was also in my thesis progress committee and gave very critical feedback at times when I needed help. I am also grateful for the support of Prof. Neş'e Bilgin and Ibrahim Yaman in my protein studies, Dr. Cemalettin Bekpen in my bioinformatic studies, Prof. A. Nazlı Başak and Prof. Nesrin Özören in my times of rotation, and Assoc. Prof. Stefan Fuss for his feedback and suggestions.

I have been a part of the fly lab from the very beginning and I had very amazing lab mates who have accompanied me in my journey and changed my life. Duygu Koldere and Gamze Akgün are among the very special ones who were just incredible at each stage of my PhD thesis including the writing part. Without my 'thesis writing first aid kit' and

‘emergency call center team’, it would be very hard to see the finish line. I am proud to be a member of the ‘free women club’ and I am looking forward to see our dreams come true together. Dr. Bahar Şahin and Dr. Stefan Koestler have been the two postdocs of our lab who were there at both good and bad times. They are very valuable friends who I am so glad to come across them and I would like to thank for their moral and professional support. I would also like to express my gratitude towards our first graduate group Arzu Öztürk, Sercan Sayın, and Mustafa Talay with whom we shared laughter, tears and very memorable moments while we were trying to learn fly work. Also I am so happy to have met two other former graduates Selen Zülbahar and Kaan Mika whom I will always remember with a big smile. I won’t forget our ‘Unzipped’ discussions and our days-nights in the lab. We also had wonderful technicians at times: Arzu Arat, Güneş Tunçgenç, and Eren Şahin all had very colourful personalities and were the joy of the lab in addition to making life a lot easier for us by making hundreds of vials of fly food. I would also like to acknowledge our former and present young padawans Kaan Apaydın, Filiz Taşçı, İlgi Uğurluoğlu, Gülce Padem, Ece Sönmez, Cağatay Aydın, Ayşegül Kılıç, Gizem Dedeoğlu, Ayşe Candayan, Ayça Yörükoğlu, and our current lab member Ferdi Rıdvan Kral for their friendship and being part of our little ‘fly community’. Çağrı Çevrim joined the lab a year after me has been in the lab since then, being my longest lab mate and a very close friend of mine. I am grateful for the times that we shared and will share.

I would also like to thank my brother lab ‘the Fish lab’, which we shared a lot in common including our space and lab material. I am grateful especially to my ‘brother’ Xalid Bayramlı who has been an incredible support both in the lab and outside of the lab, and was always there for me. I would also like to thank the former post-doc Tuba Özacar for the order that she has established in the lab and for being my dear friend. I would also like to thank the other fish lab members Gizem Sancer, Büşra Çoban, Ahmet Burak, Serdar Çapar, and Burak Bali.

I had a chance to spend some time with the members of other labs, which added sparkles to my life. The ‘lemonade drinking team girls’ Burçak Özeş, Neslihan Zöhrap, Aslı Uğurlu, Elif Eren, Cansu Küey, and Elif Begüm Gökerküçük were there night and day together with me and whenever I needed some fresh air and support. I would also like to thank our neighbour lab members Tuncay Şeker, Güzem Gül, and Ali İşbilir for being the

midnight support team and even finding food at nights when we were starving. I would like to express my gratitude for the former PhD students Aslıhan Özoğuz, Serkan Uğurlu, Duygu Dağlıkoca, İnanç Değer Fidancı, Özlem Yalçın Çapan, Çiğdem Köroğlu, Carolin Pirkevi, and the present ones Suna Lahut, Mahmut Can Hız, Sunay Usluer, Ceren Saygı, Aybüke Garipcan, Ayşin Demirkol, Burçin Duan, Ceren İskender, and Ulduz Avsar. The former ones passed on their experiences and knowledge, while we overcame the difficult times of PhD life with the present ones. I would also like to thank my other 'mother' PhD friend Zeynep Özcan for her valuable support and friendship at my hardest times, and sharing both academic and parental issues with me. I did my rotations in AKİL and NDAL and I am grateful to have spent time with their former members Damla Erdoğan, Burcu Sümer, Metehan Çifdalöz, Zeynep Okray, Didem Erbahar Eruslu, Pınar Aksoy, Gönenç Çobanoğlu, and Yetiş Gültekin, who became very close friends of mine. In addition, I want to thank Duygu Demiröz and Levent Baş who not only became my friends, but also a part of my family.

I also would like to acknowledge the non-academic team, especially Ümit Bayraktar who was an incredible support in all bureauctratic issues, Cenan Bakır for his help in technical issues, and Arzu Temizyürek with the animal facility. Selda Dağdeviren and İlknur Yıldız Aydın always had a cup of coffee for me and I would also like to thank Fatma 'abla', Aslı Gündoğdu Eken, and Derya Dikbıyık.

I would like to thank my parents Hasan Terzioğlu, Tülin Terzioğlu, Sabahattin Kara, and İnci Kara in addition to my brothers Evren Kara and Enis Terzioğlu for their unconditional understanding, support, and love. Last but not least, none of this would be possible without my husband Derya, who was always my biggest support and the luck of my life. Together with our little son Alp and his sister to come, he was the reason for me to carry on and I am very grateful for having him in my life.

I would also like to thank BAP10B01D4, BAP11B01D29, and TUBITAK 111T446 for supporting my work. I would also like to acknowledge the Center of Life Sciences and Technologies for providing the opportunity to use the animal facility.

ABSTRACT

ELUCIDATING THE ROLE OF UNZIPPED IN THE VISUAL SYSTEM OF *DROSOPHILA*

The *Drosophila* eye is composed of 800 ommatidial units, each containing eight photoreceptors (PR). The outer PRs R1-R6 are responsible for motion detection, while the inner PRs R7 and R8 and are responsible for colour vision. The outer PRs express Rhodopsin1 (Rh), while the inner PRs express Rh3-Rh6. The pale subtype is formed when the R7 cells express Rh3 and the coupled R8 cells express Rh5, while in the yellow subtype R7 cells express Rh4 and the coupled R8 cells express Rh6. This final state of differentiation is reached after a sequential recruitment process of PRs at the 3rd instar larval stage. At the initial stage, the PR cells start differentiating and their axons target to their temporal layers. At the terminal stage the inner and outer PRs are distinguished from each other, each PR expresses a specicific Rh molecule, and the axons target to their final layers in the optic lobe. The aim of this study was to identify new molecules involved in inner PR differentiation, mainly focusing on three genes expressed in R8 cells that have been identified in a previously performed enhancer-trap screen. One of these genes, *unzipped* was chosen for further analysis because of its function as cell adhesion molecule (CAM). By immunostainings the expression of Uzip was revealed to be in R8 cells and a subgroup of glial cells at the 3rd instar larval stage, R8 cells and glial cells at the 48 hour pupa stage, and glial cells in the adult stage where some of them project to the medulla. Immunostainings showed that Uzip does not have a direct effect on PR formation and glia expression at the 3rd instar larvae and pupae stages; or on subtype specification at the adult stage. For axonal targeting both the downregulation of Uzip in the target area and the misexpression in neighboring PRs and glia, which are not in the target region, lead to an increase in axonal misprojection phenotype. According to our suggested model, Uzip expressing R8 cells follow the adhesive signal from the Uzip expressing glial cells at the target region of projection. This study identifies Unzipped and describes its expression and involvement in axonal targeting the visual system.

ÖZET

UNZIPPED GENİNİN *DROSOPHILA* GÖZ SİSTEMİNDEKİ ROLÜ

Drosophila gözü, herbiri sekiz fotoreseptör içeren 800 adet birimden oluşur. R1-R6 dış fotoreseptörleri Rhosopsin1'i (Rh1) ifade edip hareketi algılarlarken, R7 ve R8 iç fotoreseptörleri Rh3-Rh6'yı ifade edip renklerin algılanması sağlarlar. İfade edilen Rh molekülüne göre R7 ve R8 hücreleri alt gruplara ayrılmaktadır. Rh4'ü ifade eden R7 ile Rh6'yı ifade eden R8 çifti 'sarı' altgrubu oluştururken, Rh3'ü ifade eden R7 ile Rh5'i ifade eden R8 çifti 'soluk' altgrubu oluşturur. PR'lerin farklılaşma süreci, üçüncül instar larva aşamasında başlar ve iki aşamada tamamlanır. İlk aşamada PR hücrelerinin farklılaşması başlar ve aksonları beyinde geçiçi katmanlarına yönelir. İkinci aşamada, içteki ve dıştaki PR'ler birbirlerinden ayrılırlar, her PR bir Rh molekülü ifade eder ve aksonlar optic lobda gitmeleri gereken katmanlarına uzanırlar. Bu çalışmanın amacı, daha önceden gerçekleştirilmiş olan yükseltici taraması baz alınarak iç fotoreseptörlere, özellikle de R8 hücreleri üzerine odaklanarak, iç PR'lerin farklılaşmasında görevli yeni molekülleri ve yolakları bulmaktı. Yükseltici taramasında bulunan ve R8 PR'ında ifade edilen üç aday genden *unzipped* geni bir hücre yüzey molekülü olması sebebiyle daha detaylı analiz yapmak üzere seçildi. İmmünoboyamalar ile ortaya çıkan ifade örüntüsüne göre Uzip üçüncül instar larva safhasında R8 hücrelerinde ve glia hücrelerinin bir alt grubunda, 48 saat pupa safhasında R8 hücrelerinde ve yetişkin safhada da bir kısmı medullaya uzanan alt grupta olmak üzere glia hücrelerinde ifade edilmekte. Yine yapılan immünoboyamalara göre Uzip üçüncü instar ve pupa aşamasında PR oluşumu ve glia ifadesinde, yetişkin safhasında da Rh ifadesine bağlı altgrup özelleşmesinde direkt bir etkiye sahip değil. Akson yönelmesinde ise Uzip hedef bölgedeki glialarda baskılandığı ve normalde ifade edilmeyen komşu fotoreseptörlerle farklı glialarda ifade edildiği zaman, akson projeksiyonlarında sapma görüldü. Bu çalışma sonucunda öngördüğümüz modele göre Uzip'i ifade eden R8 hücreleri, projeksiyonlarının hedef bölgesinde bulunan Uzip'i ifade eden glia hücrelerinden gelen adhezyon sinyalini takip etmekte. Bu çalışma Unzipped'in görsel sistemdeki ve aksonal uzanımdaki ifadesini ve rolünü göstermektedir.

TABLE OF CONTENTS

LIST OF FIGURES

LIST OF TABLES

LIST OF SYMBOLS

ml	Mililiter
mM	Milimolar
ng	Nanogram
v	Volume
w	Weight
µg	Microgram
µm	Micrometer
µl	Microliter

LIST OF ACRONYMS/ABBREVIATIONS

APF	After Puparium Formation
Ato	Atonal
BAC	Bacterial Artificial Chromosome
bp	Base pair
CADN	N-Cadherin
CAM	Cell Adhesion Molecule
caps	Capricious
CC	Cone cells
CNS	Central Nervous System
Dac	Dachsund
Dpp	Decapentaplagic
DRA	Dorsal Rim Area
Dscam	Down Syndrome Cell Adhesion Molecule
Dve	Defective proventriculus
Eg	Epithelial glia
EGFR	Epidermal Growth Factor Receptor
Eph	Ephrin
EY	Eyeless
EYA	Eyes absent
EYG	Eye gone
Fmi	Flamingo
Fra	Frazzled
GCPR	G-coupled Protein Receptor
GFP	Green Fluorescent Protein
Gogo	Golden goal
GPC	Glial Precursor Cell
Hh	Hedgehog
HRP	Horse Radish Peroxidase
Hth	Homothorax

IOC	Interommatidial cells
Ig	Immunoglobulin
IPTG	Isopropyl-ß-D-1-thiogalactopyranoside
Lats	Large tumor supresser
LG	Longitudinal Glia
LH	Lateral Horn
LN	Local Interneuron
MF	Murphogenetic Furrow
MFS	Major Facilitator Superfamily
MG	Marginal Glia
MS	Mass Spectrometry
N	Notch
NGS	Normal Goat Serum
Otd	Orthodenticle
PBS	Phosphate Buffered Saline
PCP	Planar Cell Polarity
PFA	Paraformaldehyde
PH	Pleckstrin homology
pH	Power of Hydrogen
PR	Photoreceptor
RBG	Retinal Basal Glia
RD	Retinal Determination Genes
Repo	Reversed Polarity
Rh	Rhodopsin
Ro	Rough
Sens	Senseless
Seq	Sequoia
Svp	Seven-up
Sim	Single-minded

SO	Sine Oculis
Ss	Spineless
TF	Transcription Factor
TOY	Tween Of Eyeless
UAS	Upstream Activating Sequence
Uzip	Unzipped protein
VNC	Ventral Nerve Chord
Wg	Wingless
Wt	Wild Type

INTRODUCTION

1.1. Drosophila melanogaster as a Model Organism

Drosophila melanogaster, also known as the fruit fly, is a widely used model organism. It has many scientific advantages such as its fully sequenced genome, the variety of available genetic tools, and the commercially available fly lines with different genotypes. Additionally it has maintenance advantages such as short life-cycle, high progeny number, low cost maintenance, and small area requirement for large number of flies. These properties, especially when compared to vertebrate models such as mice, are important advantages for working with a model organism. Since the discovery of the *white* gene by Thomas Hunt Morgan in 1910, which brought him the Nobel Prize, outstanding discoveries were made in *Drosophila* that found many application areas and lead to discoveries in other organisms (Bellen *et al*., 2010; Morgan, 1910).

One of the key features that make *Drosophila* an outstanding model in studying the nervous system development is its simple and well-defined sensory system, which shows high similarity to vertebrates on the developmental and functional level (Gehring, 2005). For this reason the fruit fly has had a great contribution to the understanding of neuroscience especially in the fields of cell fate determination, tissue specification, and neuronal differentiation studies (Rister *et al*., 2013; Sanes and Zipursky, 2010; Wernet and Desplan, 2004).

1.2. The Visual System of *Drosophila melanogaster*

The camera-like eye structure of vertebrates look different than the compound structure of insect eyes, but they have many traits in common like the perception of visual stimulus and the processing of it. The factors involved in their specification and patterning are highly conserved (Kumar, 2001; Sanes and Zipursky, 2010).

The compound eye of *Drosophila melanogaster* is composed of 800 hexagonal units called 'ommatidia'. Each ommatidium consists of 20 cells: eight photoreceptor (PR) neurons, located at the core of the ommatidium; and twelve accessory cells composed of six pigment cells (primary, secondary, and tertiary), four cone cells, and two mechanosensory bristles (Wolff and Ready, 1993; Kumar, 2001). The outer photoreceptors R1-R6 reside in the outer ommatidia forming a trapezoid, while the inner photoreceptors R7 and R8 are placed in the middle. R7 spans the upper half of the retina sitting on top of R8 and is UV sensitive. R8 is at the lower half of the retina and is sensitive to either blue or green light depending on the subtype (Hardie, 1979; Katz *et al*., 2009).

Each PR expresses a specific type of Rhodopsin (Rh) protein, a member of the 'opsin' family. Opsins are visual pigments, placed on the apical outer membrane of the PRs, where they collect light. According to the type of Rh they express, different PRs are sensitive to a different part of the light spectrum. The outer photoreceptors R1-6 express Rh1, which has a broad spectrum and is involved in dim light vision, orientation, and motion detection (O'Tousa *et al*., 1985; Zuker *et al*., 1985). The inner PRs express a different set of Rhs. The R7 cells express Rh3 or Rh4, which are both UV sensitive. If R7 expresses Rh3, the R8 in the same ommatidium expresses the blue-sensitive Rh5, forming the pale subtype, which makes up 30% of all ommatidia. When R7 expresses Rh4, the R8 coupled to it expresses green-sensitive Rh6, forming the yellow subtype, which makes up 70% of the ommatidia (Gao *et al*., 2008a; Yamaguchi *et al*., 2010). By expressing different sets of Rhodopsins, the inner photoreceptors are responsible for color vision and wavelength discrimination.

Vision starts by reception of light by the PRs, which is processed further by phototransduction. Here, the light stimulus is converted to a neural signal, and is finally transmitted to the optic lobe to be analyzed as an 'image' (Cook and Desplan, 2001). The PR neurons are photosensitive cells, which convert light input to electric signal. They project from the retina to the optic lobe for the transmission of the signal. The Rhs expressed by each PR cell are G-protein coupled receptors (GPCR) that are bound to light-sensitive chromophores. When excited by a photon, they initiate a signal transduction pathway called phototransduction (Borst, 2009; Rister and Desplan, 2011; Terakita, 2005).

The processing of the visual stimuli is similar in vertebrates. The 'rods' are highly sensitive PRs that can respond to a broad spectrum and they all express rod opsins. Similar to the outer PRs, rods are responsible for processing of dim light and motion detection. They are placed in the periphery of the retina. At the center of the retina is the fovea region, which is mostly composed of cone PR cells that express one of the cone opsins. Human cones have three subtypes absorbing light at different wavelengths: S for short (<500 nm, blue), M for medium (~530 nm, green), and L for long (~560 nm, red). The cones are responsible for high-resolution image formation and colour perception (Figure 1.1) (Cook and Desplan, 2001; Xiao and Hendrickson, 2000).

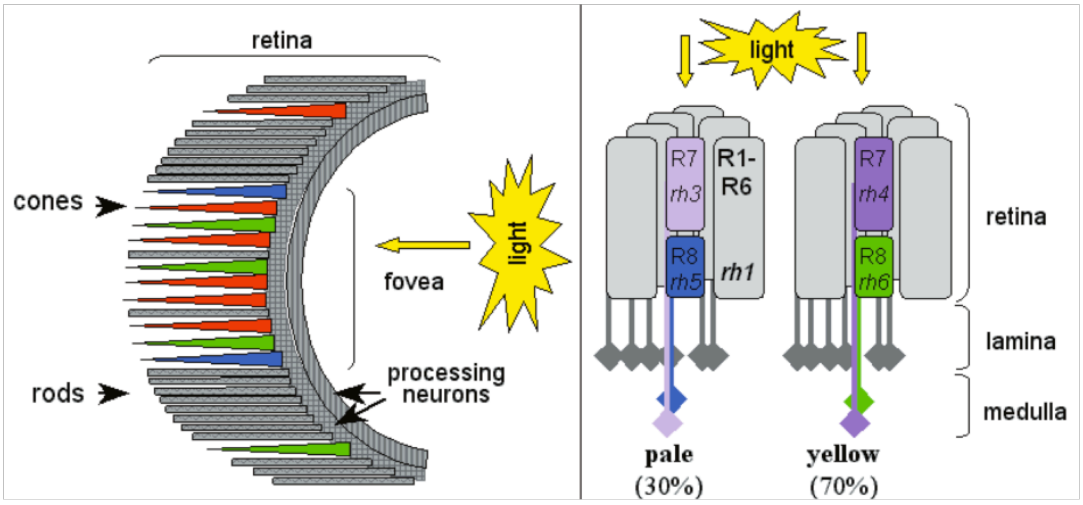

Figure 1.1. Photoreceptor subtypes in humans and flies. In the humans the M (green), L (red), and S (blue) cone cells, which are involved in color vision and generation of high-resolution images, reside in the central region of the retina called the 'fovea'. The rod cells which are important for dim light vision are found in the outer layer of the retina and express rod 'opsin's, rhodopsin (Cook and Desplan, 2001).

For both vertebrates and invertebrates, the general rule behind the expression of receptors in the visual system is the same as in the most of the sensory systems: 'one receptor per cell'. This is to prevent sensory overlap, and with rare exceptions this is the reason for a single PR expressing a single opsin (Mazzoni *et al*., 2004). Considering the basic principles and similarities between the visual systems of vertebrates and *Drosophila*,

Drosophila is a great model to reveal the regulation mechanism of Rhodopsin expression (Pichaud *et al.*, 1999; Rister and Desplan, 2011).

1.2.1. The Formation of the *Drosophila* Eye and PR Cell Specification

The development of the *Drosophila* eye starts when a group of cells get determined to form the eye at the embryonic stage. The specification of the eye primordium is established by the Wnt and TGF-β signalling pathways, enabling the activation of a set of nuclear genes called the 'retinal determination genes' (RD) (Domínguez and Casares, 2005; Kenyon *et al.*, 2003; Kumar, 2009). These are members of TF (Transcription Factor) families: *eyeless (ey)*, *eye gone (eyg*), *sine oculis (so*), *eyes absent (eya*), *dachshund (dac*), and *teashirt (tsh)* (Sahin and Celik, 2013; Silver and Rebay, 2005; Tsachaki and Sprecher, 2012). *ey* and *twin of eyeless (toy)* are highly related genes that initiate differentiation. They are the homologues of the vertebrate gene *pax6*, which is highly conserved and initiates the formation of the eye in many organisms (Czerny *et al*., 1999; Jang *et al*., 2003). The rest of the RD genes are at the downstream of the regulatory pathway, but there is a high level of crosstalk, feedback loops, and interaction among them. For that reason they are referred to as the 'RD network'. These molecules are essential for the formation and differentiation of the eye: their ectopic expression causes the formation of an eye in other tissues while their absence causes severe deficiency in the formation of the eye (Bonini *et al*., 1997; Halder *et al*., 1995; Shen and Mardon, 1997).

At the third instar larval stage, the cells of the eye-antenna imaginal disc form a monolayer epithelial sheet. A wave of differentiation sweeps from the posterior end of the eye disc towards the anterior end, called the morphogenetic furrow (MF), which makes an indentation in the smooth sheet leaving differentiated cells behind as it moves along (Ready *et al*., 1976; Wolff and Ready, 1991). The differentiating cells do not migrate with this wave; instead, their thickness, morphology, and cell-cycle state changes along the anterior/posterior axis. In the MF, there are many TFs and differentiation molecules that initiate PR formation. Hedgehog (*hh*), Decapentaplegic (*dpp*), and Ecdysone are the major signalling molecules that initiate the MF (María Domínguez and Hafen, 1997; Niwa *et al*., 2004; Ready *et al*., 1976). *dpp* is involved in the progression of the MF, while *wingless*

(*wg)* regulates the MF negatively in order to prevent inaccurate retinal specification (Baonza and Freeman, 2002; Heberlein *et al*., 1993).

As the MF moves along, it first induces the TF *atonal* (*ato*), which starts the differentiation of the precursor R8 cells: the first PR to differentiate (Domínguez, 1999; Jarman *et al*., 1994). *Hh* and *ato* form a feedback loop where the secretion of *Hh* by differentiated cells induces *ato*, and *ato* in return promotes *Hh* secretion (Lopes and Casares, 2010). The R8 cells are chosen from a group of ato-expressing cell cluster, which are evenly distributed. *Ato* activates *senseless (sens),* a zinc-finger TF which is required for R8 differentiation. Lateral inhibition mediated by Notch decreases the number of ato-expressing cells in the cluster to one cell, which continue to express *sens* and become R8 (Frankfort and Mardon, 2002). *Sens* represses *rough* (*ro*) in order to maintain the R8 fate. The R2 and R5 cells, which are the next ones to differentiate, express *ro* (Frankfort *et al*., 2001; Pepple *et al*., 2008).

Once the founder R8 cells start differentiating, the other PRs follow; the initial differentiation wave is mediated by epidermal growth factor receptor (EGFR) and Notch (N). The EGFR ligand Spitz is secreted by R8 leading to the differentiation of R2/R5 and then R3/R4. There are also other factors involved in the differentiation of R3/R4 such as *seven-up (svp*), which is a nuclear hormone, the TF *spalt*, and the non-canonical Wnt pathway Fz/PCP (Mlodzik *et al*., 1990; Mlodzik, *et al*., 2004; Strutt *et al*., 2002). These five PRs (R8, R2, R5, R3, R4) form a cluster (Freeman, 1996). They are arrested at the G1 phase and differentiate with the EGFR signal.

The undifferentiated cells around the cluster, enter cell cycle with a second mitotic wave where R1/R6 cells are recruited in response to EGFR and express *svp* (Baker and Yu, 2001; Mlodzik *et al*., 1990). Finally the UV-sensitive R7 PR is formed as a result of two signalling pathways: R8 cells express Bride-of-Sevenless (*Boss*), which binds to Sevenless (Krämer *et al*., 1991), and R1/R6 express Delta, which activate the Notch receptor on the potential R7 cell (Figure 1.2) (Cooper and Bray, 2000; Tomlinson and Struhl, 2001). After the differentiation of PRs is completed, the non-neural cone cells form.

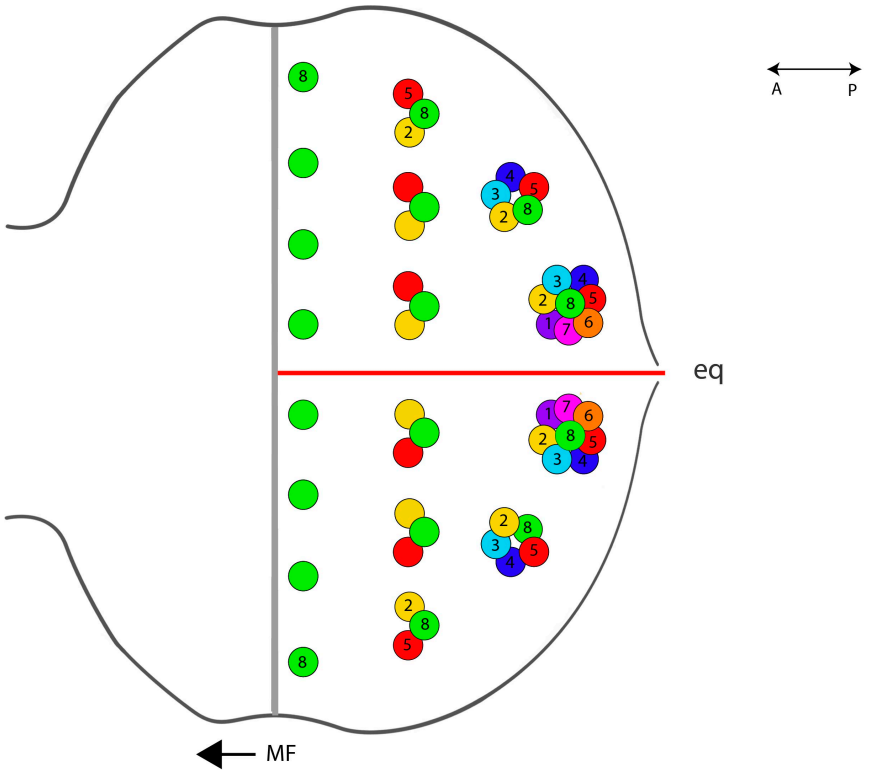

Figure 1.2. PR specification at the 3rd instar larval stage. As the MF sweeps from the posterior end to the anterior end of the eye disc, first the founder R8 cells are specified (green), then R2 and R5 (yellow and red respectively), and later R3 and R4 (pale and dark blue). After the second mitotic wave sweeps through, the last PRs R1-R6 (purple and orange) and finally R7 (pink) become specified.

The variety of the morphogens, hormones, and TFs involved in PR specification and the complexity of their interactions, indicate that PR specification requires a highly controlled network, and the correct regulation is very important for the functioning of the visual system.

1.2.2. Terminal Differentiation of PRs and Subtype Specification

Once the initial PR specification is completed, the terminal stage starts where the cells in the ommatidia are formed and the differentiation is completed. The pigment cells and the mechanosensory bristles are added to the periphery of the ommatidia. The undifferentiated cells remaining are removed by apoptosis, and the non-neural accessory

cells, which provide support, isolate the ommatidium from its neighbours. Additionally, during the pupal stage the PR cells acquire the characteristic apical membrane structure called the 'rhabdomere'. These are the locations where Rhodopsin molecules reside. At the first half of the pupation period the formation of the PRs, cone cells (CCs) and pigment cells are completed. During the last half of pupation, the flat epithelial sheet starts to form the three dimensional adult *Drosophila* eye structure. 50 hours After puparium formation (APF), PRs project to the brain to make their specific connections. In addition to pigments, corneal lens and the pseudocone are also secreted at this stage (Wernet and Desplan, 2004).

The first step in terminal PR differentiation is to gain the inner/outer PR cell fate. The inner PRs R7 and R8 express the zinc finger TF complex *spalt*, which distinguishes the inner PRs from the outer ones (Domingos, *et al*., 2004; Mollereau *et al*., 2001). Then the R7 and R8 cells are specified. *Prospero,* which is another TF, is expressed in R7 cells and represses the expression of R8 Rhodopsins Rh5 and Rh6 in the R7 cell by binding to their promoters. Additionally *prospero* is involved in the positioning of R7 cells (Cook *et al*., 2003) while R8 cells require the specific expression of *sens*, a zinc-finger TF, for its cell fate decision. *Sens* represses the R7-specific Rh3 and Rh4 in R8 cells (Xie *et al*., 2007). In summary, *spalt* leads to an inner PR fate, while *prospero* and *senseless* lead to further differentiation where the inner PRs gain the R7 and R8 fates, respectively.

After R7-R8 specification has taken place, Rhodopsin molecules are expressed and the PR differentiation is completed. The expression of Rh genes starts at 78% APF and requires a broad network of transcriptional activators and repressors. First Rh1 is expressed in the outer PRs, which is shortly followed by the expression of Rh3, Rh4, Rh5, and finally Rh6 in the inner PRs (Earl and Britt, 2006).

The inner PRs of the ommatidia that are responsible for color vision are divided into two subtypes: yellow subtype, which expresses Rh4 and Rh6 in a coupled manner in 70% of the ommatidia, and pale subtype, which expresses Rh3 and Rh5 and form 30% of the ommatidia (Jukam and Desplan, 2009; Morante *et al*., 2007; Papatsenko *et al.*, 1997). This ratio is also conserved in different organisms including flies that are evolutionarily distant like the blowfly *Calliphora* and the housefly *Musca* (Kirschfeld and Franceschini, 1977; Schmitt *et al*., 2005).

The distribution and patterning of subtype specification is stochastic. The first step of this choice is made by the expression of a bHLH TF named *spineless (ss)*. Ss is expressed in 70% of R7 cells and induces the expression of Rh4 specifying the yellow subtype. The remaining R7 cells that do not express *ss* express Rh3 and form the pale subtype (Wernet *et al*., 2006). The upstream of this signal or how *ss* is expressed stochastically in 70% of the retina remains to be elucidated. *Ss* activates the expression of *defective proventriculus* (*dve),* which is a K50 homeobox protein, in the yellow R7 cells. Dve represses the expression of Rh3. It is also strongly expressed in the outer PR's where it represses Rh3, Rh4, and Rh6 expression. In contrast, in the pale subtype *dve* is repressed by *sal* so that the expression of Rh3 can be activated by *orthodenticle (otd)* (Johnston *et al.*, 2011).

Once the decision is made by the R7 cells to acquire the yellow or pale subtype, this information is conveyed to the underlying R8 cell. When there is no signal from the R7 cell, the R8 cells expresses Rh6 by default (Chou *et al*., 1996; Papatsenko *et al*., 1997). While the identity of the signal that is conveyed from the R7 cell to the R8 cell is not known, the signalling pathway that maintains the subtype choice in the R8 cell has been revealed. *Warts* and *melted* are two genes that have opposite roles and regulate each other in a bistable loop. *Warts* is a Ser/Thr kinase that is similar to the Large Tumor Suppressor in humans (*lats*). Both *warts* and *lats* are part of the *Lats/Hippo/Salvador* tumor suppressor pathway, which normally prevents proliferation by enforcing cell death. *Warts* is expressed in R8 cells of the yellow subtype, and its loss of function causes all R8 cells to express Rh5, transforming the yellow subtype R8 to a pale subtype R8. The *Melted* protein has a pleckstrin-homology (PH) domain, and is a member of the *Tor/Insulin* growth control pathway. It is expressed in the pale R8, and its loss of function causes all R8 cells to express Rh6 as if no signal is received from the R7 cell. *Melted* is activated upon receiving the signal coming from the pale R7 cells and it converts the coupled R8 cell to the pale subtype. *Warts,* on the other hand induces the expression of Rh6 when there is no signal received from the R7 cell, leading to the acquisition of the yellow phenotype in R8 (Mikeladze-Dvali *et al.*, 2005; Morante *et al*., 2007; Quan *et al.*, 2012).

The differentiation of inner PRs in the dorsal retina depends on regional differentiation rather than stochastic choice mechanisms and leads to the generation of two

subtypes called dorsal rim area (DRA) and dorsal y. The DRA is present in the two dorsal-most rows of the retina and is responsible for the detection of the e-vector and polarized light. The ommatidia in this region have larger inner rhabdomeres and stacks of microvilli that serve as polarizing filters. Both R7 and R8 cells in this area express the same rhodopsin, Rh3. *wg* expression in the head cuticle and *IroC* expression in the dorsal half of the eye lead to the local expression of the homeoprotein homothorax (*hth*) in one-two rows at the dorsal edge (Wernet *et al*., 2003). The dorsal y ommatidia are located at the dorsal third of the retina and co-express UV-sensitive Rh3 and Rh4 in the R7 cells and Rh6 in R8 cells. These ommatidia are thought to be responsible for distinguishing the solar and antisolar halves of the sky, which is required for proper navigation skills. The dorsal y subtype is interesting as it presents the only exception breaking the 'one receptor one neuron' rule. This mechanism of co-expression is regulated by *IroC*, which induces the expression of Rh3 in the yellow subtype (Figure 1.3) (Mazzoni *et al*., 2008).

1.2.3. Axonal Projection in the Visual System

The visual system of *Drosophila* is organized in columnar and layered circuits. The axons of the PRs project to the optic lobe. The optic lobe is composed of 4 ganglia: the lamina, medulla, and the lobula and the lobula plate which form the lobula complex (Sanes and Zipursky, 2010). The axons of the outer PRs R1-R6 terminate in the lamina in a columnar organization (Hakeda-suzuki and Suzuki, 2014; Meinertzhagen *et al*., 1991; Morante and Desplan, 2004). The inner PRs R7 and R8 project to the medulla. The medulla neuropil is divided in to 10 parallel layers, M1 to M10. The R8 axons terminate in the M3 layer while the R7 axons terminate in the M6 layer. There is also a similar organization in the medulla. Each column is composed of lamina neurons L1-L5, which elongate from the lamina cartridges, 35 medulla neuron subtypes, and other neurons that form branches in defined patterns (Figure 1.4) (Fischbach and Dittrich, 1989; Melnattur and Lee, 2011; Morante and Desplan, 2008).

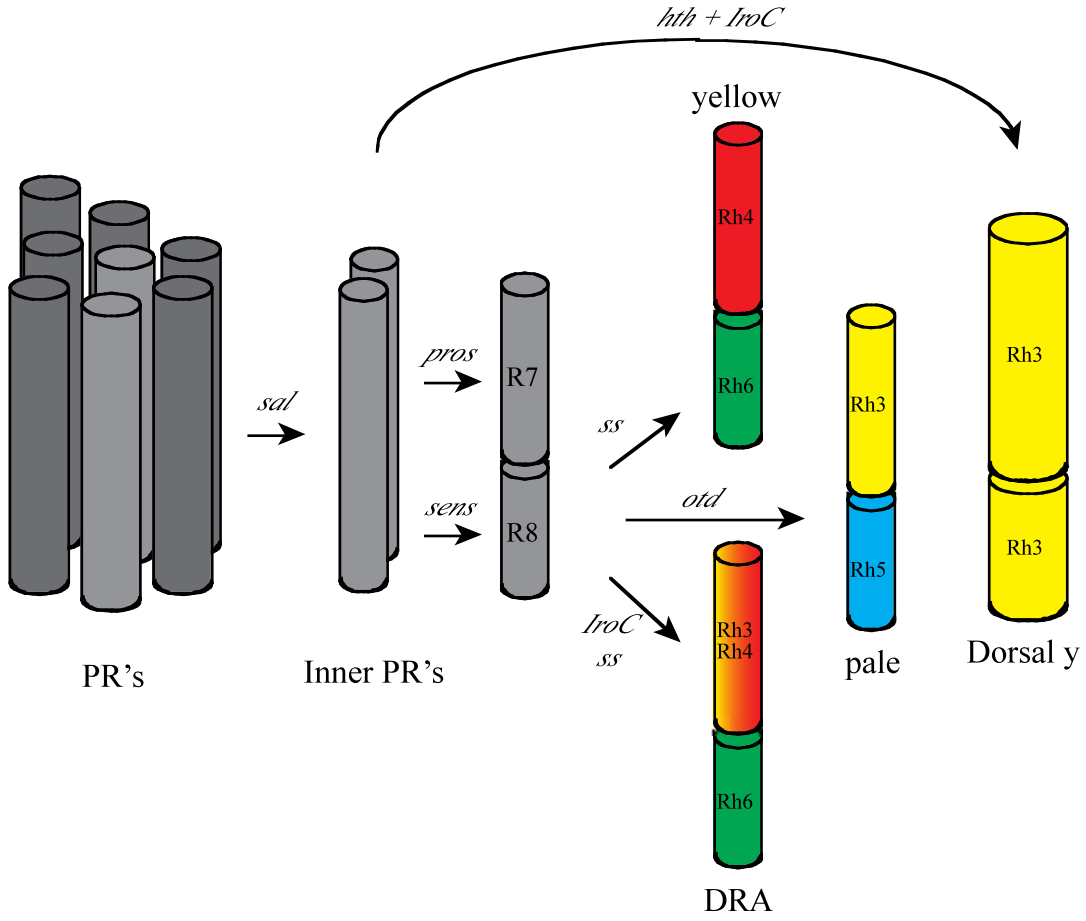

Figure 1.3. Terminal differentiation of PRs. The PR cells start expressing Rhs at the pupal stage. First the inner PRs are differentiate by expression of the TF complex *sal*. Then four ommatidial subtypes are generated depending on the type of Rh expression in the inner PRs.

The initial targeting and the formation of the retinotopic map starts at the 3rd instar larva stage. At this stage neurogenesis, gliogenesis, projection to the optic lobe, and the formation of the optic lobe happen in parallel. The first stage in the projection of an R-cell axon is its projection from the eye disc. As the PR differentiate row by row at the posterior side of the MF, they extend their axons through the optic stalk towards the optic lobe to temporal layers (Roignant, Jean-Yves and Treisman, 2009). In doing so they rely on glial cells which originate in the optic lobe and migrate into the eye disc. The PR cells projecting to the optic lobe are also involved in the differentiation and formation of the optic lobe.

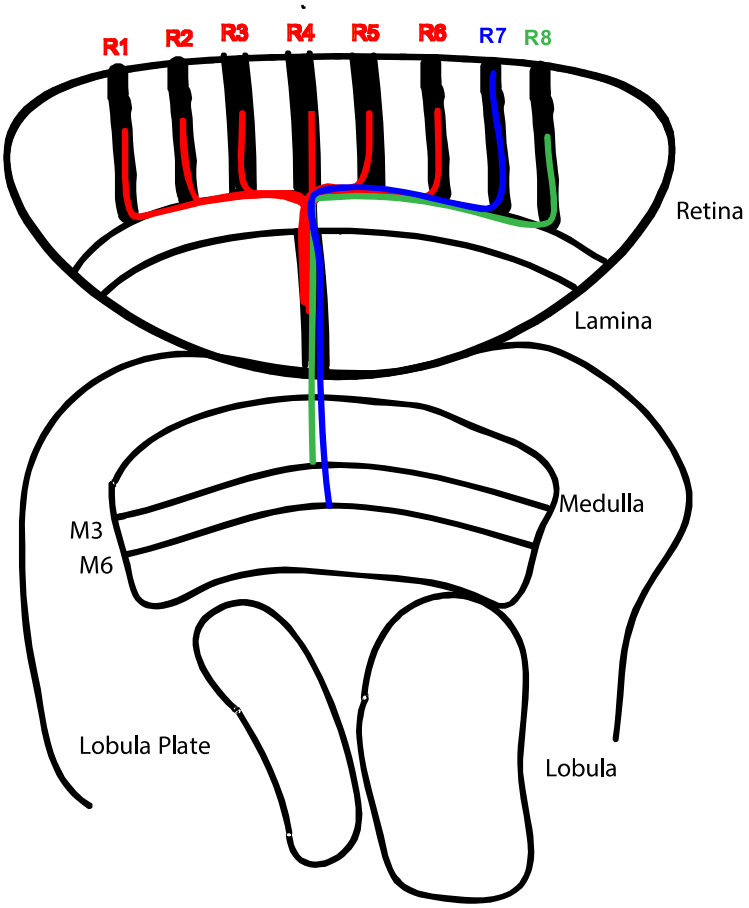

Figure 1.4. PR projections in the adult brain. The retinotrophic map formation and the curved nature of the *Drosophila* eye leads to different PRs from adjacent ommatidia to project through the same cartridge at the lamina. The R1-R6 cells terminate in the lamina layer while the R7 and R8 axons move on to the medulla. The R8 cells stop at the M3 layer while the R7 cells stop at the M6 layer.

First the founder PR, R8 enters the developing optic lobe and starts the establishment of the retinotopic map by activating *Wnt4* (Sato *et al*., 2006). The axons of R8 cells terminate in a temporal layer in the medulla, which requires two transmembrane receptors *Flamingo (fmi*) and *golden goal* (*gogo*) in addition to *Hu-li tai shao (Hts),* which is the *Drosophila* homolog of Adducin (Lee *et al*., 2003; Ohler *et al*., 2011; Senti *et al*., 2003). Then R1-R6 cells project to the lamina, terminating between two rows of glia called epithelial glia (eg) and marginal glia (mg) in the lamina, which provide the 'stop signal' required for the axons to terminate (Chotard and Salecker, 2007; Poeck *et al*., 2001). The genes involved in this process are: *nonstop*, *JAB1/CSN5*, *glial cells missing (gcm)* and

gcm2 (Toshihiko Hosoya *et al*., 1995; Jones *et al*., 1995; Suh *et al*., 2002). These glial layers later on become intermediate targets as the R1–R6 cell axons choose their final synaptic partners at later stages. Finally, R7 axons pass through the lamina and extend towards the developing medulla. The R8 and R7 axons at the larval stage, project closely adjacent to each other in an evenly spaced manner into the medulla neuropil (Lee *et al*., 2003; Tomasi *et al*., 2008). The axon bundles entering the optic lobe lead to the activation of two anterograde signals: *Hh* and *Spitz*. These cause the differentiation of lamina neurons. Additionally the expression of *single-minded (Sim*) is activated in lamina neurons by *Hh*, which mediate their assembly into the columnar lamina cartridge structure (Huang and Kunes, 1998; Zhen Huang and Kunes, 1996; Zhen Huang *et al*., 1998; Umetsu *et al*., 2006). The targeting process of PR cells to their temporal layers continues throughout the pupal stage and finalizes towards its end.

At the pupal stage both the outer and the inner PR's project to their final layers. The targeting of R7 and R8 is acquired in two steps: First the R8 cells reside at the temporal layer, which is at the distal medulla neuropil border, while the R7 cells go to the deeper layers of the medulla. After mid-pupal stage they both target to their final layers. The temporal projection of R8 depends on *gogo*, which is the only molecule known to affect the first step of R8 growth and causes the axons to stop at the R8 temporary layer at 48 hr APF. Phosphorylated *gogo* enhances the adhesive interaction of R8 with the R8 temporary layer, whereas dephosphorylation provides a permissive signal that allows the axon to leave the temporary layer and project to the M3 targeting layer (Mann *et al*., 2012). However, even in *gogo* mutants, only a few R8 axons pass through the R8 temporary layer and mistarget to the deeper layer, suggesting that there are other factors involved in the early targeting process. The second step of medulla targeting occurs after all the axons of R7, R8, and lamina neurons reach their respective temporal layers, when R8 axons start to extend thin filopodia towards their final targets at around 50 hr APF. At this stage Netrin B, one of the two Netrin isoforms expressed in *Drosophila*, is also involved. It is expressed in the M3 layer starting at 42 hr APF and is strongest at 55 hr APF. The R8 cells expressing Frazzled (Fra), the Netrin receptor, recognize Netrin at the target area and project towards it. Net/Fra has an instructive role in R8 axon attraction, which leads them to the proper layer (Timofeev *et al*., 2012). By 70 hr APF, R7 and R8 axons reach their final target layer, develop mature terminals, and undergo synaptogenesis (Figure 1.5).

As for the outer PR's from the 3rd instar larval stage to approximately 30 hours APF, the growth cones from one ommatidial cluster terminate adjacent to each other in the lamina. Then the R1–R6 growth cones leave their original fascicle and extend to neighboring sets of lamina neurons L1–L5. Analysis of *fmi*, *CadN*, *Lar*, and *Liprin-a* mutants show that the outgrowth and selection of the target neuron sets are regulated by interactions between R1–R6 axons; and between R-cell axons and lamina neurons. Starting from the mid-pupal stage, growth cones elongate and develop into mature terminals, which establish synaptic contacts with lamina neurons L1–L3 and other neuron subtypes. In order to have a further insight and understanding of the factors involved in axonal growth, targeting, and positioning of PRs, forward genetic screens were performed (Hadjieconomou *et al*., 2010).

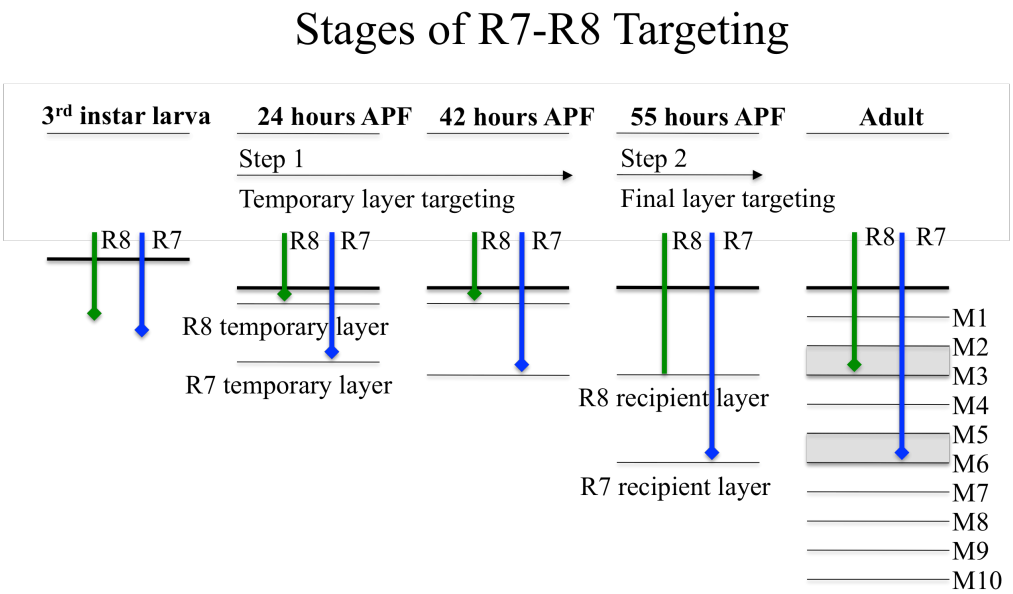

Figure 1.5. Developmental stages of R7 and R8 targeting. Axonal targeting of the inner PRs starts at the 3rd instar larval stage, at the early pupal stage the R8 axons project to the M1 layer while the R7 cells project to the M3 layer temporarily. At the late pupal stages both R7 and R8 project to their final layers M6 and M3 respectively (modified from Hadjieconomou *et al*., 2010).

The R8 and R7 axons project to different layers in the medulla, thus their projection involves a different set of molecules. The targeting of R8 axons are regulated mainly by three cell surface proteins which are *Fmi*, *gogo* and *caps* (Lee *et al.*, 2003; Tomasi *et al*., 2008; Senti *et al*., 2003). Both *fmi* and *gogo* are expressed in all PRs, including the inner PRs. Additionally *fmi* is also expressed in lamina and medulla neuron subtypes. The expression of *gogo* also shows variation by decreasing at the mid-pupal stage. In the absence of *fmi* and *gogo*, the inner PR axons are stuck at the medulla neuropil border, where they project temporarily at the pupal stage (Senti *et al.*, 2003 ; Tomasi *et al*., 2008). *Caps*, which is a CAM expressed in R8 cells and target neurons including the M3 layer, is also involved in the projection process. In the previous report it was shown that its deficiency causes early or late termination in addition to surpassing to neighbor columns while its overexpression leads to the termination of R7 axons in the M6 layer, showing that it has an instructive role in R8 targeting (Shinza-Kameda *et al*., 2006). However a recent paper showed that *Caps* does not mediate R8 axon targeting by R8 axon-target adhesion and its mutation causes a milder phenotype than the one described previously (Berger-Müller *et al*., 2013). Still, *caps* is one of the factors affecting the targeting of R8 cells and its milder affect indicates the presence of other players. *Netrin* is another molecule, which localizes to M3. The R8 axons which do not express its receptor Fra stop at their temporary layer and fail to extend towards their final target. Although Netrin usually functions in long range signals as a secreted molecule, it is shown that it acts locally (Timofeev *et al*., 2012). Jelly belly and Alk are other factors that are involved in the control between the afferent axon and target neuron interactions. They are required for the assembly of the cartridge for the R1-R6 neurons in addition to layer and column specific targeting of the medulla (Bazigou *et al*., 2007).

R7 axons, which are different both in structure and axonal projection, have a different regulation mechanism compared to the R8 cells. The regulation factors of R8 have more restricted expression patterns while the R7 axon guidance determinants have broader expression patterns such as CadN. CadN is shown to be involved in the targeting of R7 both to its temporary and final targets. Its total absence or being missing in target neurons leads to similar defects: the early termination of R7 cells in the M3 layer instead of M6, which implicates that the layer specificity of the targeting might be related to the target neurons (Lee *et al*., 2001; Nern *et al*., 2005; Ting *et al*., 2005; Yonekura *et al*.,

2007). PTP69D and Lar, which are both receptor tyrosine phosphatases, and Liprin-α are other factors that R7 depends on while targeting. Lar is involved in stabilizing the layer-specific connections and is known to recruit molecules such as CadN and Liprin-a into a complex. In its absence the R7 cells target to the correct layer in the first place, but then draw back and mistarget to M3 (Hofmeyer and Treisman, 2009; Choe *et al*., 2006). The Activin/TGF-β receptor *Baboon*, its downstream effector *dSmad2*, and *Importin-a3* also play a role in R7 targeting and their absence cause the invasion of adjacent columns (Ferguson *et al*., 2009).

There are also factors, which are expressed in both R7 and R8 cells like the Zinc finger TF *sequoia* (*seq*). It is transiently expressed first in R8 cells and then in R7 cells when their axons are projecting to their temporary layers. Its deficiency leads to early termination of R7 cells in the M3 layer while its prolonged expression causes the mistargeting of R8 axons to the M6 layer. *Seq* also regulates the level of *CadN* expression which in return affects the R7 targeting (Petrovic and Hummel, 2008). TFs also regulate the targeting of PR cells in addition to subtype specificity. *Sens* in R8 cells activates the expression of *caps* in addition to its role in Rh5/Rh6 activation and Rh3/Rh4 repression. In R7 cells NF-YC represses *sens* and in return the expression of *caps* to prevent mistargeting to the M3 layer (Morey *et al*., 2008). Although a large variety of permissive and instructive factors and their interrelations have been revealed to have a role in axonal projection, considering the complexity of the neural connections, there are many more networks and pathways to be elucidated (Figure 1.6).

For the outer PR projections there is a different system. Due to the curved nature of the *Drosophila* eye, the information from different ommatidia are combined in order to obtain a proper visual image. The ommatidia project each outer PR to a different cartridge in the lamina. As a result, one cartridge contains the outer PRs of six different ommatidia and a set of lamina neurons. The PR cells containing the same visual information connect with the same target neurons, called neural superposition, increasing the light detection sensitivity (Clandinin and Zipursky, 2000). The R1-R6 cells are sensitive to *fmi* levels in the neighboring axons. *Fmi* is a CAM, which mediates the interactions between R cells by positioning them relative to each other and leading them to their correct columns (Chen and Clandinin, 2008; Lee *et al*., 2003). N-Cadherin (CadN), which is another CAM, is also

involved in the targeting of outer PRs stabilizing the interactions between the PR axons and lamina neurons. In its absence the R1-R6 cones cannot position themselves in neighboring columns (Lee *et al*., 2001; Prakash *et al*., 2005). Leukocyte antigen-related (Lar) and Liprin-α are the other factors which are known to be involved in the regulation of PR cell targeting (Clandinin *et al*., 2001; Choe *et al*., 2006).

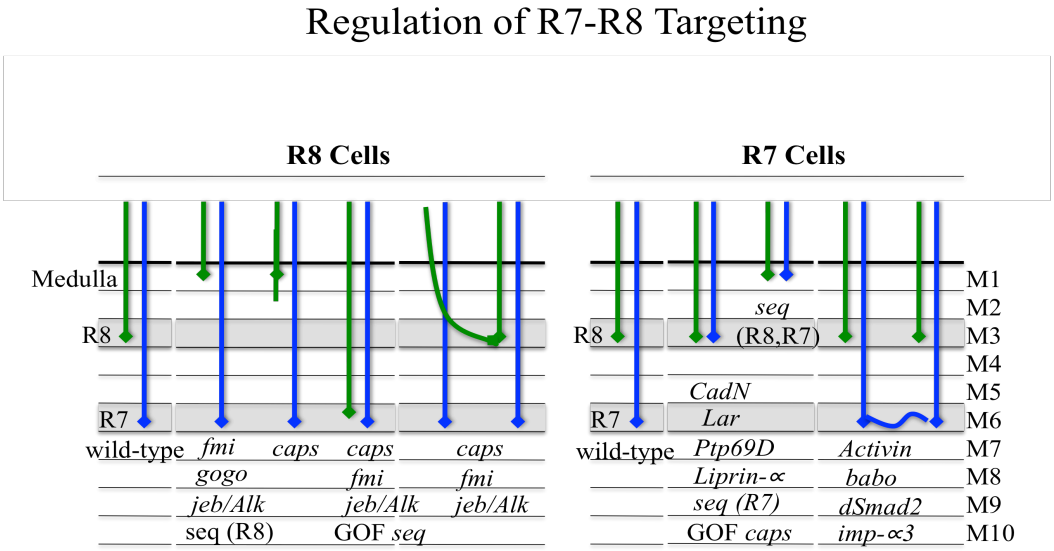

Figure 1.6. The regulation of R7-R8 targeting. The axonal targeting of the inner PRs is a complex process and the presence or absence of the regulatory molecules can lead to different phenotypes, while they are not sufficient for leading the targeting alone. The known molecules, which have a role in this process are listed, but there are more to be elucidated (adapted from Hadjieconomou *et al*., 2010).

1.2.3.1. Role of Glial Cells and Axon-Glia Interactions in Axonal Projection. The functioning of the nervous system depends on the interaction of two different cell types: neurons and glial cells. Studies in both vertebrates and invertebrates show that the highly conserved nervous system requires a very tight regulation and both the role of glia and neuron-glia interactions are far more complex than anticipated. First of all neurons and glia are required for each other's survival. In addition, glia regulate axonal outgrowth during injury repair, act as guidepost cells and intermediate target cells, form boundaries for developing axons, and are involved in axon pruning. Axons, in return, guide glial migration, which is critical since glial cells are usually born far away from their final targets and have to migrate to their final destination (Chotard and Salecker, 2004).

1.2.3.2. Glial Cells in the Visual System of *Drosophila melanogaster.* The *Drosophila* visual system has fewer glial cells compared to vertebrates, while the mechanisms of communication between neurons and glial cells are conserved. At the 3rd instar larva stage, as the PR cells differentiate and project to the optic lobe through the optic stalk, the retinal basal glia (RBG) also called the subretinal glia, originate from the optic stalk. They migrate to the eye disc and move from the basal surface up to the area where the youngest PR cells start to form their axons. This migration process is independent of the differentiation of PR cells, however the formation and projection of the PR cells depend on the migration of the glial cells to the eye disc (Rangarajan *et al*., 1999).

The outermost glial cells are the perineural cells. Just beneath them are the subperineural cells, which are epithelial-like and are connected by tight septate junctions. In the developing eye, there are two enlarged subperineural cells called the carpet cells (Silies *et al*., 2007). These two types of glial cells form the blood-brain barrier of *Drosophila*, providing a protection shield from the high K^+ concentration in the hemolymph. (Choi and Benzer, 1994; Hummel *et al*., 2002). Just underneath this barrier is the wrapping glia, which is formed by the differentiation of the perineural glia after contacting PR cells. They form a glial sheath around the PR cells, wrapping them and following them to the optic lobe (Silies *et al*., 2010). A fourth type of glia called the edging glia, has been anatomically defined, but its genetic profile or function are not known (Figure 1.7) (Silies *et al*., 2007).

Glial cells migrate from the optic stalk towards the eye disc. At this stage the FGF8-like protein Pyramus, which is among the Htl ligands, is secreted by glia and directs glial proliferation and migration. After the glial cells reach the differentiated eye disc, they come across a second FGF8-like protein signal, Thisbe. It is expressed by the developing PR neurons and is required for the formation of the glial sheath around the extending PR axons. At this stage the glia-glia signal switches to the neuron-glia signal. Since it is known that these two FGF-8 like proteins can also substitute for each other, other signals that differentiate between these two types of interactions must exist (Franzdottir *et al*., 2009; Silies *et al*., 2010).

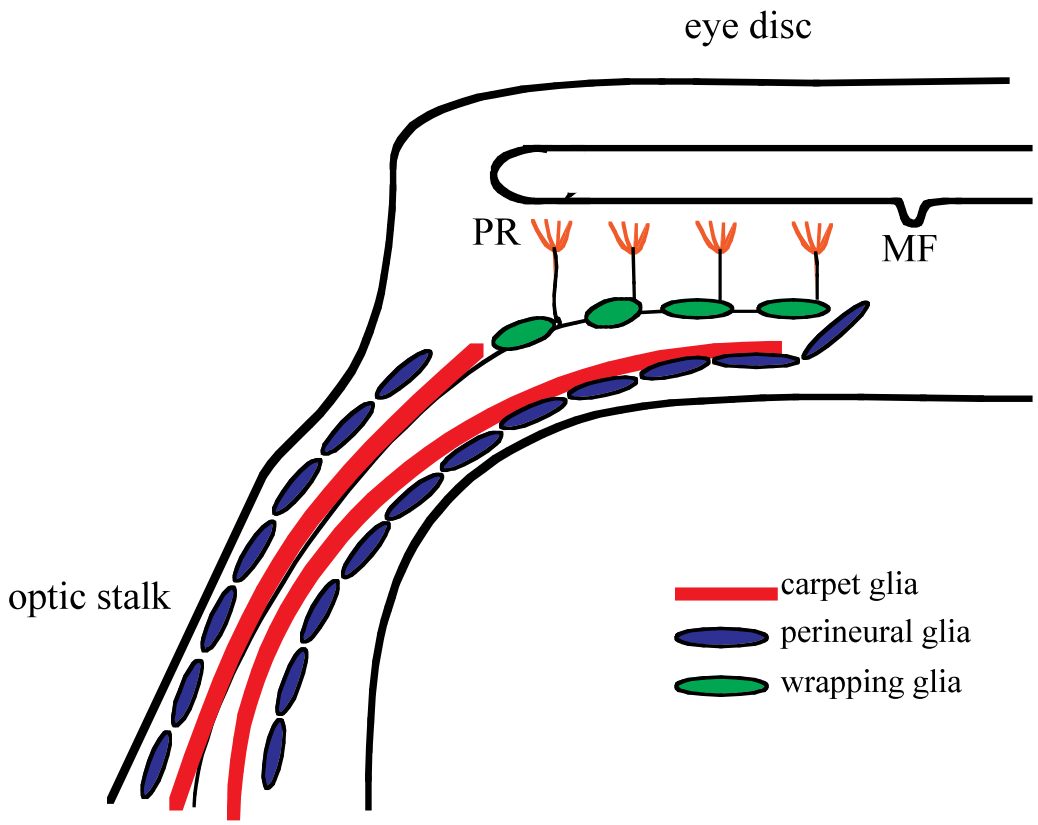

Figure 1.7. Glial cells in the 3rd instar larval eye disc. There are four major types of glia in the 3rd instar larval eye disc. Glial cells migrate from the optic lobe to the eye disc. First the carpet glia move and then the perineural glia move over the carpet glia. As the perineural glia come into contact with the differentiating axons, they turn into wrapping glia and start wrapping the PR axons.

The satellite glia ensheath the cell bodies of lamina neurons as they mature. The other glia in the optic lobe are neuropil-associated glia. The R1-R6 axons stop in the lamina between distal epithelial and proximal marginal glial cells, forming a thin layer or neuropil called lamina plexus. These two groups of glial cells are derived from the glial precursor cell (GPC) region, which contain multipotent progenitors (Chotard and Salecker, 2007). The committed cells in this area express *glial cells missing* (*gcm*) and *gcm2*, which are two transcriptional regulators essential for glial cell specification. It is important to note that *gcm* is also expressed in a few cells, which are not glial cells like macrophages or neural precursors (Chotard and Salecker, 2004; T Hosoya *et al*., 1995; Jones *et al*., 1995). The third row of glial cells beneath the lamina plexus, is the medulla glial cells, which

reside in the lamina-medulla boundary (Chotard and Salecker, 2007). All glia subtypes in the visual system express a homeodomain protein: *reverse polarity gene* (*repo*). Repo is a widely used marker for glial cells in the early, developing, and adult stages of *Drosophila*. At the third instar larva stage in addition to the eye imaginal disc, it is also expressed in the LPC region in the optic lobe and in the glial cells in the lamina plexus region, which are epithelial, marginal, and medulla glial cells. Only a few cells are Repo positive in the GPC region margins as they come into contact with PR axons (Poeck *et al*., 2001). The loss of Repo affects the glial differentiation both in the eye and the optic lobe (Figure 1.8) (Halter *et al*., 1995; Xiong *et al*., 1994).

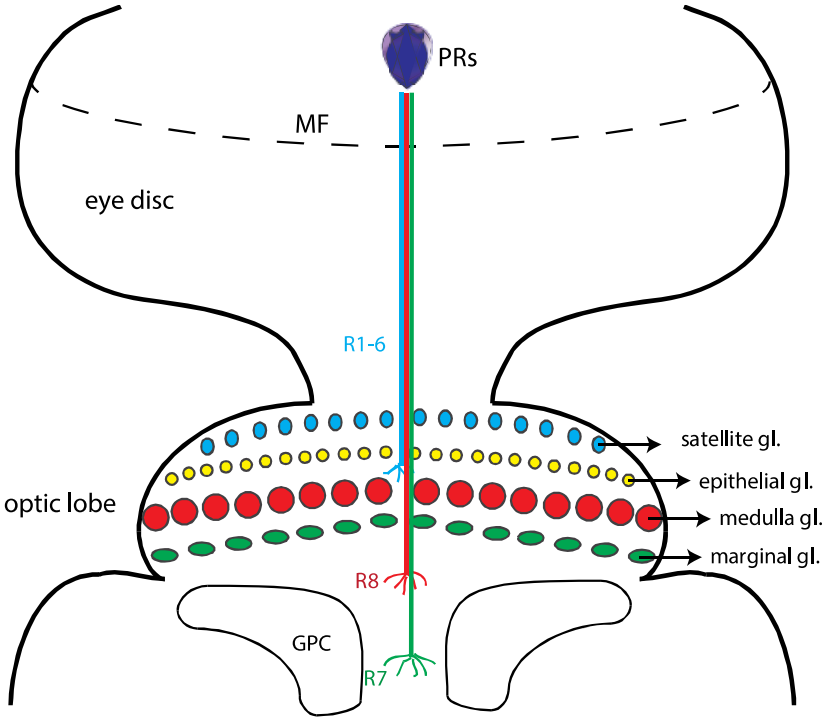

Figure 1.8. Glial cells in the optic lobe and their role in axonal projection in 3rd instar larva. The glial cells in the optic lobe are involved in axonal targeting. The satellite glia ensheath the cell bodies of lamina neurons, the other glia are neuropil-associated. The R1-R6 axons stop between the epithelial and medulla glia, which provide a stop signal, while the R7 and R8 axons pass the marginal glia to project to their temporal layers in the medulla.

Apart from *gcm* and *repo*, which are expressed widely in glia in the early visual system, there are not many other markers to reveal the subtypes of glia. Instead, enhancer traps are used in order to identify the expression of different subtypes of glia in the optic

lobe and the eye imaginal disc. The carpet glia are known to express *moody* and *moody-Gal4* line can be used to drive their expression while the *c527-Gal4* reporter line is used for the visualization of the perineural glial cells. The wrapping glia are marked by *Mz97-GAL4* (Hummel *et al*., 2002; Silies *et al*., 2010).

Glia also exists in the adult visual system. Although the eye lacks them, three classes of glia are present in the lamina: surface, cortex, and neuropil glia. Each group has two subtypes which are: fenestrated, pseudocartridge, distal, proximal, epithelial and marginal glia, respectively. Most glial cells in the adult system cannot be matched to the ones at the larval stage except for a few. For example, the fenestrated glia are equivalent to perineural glia in the larva and the pseudocartridge glia are thought to be equivalent to subperineurial surface glia. These two groups are just below the retina and are involved in the formation of the blood-brain barrier. There are also many other types of glia which are functionally unknown and their expression patterns can only be predicted with the help of different enhancer trap lines (Figure 1.9) (Edwards *et al*., 2012). Details of neuron-glia interactions will be revealed to a great extent with the discovery of the roles of these new classes of glial cells in visual processing.

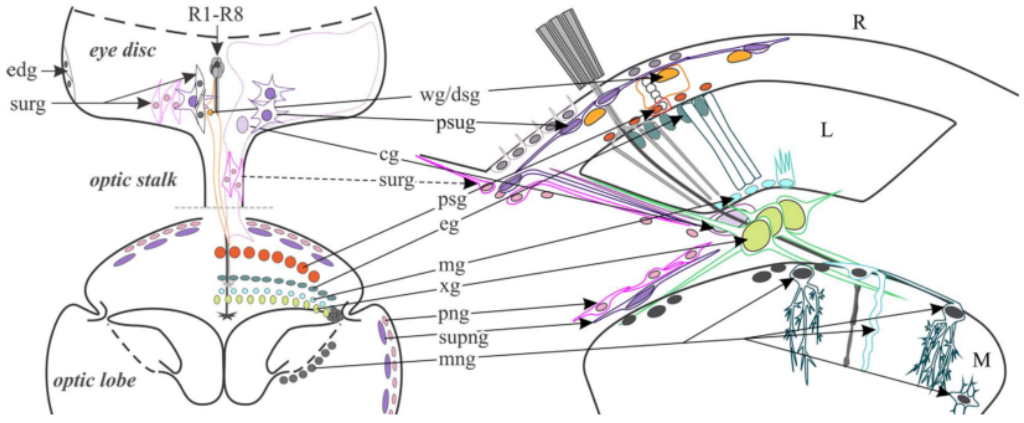

Figure 1.9. Glial subtypes and their fates in the *Drosophila* visual system. Some of the known ones are (perineurial, pink; subperineurial, shades of purple), cortex (distal satellite, orange; proximal satellite, red), neuropil (astrocyte-like, blue; ensheathing, light blue), and chiasm (green). Abbreviations: cg, carpet glia; edg, edging glia; mng, medulla neuropil glia; png, perineurial glia; surg, surface glia; wg, wrapping glia (Edwards *et al*., 2012).

1.2.3.3. Cell Adhesion Molecules (CAMs). CAM's are essential players in neuron-glia interactions. They have many functions such as axon guidance, targeting, synaptogenesis, and fasciculation. Some are expressed specifically in neurons, some are expressed in glial cells, and some are expressed in both (Silies and Klambt, 2011). They interact in homophilically or heterophilically. They do not always have attractive roles, but are also involved in the repulsion of the neurons in the process of guiding them to their correct targets (Figure 1.10).

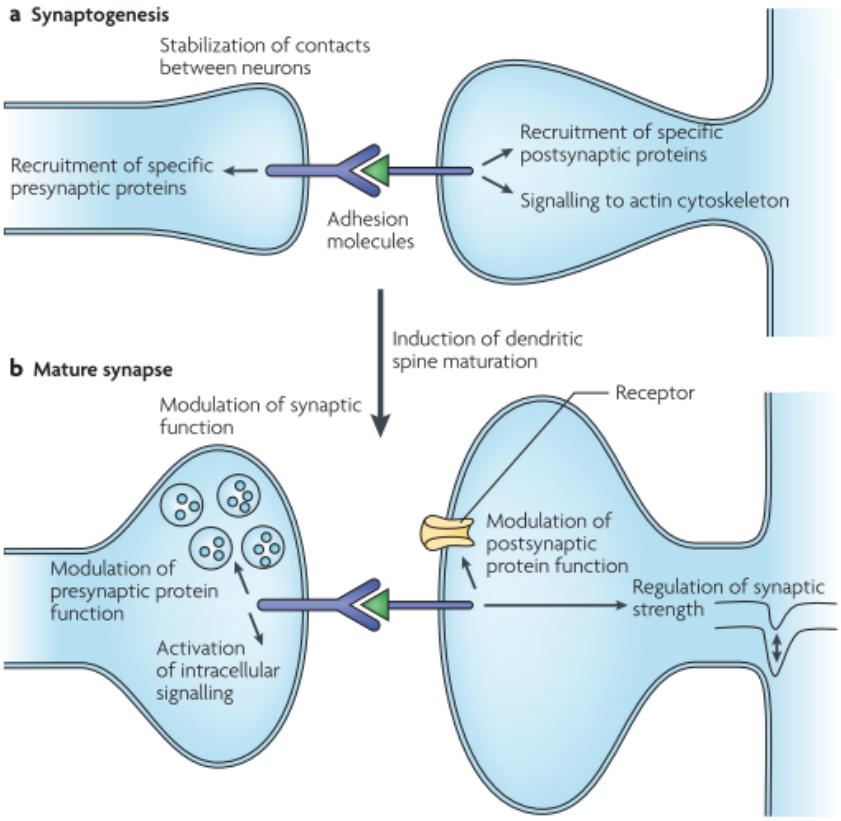

Figure 1.10. Role of CAMs in synaptogenesis and mature synapse. Synaptic adhesion molecules are essential in the formation of a synapse. They are involved in the stabilization of the first initial contact between axons and dendrites by recruiting specific pre-synaptic and post-synaptic proteins (Dalva *et al*., 2007).

There are a few major classes of CAMs. One of the biggest CAM families is cadherins. It's a large superfamily with 80 known members in mammals and 17 members

in *Drosophila*. The members of this family are usually found at synapses and are very active in the development of the nervous system. They have a tandemly repeated extracellular calcium-binding domain, which is called the cadherin motif or EC domain, allowing them to form homophilic interactions. They mediate homotypic interactions between presynaptic and postsynaptic cells, contributing to the specificity of axon targeting. There are three classic Cadherins in *Drosophila*: E-Cadherin, Neuronal (N)-Cadherin, and N-Cadherin2, but N-Cadherin has 9 isoforms due to alternative splicing. Both E-Cadherins and N-Cadherins are expressed in PRs and their targets in the lamina (Lee *et al*., 2001; Prakash *et al*., 2005). Another CAM is the family of presynaptic neurexins and postsynaptic neuroligins that also act in a calcium-dependent manner. Another class is Ephrins (Ephs) and ephrin-s. Ephs belong to the receptor tyrosine kinase family, which are divided in to classes A and B based on their affinity for ephrin-A and ephrin-B ligands. Both ephrin classes are membrane bound. The fourth class is the Immunoglobulin (Ig) superfamily which have variable numbers of globular extracellular cysteine-looped domains (Dalva *et al*., 2007). Many Ig family members were shown to have roles during synapse development. Down syndrome cell-adhesion molecule (Dscam) in *Drosophila* is a well- studied member of the Ig family. Dscam receptors are single-pass transmembrane proteins with characteristic Ig domains. Alternative splicing generates different Dscam isoforms with up to 38,016 different ectodomains. Dscam is important for neuronal wiring and it is suggested that its homophilic binding property allows the specificity and molecular recognition (Sanes and Zipursky, 2010; Schmucker, 2007).

1.3. Gal4-UAS System

The Gal4-UAS system in *Drosophila,* was first extensively described by Brand and Perrimon in 1993. Since then, this tool has been one of the most outstanding strengths of *Drosophila* as a model organism. Gal4 encodes for an 881 amino acid protein, which was initially identified in the yeast *Saccharomyces cerevisiae.* It binds to the DNA and activates the transcription of the target gene by binding to the 17 base pair (bp) site, which defines an Upstream Activating Sequence (UAS). The Gal4 and UAS elements are not endogenously expressed in *Drosophila*, however when ectopically expressed, the Gal4 element activates UAS in *Drosophila* as it does in yeast. In addition, their expression does

not lead to any phenotypic defect in *Drosophila*. These findings all lead to the elegant work of Brand and Perrimon describing the areas where the Gal4-UAS system can be used in *Drosophila* (Brand and Perrimon, 1993).

In this bipartite system, there are two components: the driver and the responder. These two are maintained in different parental lines, which gives the system its strength. The manipulations in genes leading to toxicity, lethality, or reduced viability can be controlled with temporal and spatial expressions. In addition, toxic effects or programmed cell deaths can also be induced locally by this system for targeted studies. Gal4 is not active on its own and is activated only when there is an enhancer in front of it. By using this feature, the enhancers, which do not have a known expression pattern but reside in front of a Gal4 element, can be characterized. By crossing these to reporter lines, which are usually UAS-galactosidase (UAS-lacZ) or UAS-Green Fluorescent Protein (UAS-GFP) the tissue and time the enhancer is active can be revealed. This also enables the study of genomic regions, which do not have a known function, and provides a starting point for revealing their role. The wide range of combinations which can be established with these drivers and reporters in addition to their commercial availability, makes *Drosophila* a very strong model for studying the effect of many genes in different tissues and time intervals (Duffy, 2002).

1.4. Enhancer Trap Screen

In order to identify novel genes, that are involved in a particular process of interest an enhancer-trap screen can be used as an unbiased approach. In an enhancer-trap screen, a Gal4 containing transposable element is directed to insert randomly to the genome. Then, these flies with the Gal4 element are crossed to flies carrying the UAS-reporter gene construct. The F1 generation carrying the enhancer-Gal4>UAS-reporter constructs are selected according to the activity of the enhancer (Brand and Perrimon, 1993). By screening the tissue of interest at a specific developmental stage, one can find novel genes and enhancer regions that are involved in the regulation of a pathway of interest (Figure 1.11). After Brand and Perrimon's initial screen, this method was developed and modified using different transposons which insert to different regions in the genome and variations

in the reporter (Duffy, 2002; Horn *et al*., 2003; Mollereau *et al*., 2000; Sepp and Auld, 1999).

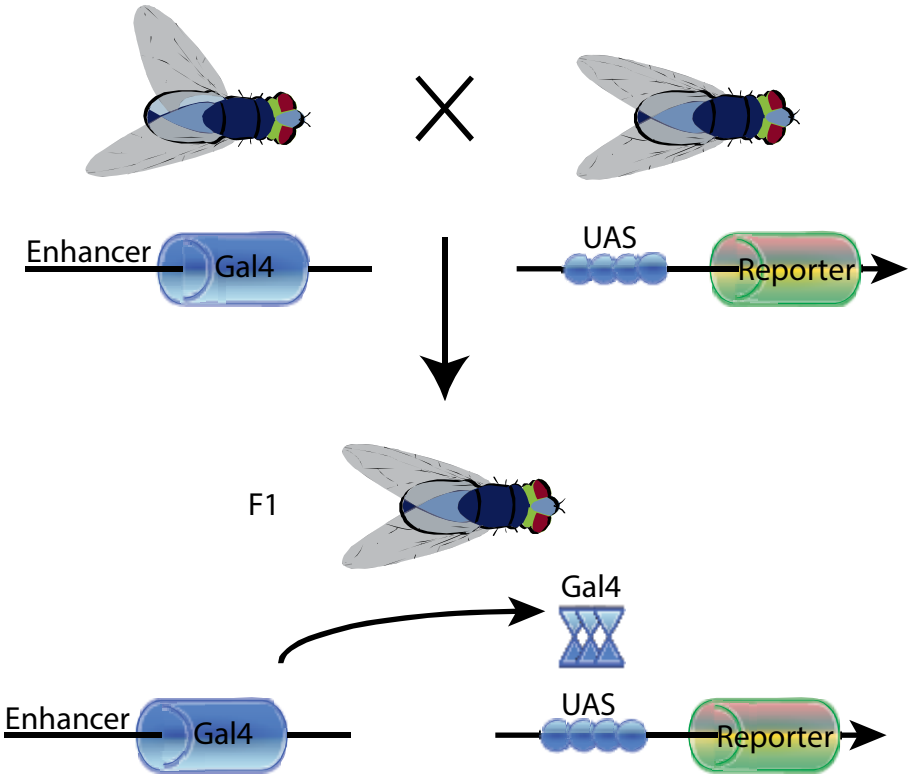

Figure 1.11. Enhancer Trap Screen. The Gal4 containing element is inserted into a random region in the genome. If there is an enhancer in that area, the Gal4 gets activated and binds to the UAS element, which drives the reporter.

2. AIM OF THE STUDY

The nervous system is the most complex structure in our body and its proper functioning relies on the correct specification of cells and the establishment of proper connections during development. The fly visual system represents an excellent model system because the mechanisms of specification and differentiation including axonal targeting to the brain are well studied.

Here, we identify an R8 cell specific gene, *unzipped*, which encodes a cell adhesion molecule, and we aim to investigate its function in visual system development. Its function as a CAM and its involvement in axonal projection makes it a strong candidate for PR differentiation and projection. As this gene has not been studied extensively and has not been investigated in the visual system, one of our major aims was to generate all the necessary tools to study its function.

The developmental expression pattern of *unzipped* will be analyzed by using enhancer-trap lines, generating tools to study the endogenous gene expression, and characterizing the mcherry-tagged fusion protein in transgenic flies.

Our major aims can be summarized as finding the function of Unzipped in the early specification of PRs, subtype specification, and axonal targeting of R8 cells based on the expression pattern of Unzipped.

3. MATERIALS AND METHODS

3.1. Biological Material

Unless stated otherwise, all fly stocks were kept in incubators with 80% humidity and a 12:12 day:night cycle at 25°C. Fly food (Nutri-FlyTM Bloomington Formulation) was obtained commercially and prepared every week with the addition of 4.8 ml of propionic acid per liter of fly food. *Drosophila melanogaster* lines used in the experiments are listed and described in Table 3.1.

Table 3.1. *Drosophila melanogaster* strains used throughout this study.

Name of line	Chr. No	Description
AC109-Gal4	III	Enhancer trap line with Gal4 insertion in the second intron of *CG14160*
AC783-Gal4	II	Enhancer trap line with Gal4 insertion in the first intron of *uzip*
CantonS		Wt
DGRC 104787	III	Enhancer trap line with Gal4 insertion in the 5'UTR region of uzip
Elav-Gal4	III	Expresses Gal4 in post-mitotic neurons under the control of *elav* enhancer
Gcm-Gal4	II	Expresses Gal4 in glial cells under the control of *gcm* enhancer
lGMR-Gal4	II	Expresses Gal4 in photoreceptor cells under the control of *lGMR* enhancer
lGMR-Gal4	III	Expresses Gal4 in photoreceptor cells under the control of *lGMR* enhancer
Moody-Gal4	II	Enhancer trap line with Gal4 insertion, used as carpet glia driver
Mz97-Gal4	II	Enhancer trap line with Gal4 insertion, used as wrapping glia driver
QB	I, II, III	Quadriple balancer, used for balancing flies
Repo-Gal4	II	Expresses Gal4 in all glial cells, except the midline glia, under the control of repo

Table 3.1. *Drosophila melanogaster* strains used throughout this study (cont.).

Rh3-LacZ	III	Expresses LacZ under the control of Rh3 promoter
Rh4-LacZ	III	Expresses LacZ under the control of Rh4 promoter
Rh5-LacZ	III	Expresses LacZ under the control of Rh5 promoter
Rh6-LacZ	III	Expresses LacZ under the control of Rh6 promoter
Senseless-Gal4	III	Expresses Gal4 under the control of *senseless* enhancer
UAS-CD8::GFP	III	Expresses mCD8-tagged GFP under the control of UAS sequences
UAS-GFP.nls	X	UAS fusion to cDNA of GFP with a nuclear localization signal
UAS-Uzip	II	UAS line with full length Uzip tagged with a cyano fluorescent protein (CFP)
UAS-Uzip-RNAi	II	Expresses double stranded RNAi of uzip under the control of UAS (VDRC KK line)
UAS-Uzip-RNAi	III	Expresses double stranded RNAi of uzip under the control of UAS (TRIP)
$Uzip^{D43}$	II	Null *Uzip* allele
$Uzip^{23}$	II	Hypomorphic *Uzip* allele
Uzip::mCherry	III	Uzip transgenic flies express mCherry tag
General Stocks		
y w	I	Yellow body color and white eye phenotype
w^{1118}	I	White eye phenotype
Balancers and Markers		
CyO	II	Balancer chromosome with curly wings
sp	II	Supernumerary bristles marker
TM2	III	Balancer chromosome with large halteres and/or with bristles on halteres
TM6B	III	Balancer chromosome with humeral and tubby markers

3.2. Chemicals and Supplies

Unless stated otherwise, all chemicals used in this study were purchased from Fisher Scientific, Sigma, Molecular Probes or Roche.

3.2.1. Chemical Supplies

Table 3.2. Chemicals

Chemical	Company
Acrylamide/bis-Acrylamide	Sigma Aldrich (A3574)
PageBlue Staining Solution	Thermo Scientific (24620)
NaCl	Sigma Aldrich (S7653)
Paraformaldehyde	Sigma Aldrich (A9647)
Protease Inhibitor Cocktail	Roche (11836153001)
Protein Ladder	Precision Plus Protein (161-0374)
Sodium Deoxycholate	Sigma (30970)
Tris	Sigma (T6066)
Triton X-100	AppliChem (A4975)
Tween 20	Sigma Aldrich (S36285-326)

3.2.2. Buffers and Solutions

Buffers and solutions used in this study is listed in Table 3.3.

Table 3.3. Buffers and solutions.

Buffer/Solution	Content
APS (10%)	1 g APS in 10 ml H_2O
BBT	1X PBS 0.1% BSA 0.1% Tween20
Blocking Solution	10% BSA in TBS-T
BNT	1X PBS 0.1% BSA 0.1% Tween20 250mM NaCl

Table 3.3. Buffers and solutions (cont.).

Buffer A (for DNA isolation)	100mM Tris (pH 7.5) 100mM EDTA 100mM NaCl 0.5% SDS H_2O
Buffer B (for protein purification)	7 M urea 0,1 M NaH2PO4 0,01 M Tris-Cl pH 8
Buffer C (for protein purification)	8 M urea 0,1 M NaH_2PO_4 0,01 M Tris-Cl pH 6,3
Buffer E (for protein purification)	8M urea 0,1 M NaH_2PO_4 0,01 M Tris-Cl pH 4,5
Coomassie Blue Stain	40% MetOH 10% Acetic acid 1 g/l Coomassie blue
Destain Solution	30% propanol 10% Acetic acid 60% dH_2O
Dough Solution	167 mM Tris-Cl (pH 6.8) 0.5 % SDS 10 % (w/v) sucrose 25 µl/ml beta-mercaptoethanol 0.01 %(w/v) bromophenol blue
DTT (1.5M)	4.635 g DTT 0.01M NaOAc (pH 5.2) In 20 ml ddH_2O
Fly Head Lysis Buffer	20 mM Tris-Cl pH 8.0 50 mM NaCl 1% NP-40 2 mM EDTA 1X Roche Protease Inhibitor Cocktail®
Grape Agar Premix	Genesee Scientific
Incomplete Adjuvant	Freund's Sigma (F-S506)

Table 3.3. Buffers and solutions (cont.).

Laemmli's Sample Buffer (3X)	50 mM Tris-Cl pH 7.5 2% SDS 10% Glycerol 0.1% Bromophenol blue 100 mM DTT
LumiGlo® Western Blotting Substrate	Cell Signaling, USA
Normal Goat Serum	Millipore, Germany
OCT medium	Tissue Tek
PAXDG	10 g BSA 3 g Sodium Deoxycholate 3 ml Triton X-100 50 ml Normal Goat Serum 100 ml 10X PBS in 1 L
PBS (1x)	137 mM NaCl 2.7 mM KCl 10 mM Na_2HPO_4 1.8 mM KH_2PO_4
PBT	0.2% Triton X-100 in 1X PBS
PBX3	0.3% Triton X-100 in 1X PBS
PBX5	0.5% Triton X-100 in 1X PBS
PFA (16%)	8 g paraformaldehyde in 50 ml 1 N NaOH until it dissolves completely
Reagent Diluent	1 % BSA in PBS pH 7.2-7.4 0.2 µm filtered (R&D System #DY995)
Running Buffer	25 mM Tris Base 190 mM Glycine 0.1% SDS pH adjusted to 8.3 with HCl
SDS (20%)	20 g SDS in 100 ml
Stop Solution	2 N H2SO4 (R&D System #DY994)

Table 3.3. Buffers and solutions (cont.).

Strip Buffer	50mM KH_2PO_4 (pH 7.5) 0.3M NaCl 100mM EDTA (pH 8) in dH_2O
Substrate Solution	1:1 mixture of Color Reagent A (H_2O_2) and Color Reagent B (Tetramethylbenzidine) (R&D System #DY999)
TBS-T	20 mM Tris Base 150 mM NaCl 0.1% Tween-20 pH adjusted to 7.6 with HCl
Transfer Buffer	25 mM Tris Base 190 mM Glycine 20% Ethanol/Methanol
Tris-HCl (pH 6.8, pH 8.8, 1M)	121.1 g Tris base in 1L Adjust pH with HCl
Urea Lysis Buffer (8M)	10 mM NaH NaH NaH_2PO_4 10 mM Tris-HCl (pH 8) 10 mM Imidazole 8M Urea 10 mM 2-mercaptoethanol 0.5% NP40
Wash Buffer	0.05% Tween 20 in PBS pH 7.2-7.4 (R&D System #WA126)

3.2.3. Antibodies

Antibodies used throughout Western blot experiments are listed in Table 3.4. Antibodies used during immunohistochemistry experiments are listed in Table 3.5.

Table 3.4. Antibodies used in the Western blotting experiments.

Name	Antigen	Species	Dilution	Source
Primary Antibodies				
Anti-Uzip	Uzip	Mouse	1:100	from Huang group
Anti-Uzip	Uzip	Rabbit	1:200	from Huang group
Anti-Uzip	Uzip	Rabbit	1:10000	generated in our lab
Anti-His	His	Mouse	1:1000	Genscript
Secondary Antibodies				
Anti-mouse IgG, HRP linked	IgG	Mouse	1:1000	Cell Signalling (Nr.7076)
Anti-rabbit IgG, HRP linked	IgG	Rabbit	1:1000	Cell Signalling (Nr.7074)

Table 3.5. Antibodies used in the immunohistochemistry experiments.

Name	Antigen	Species	Dilution	Source
Primary Antibodies				
Anti-βGal	β-galactosidase	Rabbit	1:1000	Cappel
Anti-Chp	Chaoptin	Mouse	1:20	DSHB (24B10)
Anti-dsRed	mCherry	Rabbit	1:5000	
Anti-Elav	Elav	Rat	1:50	DSHB
Anti-NCad	N-Cadherin	Rat	1:20	DSHB
Anti-Pros	Prospero	Mouse	1:10	DSHB
Anti-Repo	Repo	Mouse	1:20	DSHB
Anti-Rh5	Rh5	Mouse	1:50	DSHB
Anti-Rh6	Rh6	Rabbit	1:100	DSHB
Anti-Uzip	Unzipped	Mouse	1:10	from Huang group
Anti-Uzip	Unzipped	Rat	1:20	from Huang group
Anti-Uzip	Unzipped	Rabbit	1:1000	generated in our lab
Secondary Antibodies				
Alexa 488	Mouse	Goat	1:800	Invitrogen
Alexa 488	Rabbit	Goat	1:800	Invitrogen
Alexa 546	Rat	Goat	1:800	Invitrogen
Alexa 555	Mouse	Goat	1:800	Invitrogen
Alexa 647	Rat	Donkey	1:800	Invitrogen
Alexa 647	Mouse	Goat	1:500	Invitrogen

3.2.4. Disposable Labware

Table 3.6. Disposable labware used during this study.

Name of product	Provider
Filters	Millipore
Filter Tips	Greiner Bio-One, Belgium
Microscope cover glass	Fisher Scientific, UK
Microscope slides	Thermo Scientific, UK
Petri Dish	Greiner Bio-One, Belgium
Pipette Tips	VWR, USA
Plastic Cover Slips	Rinzle (72261-50)
Test Tubes, 0.5 ml	Citotest Labware Manufacturing, China
Test Tubes, 1.5 ml	Citotest Labware Manufacturing, China
Test Tubes, 2 ml	Citotest Labware Manufacturing, China
Test Tubes, 15 ml	Becton, Dickinson and Company, USA
Test Tubes, 50 ml	Becton, Dickinson and Company, USA
Syringe (1 cc)	Becton, Dickinson and Company, USA

3.2.5. Equipment

Table 3.7. Equipment used during this study.

Name of equipment	Provider
Autoclave	Astell Scientific Ltd., UK
Centrifuges	Eppendorf, Germany (Centrifuge 5424, 5417R)
Cold Room	Birikim Elektrik Soğutma, Turkey
Confocal Microscope	Leica Microsystems, USA (TCS SP5)
Cryostat	Leica CM3050 S-USA
Electrophoresis Equipment	Bio-Rad Labs, USA (ReadySub-Cell GT Cells)
Environmental Test Chamber	Sanyo, Japan (MLR 351H)
Freezers	Arçelik, Turkey
Fluorescence Stereomicroscope	Leica Microsystems, USA (MZ16FA)
Heating Block	Fisher Scientific, France (Dry-bath incubator)
Heating magnetic stirrer	IKA, China (RCT Basic)
Homogenizer	Kontes, USA (749540-0000)

Table 3.7. Equipment used during this study (cont.).

Incubator	Weiss Gallenkamp, USA (Incubator Plus Series)
Inverted Microscope	Zeiss, USA (Axio Observer, Z1)
Laboratory Bottles	Isolab, Germany
Micropipettes	Eppendorf, Germany
Microplate Reader	Versa Max, USA
Microwave oven	Vestel, Turkey
Spectrophotometer	NanoDrop (ND-1000 NanoDrop-USA)
pH meter	WTW, Germany (Ph330i)
PVDF Membrane Visualization	Stella, Raytest, Germany
Refrigerators	Arçelik, Turkey
SDS-PAGE Electrophoresis System	Bio-Rad Labs, USA (Mini PROTEAN® Tetra Cell)
SDS-PAGE Transfer System	Bio-Rad Labs, USA (Mini Trans-Blot® Electrophoretic Transfer Cell)
Stereo Microscope	Olympus, USA (SZ61)
Vortex Mixer	Scientific Industries, USA (Vortex Genie2)

3.2.6. Oligonucleotide Primers

Primers used for cloning and sequencing can be found in Table 3.8.

Table 3.8. Primers used for inverse PCR.

Primer Name	**Primer Sequence (5'→3')**
AC-19	CTTGACCTTGCCACAGAGGACTATTAGAGG
AC-20	CAGTGACACTTACCGCATTGACAAGCACGC
AC-37	GGTCAACTTCAAAGTCCACGAG
AC-38	CGGCGACTGAGATGTCCTAAATG
F1	CCAGTTCCGAGTATCACAGCCAGATG
F2	CTAACGTGCAGCCAGGAATTATCG
F3	GGGCACGTTCGACCTAARAAG
R1	GCACCCAGAAAGAACGGCAACAATCG
R2	GTCAGATATGCAGGGGACGTTC
R3	CCGAGCTGTTGCTCTCCATTTTGGGCC

3.3. Biochemical Methods

3.3.1. Protein Extraction

Protein extraction experiments were carried on with young adult flies by extracting total protein from wt and *Uzip*^{D43} fly heads. 15 fly heads from each genotype were homogenized in 60 µl lysis buffer using a homogenizer. The mixture was kept on ice for 30 min to let tissues completely dissolve in the buffer. The protein extract was centrifuged at 4°C at 10000 rpm for 10 min. Without disturbing the pellet of tissue debris, which contains the cuticle and the hard tissue that can not be lysed, and the lipid rich upper layer; 50 µl of the supernatant was transferred into a clean tube. 25 µl of 3X Laemmli's buffer was added to the supernatant. In order to denature the proteins and reduce their disulfide bonds, samples were heated at 99°C for 5 min before loading onto the gel.

3.3.2. SDS-PAGE

Polyacrylamide gel was prepared in standard way. In order to be able to observe smaller proteins easier, a 15% gel was preferred. 4 µl of a ready-to-use protein ladder (Roche) and 20 µl of protein extract were loaded. The gel was run in 1X running buffer under 30 mA constant current. Table 3.9 shows the amount of solutions and chemicals used for SDS-PAGE gel preparation.

Table 3.9. SDS-PAGE gel preparation.

Gel components	Resolving gel, 5 ml	Stacking gel, 3 ml
ddH_2O	550 µl	2.175 ml
Tris-Cl	1.875 ml (pH 8.8)	375 µl (pH 6.8)
Acrylamide-Bisacrylamide 29%-1%	2.5 ml	397.5 µl
SDS 20%	25 µl	15 µl
APS 10%	50 µl	30 µl
TEMED	2 µl	7.5 µl

3.3.3. Coomassie Blue Staining

4 µl of ready-to-use protein ladder and 20 µl of protein extract were loaded to the SDS-PAGE gel. The gel was run in 1X running buffer under 30 mA constant current. Then it was stained with Coomassie Blue staining solution for 15 min. As the following step it was rinsed and washed with destain solution. The protein bands were observed.

3.3.4. Western Blotting

Activation of the PVDF membrane was done in methanol for 1 min and it was stabilized in 1X transfer buffer. Transfer to the PVDF membrane was performed in cold 1X transfer buffer under 200 mA constant current for 2 hours. Then the membrane was washed with TBS-T and blocked in 10% BSA dissolved in TBS-T for 1 hour at room temperature while shaking. The primary antibody was dissolved in 5% BSA (in dilutions stated in (Table 3.5) in TBS-T. The membrane was incubated with the primary antibody solution overnight at 4°C while shaking. The following day unbound and non-specifically bound antibodies were removed by washing 3 times with TBS-T for 10 min. HRP coupled secondary antibody (host species stated in Table 3.5) was dissolved in 5% BSA at a dilution of 1:1000 and incubated with the membrane at room temperature for 2 hours. As previously, three washing steps were performed. The membrane was incubated with HRP revealing kit 20X LumiGlo® diluted to 1X in ddH_2O for 3 min. The Stella documentation system was used to record the chemiluminescent signal. Images were processed with Adobe Photoshop.

3.4. Histological Methods

3.4.1. Antibody Preabsorbtion

3.4.1.1. Embryo Fixation. Grape agar plates were prepared by using Grape Agar Premix left overnight to dry. Young adults were collected and transferred into an embryo

collection chamber. Then the embryo collection chamber was placed onto Grape agar plate and yeast extract was added before the adults were placed in the chamber. The system was incubated at 25^{o}C for maximum 16 hours. In the next step, adult flies were removed and the chamber was separated from the agar plate. Remains from the agar were washed out with H_2O. In order to dechorionate embryos, the chamber was dipped into 50% bleach solution for 2-3 minutes. After a second washing step, embryos were left to dry a while. In the following step, embryos were shaken for 20-30 minutes in heptane and 4% formaldehyde (1:1) solution. The lower phase of the solution was removed. After adding 1 ml of heptane and 1-3 ml of methanol to the solution, it was shaken vigorously. Then the embryos were left to settle and the supernatant was removed. After washing 2-3 times with methanol, the embryos were stored at -20^{o}C.

3.4.1.2. Embryo Preabsorption of Antibodies. Embryos were transferred to an Eppendorf tube and the methanol was removed. They were washed with BBT four times for 20 minutes. The antibody was diluted 1:100 in BBT with the embryos and left to rotate overnight at 4oC. After embryos settled, the supernatant was transferred into a fresh tube and stored at 4oC.

3.4.2. Preparation of *Drosophila* Tissues for Immunohistochemistry

3.4.2.1. Preparation of Larval Eye Imaginal Discs. 3rd instar larvae were dipped into ice-cold PBS. A hole was pinched on the body with the forceps just below the third-most anterior segment. Next, pulling from the mouth hook by one pair of forceps and from the body with the other, the eye-antennal disc attached to the brain was pulled out and transferred into cold PBS.

3.4.2.2. Preparation of Pupal Eye Discs. Pupae of the desired stage were carefully removed from the vials and transferred into 4% PFA on a silicon plate. The operculum was grabbed carefully and the pupal case was removed. A little hole was pinched into the anterior side and enlarged carefully to take out the eye-brain complex and the tissue was transferred into fresh 4% PFA. Then the retina was removed carefully from the eye-brain complex. The dissection procedure should not take longer than 30 min to avoid tissue degradation.

3.4.2.3. Preparation of Adult Brains. Selected flies were anesthetized with CO_2 and dipped into 70% ethanol in a glass dish. They were washed 3 times with PBS and dissection was carried on a silicon plate in a drop of ice-cold PBS. First, the proboscis was removed. Then, the hole that the proboscis has left was used to grab and remove the head exoskeleton. The brain was detached from the head. The residual trachea was cleaned, and the brain was placed into ice-cold PBS.

3.4.2.4. Preparation of Adult Retinas. Selected flies were anesthetized with CO_2 and their heads were cut off and placed in ice-cold PBS on the dissection pad. Gently, proboscis was pulled out and by entering through the hole in the base of the head the head was cut into two halves. The brain and cuticles were removed gently to ease access to the retina. Then, the circle of tissue at the base of the retina was removed. After fixation with 4% PFA, the lamina tissue attached to the retina was removed and the washing steps were performed as written in the protocol. The dissection procedure should not take longer than 30 min to avoid tissue degradation.

3.4.2.5. Preparation of Adult Eye Sections. Adult fly heads were cut off on CO_2 pads and immediately put in OCT-filled rubber molds. After embedding the heads into the molds and the air bubbles were cleaned, the molds were put into the -80ºC freezer for 15 minutes. Then, within one hour the frozen blocks were sectioned in 12 μm slices at -20ºC using a cryostat. The sections were picked up using positively-charged slides and stored at -20ºC till the end of the sectioning. Once all the sections were taken, they were dried on the slides for 5 minutes at RT and then for 2 hours at 65ºC.

3.4.3. Immunohistochemistry

3.4.3.1. Immunohistochemical Stainings of Larval Imaginal Discs. Tissues were fixed in 4% PFA in PBS for 20 minutes at room temperature while shaking at 100 rpm. Then, tissues were washed three times for 10 minutes with PBX3. For blocking, tissues were incubated in BNT solution for one hour at room temperature. After blocking, tissues were incubated in primary antibody solution overnight at 4°C while shaking at 100 rpm. Primary antibodies were diluted in BNT in dilutions listed in Table 3.4. Tissues were washed three

times for 10 min with PBX3 and then, incubated in secondary antibody solution prepared in BNT in dilutions listed in Table 3.4 for 2 hours at room temperature while shaking at 100 rpm. Then, they were washed 3 times with PBX3 for 10 minutes and mounted in Vectashield embedding medium, and stored at 4°C in dark. The samples were visualized using confocal microscopy.

3.4.3.2. Immunohistochemical Stainings of Pupal Eye Discs. Tissues were fixed in 4% PFA in PBS for 20 minutes at room temperature while shaking at 100 rpm and then washed three times for 10 minutes with PBX3. Then, tissues were blocked in 1:10 goat serum in BNT for 20 min at room temperature. Primary antibodies were diluted in BNT in dilutions listed in Table 3.4 and tissues were incubated in primary antibody solution overnight at 4°C while shaking at 100 rpm. After that, tissues were washed three times for 10 min with PBX3. Then, tissues were incubated in secondary antibody solution prepared with BNT in dilutions listed in Table 3.4 for 2 h at room temperature while shaking at 100 rpm. After three washes for 10 min with PBX3, tissues were mounted in Vectashield embedding medium, and stored at 4°C in the dark. Finally, samples were visualized using confocal microscopy.

3.4.3.3. Immunohistochemical Stainings of Wholemount Adult Brains. Tissues were fixed in 4% PFA in PBS for 30 minutes at room temperature while shaking at 100 rpm. Then, they were washed three times for 15 minutes with PBX3 and blocked in PAXDG for 2 h at room temperature. Primary antibodies were diluted in PAXDG and tissues were incubated in primary antibody solution overnight at 4°C while shaking at 100 rpm. After three washes for 15 min with PBX3, tissues were incubated in secondary antibody solution prepared in PAXDG for 2 h at room temperature while shaking at 100 rpm at dark. After the incubation in secondary antibody solution, tissues were washed three times for 15 min with PBX3. Then, they were mounted in Vectashield embedding medium, and stored at 4°C in dark. Finally, the samples were visualized using confocal microscopy.

3.4.3.4. Immunohistochemical Stainings of Wholemount Adult Retinas. Tissues were fixed in 4% PFA in PBS for 15 min at room temperature. After removing the lamina of retinas, tissues were washed three times for 30 minutes with PBX5. For blocking, tissues were incubated in 10% normal goat serum in BNT for 1 h at room temperature. Afterwards,

primary antibodies were diluted in PAXDG and tissues were incubated in primary antibody solution for two nights at 4°C while shaking at 100 rpm. Then, tissues were rinsed quickly two times with PBX5 and washed three times for 10 minutes with PBX5. Tissues were then washed once with 4% PFA for 5 min. After that, they were washed three times for 10 minutes with PBX5. Then, they were incubated in secondary antibody solution prepared with BNT for 2 h at room temperature while shaking at 100 rpm. After the incubation, tissues were rinsed quickly two times with PBX5 and washed three times with PBX5 for 10 min. White-eyed retinas were mounted immediately, but red-eyed retinas washed with PBX5 for 2 more days at 4°C before mounting. Finally, the samples were visualized using confocal microscopy.

3.4.3.5. Immunohistochemical Stainings of Adult Eye Sections. Sections were fixed for 15 minutes at RT by using 4% paraformaldehyde (diluted in PBS). Then, the slides were washed for three times with PBX3 for 15 min. For blocking, slides were incubated in BNT for 1 hour at RT. Then, 40-50 µl of primary antibody diluted in BNT was added onto each slide. Plastic coverslips were used to cover the slides and they were left in humidity chamber overnight at 4ºC. After that, slides were rinsed for three times with PBX3 for 10 minutes and incubated for 2 hours in the dark with the secondary antibody solution prepared in BNT. Finally, the slides were washed for three times with PBX3 for 10 minutes.

3.5. Antibody Generation

3.5.1. Protein Expression and IPTG Induction

3.5.1.1. For Growth Curve Testing. For growth curve testing, a strike of glycerol stock was taken by using a filter tip and placed into 5 ml LB with antibiotic solution. Then, it was put on a shaker and left overnight at 37ºC. After that, 500 µl of the solution was taken and added to 50 ml of LB Broth medium with antibiotic solution. A 1 ml sample was taken every hour. 3 hours later 1 mM IPTG was dissolved in dH_2O added to the rest of the culture. Every hour, a 1 ml sample was taken and centrifuged. The supernatants were discarded and the sample was put at - 20ºC. This procedure was continued for 4 hours.

After centrifuging the rest, the supernatant was removed and put at -20ºC. 100 µl of 10% TCA was added to each pellet. The tubes were vortexed and left on ice for 10 minutes. After that, they were centrifuged for 1 minute at maximum speed in a tabletop centrifuge. TCA was removed as much as possible using a micropipette. This step was followed by the addition of 1 ml of acetone and centrifugation for 1 minute at maximum speed. Then, the supernatant was discarded, a quick spin down was performed and the remaining acetone was removed. For a complete evaporation of the acetone, the Eppendorf was left at 65ºC with an open lid for 2 minutes. Afterwards, 100 µl of dough solution was added and boiled at 95ºC for 2 minutes to make the sample ready to load to a SDS-Page gel.

3.5.1.2. For Denaturing Conditions. As a first step, a strike of glycerol was taken with a filter tip and put into 5 ml LB with antibiotic solution. It was placed onto a shaker and left overnight at 37ºC. Then, 1 ml of solution was added to 250 ml Terrific Broth with antibiotic solution. 2 hours later, the OD was checked and this was repeated every 30 minutes. When the OD reached 1, 1 mM IPTG dissolved in dH_2O was added to the rest of the culture. After 4 hours, the bacteria were centrifuged at 7500 rpm at 4ºC for 15 minutes and the supernatant was removed.

3.5.2. His-tagged protein purification with Ni-NTA cartridges

3.5.2.1. Preparation of the Ni-NTA Cartridge. In order to purify the His-tagged protein, Ni-NTA cartridges were used. First, the column was cleaned by adding several solutions in the following order: 10 ml dH_2O, 2-3 ml 0,1 M NaOH, 30 ml dH_2O (pH should be at most 9), 10 ml 70% EtOH, 10 ml dH_2O. Then, 10 ml strip buffer was added to remove all chemical traces like previous proteins and Ni, which may be left from previous experiments. After stripping, 20 ml dH_2O was passed through the column. In order to coat the column with Ni, $NiSO_4$ solution was passed through the column for 10 minutes as a loop. Then, 10-20 ml dH_2O was added and finally 5 ml of buffer B was passed through the column for equilibration.

3.5.2.2. Protein Purification with Ni-NTA Cartridges. In order to purify the protein, the pellet was dissolved in a mixture of Buffer B and 3µl Dnase (3000 unit/ml). Then, it was

put onto a shaker for 15 minutes at RT and then centrifuged at 16000 g at 4ºC for 30 minutes. After centrifuging, the supernatant was collected and loaded to the column. 5 ml of Buffer B and 15 ml of Buffer C was passed through the column, respectively. Finally, Buffer E was added to the column and 20 ml of the protein was eluted.

3.5.3. Ammonium Persulfate Precipitation

Ammonium persulfate precipitation was used at two different steps. The first step was when increasing the concentration of the Uzip protein for injection to get rid of the low pH solution and urea before injection. The second step was when increasing the antibody concentration after isolating the serum from Uzip protein-injected rabbits. For the second step 40 ml blood was taken from the rabbit after sacrification. The blood sample was centrifuged at 4500 rpm and the serum was extracted. After centrifugation, 20 ml of serum was obtained and added to 12 ml ammonium persulfate (saturated pH 6.8) and put into a dialysis membrane, which was placed into cold PBS in a graded cylinder. After overnight dialysis at 4ºC, the precipitate in the dialysis membrane was diluted by adding 1:30 PBS. Then, 300-500 ml PBS was added to the graded cylinder. Every 1-2 hours, PBS in the graded cylinder was replaced with fresh PBS solution (for 3 times). Finally, the precipitate in the dialysis membrane was collected and diluted in 10 ml PBS.

3.5.4. Injection

For the injection process, 100 µg of protein was taken (at least 100 µl, at most 200 µl per animal) and mixed with complete adjuvant complex in a ratio of 1:1 for the first injection. The solution was taken up into a 2 ml insulin syringe while avoiding air bubbles and taken to the Vivarium (Boğaziçi University animal facility) where injection was performed. The following injections were performed by mixing 100µg protein with incomplete adjuvant complex in a ratio of 1:1. Two New Zealand rabbits at the age of 1 were used for injection and the injection was repeated 6 times with 15 day intervals.

3.5.5. ELISA

In order to prepare the plates, the Uzip protein extracted previously was diluted in PBS. Then different dilutions of 100 µl of the protein were loaded into each well of the 96-well plate. The plate was sealed and incubated overnight. After the incubation, the plate was aspirated and washed with 400 µl wash buffer for three times. Blocking of the protein added wells was performed by adding 200 µl BSA (1% in PBS), and incubating the plate for one hour at RT. Then washing was performed for three times by using wash buffer.

After the plate was ready, 1 ml blood sample was taken from the ear of the rabbit. The sample was centrifuged in a tabletop centrifuge for 2 minutes at 13000 rpm. After centrifugation, the serum was collected and diluted in reagent diluent in concentrations of 1/100, 1/500, and 1/1000. 100 µl of the diluted serum was added to each well. After incubation the wells were washed for 3 times with wash buffer. Then, rabbit HRP secondary antibody (1/1000 diluted in reagent diluent) was added to the plate and incubated 1 hour in the dark. After incubation, washing was done using washing buffer for 3 times. Then, 50 µl reagent substrate was added to each well. After 20 minutes, the stop solution was added to end the reaction and the results were analyzed in the plate reader.

3.5.6. Antibody Purification

In order to purify the antibody, a NHS-activated agarose dry resin column was used. First, the column was washed with isopropanol and activated by using 1mM HCl. Then, the protein was loaded to the column and left for 2 hours at RT. Afterwards, the column was washed with 6 ml PBS. Then, the column was treated with 5 ml of 1M Tris (pH 7.4) for 15 minutes at RT. After washing the column with 3 ml PBS, the column was treated with 5 ml 1M Tris (pH 7.4) for 15 minutes at RT and the buffer was allowed to pass from the column. Then, the washing step was repeated with 15 ml PBS. After that, 10 ml serum was passed through the column twice to bind to the protein-coated column. Then 20 ml PBS was passed through the column for washing and finally the antibody was eluted in 10 ml 1X PBS.

3.6. Molecular Biological Techniques

3.6.1. Isolation of Genomic DNA

15 flies were homogenized with the help of a homogenizer in 200 µl Buffer A and incubated at 65°C for 30 minutes. 114 µl of 6M LiCl and 286 µl of 5M KoAc were added in homogenized solution and tubes were incubated on ice for 10 minutes. Then tubes were centrifuged at 14000 rpm for 15 minutes. The DNA was extracted from supernatant by using 600 µl phenol:chloroform (1:1) and precipitated by 0.7 volume of isopropanol. After centrifugation at 14000 rpm for 15 minutes at room temperature, the pellet was washed with 70% ethanol. The pellet was left to air dry and dissolved in 75 µl dH_2O.

3.6.2. Restriction Digestion of DNA

5 µl of genomic DNA were digested with 10 units of TaqI at 65°C for 3 hours.

3.6.3. Ligation

Ligation was performed with 10 µl of the digested DNA in a total volume of 400 µl, using 2 µl of T4 DNA ligase at 16°C overnight in the presence of 40 µl T4 DNA ligase buffer (10x). In the next step, 40 µl 5M NaOAc and 1100 µl 100% ethanol were added into the tubes and the samples were incubated at -20°C for one hour. Centrifugation was performed for precipitating DNA at 14000rpm for 15 minutes at 4°C. The pellet was washed with 70% ethanol and the solution was centrifuged again at 14000 rpm for 10 minutes at 4°C. In the final step, the pellet was airdried and resuspended in 65 µl of distilled water.

3.6.4. Inverse PCR

The inverse PCR is composed of two consequent PCR reactions. In the first reaction, 15 µl of DNA from the ligation step was used as a template. In a total volume of

50 µl, the reaction ingredients were; 10 mM of dNTP, 5U of Taq polymerase, 1x Roche Taq polymerase buffer and 20 mM of each primer AC-19 and AC-20 listed in Table 3.7. The reaction conditions were: 5' 95^0C, (30'' 95^0C, 1' 62^0C, 2' 72^0C) X 40, 7' 72^0C. For the second PCR reaction, 2 µl of the PCR product from the first reaction was used as a template. 6 reaction with 6 different sets of primers were prepared: AC38-F1, AC38-F2, AC38-F3; and AC37-R1, AC37-R2, AC37-R3 listed in Table 3.7. The ingredients were the same as the first reaction except for primers and the reaction cysles. The reaction conditions were: 5' 95^0C, (30'' 95^0C, 1' 61^0C, 2' 72^0C) X 35, 7' 72^0C. PCR products of both reactions were run on a %1 agarose gel.

3.7. Fly Crossing Schemes

The flies with the correct genotype for the projection analysis were generated in a few crosses. The crosses set for the analysis of knockout mutants (Figure 3.1), downregulation experiments (Figure 3.2), and misexpression experiments (Figure 3.3) are seen in the following figures.

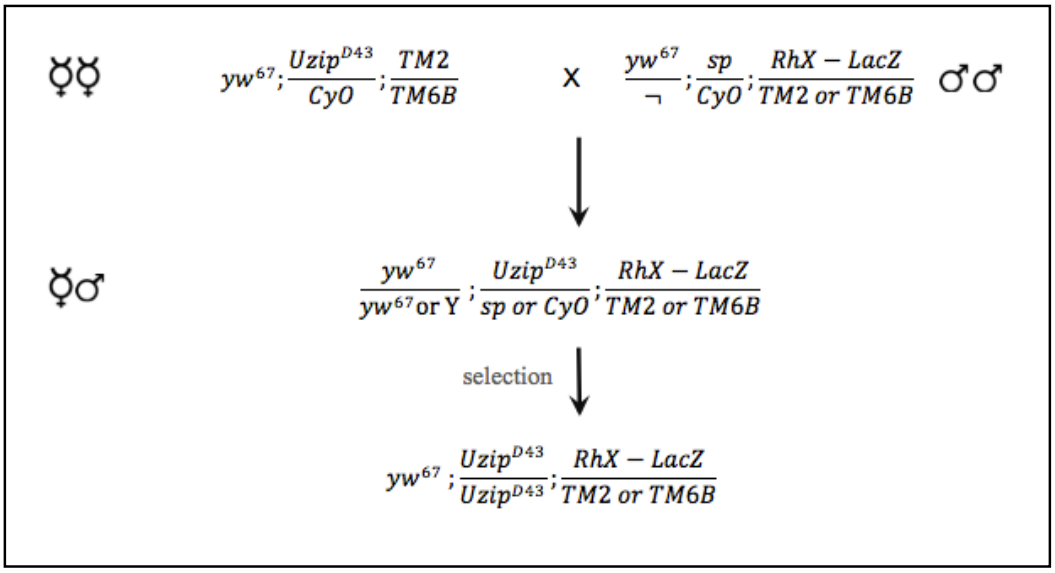

Figure 3.1. Cross schemes set up for the projection analysis of Uzip knockout mutants. The null mutants were crossed with Rh3-lacZ, Rh4-lacZ, Rh5-lacZ and Rh6-lacZ flies. Then the desired alleles were selected and the homozygous null mutant flies were selected for dissection.

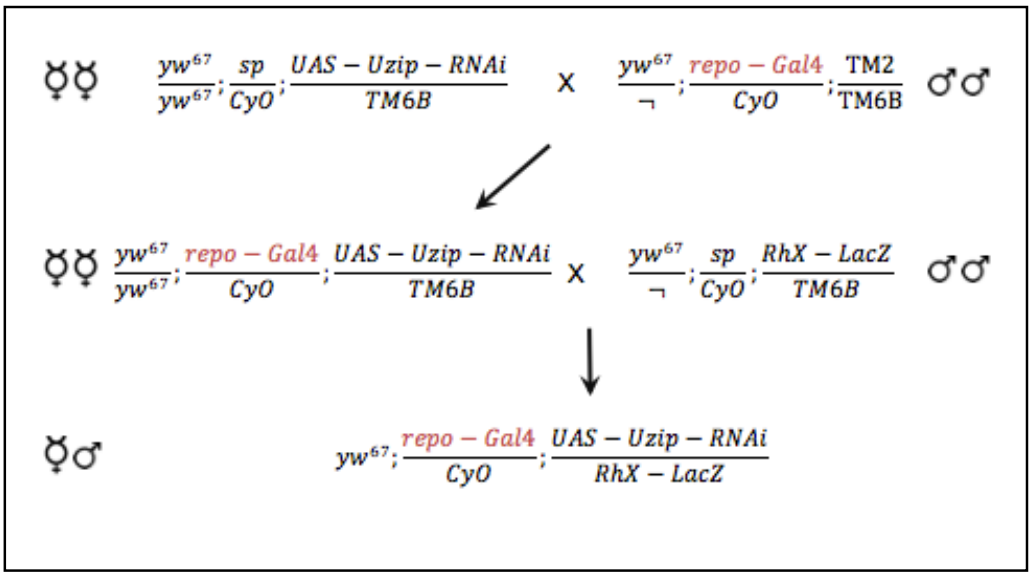

Figure 3.2. Cross scheme set up for the projection analysis of Uzip downregulation. The Uzip-RNAi lines were crossed with the appropriate driver lines represented with repo-Gal4 in the scheme. Then the desired alleles were selected and crossed with the Rh5-lacZ and Rh6-lacZ lines. The flies containing the driver, UAS-RNAi reporter, and the RhX-lacZ line were selected from the progeny and stained.

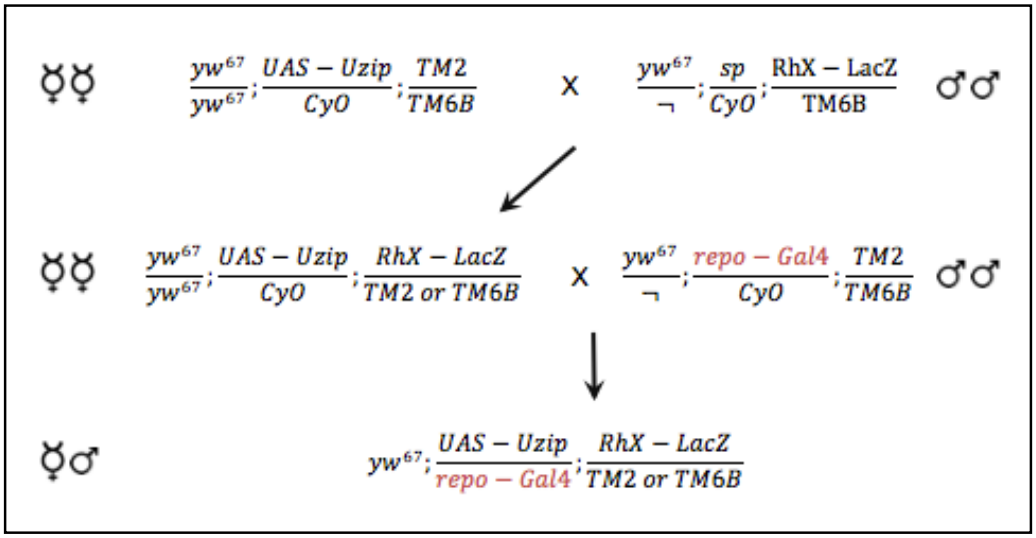

Figure 3.3. Cross scheme set up for the projection analysis of Uzip misexpressing flies. The UAS-Uzip lines were crossed with the Rh5-lacZ and Rh6-lacZ lines. Then the desired line was chosen and crossed with the appropriate driver lines represented by repo-Gal4 in the scheme. The flies containing the driver, UAS-Uzip line, and the RhX-lacZ line were selected from the progeny and stained.

4. RESULTS

4.1. Enhancer-Trap Screen for R8 Specific Lines

Enhancer-trap screens in flies have been established as early as 1993 by the pivotal work of Brand and Perrimon and many screens were made based on the P-element transposon (Brand and Perrimon, 1993). However, all those screens did not result in the saturation of the genome with P-element insertions. This is due to the fact that P-element favor exons rather than introns for insertion and thus results in many hotspots of insertion (Ryder and Russell, 2003). The piggyBac element transposon, a more recently used transposable element, has a different insertional specificity favoring more intronic regions when compared to P-elements (Hacker *et al.*, 2003).

A piggyBac based enhancer-trap screen was performed previously in order to identify novel genes that might be involved in photoreceptor specification, differentiation, and projection. The enhancer-trap fly lines were crossed with UAS-GFP flies and screened at the pupal stage for expression in the eye (Çelik and Desplan, unpublished data). The candidates were then analyzed further for any R8-specific expression starting from the 3rd instar stage, since PR specification starts at this stage. Immunostainings were performed with the candidate lines and four of them were found to be R8-specific at the 3rd instar larva stage: AC109, AC783, AC1000, and AC1012 (Arzu Öztürk, 2010). Using the inverse PCR method, the insertion site for R8-specific AC109 was mapped to *CG14160,* and AC1000 and AC1012 mapped to slightly different sites upstream of the gene *capricious* (Çelik and Desplan, unpublished data); (Arzu Öztürk, 2010). While the R8-specific line AC783 was mapped to the first intron of the gene *unzipped*, its exact localization could not be determined (Arzu Öztürk, 2010).

In the interest of finding novel candidates for photoreceptor differentiation with a specific focus on R8 regulation the insertion sites of these enhancer-trap lines, their expression patterns during developmental stages, and the potential role of the associated genes were further analyzed. *Capricious*, for which a role in photoreceptor differentiation

and axonal guidance of photoreceptor subtypes has been determined previously was excluded from this study (Morey *et al*., 2008).

4.1.1. The Expression Pattern of AC109 and CG14160

In the enhancer-trap line AC109, the piggyBac element had inserted into the second intron of an uncharacterized gene named *CG14160*. *CG14160* encodes a putative transporter gene (Figure 4.1).

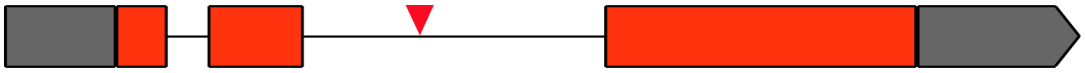

Figure 4.1. The piggyBac element in the line AC109 has inserted to the second intron of *CG14160*.

Bioinformatic analysis using the InterPro domains revealed that CG14160 is a member of the major facilitator superfamily (MFS), which is a transporter family with 12 transmembrane helices (Figure 4.2). The protein domains were analyzed using the 'simple modular architecture tool' available from the EMBL web-site (http://smart.embl-heidelberg.de/smart/change_mode.pl), confirming the presence of 12 transmembrane domains in CG14160.

Figure 4.2. Predicted transmembrane domains of CG14160. 12 transmembrane domains were predicted for CG14160 with SMART.

The genome-sequencing data molecular investigations have revealed more than hundreds of primary and secondary transporters exist. Two of these families were found to

occur ubiquitously in all living organisms, which are the ATP-binding cassette (ABC) superfamily and the major facilitator superfamily (MFS). MFS proteins are composed of transmembrane helices connected by hydrophilic loops; both N and C termini are located in the cytoplasm. They usually consist of 400-600 amino acids and 25% of the known membrane transport proteins are members of this large family. Transport groups regulate the intake of essential nutrients and ions, while excreting the toxic substances. MFS's are single-polypeptide secondary carriers, which transport only the small solutes and they function with three major kinetic mechanisms: uniporters transport a single type of substrate, symporters transport two or more substrates in the same direction at the same time, and antiporters transport two or more substrates in opposite directions across the membrane. The substrates of this family show a large variation including ions, sugars, sugar phosphates, drugs, neurotransmitters, nucleosides, amino acids, and peptides (Reddy *et al.*, 2012; Saier *et al*., 1999). CG14160 is conserved only among *Drosophila* species and it does not have any identified orthologs in non-insect arthropods or mammals (Figure 4.3) (Pao, *et al.*, 1998; Walmsley *et al*., 1998).

The expression pattern of the AC109 enhancer-trap line was analyzed at three different stages. The 3rd instar larval stage was chosen because PR specification starts at this stage. At the midpupal stage PR axons have already projected to the optic lobe, but expression of Rh genes has not started yet. In the adult stage the expression of Rh has finalized and the PR subsets are established.

The enhancer-trap lines were crossed to nuclear GFP reporter lines to determine the cell types in which these genes are expressed. The R8-specific transcription factor senseless has been used as a marker to visualize the R8 cell. Elav is the fly homolog of Hu proteins and specifically marks neuronal cell nuclei.

These results indicate that at the larval stage AC109 co-localizes with the R8 marker *senseless*, confirming that AC109 is an R8-specific line. The expression starts as early as row 8 in some of the ommatidia, and AC109 is expressed in all of the rows starting around the 14-15th row until the very posterior end of the eye disc (Figure 4.4).

A

Description	Max score	Total score	Query cover	E value	Ident
Drosophila melanogaster chromosome 3L	4787	4787	100%	0.0	100%
Drosophila simulans strain mixed chromosome 3L, whole genome shotgun sequence	4091	4091	99%	0.0	94%
Drosophila sechellia strain Rob3c scaffold_0, whole genome shotgun sequence	4006	4006	99%	0.0	93%
Drosophila yakuba strain Tai18E2 chromosome 3L, whole genome shotgun sequence	3092	3092	99%	0.0	86%
Drosophila erecta strain TSC#14021-0224.01 scaffold_4784, whole genome shotgun sequence	1984	2949	93%	0.0	87%
Drosophila ananassae strain TSC#14024-0371.13 scaffold_13337, whole genome shotgun sequence	857	1300	74%	0.0	76%
Drosophila pseudoobscura pseudoobscura strain MV2-25 chromosome XR unlocalized genomic scaffold ChXF	677	1003	68%	0.0	73%
Drosophila persimilis strain MSH-3 scaffold_27, whole genome shotgun sequence	673	992	68%	0.0	73%
Drosophila willistoni strain TSC#14030-0811.24 scf2_1100000004837, whole genome shotgun sequence	576	736	57%	2e-159	71%
Drosophila virilis strain TSC#15010-1051.87 scaffold_13049, whole genome shotgun sequence	556	754	57%	2e-153	71%
Drosophila mojavensis strain TSC#15081-1352.22 scaffold_6680, whole genome shotgun sequence	533	696	57%	2e-146	70%
Drosophila grimshawi strain TSC#15287-2541.00 scaffold_15110, whole genome shotgun sequence	518	678	57%	5e-142	70%
Pseudopodoces humilis unplaced genomic scaffold, PseHum1.0 scaffold325, whole genome shotgun sequenc	59.0	59.0	1%	0.001	85%
Pteropus alecto unplaced genomic scaffold, ASM32557v1 scaffold146, whole genome shotgun sequence	55.4	55.4	2%	0.017	83%
Phaseolus vulgaris cultivar G19833 chromosome 1, whole genome shotgun sequence	53.6	53.6	1%	0.060	83%

B

Description	Max score	Total score	Query cover	E value	Ident
CG14160 [Drosophila melanogaster]	982	982	100%	0.0	100%
GD12876 [Drosophila simulans]	972	972	100%	0.0	98%
GM24824 [Drosophila sechellia]	868	868	100%	0.0	94%
GE20286 [Drosophila yakuba]	858	858	100%	0.0	95%
GG13990 [Drosophila erecta]	851	851	100%	0.0	95%
GF23847 [Drosophila ananassae]	835	835	100%	0.0	87%
GL11828 [Drosophila persimilis]	783	783	100%	0.0	82%
GA12795 [Drosophila pseudoobscura pseudoobscura]	767	767	100%	0.0	82%
GK24105 [Drosophila willistoni]	758	758	100%	0.0	79%
GH16565 [Drosophila grimshawi]	748	748	100%	0.0	76%
GJ11718 [Drosophila virilis]	714	714	100%	0.0	77%
GI13855 [Drosophila mojavensis]	692	692	100%	0.0	75%
CG14160-like protein [Drosophila affinis]	493	493	66%	2e-169	82%

Figure 4.3. Blast analysis of CG14160. The nucleotide blast analysis of CG14160 (BLASTn) (A) and protein blast analysis of CG14160 (blastp) (B). (http://blast.ncbi.nlm.nih.gov/Blast.cgi)

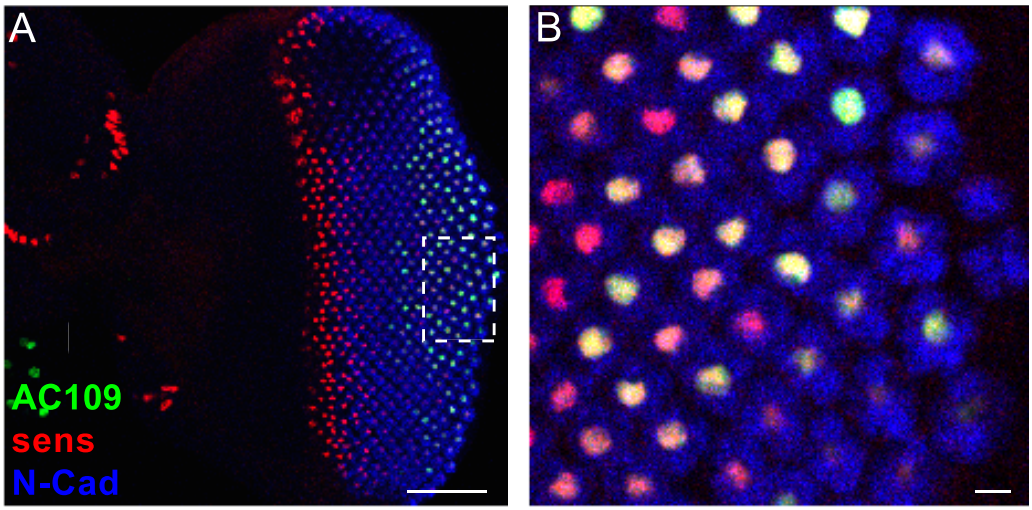

Figure 4.4. AC109 expression in 3rd instar larva. Immunostainings were performed against GFP to mark the enhancer trap line, Sens for R8 cells, and ElaV for neuronal cells. AC109>UAS-nGFP is expressed in R8 cells and colocalizes with the R8 marker senseless starting from row 8. Scalebars represent 50 μm (A) and 25 μm (B) respectively.

At 48 hrs APF, the AC109 enhancer-trap continues to drive expression in the R8 cell of 95% ommatidia, which was confirmed by co-staining with the R8 marker *senseless* (Figure 4.5). AC109 enhancer-trap is also expressed in R7 cells in ~ 50% of the ommatidia. This was inferred from the position of the GFP-expressing PR cell in relation to the *senseless*-expressing cell. A few ommatidia express the AC109 enhancer in a third PR, but the position of that PR changes.

At the adult stage both the UAS-nGFP (nuclear GFP) and UAS-CD8::GFP (membrane-bound GFP) reporters were used for co-localization studies. The nuclear localization of GFP will allow the identification of the cell types in which the enhancer drives expression, as all known markers are nuclear. Visualization of axonal projections in the optic lobe using the membrane-bound GFP can also help with the identification of cell types. These experiments show that the AC109-Gal4 enhancer is no longer expressed in PR cells in the adult. Instead, expression is observed in a group of neuronal cells at the medulla border and the lobula (Figure 4.6 A-B). Co-staining with the glial marker Repo and the neuronal marker Elav revealed co-localization with Elav (Figure 4.6 A). Analysis

of axonal projections revealed localization to the lamina, medulla, and the lobula (Figure 4. 6 C-D).

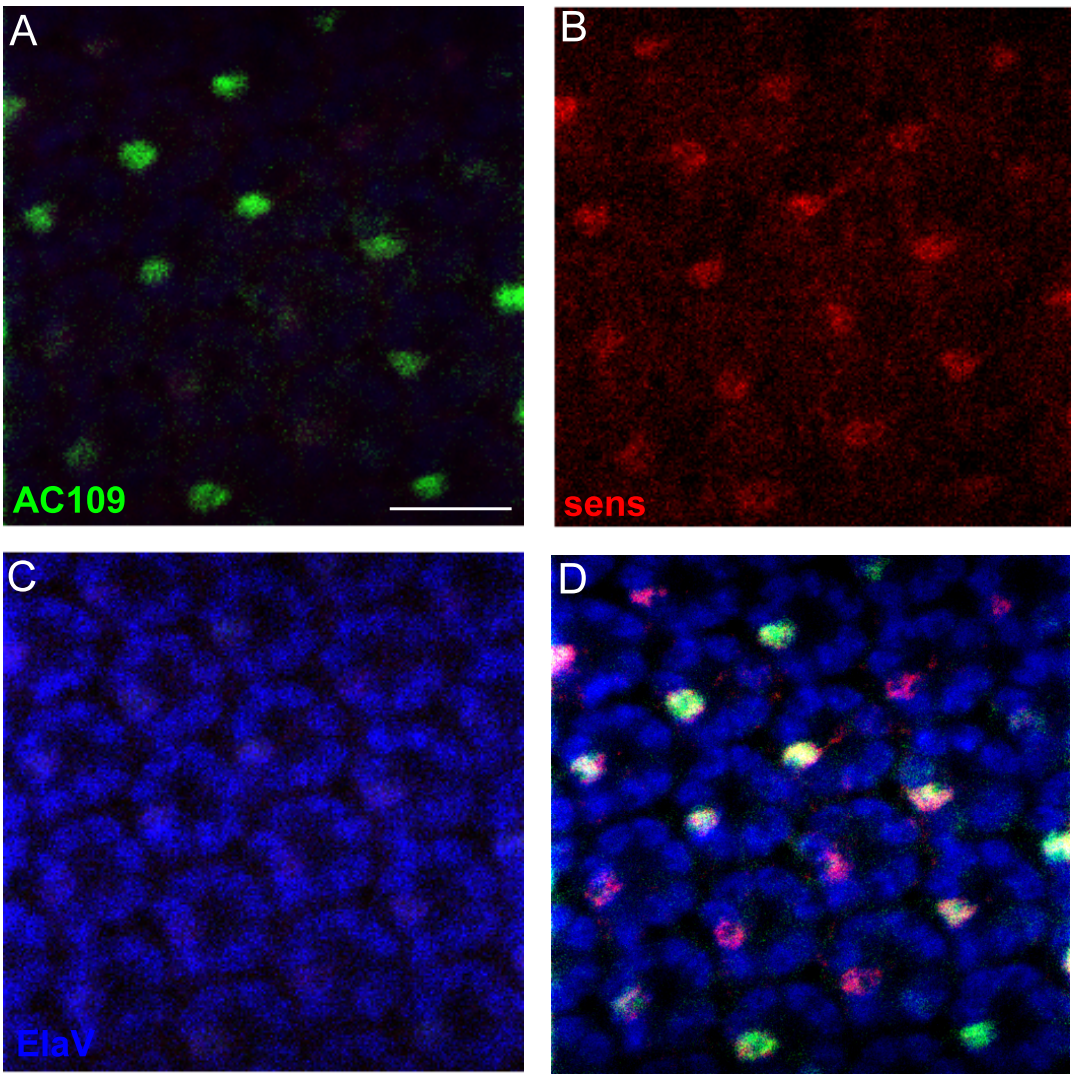

Figure 4.5. AC109 expression in midpupa retina. Immunostainings were performed against GFP to mark the enhancer trap line, Sens for R8 cells, and Elav for neuronal cells. AC109>UAS-nGFP is expressed in 95% of R8 cells in the midpupa stage and it co-stains with *senseless*. AC109-Gal4>UAS-nGFP- green (A), sens-red (B), Elav-blue (C) merge (D). Scalebar: 10 μm.

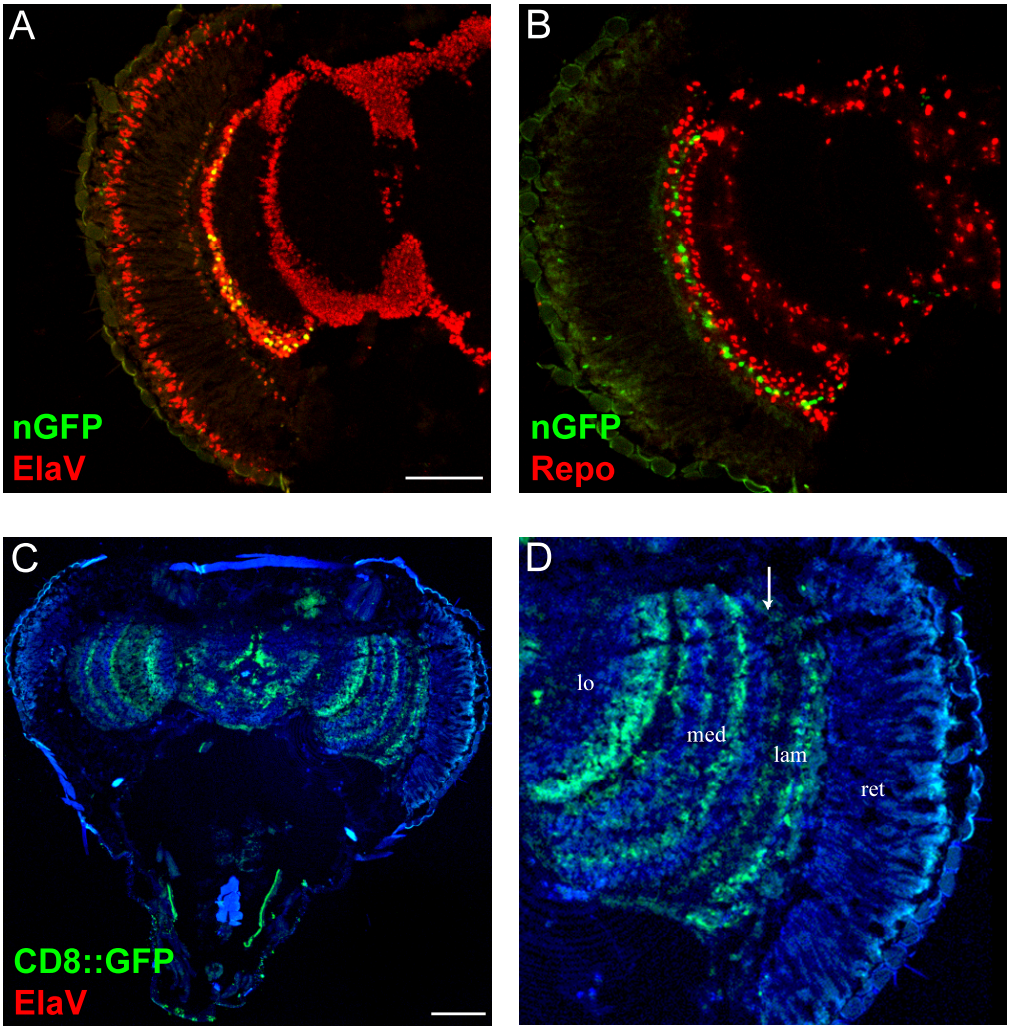

Figure 4.6. Expression of nuclear and membrane bound GFP under the control of the AC109 enhancer in the adult stage. AC109>UAS-nGFP is expressed in a subgroup of neuronal cells at the lamina border (A) and co-localize with Elav, but not with Repo (B). AC109>UAS-CD8::GFP-expressing cells project to the lamina, lamina-medulla border (arrow), medulla (med), and lobula (lo) (C-D). Scalebars: 50 µm (A-B), 100 µm (C-D).

4.1.2. The Expression Pattern of the Enhancer-Trap Line AC783 and Its Associated Gene Unzipped

4.1.2.1. The Localization of the AC783 Enhancer-Trap Line to Unzipped. Previously, it was shown that the enhancer-trap line AC783 was localized to the first intron of the gene

unzipped, but its exact position and direction could not be determined (Arzu Öztürk, 2010). Repetition of inverse PCR experiments, cloning of the amplified region before sequencing, or using different primers did not give accurate results, thus a different strategy was followed. Considering the blast hits, the candidate region to which the enhancer-trap had inserted to was narrowed down to 2500 bp within the first intron of *unzipped*. Three forward and reverse primers were designed within this region in order to determine the location and direction of the enhancer-trap insertion (Figure 4.7). The region was amplified using primers located in the piggyBac transposon and first intron of *unzipped*. The genome was digested randomly with the TaqI enzyme, which does not cut the region with the transposon. The randomly digested pieces of genomic DNA were ligated, forming circular pieces of DNA. One of those pieces contains a part of the transposon, and the part of genomic DNA where the transposon has inserted is the region we are searching for. After ligation, PCR was made with the new set of primers, which are from within the transposon region and from the intronic region. PCR was made with both forward and reverse primers since the orientation in which the transposon inserted was not known. The forward primers amplified three regions with the size of 250 bp, 750 bp, and 1250 bp, indicating that the enhancer-trap had inserted to the genome in a forward position. After sequencing and blasting the results with the *Drosophila* genome, it was concluded that the Gal4 enhancer-trap had inserted to the 645^{th} bp of the first intron of the *unzipped* gene in a positive orientation (Figure 4.7 C and Appendix).

While we were trying to generate tools for its further characterization, the first paper characterizing *unzipped* was published in 2011 (Ding *et al.*, 2011). In this study Unzipped was shown to be a 488 aa CAM with no homology to other CAMs. Additionally, this protein did have any known domains. It was shown that two forms of Unzipped exist: a secreted and a membrane-bound form, and when expressed in *Drosophila* S2 cells, cell aggregation was triggered through homophilic binding. In the embryonic Central Nervous System (CNS) Uzip was mostly produced by the longitudinal glia (LG), but it was also found in axons. Unzipped was shown to have a function in the guidance of longitudinal axons in *Drosophila*. Although the loss of *uzip* alone did not cause any defects in axonal patterning, its deletion enhanced the projection defects observed in N-Cadherin and Wnt5 mutants (Ding *et al*., 2011). Unzipped has no mammalian ortholog, however it is conserved among insects.

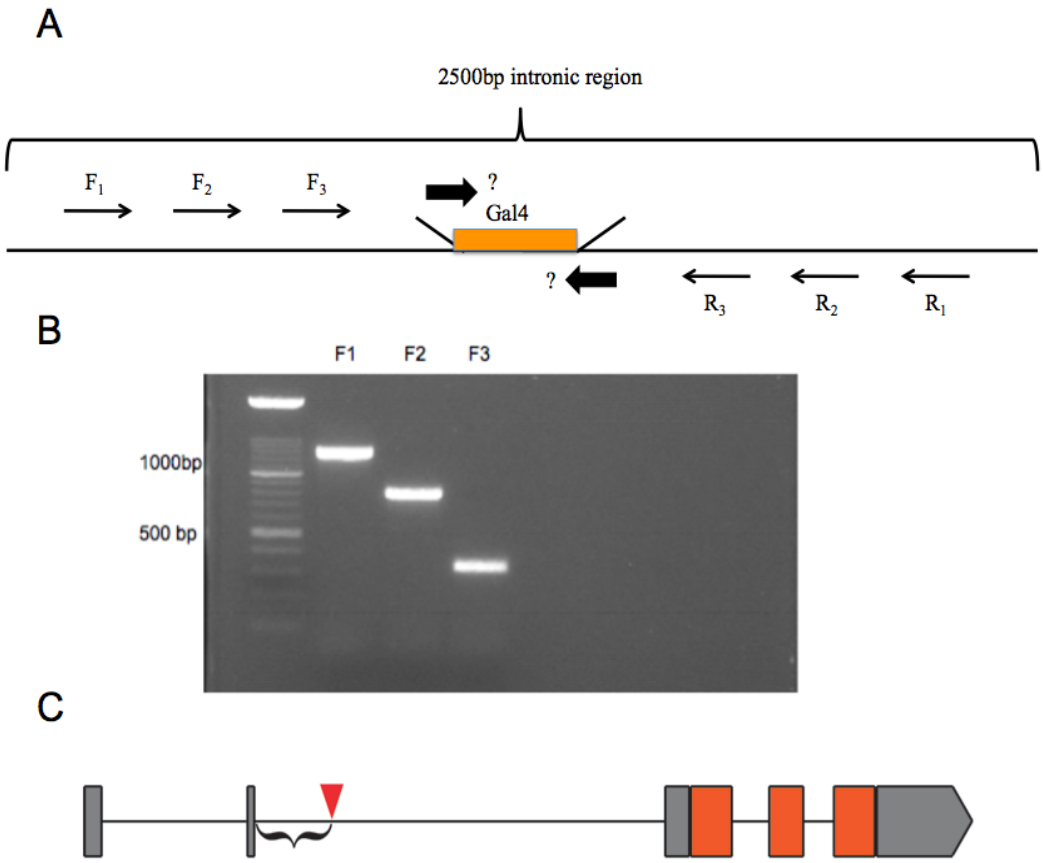

Figure 4.7. PCR amplification of the candidate region and localization of AC783. PCR amplification was performed with different forward and reverse primers designed from the 2500 bp intronic region (A). The forward primers designed from the intronic region and the reverse primers designed from the PiggyBac region amplified PCR products of 250 bp, 750 bp, and 1250 bp (B). AC783 is localized 645 bp into the first intron of *unzipped* (C).

4.1.2.2. Domain Prediction and Bioinformatic Analysis of Unzipped. Cell aggregation assays suggested that Unzipped is a CAM, however no sequence or domain relevant to CAMs could be identified or predicted. The only identifiable domains were the transmembrane region and the signal peptide (Ding *et al*., 2011). In order to identify possible domains and conserved regions, two major databases were used: SMART (Simple-Modular-Architecture-Research-Tool) for regional sequence analysis and PFAM, which is a database of protein families that includes their annotations and multiple

sequence alignments for domain analysis. Performing domain analysis using SMART following results were obtained:

- 1-25 aa: signal peptide
- 26-379 aa: unknown
- 380-400 aa: low complexity
- 401-463 aa: unknown
- 464-486 aa: transmembrane domain

These results were in line with previous findings (Ding *et al*., 2011). Further domain analysis using the PFAM tool did not provide any further information on conserved regions. Taken together, no additional domains or sequences could be identified by the bioinformatic analysis performed here.

4.1.2.3. The Expression Pattern of the Enhancer-Trap Line AC783. The enhancer-trap line AC783 colocalizes with the R8 marker Senseless at the third instar larva stage and is expressed in some of the ommatidia starting from row 8 (Figure 4.8 A-B). It is expressed in all ommatidia after row 14 until the posterior end of the eye disc. It is also expressed in a subset of glial cells in the eye disc as identified by Repo staining (Figure 4.8 C-D). The glial cell subsets could not be characterized in detail as no antibodies are available to label different glial cell subtypes. The only available tools are different enhancer-trap lines. However, as AC783 is also an enhancer-trap line, double labeling could not be performed. Still, by analyzing the labeled cells, we suggest that the enhancer-trap line drives expression in carpet glia. Carpet glial cells comprise a subset of glia located in the eye disc with a big nucleus that can easily be distinguished from other cells (Figure 4.8) (see arrows in Figure 4.8 D).

At the mid-pupal stage AC783 continues to drive expression in R8 cells and colocalizes with Senseless (Figure 4.9). At the adult stage, AC783 driven nuclear GFP colocalizes with Repo cells but not Elav cells, showing that it is expressed in a group of glial cells but not neuronal cells (Figure 4.9 A-C).

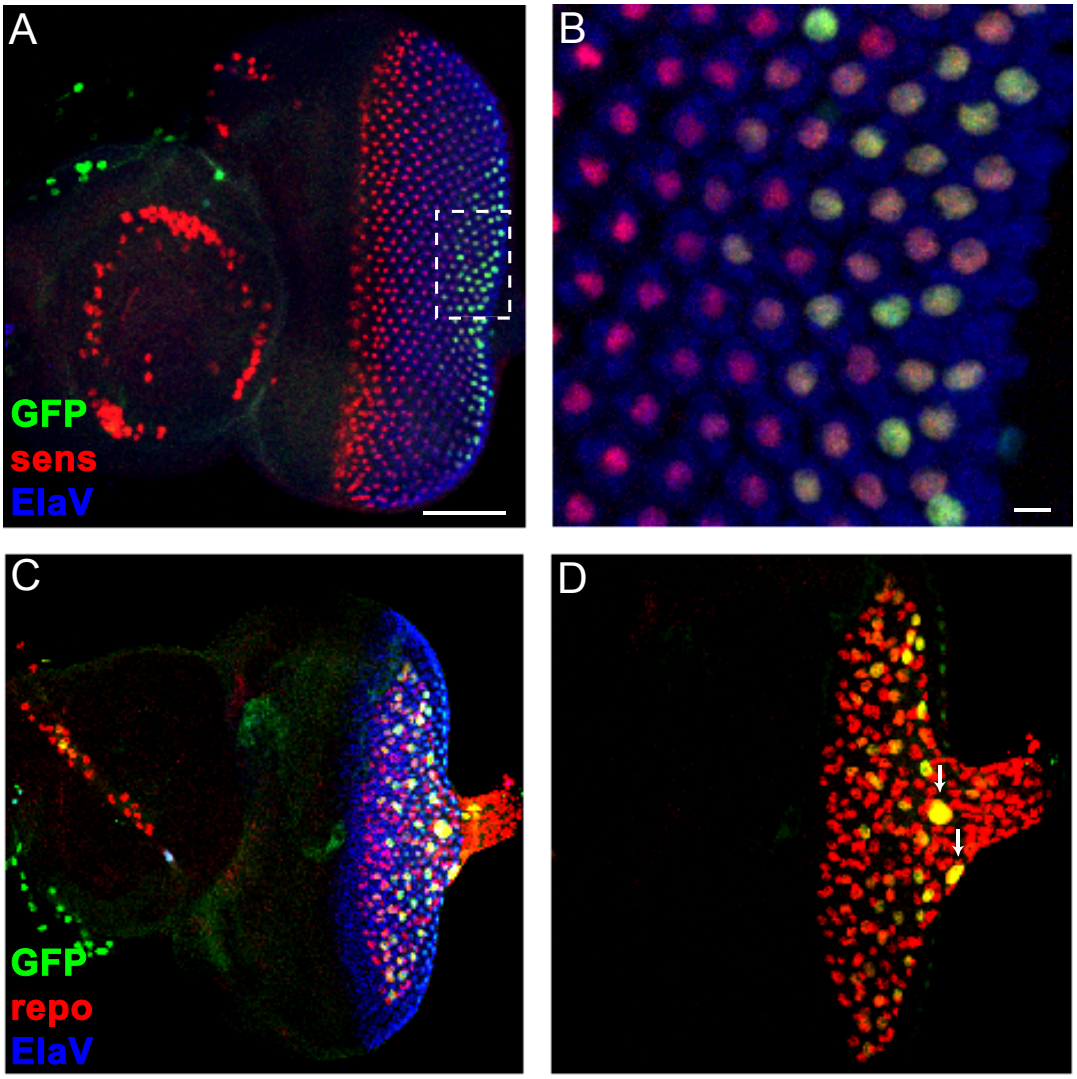

Figure 4.8. AC783-Gal4 driven expression in the 3rd instar larval stage. Immunostainings were performed against GFP to report the enhancer activity of AC783, Elav for neuronal cells, Sens for R8 cells, and Repo for glial cells. AC783>UAS-nGFP colocalizes with Senseless starting from row 8 after the MF (A-B). It is also expressed in a subset of glial cells (C-D). Arrows show carpet glia cells (D). Scalebars: 50 μm and 25 μm.

AC783-Gal4 driven reporters expressed in the cell membrane project both to the lamina, medulla, and the lobula (Figure 4.10 D-F). In the lamina single GFP-positive cells are scattered randomly throughout the layer. The phenotype and structure of the cells suggest that they might be glial cells, which reside in the lamina (Figure 4.10 A-C). When AC783 drives the GFP reporter that localizes to the cell membrane, those cells are

expressed at the membranes surrounding the PR cells and project to the medulla. They also stop at the exact location as the PRs. These cells do not colocalize with the PR cells suggesting that they might also be glial cells wrapping the PR cells (Figure 4.10 F).

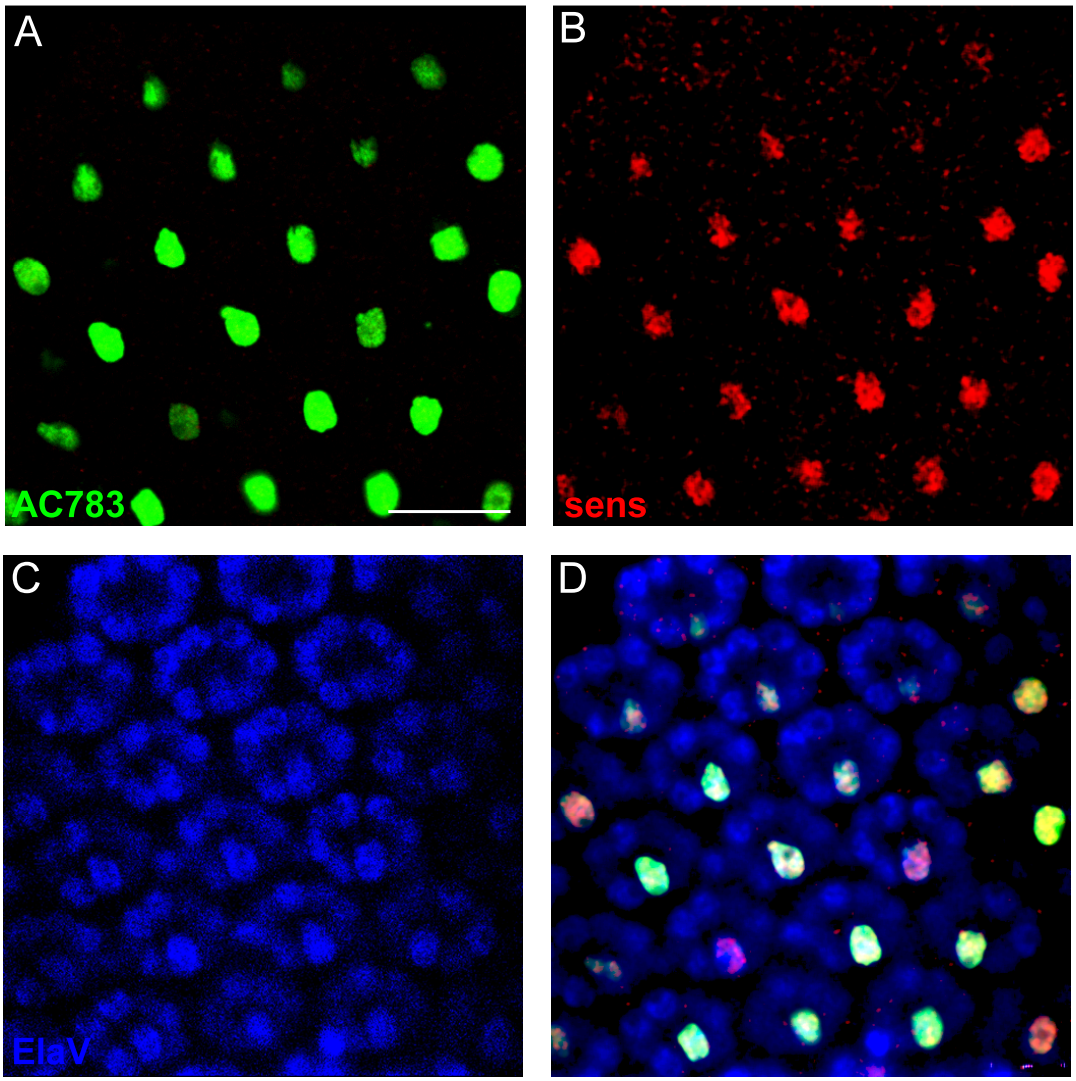

Figure 4.9. AC783 expression in mid-pupal stage. Pupal immunostainings were performed against GFP to mark the enhancer-trap line, Sens for R8 cells, and Elav for neuronal cells. AC783>UAS-nGFP is expressed in R8 cells at the mid-pupal stage, colocalizing with Senseless. AC783-Gal4>UAS-nGFP- green (A), sens-red (B), Elav-blue (C) merge (D). Scalebar represents 10μm.

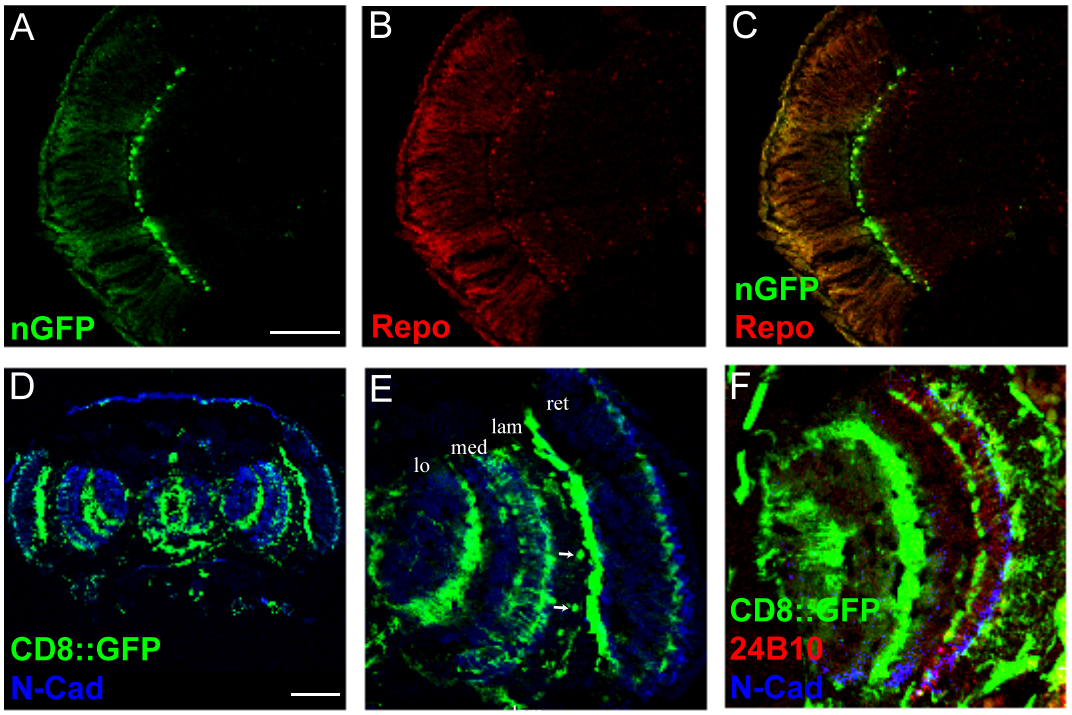

Figure 4.10. AC783 expression in the adult stage. AC783>nGFP is expressed in glial cells at the lamina border (A-C) AC783>CD8::GFP expressing cells project to the lamina (la), medulla (med), and lobula (lo) border (D). At the lamina there are single GFP-labelled cells (arrows) (E). At the medulla the AC783 driven reporters project to the same layer as the PRs that are labelled with 24B10 (red) (F). Scalebars: 50 µm (A-B) and 100 µm (C-D).

4.2. Unzipped is a Candidate for the Regulation of PR Differentiation and Targeting

Using an enhancer-trap line inserted into the first intron of the Unzipped gene we showed that this gene is expressed both in R8 cells and a subgroup of glial cells. The R8 cell is the first cell that is specified in the larval retina and directs the specification of all other PRs. It is also special as R8 axons are the first ones that project to the optic lobe. These axons are later followed by the other PR axons. R8 axon outgrowth does not start before glial cells from the optic lobe migrate to the eye imaginal disc and contact the R8 cells. The R8 cells than use the glial cells to project their axons to the optic lobe. Many of the molecules that have been identified so far and are involved in axonal targeting are

expressed both in neurons and in the target regions or glial cells. Considering its putative role as a cell adhesion molecule involved in axonal targeting (Ding *et al.*, 2011) we decided to investigate its function in the visual system of *Drosophila*.

4.3. The Expression Pattern of Unzipped

In order to have a better insight into the function of Unzipped, the expression pattern should be revealed as an initial step. Since AC783 is an enhancer trap line, it only gives a general idea, but does not show the full expression. Since the Gal4 element had inserted to a specific location in the intronic region, it is possible that other regions involved in the expression of Unzipped might not be affecting the enhancer trap due to the distance or direction of insertion. In order to understand the exact expression pattern of Unzipped, another enhancer trap line, which had inserted to a different location, the 5'UTR region, was immunostained to see if the expression matched AC783. In addition, different antibodies and a mCherry-tagged BAC construct were used in order to understand the expression pattern of Unzipped.

4.3.1. The Expression Pattern of the DGRC Enhancer Trap Line

Apart from AC783, there is another commercially available enhancer-trap line from the Drosophila Genetic Resource Center (DGRC) with the code 104787. Different from AC783, 104787 has inserted to the 5'UTR region in a reverse orientation (Figure 4.11).

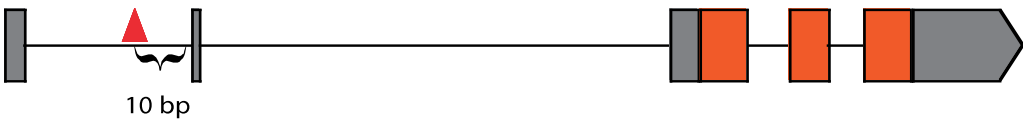

Figure 4.11. In the DGRC 104787 enhancer trap line the Gal4 element has inserted into the 5'UTR region of *unzipped* in a reverse orientation.

104787 was immunostained at the third instar larva and adult stages to see if the expressions of the two enhancer trap lines matched. At the third instar larva stage of the 104787>UAS-CD8::GFP flies, the membranes of the cells driven by 104787 colocalized

with R8 cells, which were visualized with *senseless* (Figure 4.12). No other PR was stained by 104787, indicating that the DGRC enhancer trap line is specific to R8 cells like AC783. Additionally a group of cells just above the PR level, where the glial cells reside, were also stained starting from row 8 after the MF (Figure 4.12 C). This is the same starting point as the AC783 line, only at the glial level. The nuclear stainings with *104787>UAS-nGFP* flies were also similar to AC783 stainings, and at the glial level both the subgroup of glial cells and the carpet glia nuclei can be seen (Figure 4.12 D).

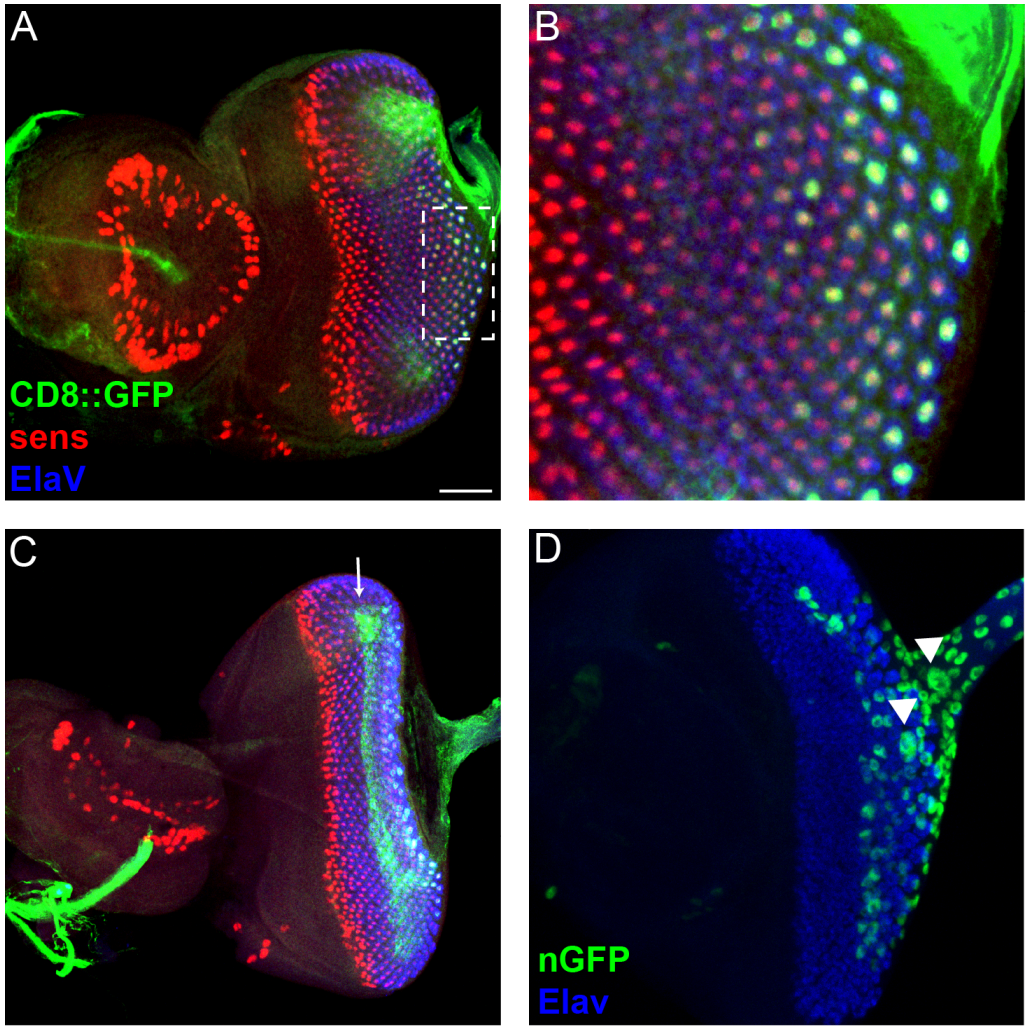

Figure 4.12. The expression pattern of the DGRC 104787 enhancer-trap line at the 3rd instar larva stage. At the 3rd instar larva stage, 104787>UAS-CD8::GFP flies expressed GFP in the membranes of R8 cells (A-B). There was expession also at the glial cell level starting from row 8 (arrow) (C). The 104787>UAS-nGFP flies stained a group of glial cells including the carpet cells (arrow heads) (D). Scalebar 50 µm.

In the adult stainings of the *104787>UAS-CD8::GFP* flies, the GFP stained membrane of the reporter driven by 104787 projected to the same layer as the PR cells. In addition, there was also a lesser amount of staining at the M3 layer, where the R8 cells project. In the nuclear staining of the DGRC enhancer trap line, the cells were big and surrounded both the lobula and the medulla. They did not exist in the medulla where the PRs project to, suggesting that 104787 driven reporters project to the PR target terminals (Figure 4.13). These findings are in accordance with the AC783 enhancer-trap line results. Although the enhancer traps had inserted to two different regions and in different directions, the similarities in their expression patterns suggest that AC783 and 104787 might be close to the endogenous expression of *unzipped*, or both enhancer traps are close to the regulatory region of *unzipped* so that both are regulated in the same way.

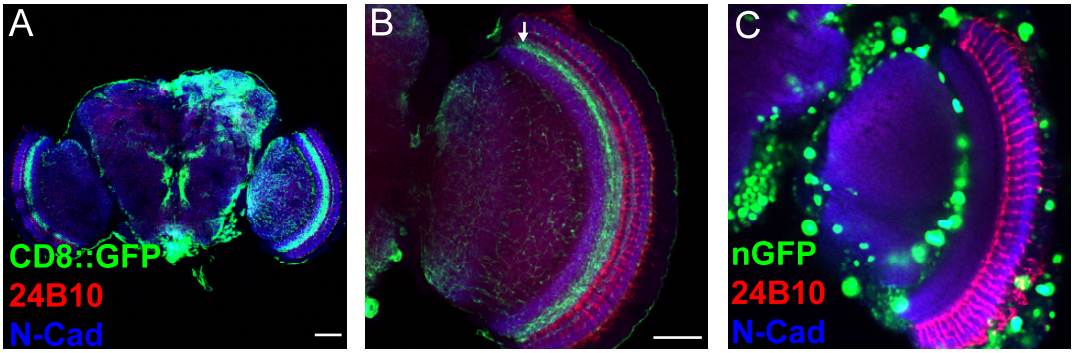

Figure 4.13. The expression pattern of the DGRC 104787 enhancer trap line at the adult stage. The 104787>UAS-CD8::GFP lines projected to the same layer as the PR cells project (arrow) (B). The 104787>UAS-nGFP expressing cells surround the medulla and the lobula. 104787-Gal4>UAS-CD8::GFP – green, 24B10-red, Elav-blue (A-B), 104787-Gal4>UAS-nGFP, 24B10-red, Elav-blue (C) Scalebars: 50 µm (A) and 100 µm (B).

4.3.2. The Endogenous Expression of Unzipped

Enhancer-trap lines give a good idea about the expression pattern of a gene. However, if they fully reflect the endogenous expression needs to be assessed first. Usually, Gal4 enhancer-trap lines are expressed with a slight delay compared to the endogenous expression. Since the expression of Gal4, synthesis of the protein, its binding to the UAS sequence, and the synthesis of the reporter protein takes some time. Thus, in

the next section we investigated the endogenous expression and localization of the Unzipped protein using antibodies raised against Unzipped.

4.3.2.1. Localization of Unzipped with Anti-Unzipped Antibodies from the Huang Group. Two antibodies were previously raised against different regions of Unzipped (Ding *et al.*, 2011). One of them is a polyclonal rabbit antibody generated against a 8kDa sequence between 294-311 aa referred to as the short fragment. The other one is a mouse monoclonal antibody generated against a 35kDa region between 174-405 aa referred to as the long fragment. Both of these regions reside in the conserved region, which was shown to be important for Unzipped function (Ding *et al*., 2011) (Figure 4.14).

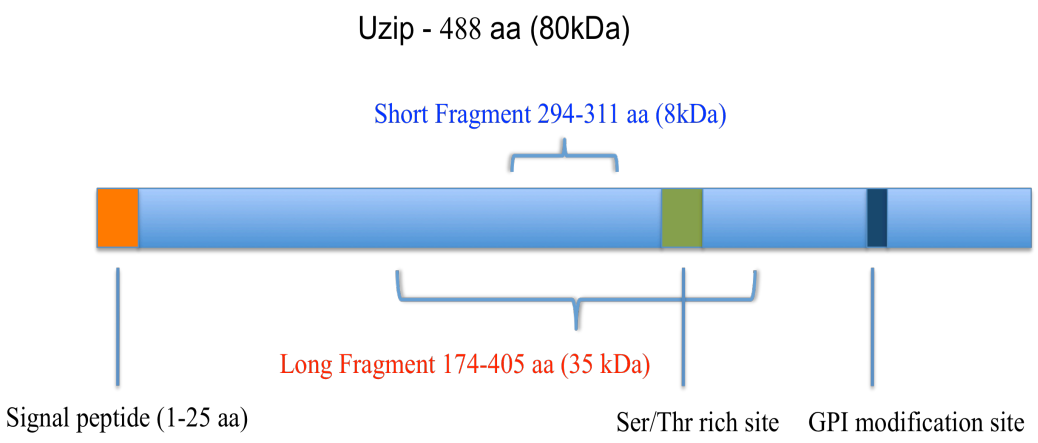

Figure 4.14. The regions used for Unzipped antibody generation by the Huang group. The antibodies were generated against two regions in the Unzipped protein. The 8kDa short fragment between 294-311 aa is a rabbit polyclonal antibody and the 35 kDa long fragment between 174-405 aa is a mouse monoclonal antibody.

The antibodies were first tested against a N-Terminal His tagged Uzip protein that was generated from the 175-405 aa (35kDa) region of Unzipped in our lab. It was expressed and purified from E. Coli. Western blots were performed with both the mouse (long fragment) and the rabbit (short fragment) antibodies and both antibodies recognized the 35kDa Uzip protein. Thus, the antibodies were working on Western blots (Figure 4.15).

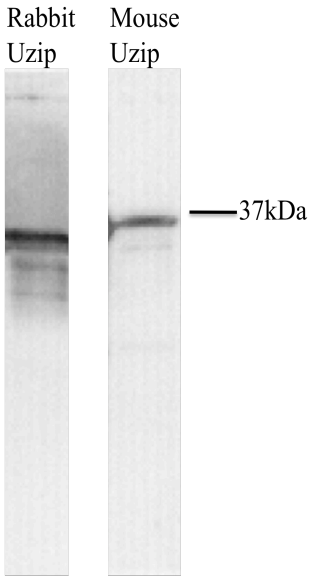

Figure 4.15. Western blots for the rabbit and mouse Uzip antibodies generated by Ding *et al.,* 2011. Western blots were performed with the rabbit and mouse Uzip antibodies. Both antibodies recognized the partial Unzipped protein (35kDa) that was expressed and purified in our lab.

In order to assess if these antibodies work in immunohistochemistry and the enhancer-trap line reflects endogenous expression third instar larval eye imaginal discs of AC783-Gal4 flies were stained with both antibodies from Ding *et al.,* 2011. The mouse Unzipped antibody was used in different dilutions but revealed no expression. On the contrary the rabbit Unzipped antibody gave a very unspecific expression, which was uniform all over the eye disc, suggesting that it might be recognizing epithelial tissue (Figure 4.16). The rabbit Unzipped antibody staining was repeated after pre-absorption with null mutant embryos to reduce the background with no significant effect on previous results.

The preabsorbed rabbit anti-Unzipped antibody was also tested on adult *wildtype (wt)* flies. In the adult flies a group of cells lining the M3 level of the medulla, similar to the expression observed with the enhancer-trap lines was visualized. There are also many other labelled cells in the medulla cortex (Figure 4.17). Since preabsorption did not work in the 3rd instar eye imaginal discs, it is difficult to distinguish the specific expression from the unspecific stainings.

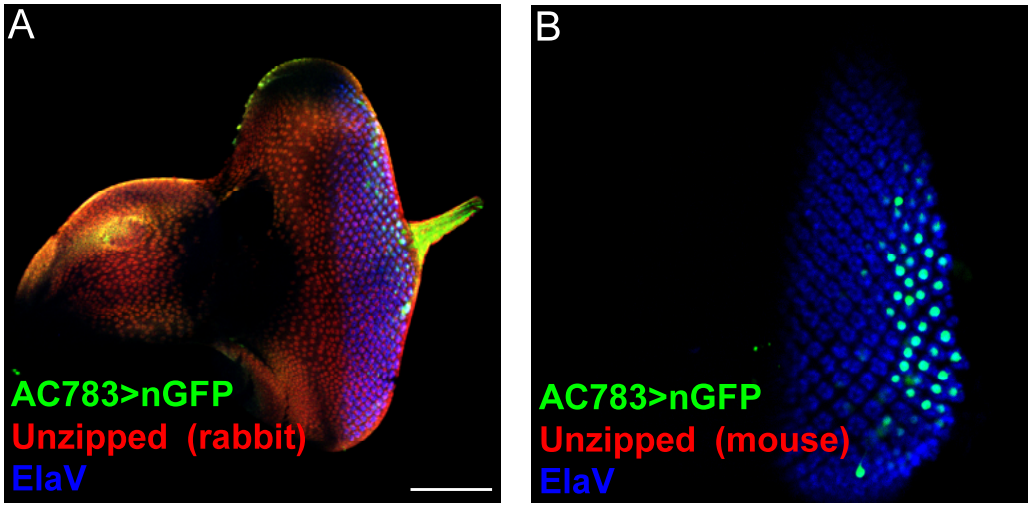

Figure 4.16. 3rd instar larval eye disc stainings with rabbit and mouse antibodies from Huang group. Immunostainings against GFP was used for AC783>nGFP, Unzipped (rabbit) and Unzipped (mouse) for endogenous Unzipped, and Elav for neurons. The rabbit antibody gave unspecific expression all over the eye-imaginal disc and did not colocalize with PR or glial cells (A). The mouse antibody gave no expression (B). Scalebar: 100 μm.

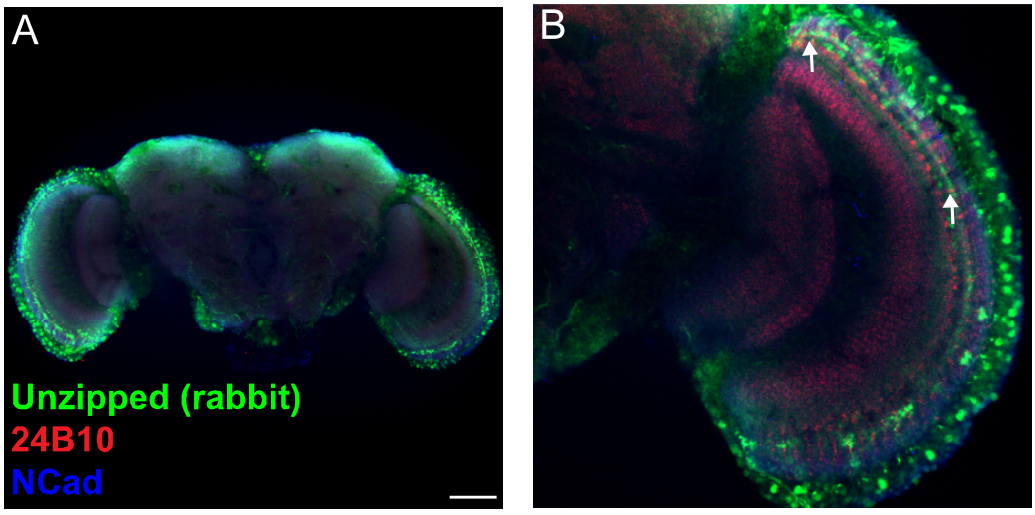

Figure 4.17. Adult expression of the short fragment rabbit antibody. Adult wholemount immunostainings against Unzipped (rabbit) were performed to identify the localization of Unzipped (green), Chaoptin (red) antibody was used to visualize PR axonal projections, and N-Cadherin (blue) antibody to label the neuropil structure. Expression is observed both at the medulla cortex and the M3 layer of the medulla (arrows) (B). Scalebar: 50 μm.

4.3.2.2. The Generation of the Unzipped Antibody. The functional antibody is not only important for the assessment of the localization of a protein, but it is also useful in elucidating the function of a protein. Thus, the availability of a functional antibody in sufficient amounts is necessary to perform detailed characterization experiments and assays. For this purpose we aimed at generating our own antibody. Since there are no known domains or functional regions in the Unzipped protein, first we tried to generate an antibody against the whole Unzipped sequence. For this purpose the coding region of Unzipped was cloned into the bacterial expression vector pET-30a(+). However, the protein could not be isolated and got stuck to the bacterial membrane, probably due to the presence of the GPI modification site.

Later two different constructs were generated by cloning the 174-405 aa and 294-311 aa parts of the Unzipped protein. This selection was based on the publication by Ding *et al.,* 2011. The major difference between these fragments and the full protein is that they lack the transmembrane domain, so there is a lower probability of the protein getting attached to the membrane. Both fragments were tagged at the N-terminal site with a His tag. The constructs were transformed to Rosetta™ 2(DE3)pLysS competent cells, which are specialized for protein expression after IPTG induction, and contain a plasmid which codes for 7 of the rare codons in *E. coli.* Successful transformation and correctness of the cloned fragments were confirmed by PCR and sequencing (Figure 4.18).

After cloning, the long and short protein fragments were induced with IPTG. No expression for the short fragment could be induced although different gel concentrations and induction methods were tried. For this reason the protein expression was continued with the long fragment.

In order to determine the best concentration and time of induction with IPTG, growth curves for untransfected competent cells, IPTG-induced cells, and uninduced cells were generated. OD values were plotted on a growth curve. The bacteria first pass through a lag phase where they start replication and get ready for protein synthesis then they start duplicating and protein synthesis. The point where there is too much bacteria in the medium and the food is insufficient, they stop replicating and their growth slows down, which is the stationary phase. The optimum point to give the IPTG is the mid-log phase,

which is between lag phase and stationary phase and is around 1 at the graphic. The decision is given based on the uninduced bacteria, but since there is not a major curve difference between the induced and uninduced, both can be considered (Figure 4.19).

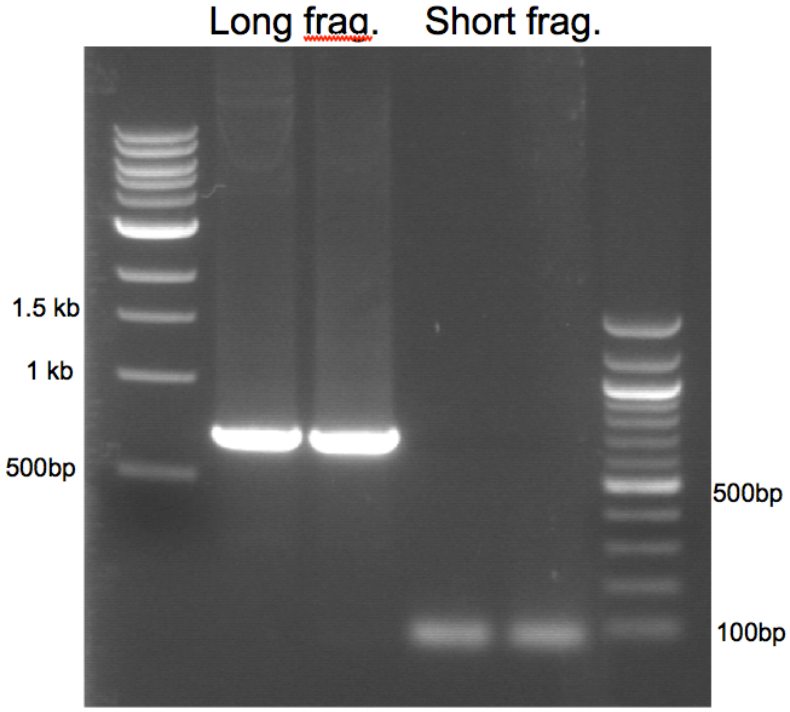

Figure 4.18. PCR confirmation of the cloned short and long fragments. The positive colonies for both long and short fragments inserted to the pET-30a(+) vector were confirmed by PCR amplification, respectively. The expected size for the short fragment is 71 bp and the long fragment is 713 bp.

The induced and uninduced sample proteins were loaded on a polyacrylamide gel and their specifity was tested by Western blot. In the Coomassie Blue staining of the gel, the competent cells and the uninduced group, which were not induced by IPTG gave unspecific bands, while the samples taken 1 hour, 2 hours, 3 hours, and 4 hours after induction gave a specific single band at the expected size (Figure 4.20). This indicated that the protein was specifically expressed upon IPTG induction. A Western blot with the anti-His antibody confirmed that the specific bands were the His-tagged Unzipped protein (Figure 4.21).

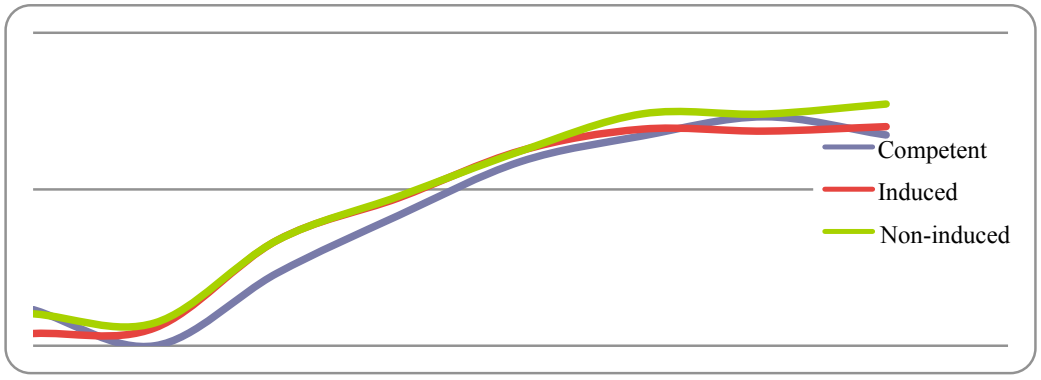

	0h	1h	2h	3h (IPTG)	4h	5h (diluted)	6h (diluted)	7h (diluted)
Competent	0.17	0.1	0.29	0.68	1.5	2.19	2.9	2.22
Induced	0.12	0.13	0.47	0.88	1.76	2.42	2.35	2.51
Non-induced	0.16	0.14	0.47	0.9	1.75	3.03	3.02	3.5

Figure 4.19. The growth curve for optimization of time and concentration of IPTG for protein induction. The midline of the exponential growth for all competent, induced, and uninduced cells was around the point 0.9-1 intersecting the graph. This is the mid-log phase, the best time point to add IPTG since the protein synthesis is the fastest at this stage. The addition of the construct or the induction with IPTG did not change the growth curve.

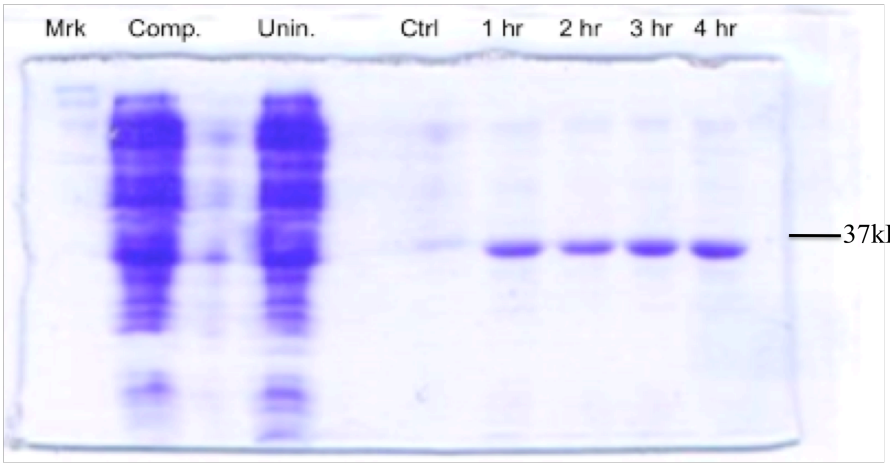

Figure 4.20. Coomassie Blue Staining of proteins extracted from the cells used in generating the growth curves. There were unspecific bands in the Rosetta2 DE3 pLYS + untransformed cells (comp.), and the Rosetta2 DE3 pLYS + transformed with the Unzipped construct but not induced with IPTG (unin.), the samples from 1-2-3-4 hours after IPTG induction gave a clear band around the expected size of 35kDa.

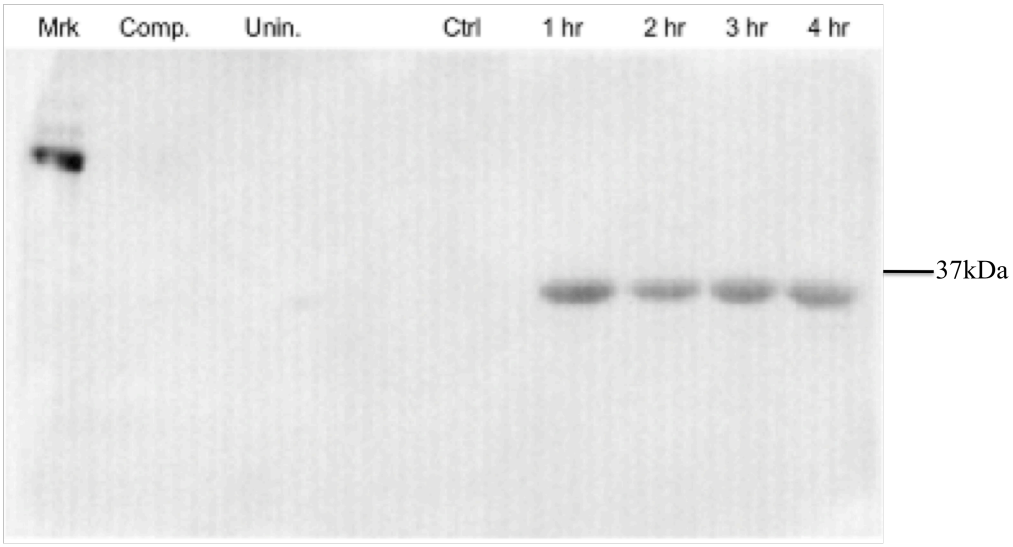

Figure 4.21. Western blot analysis of proteins extracted from competent cells used to generate the growth curve. Empty Rosetta2 DE3 pLYS + untransformed cells (Comp.), uninduced Rosetta2 DE3 pLYS + transformed with the Unzipped construct but not induced with IPTG (Unin.), and the control sample taken at the time of IPTG induction (Ctrl).

After confirming that the Unzipped protein was expressed in *E. coli* only after induction and the His antibody did not recognize any protein from the untransformed cells, uninduced cells or control cells; the Unzipped protein was purified for injection to rabbits. Ni-NTA cartridges were used to obtain proteins at optimal purity and concentration. These cartridges purify His-tagged proteins based on the recognition of their His tags. The Unzipped protein was purified under denaturing conditions with high urea and high pH solutions. Proteins obtained from the intermediate purification steps as well as the eluates were loaded on a polyacrylamide gel and visualized by Coomassie Blue staining and Western blotting with and anti-His antibody. A pure eluate was obtained at the end (Figure 4.22).

In order to decrease the high volume of eluate and make it suitable for injection, precipitation was made with ammonium sulfate and the pellet was dissolved in 1x PBS. Membrane dialysis was performed, in order to get rid of the ammonium per sulfate before injection. The purity of the protein was confirmed for the last time with the polyacrylamide gel before injection and the concentration of the protein was measured as 0.85 mg/ml (Figure 4.23).

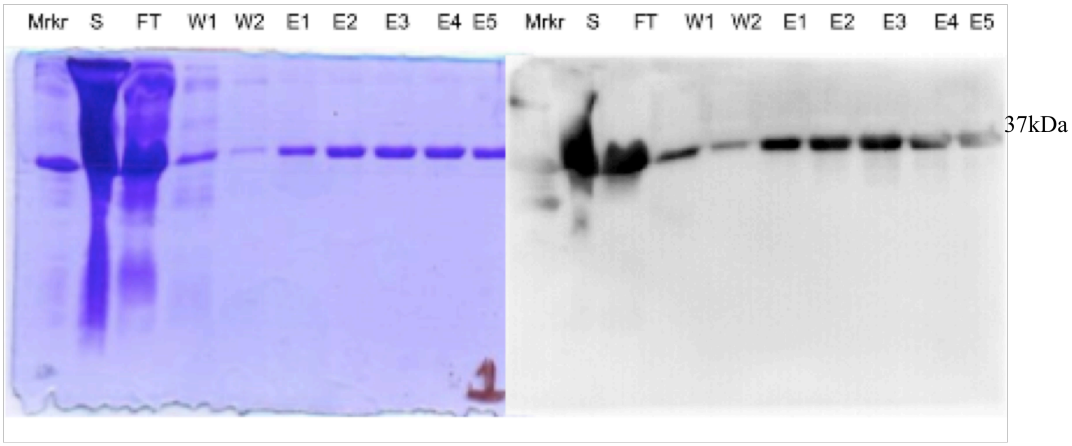

Figure 4.22. The Coomassie Blue staining and Western blot of purified Unzipped p urified by Ni NTA cartridges. The supernatant (S), which contains the induced Unzipped protein, the flow through (FT), which is the sample collected after the His-tagged protein is bound to the cartridge, two wash samples (W1 and W2) and the elutes in the following order (E1-E5) were loaded to the polyacrylamide gel.

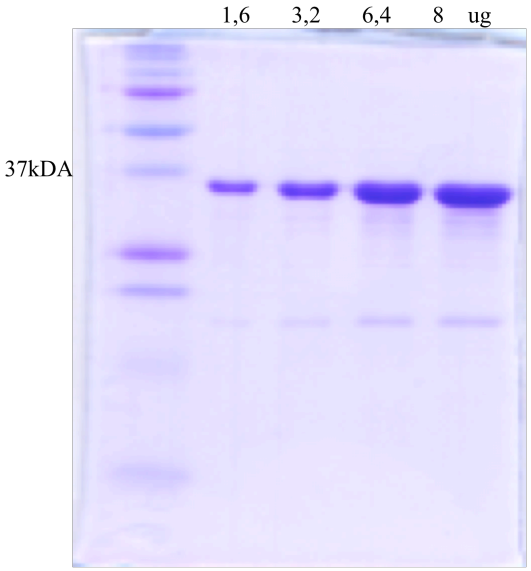

Figure 4.23. Coomassie Blue staining of purified His-tagged Unzipped protein before injection. Different concentrations of the protein were loaded to the gel to confirm the purity of the protein. The strong band seen at the expected size in the Coomassie Blue staining confirmed that our protein was pure. The slight bands seen at the lower ends were considered to be negligible.

Two one-year-old New Zealand rabbits were used for injection in order to produce the antibody. For each injection 80-100 μg of protein are required. 102 μg of protein was taken in 125 μl and mixed with 125 μl complete adjuvant complex in a (1:1) dilution in order to start the immunization. The protein was injected subcutaneously. Two weeks later a second injection was made in the same manner, this time with the incomplete adjuvant complex since the initial immunization had started. We waited for the immune reaction to take place and three days later 1 ml of blood was taken from the ear of the rabbits for testing the immune response. ELISA plates were covered with different concentrations of the Unzipped protein (50 ng – 100 ng – 250 ng). The serum was isolated from the blood, and different concentrations of serum (1/100 – 1/500 – 1/1000) were tested against different concentrations of Unzipped protein. According to the ELISA test read-outs, both rabbits appeared to be immunized by the antigen and we obtained the highest reaction with the 1/1000 serum concentration when compared to PBS only (Table 4.1).

Table 4.1. ELISA read-outs after the second immunization. The ELISA test was performed in triplicates. Different amounts of serum and different amounts of Unzipped protein were matched in the ELISA test. The highest read-out was seen in the 1/1000 diluted serum. The 50ng, 100 ng, and 250 ng proteins gave at least a fourfold response to the 1/1000 serum (bold-italic) when compared with the PBS control (italic).

Protein amount	**PBS**	**PBS**	**PBS**	**50 ng**	**50 ng**	**50 ng**
Rabbit1	1.79	0.76	*0.53*	2.03	2.25	***2.29***
Rabbit2	1.3	0.44	*0.28*	2.25	2.39	***2.4***
Serum amount	**1/100**	**1/500**	**1/1000**	**1/100**	**1/500**	**1/1000**

Table 4.1. ELISA read-outs after the second immunization (cont.).

Protein amount	**100 ng**	**100 ng**	**100 ng**	**250 ng**	**250 ng**	**250 ng**
Rabbit1	2.02	2.26	***2.35***	2.00	2.19	***2.32***
Rabbit2	2.11	2.33	***2.41***	2.20	2.42	***2.43***
Serum amount	**1/100**	**1/500**	**1/1000**	**1/100**	**1/500**	**1/1000**

Two weeks and four weeks later two additional immunizations were performed and again 1 ml of blood was taken from the ear of the rabbits in order to perform the ELISA test. This time the serum was diluted in 1/1000 ratio since it gave the best results in the previous ELISA test (Table 4.1). Although the read-out values were increasing in correlation with the increasing protein concentrations, there were some inconsistencies in the read-outs. We decided to make two more immunizations before sacrifice of the rabbits to obtain the serum (Table 4.2).

Table 4.2. ELISA read-outs of the rabbit serum after the 4th immunization. The ELISA test was performed in duplicates. There is an increase in response with the increasing concentration of the Unzipped protein, although there are some inconsistencies in the read-outs.

	PBS	PBS	50ng	50ng	100ng	100ng	250ng	250ng
Animal I 1/1000 serum	0.27	0.18	0.002	2.2	2.09	0.002	1.85	2.1
Animal II 1/1000 serum	0.95	0.63	0.008	1.8	2	0.0025	1.94	1.75

After completing the immunizations, the rabbits were sacrificed and their blood was collected. The serum was isolated from the blood, but in order to obtain the antibody,

further purification was required. Several purification systems were tested, however the highest efficiency was obtained with the NHS-activated agarose dry resin. The NHS-activated columns were first coated with the Unzipped protein, and the serum was passed through the columns twice so that the antibody recognizing the Unzipped protein got attached to the column. Then the antibody was eluted and its concentration was measured. From the total of six eluates for each animal, the one with the highest concentration of antibody was chosen for the Western blot analysis. We used protein isolated from both the Uzip null mutants and the *wt* animals. Two bands were seen in the wt lane, which were above and below the 75 kDa marker that represent the expected sizes: 65 kDa for secreted form and 80 kDa for the membrane bound version of Unzipped. For the null mutants there was no band detected for animal-I while there was a very slight band for Rabbit-II at the expected region, although it was thinner than the *wt* sample (Figure 4.24). After evaluating those results, we decided to continue with the antibody generated by Rabbit-I.

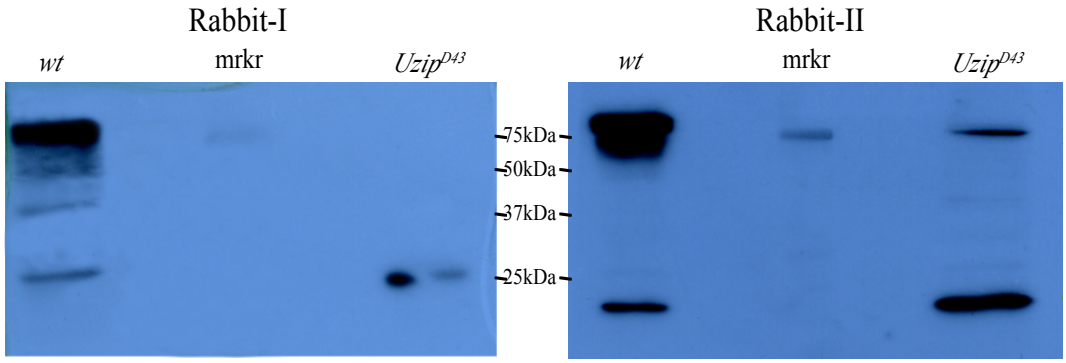

Figure 4.24. Western blot analysis with Uzip antibodies generated by Rabbit-I and Rabbit-II. Western blots were performed with the Uzip antibodies generated in Rabbit-I and Rabbit-II. Two bands above and below the 75kDa band, corresponding to the 65 kDa secreted and 80 kDa membrane bound form of Unzipped were detected that was not seen in the null mutant sample (*Uzip*^{D43}).

4.3.2.3. The Localization of the Unzipped Antibody. After testing the antibodies with Western blot, immunostainings on third instar eye imaginal discs and adults were performed. In the initial experiments a very high background was noticed, perhaps due to the small bands that were detected in the Western blot, which prevented the detection of the real signal (data not shown). To reduce this background the Unzipped antibody

generated by Rabbit II was preabsorbed against *Uzip*^{D43} null mutant embryos. The stainings were repeated using *Uzip*^{D43} null mutants obtained from the Huang group, *wt* flies, mCherry tagged BAC line generated by Kaan Mika in the lab (Kaan Mika, 2014), and the misexpression line obtained from the Huang group. The misexpression line from the Huang group is a UAS-Uzip line generated and tagged with CFP. These lines, if inserted in the right orientation can lead to the over-expression of the downstream gene, which is Unzipped in these constructs (Ding *et al*., 2011).

The null mutants and *wt* flies had some background staining all over the eye imaginal disc, no difference between the expression pattern of the two was noticed. However when the *UAS-Uzip* lines generated in our lab (1) and the Huang group (2) were misexpressed in the photoreceptors using the *lGMR-Gal4* driver, the expression of Unzipped increased in PRs a few rows after the MF, exactly at the location where the *lGMR* driver is expressed (Figure 4.25). These results suggest that our antibody is working since it recognizes Unzipped when it is misexpressed. The reason why there is no difference between the expression pattern in null mutants and wt flies can be either because Unzipped is expressed at a very low level and the difference cannot be detected, or Unzipped is not expressed in the PR cells at all.

After showing that the antibody recognizes Unzipped, we also analyzed its expression in the adult optic lobe. In wildtype flies Unzipped was expressed widely in the optic lobe, mainly in axon-like projections.

The labelled cells displayed a projection-like pattern in the M3 layer of the medulla, the termination region of R8 PR cells and was similar to the pattern compared to the short fragment rabbit antibody of the Huang group. From that layer their projections continue towards the lobula. There is also expression at the medulla cortex region, which is the region just at the entrance of the medulla. By looking at the structure and pattern, it is hard to recognize which cells and what type of cells Uzip is expressed in, however we can conclude that there is a layer to which the Uzip-expressing cells project in the middle of the medulla. This suggests that Unzipped might be projecting to the target layer in the medulla to regulate the termination of R8 PR cells (Figure 4.26).

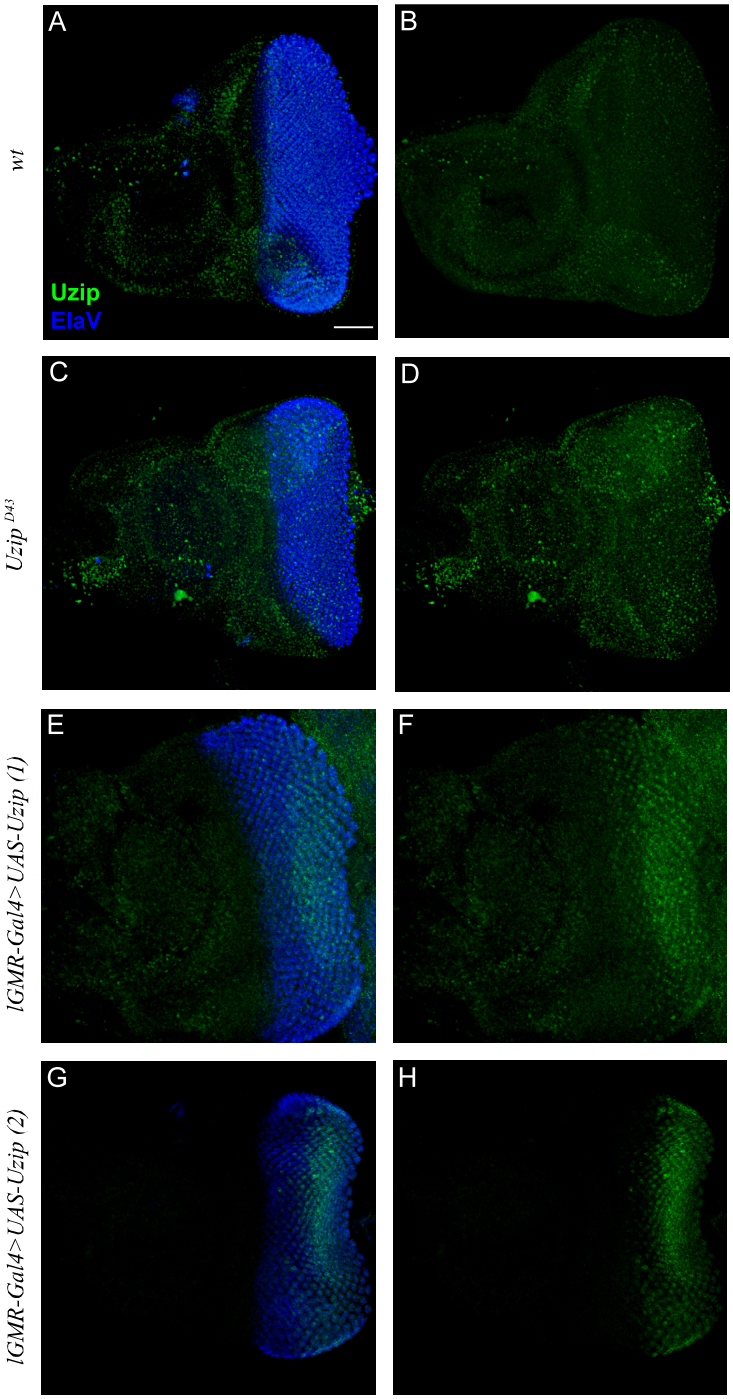

Figure 4.25. Antibody staining on 3rd instar larval imaginal eye discs using the Unzipped antibody. Immunostainings were performed with Unzipped (green), and Elav (blue). The Unzipped antibody did not give a specific expression in the *wt* (A, B) or null mutant *Uzip*^{D43} (C,D) flies, but the expression of Unzipped was detected in PRs in two different misexpression lines (E, F, G, H). Scalebar: 50 μm.

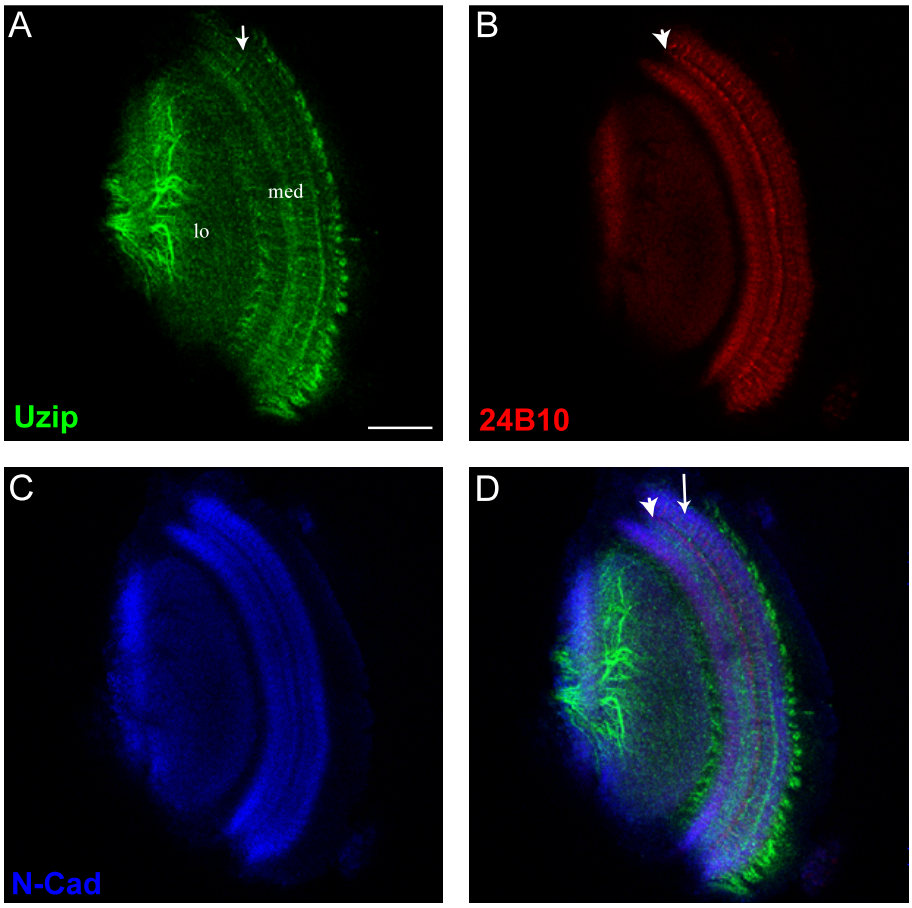

Figure 4.26. Antibody stainings with the Unzipped antibody in the whole-mount adult optic lobe. Immunostainings were performed with Uzip (green), 24B10 (red), and N-Cadherin (blue). The Unzipped expressing cells projected to the mid-layer (shown with arrow) (A) of the PR projecting cells (shown with arrowhead) (B). Uzip-green (A), 24B10-red (B), N-Cad (blue), merge (D). lobula (lo), medulla (med). Scalebar: 100 μm.

4.3.2.4. Uzip::mCherry BAC Line. A BAC transgenic line in which Unzipped was tagged at the C-terminus with the mCherry reporter has been generated by Kaan Mika in our lab in order to be used in genetic rescue experiments as well as localization studies (Kaan Mika, 2014). This line is expected to reflect the distribution of the membrane-bound form of Unzipped since it was tagged at the C terminus. This line has been used successfully in genetic rescue experiments and thus must be expressed very similar to endogenous Unzipped (Kaan Mika, 2014).

The expression pattern of Uzip::mCherry was compared with the localization data obtained from the enhancer-trap lines and antibody stainings. The Uzip::mCherry transgenic flies were stained with anti-dsRED antibody to visualize mCherry. The stainings were performed on eye imaginal discs at the third instar larval, 48hr APF pupal and adult retinas. In 3rd instar eye imaginal discs, the mCherry signal localized to the middle of ommatidia where R8 PR cells are localized (Figure 4.27). In some discs, the mCherry signal was also detected in larger cells at the glial layer, suggesting that the signal could be localizing to the membrane of the glial cells (Figure 4.27 D). These results are in accordance with the pattern observed with the enhancer-trap lines, indicating that mCherry-tagged Uzip is expressed in R8 and glial cells in the 3rd instar eye-imaginal disc.

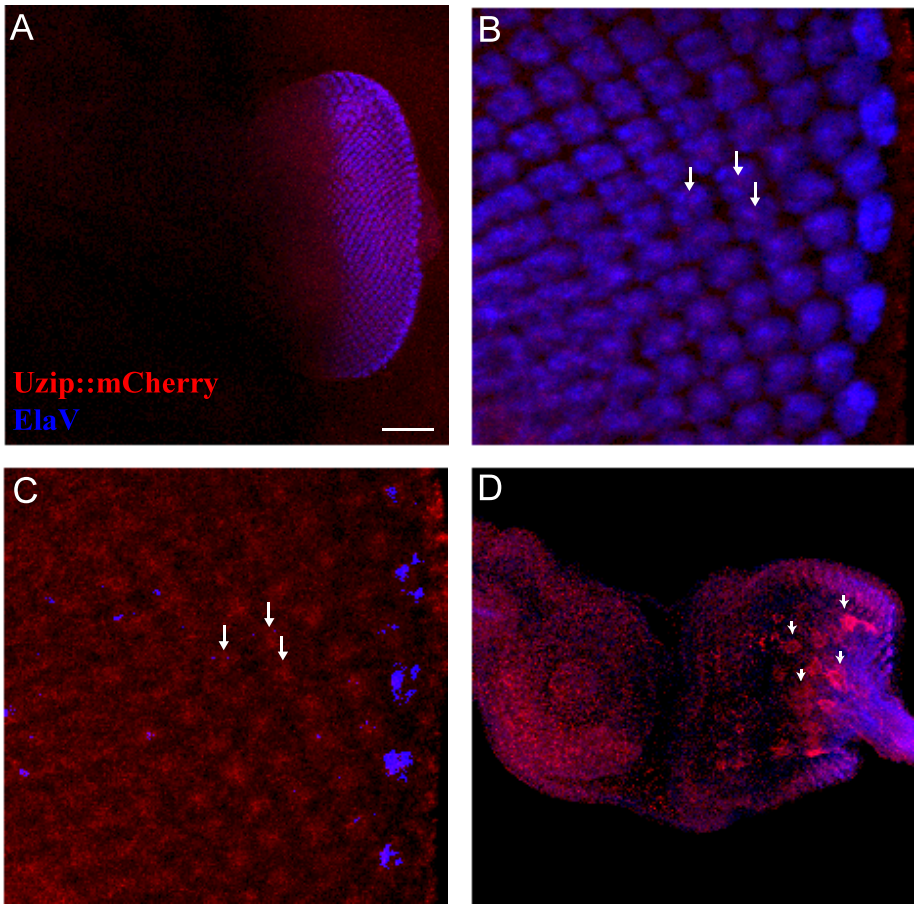

Figure 4.27. Uzip::mCherry expression in 3rd instar eye imaginal discs. Immunostainings were performed with dsRed for mCherry (red) and Elav (blue) (A). A mCherry signal was detected in the middle of ommatidia, where R8 cells reside (arrowheads) (B-C). Stainings in some glial cells were also observed (arrow) (D). Scalebar: 50 μm.

Pupal eye discs were stained with ds-Red at 48 hr APF in order to detect the expression of Uzip::mCherry. In the pupal stage there is a faint Unzipped expression coming from the R8 cells which colocalizes with *sens*, and from the middle of the ommatidia where no PR cells exist (Figure 4.28). It is possible that the membrane-bound Unzipped is expressed in adherens junctions and thus is observed in the middle of the ommatidia, where the membranes are dense. It could also be that this signal is generated by the axons of R8 cells, which leave the ommatidia from a central position. The localization to R8 cells is in coordination with the enhancer-trap expression pattern, suggesting that the membrane bound form of Unzipped is expressed in R8 cells and the enhancer-trap reflect endogenous Unzipped expression.

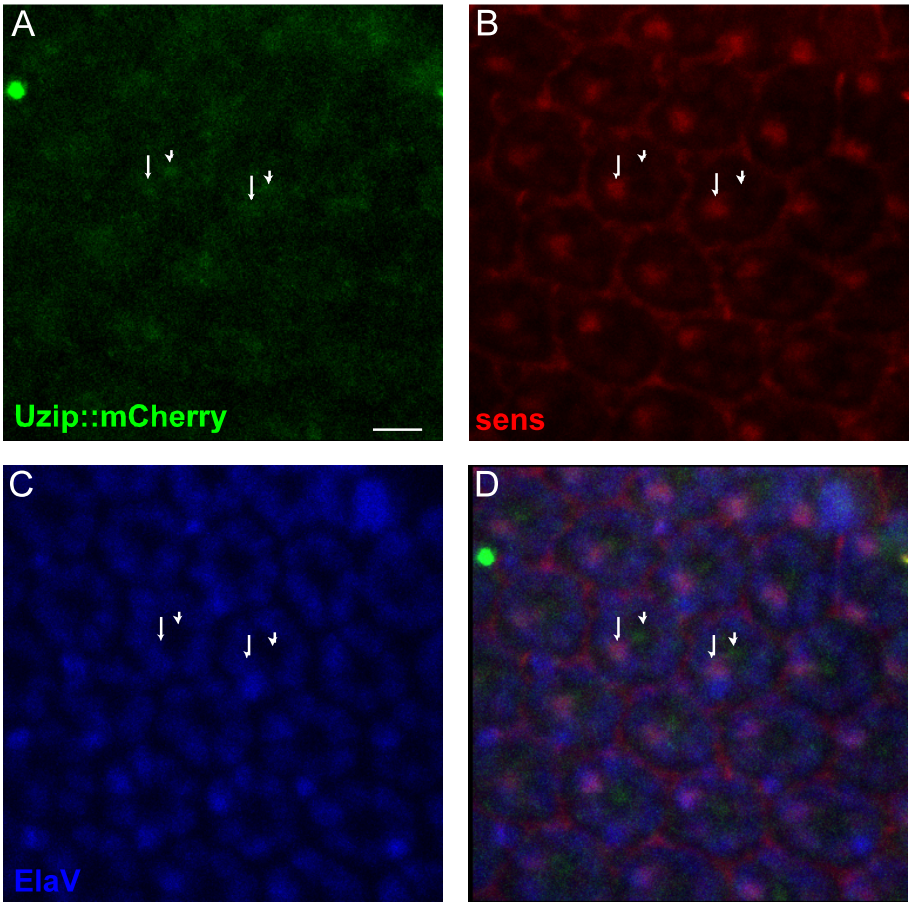

Figure 4.28. Uzip::mCherry expression in 48 hr APF. Immunostainings were performed with dsRed for Uzip::mCherry (green), Sens for R8 (red), ElaV for neuronal cells (blue). Uzip:mCherry is expressed both in R8 cells and the middle of the ommatidial cells in the 48 hr pupal retina. Uzip:mCherry (A), Sens (B), Elav (C), merge (D). Scalebar: 10 μm.

In the adult stainings, Uzip::mCherry expression was detected in axonal projections. This projection pattern was very similar to the projection observed with the 24B10 antibody, which labels PR axonal projections. Additional stainings in the optic lobe suggest that Uzip is expressed in glial subpopulations.

Uzip::mCherry is also expressed in a few cells in the lobula layer. We conclude that the membrane bound form of Unzipped localizes to the same layer as the PR cells, which is in accordance with the enhancer trap line expressions (Figure 4.29). As for the Uzip antibody stainigs from our lab and from the Huang group, Uzip localizes to the midlevel of the projection layer of the PR cells, which is presumably the M3 layer. From these results we can conclude that Uzip localizes to the M3 or M6 layer where the R8 and R7 axons project respectively.

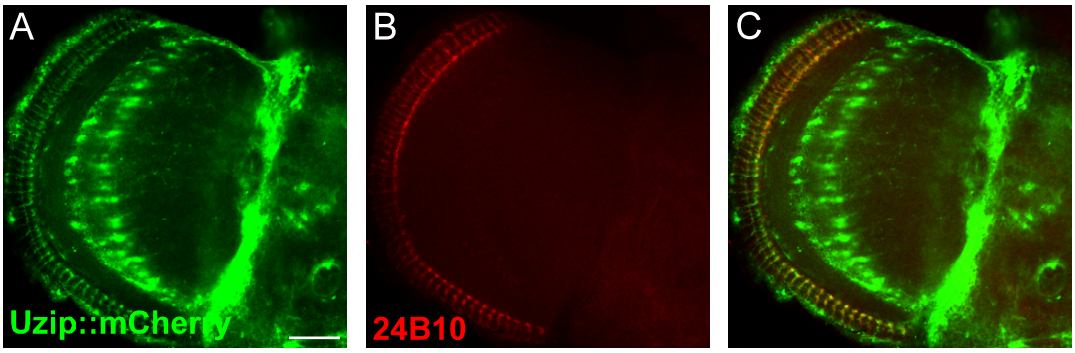

Figure 4.29. Uzip::mCherry expression in the adult optic lobe. Immunostainings were performed with dsRed for Uzip::mCherry (green) (A), and 24B10 to label PR axons (red) (B). The Uzip:mCherry-expressing projections co-localize with PR axons (C). Scalebar: 10 μm.

If we summarize the expression patterns observed in the enhancer traps, antibodies, and mCherry-tagged Uzip we can conclude that Unzipped is expressed in R8 cells and glial cells in the eye starting from the 3rd instar larva stage. Expression in the imaginal disc was not detected in wild type with the Unzipped antibodies. This might be due to a low expression level, the requirement for the optimization of the antibodies, or the localization. Since Unzipped is a CAM, it is possible that it is localized to the membrane or axons, which gives a weaker signal when scattered instead of accumulating in the nucleus. The R8-specific expression continues at the pupal stage. In the optic lobe, Unzipped localizes

mainly to projections of either neurons and/or glia. The projection pattern in the medulla resembles the PR axonal projections. The overall expression pattern is interesting and is consistent with a role of Unzipped in one or more aspects of PR differentiation.

4.4. Characterization of Unzipped Mutants

Our initial experiments showed that Unzipped is expressed in the PR R8, which is the first PR to be specified. It is also the first PR that extends its axon towards the optic lobe. As the R8 cell has a central role in these processes, a gene like unzipped which shows such specific expression might be one of the molecules mediating the functions of the R8 cell. Thus in loss of function experiments we would expect to observe problems in the specification of all other PRs, and in terms of the projection patterns we would also expect defects in the proper projection of PR axons.

In order to investigate Unzipped function in these processes we made use of mutant lines that were generated and described in the publication by Ding *et al.,* 2011. According to this there are two mutants: $Uzip^{D43}$ null mutants and $Uzip^{23}$ hypomorph mutants. The null mutants obtained from the Huang group are generated by the mobilization of two P-elements in the *f01534* and *f02244* flies and the deletion of the region in between (Figure 4.30 A). The $Uzip^{23}$ hypomorph mutants were generated by the mobilization of the P-element containing EP-C0410 line and the partial deletion of the region, but the coding sequence remained intact. Due to the partial deletion, Unzipped is expressed at a reduced level (Figure 4.30 B) (Ding *et al*., 2011).

Analysis was started at early developmental stages to assess the role of *uzip* at early stages of specification and projection.

4.4.1. Role of *unzipped* in PR specification

We have shown that Unzipped is expressed in R8 cells using various enhancer-trap lines and a fusion protein (see Figure 4.8, Figure 4.9, Figure 4.12, andFigure 4.25). The R8 cell is the first of the PRs to be specified and the specification of all other PRs depend on

it. Here, we investigate the possible role of Unzipped in the specification of PRs. For this purpose we analyzed the specification of R8 cells as well as R7 cells, which are the last to be specified.

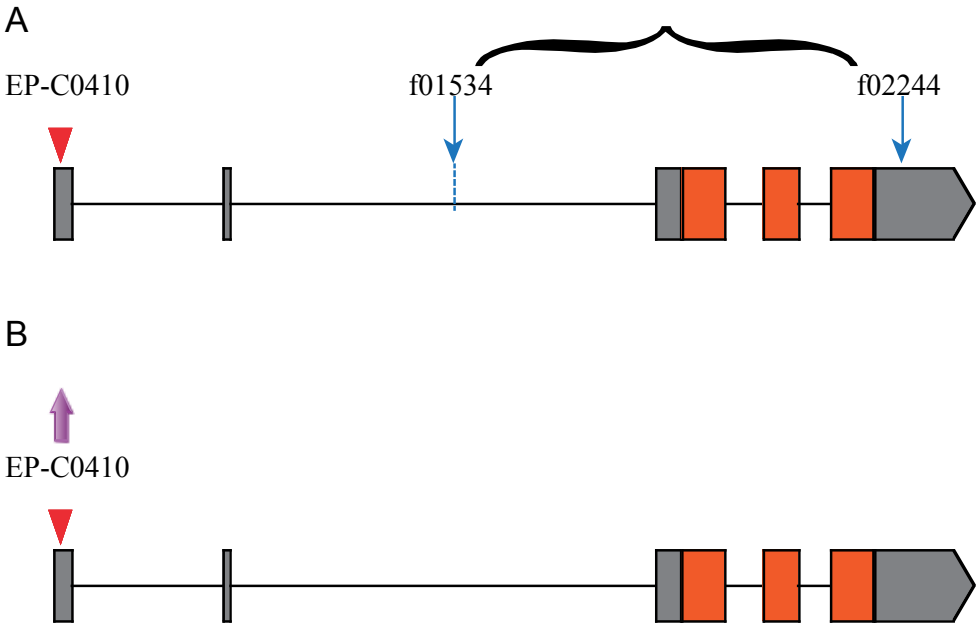

Figure 4.30. The Uzip genomic locus and description of *Uzip*^{43} and *Uzip*^{23} lines. The *f01534* and *f02244* P-element lines are mobilized and result in the deletion of the region in between, forming *Uzip*^{D43} null mutants (A). The mobilization of the EP-element results in a partial deletion of the Unzipped gene, forming *Uzip*^{23} (B). (Adapted from Ding *et al*., 2011).

4.4.1.1. Effect of unzipped on R8 specification. 3rd instar larval imaginal eye discs from *Uzip*^{D43} mutants and the *lGMR-Gal4>UAS-Uzip(1)* flies were stained with Elav and the R8 marker Senseless and the number and distribution of R8 cells were analyzed. In *Uzip*^{D43} mutants and the mis-expression background *lGMR-Gal4>UAS-Uzip(1)* one senseless-positive cell could be observed per ommatidium. Thus, no difference in R8 cell expression and distribution was observed as compared to *wt* flies. From these stainings we can conclude that the changes in Uzip levels do not affect the specification of R8 cells and the expression of Senseless (Figure 4.31).

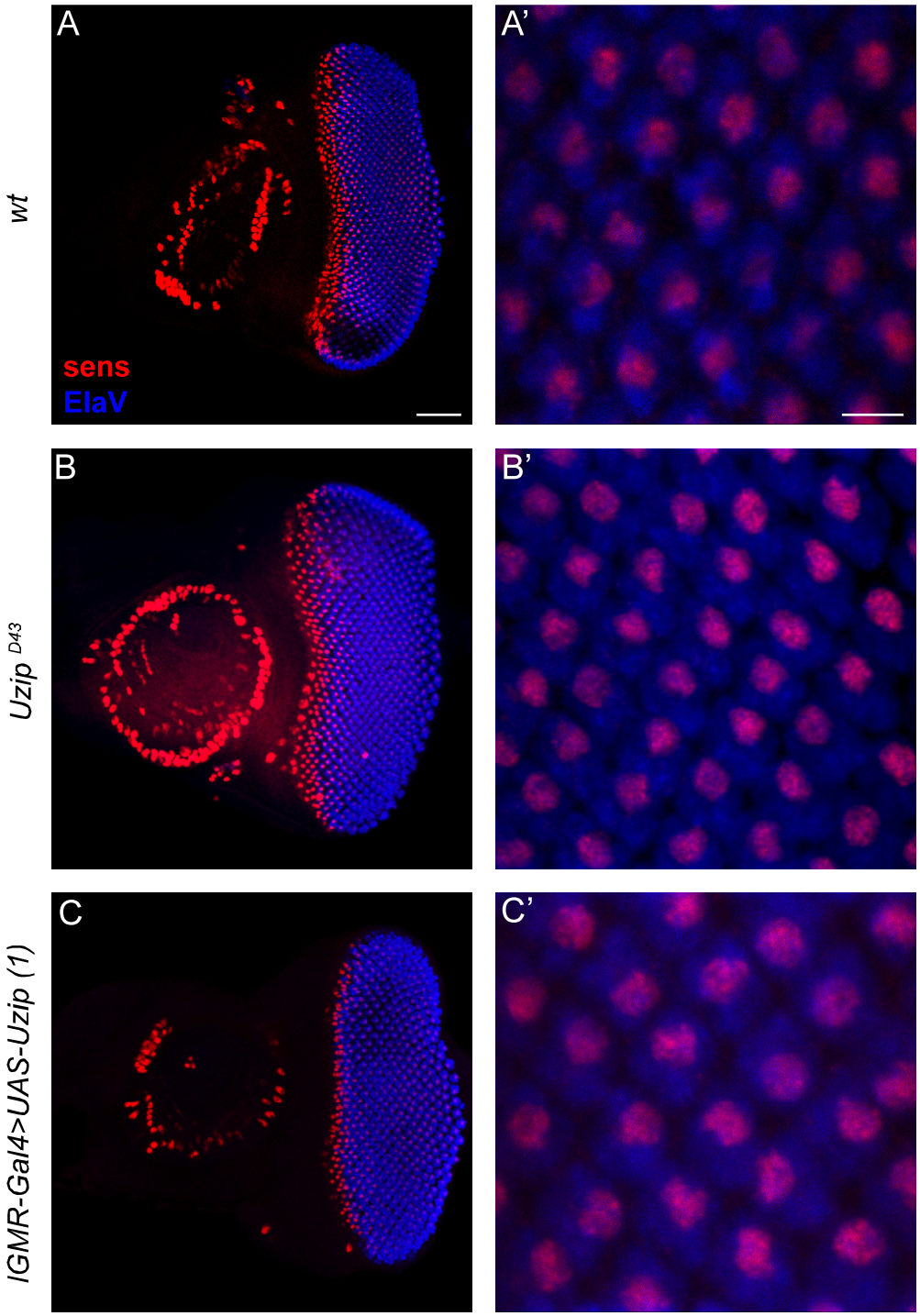

Figure 4.31. Analysis of R8 differentiation in different Uzip backgrounds in the 3rd instar eye discs. 3rd instar larva eye disc stainings were performed with Sens (red) and Elav (blue). The localization or the expression of R8 cells does not change in *Uzip*^{D43} mutants and *lGMR-Gal4>UAS-Uzip(1)* flies. *Wt* (A-A'), *Uzip* ^{D43} (B-B'), *lGMR-Gal4>UAS-Uzip (1)* (C-C') Scalebars: 75 μm and 10 μm, respectively.

Similarly, stainings of pupal retinas were also performed at the 48 hr APF in order to see if any changes could be observed at later stages of development. Retinas taken from *wt*, *Uzip*^{D43}, and *lGMR-Gal4>UAS-Uzip(1)* flies were stained with Sens and Elav. In all genotypes analyzed Senseless staining was observed in one cell per ommatidium. Thus, no change was observed in the expression or distribution of R8 cells at this stage, indicating that changing Unzipped levels does not affect later stages of R8 differentiation (Figure 4.32).

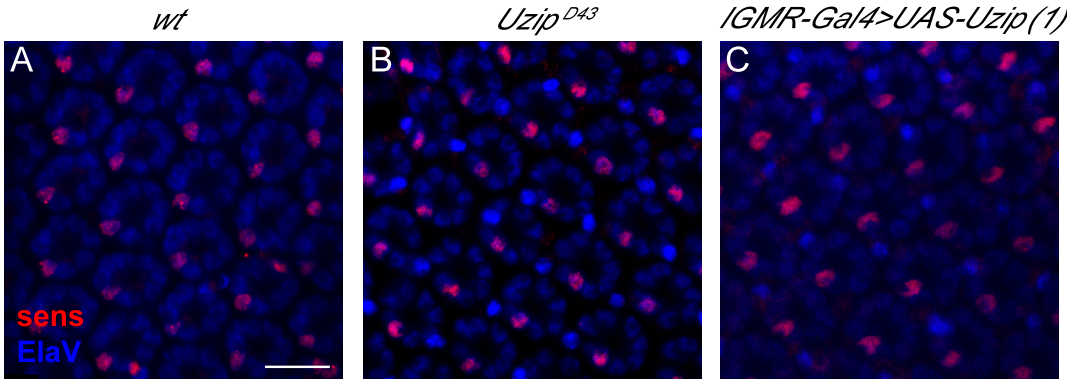

Figure 4.32. Analysis of R8 differentiation in different Uzip backgrounds 48hr APF. 48 hour pupal disc stainings were performed with Sens (red) and Elav (blue). The number and localization of R8 cells within ommatidia does not change in *Uzip*^{D43} mutants and *lGMR-Gal4>UAS-Uzip(1)* flies. *Wt* (A), *Uzip* ^{D43} (B), *lGMR-Gal4>UAS-Uzip (1)* (C). Scalebar: 10 μm.

4.4.1.2. Effect of Unzipped on R7 Specification. Unzipped is not expressed in R7 cells, however it is known that R8 cells affect the differentiation of all the other PR cells including R7 cells that are the last ones to differentiate. Since R7 and R8 interact with each other throughout the specification process, we wanted to test if the change in Unzipped levels causes a change in R7 cell specification. *Prospero*, the most commonly used R7 marker, was used to detect any potential change in the specification of R7 cells. However, since *Prospero* stains both R7 cells and cone cells, it was difficult to observe if there is any difference in R7 cell specification but the overall expression pattern in the eye discs looked similar in *wt*, *Uzip*^{D43}, and *lGMR-Gal4>UAS-Uzip(1)* flies (Figure 4.33).

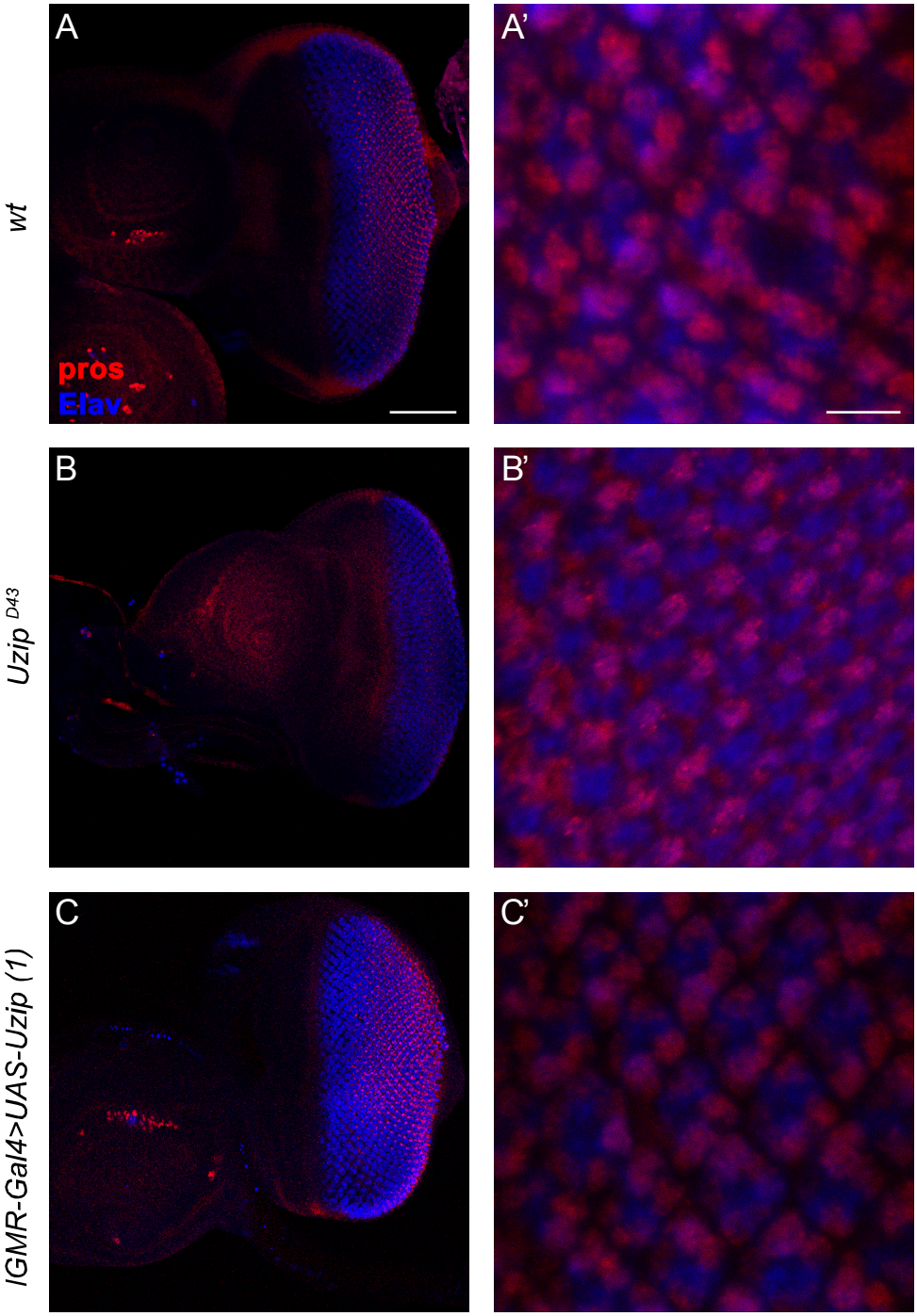

Figure 4.33. Analysis of R7 differentiation in different Uzip backgrounds at the 3rd instar larval stage. Immunostainings were performed with Prospero (red) and Elav (blue) (A', B', C'). A change in staining pattern of *Uzip*^{D43} mutants and *lGMR-Gal4>UAS-Uzip(1)* flies is not detected (A,B,C). *Wt* (A-A'), *Uzip* ^{D43} (B-B'), *lGMR-Gal4>UAS-Uzip (1)* (C-C'). Scalebars: 75 μm and 10 μm.

The stainings were repeated with 48 hr pupal discs, where R7 cells are easily distinguished from cone cells. In 48 hr APF eye discs one R7 cell per ommatidium was stained by Prospero (Figure 4.34). From these stainings, we can conclude that the changes in Unzipped levels do not affect R7 differentiation.

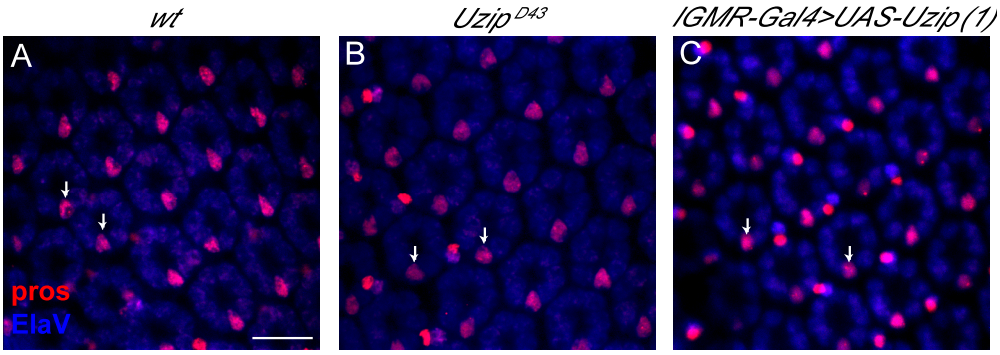

Figure 4.34. Analysis of R7 specification in different Uzip backgrounds 48hr APF. 48 hour pupal disc stainings were performed with Prospero (red) and Elav (blue). The R7 cells (arrows) can be differentiated by their localization inside the ommatidia. The R7 cells and their expression patterns do not change in *Uzip*^{D43} mutants and *lGMR-Gal4>UAS-Uzip(1)* flies. *Wt* (A-A'), *Uzip* ^{D43} (B-B'), *lGMR-Gal4>UAS-Uzip (1)* (C-C'). Scalebar: 10 μm.

4.4.2. The Effect of *unzipped* on PR Axonal Projections in Larval Stages

In order to analyze the effect of the deletion and misexpression of Unzipped on PR cell projections, the PR cell-specific CAM Chaoptin, which is a PR membrane marker, was used. *wt* (Figure 4.34 A,A'), *Uzip*^{D43}, *Uzip*^{D43}*/+,* and *lGMR-GAL4>UAS-Uzip (1)* flies were stained with Chaoptin (24B10) and Elav. In *wt* flies, a group of PR axons projected from the eye disc to the optic lobe and terminated in the lamina, forming a layer of densely packed growth cones called the lamina plexus (Figure 4.34 arrows). Looking at the morphology, these PRs that terminate in the lamina plexus were evaluated as being outer PRs (Figure 4.34). The PRs moving past the lamina plexus in an arch form are the inner PRs, which project past the lamina to their temporary layers. The PR projections of the mutants and the misexpression lines did not show any significant change in the overall pattern (Figure 4.35). With the Chaoptin (24B10) stainings, the general projection pattern is revealed, but we cannot come to a clear conclusion on the projections of specific PRs separately.

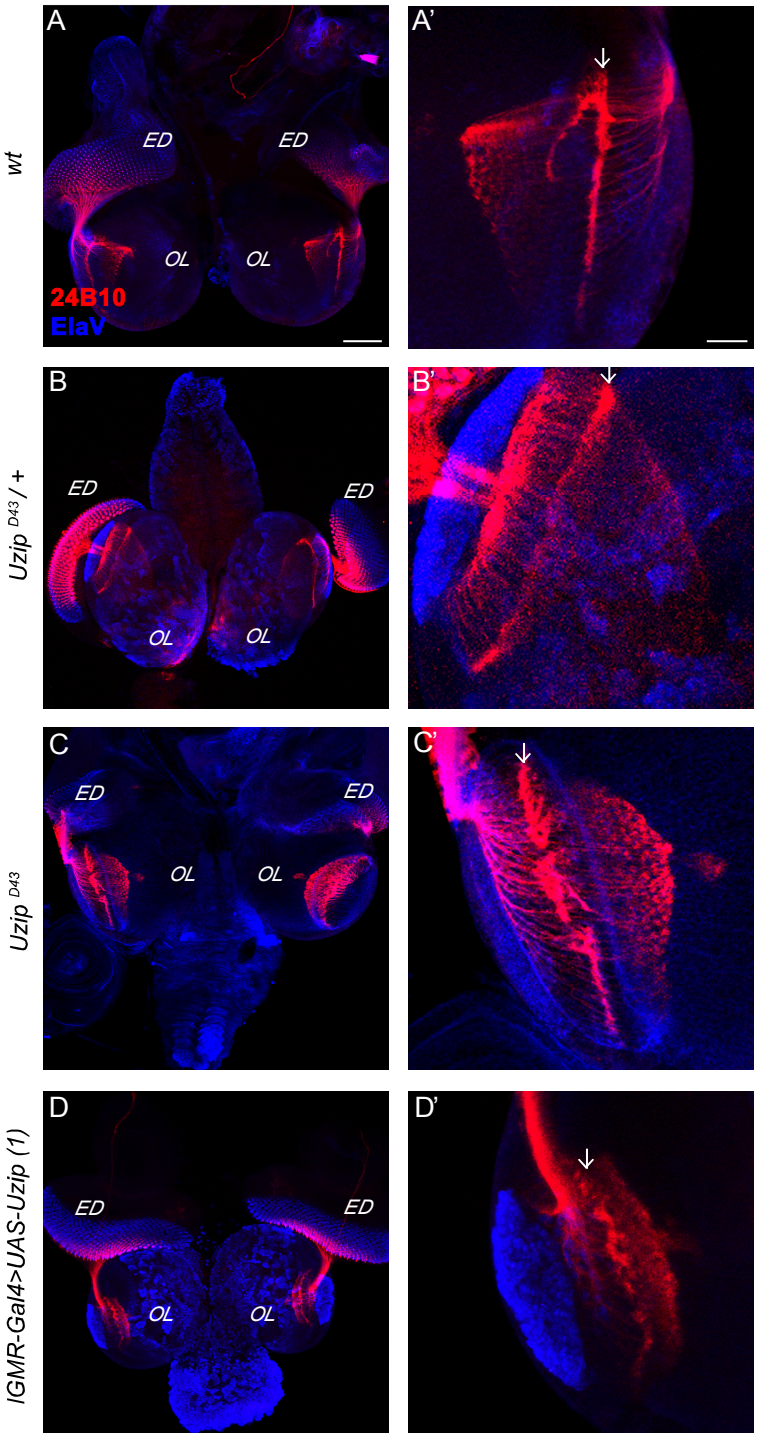

Figure 4.35. PR projection analysis of Unzipped mutants in the 3rd instar larval stage. Attached eye disc-brain stainings were performed with 24B10 (red) and Elav (blue). The lamina plexus (arrows) and the arch-like shape formed by the inner PRs in wt flies (A-A'). does not change in *Uzip*^{D43}/+ flies (B-B'), *Uzip* ^{D43} (C-C'), and *lGMR-Gal4>UAS-Uzip (1)* flies (D-D'). Eye disc (ED), Optic lobe (OL). Scalebars: 100 µm and 50 µm.

4.4.3. Effect of *unzipped* on the Glial Marker Repo

In order to observe the effect of deleting and misexpressing Unzipped on glial cells; *wt*, null mutant *Uzip*^{D43}, *lGMR-GAL4>UAS-Uzip (1)*, and *lGMR-Gal4>UAS-Uzip (2)* flies were stained with the neuronal marker Elav and the glial marker Repo. The structure of glial cells was analyzed. Additionally the extent of migration of glial cells was assessed. However, no major difference in the structure, number or migration of Repo-positive glial cells was observed (Figure 4.36). These stainings suggest that the knockout of Unzipped and misexpression of Unzipped in PR cells do not affect glial cell number or distribution.

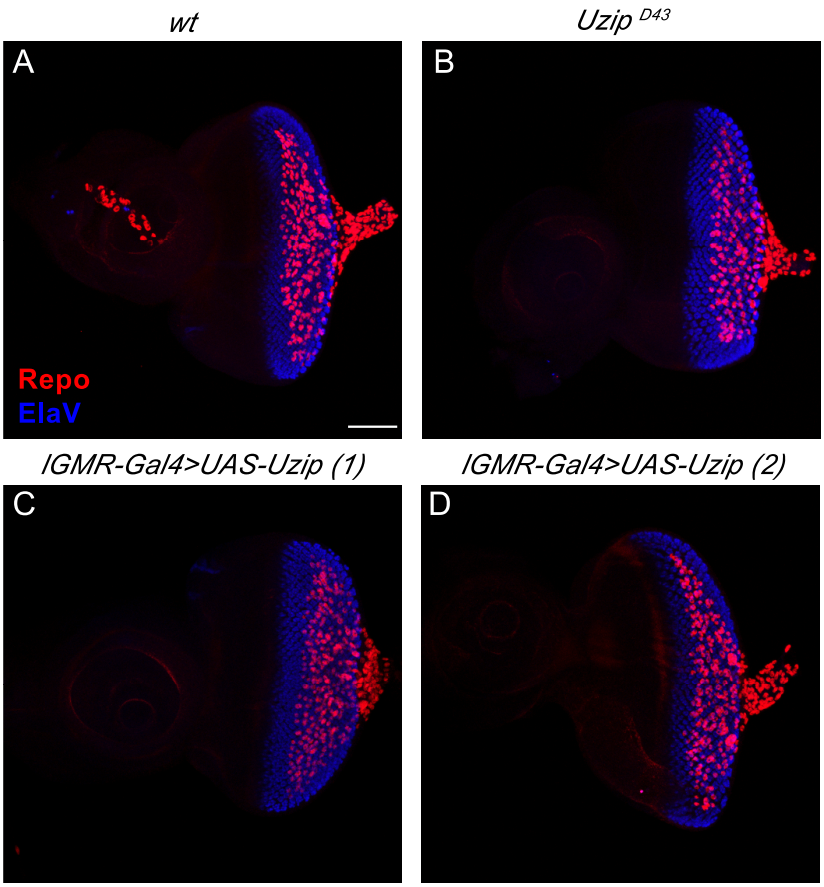

Figure 4.36. Analysis of the effect of Uzip mutation and misexpression in 3rd instar larval eye discs. Immunostainings were performed with Repo (red) and Elav (blue). The structure, number and migration of glial cells does not change in *Uzip*^{D43}, *lGMR-GAL4>UAS-Uzip (1)*, and *lGMR-Gal4>UAS-Uzip (2)* flies. *Wt* (A), *Uzip* ^{D43} (B), *lGMR-Gal4>UAS-Uzip (1)* (C), *lGMR-Gal4>UAS-Uzip (2)* (D). Scalebar: 25 μm.

4.5. Functional Analysis of *unzipped* Mutants

Although Unzipped does not appear to have a role in the early specification and differentiation of PR cells and glial cells, it is possible that it has a role in the terminal differentiation phase. At this final stage, PRs start to express subtype-specific Rhodopsins and the PR axons project to their final layers. Thus, the function of Unzipped and its potential role in subtype specification and targeting were analyzed.

4.5.1. Effect of Unzipped on Subtype Specification

In order to understand the effect of Unzipped on subtype specification, adult retinas were stained with Rh5 and Rh6, which are Rhodopsins expressed by the R8 cells. The R8 cells differentiate later than R7 cells and the subtype choice in R8 cells depends on the overlying R7 cells. Any change in the Rh5/Rh6 ratios should reveal a difference in R8 subtype specification as well as R7 subtype specification, since it directly affects the underlying R8 cell within the same ommatidium.

First the hypomorph and null mutants were analyzed for Rh5/Rh6 expression. Rh5 and Rh6 are expressed in a 30:70% ratio in the retina of wt flies. 12 retinas were dissected for the $Uzip^{23}$ hypomorphs and 15 retinas were dissected for $Uzip^{43}$ null mutants. The visual observation is not sufficient to understand the changes in the ratios, since the distribution of the Rh5 and Rh6 expressing R8 cells can change the perception. Due to this reason the Rh5 and Rh6 expressing R8 cells were quantified. The ratio of Rh5/Rh6 was 43,5 - 56,5% in $Uzip^{23}$ flies and 36-64% in $Uzip^{43}$ flies. Representative whole-mount retina stainings can be seen in Figure 4.37.

When compared with 43 – 57 %, which is the wt ratio in our stainings, the Rh5 ratio is almost the same in hypomorphic mutants with 43.5%. In the null mutants there is a slight decrease in the Rh5 expression level with 36 – 64 %. (Figure 4.38). This is a mild change and there are no factors or molecules reported in literature that give rise to such minor changes in subtype specification. There are no CAMs reported to be involved in subtype specification either, but it is important to keep in mind this slight change.

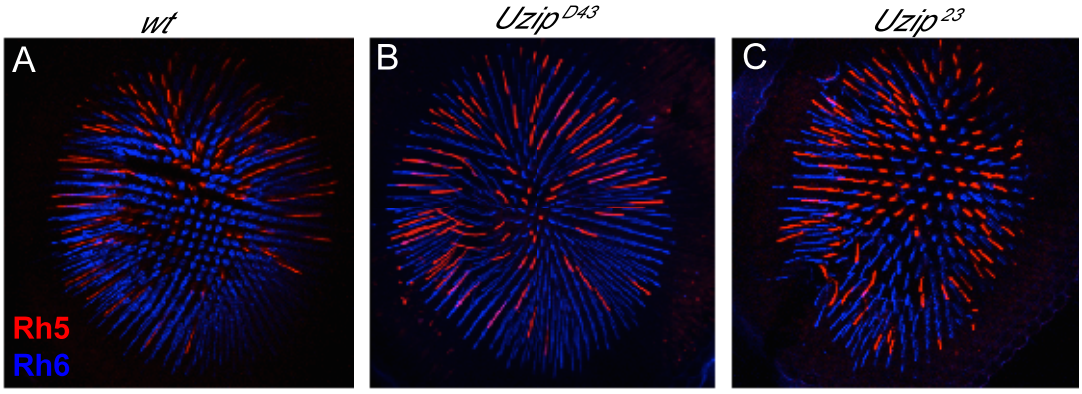

Figure 4.37. Analysis of Unzipped mutants and their effect on subtype specification. Adult, whole-mount retinas were stained with anti-Rh5 (red) and anti-Rh6 (blue) antibodies. Each R8 expressing Rh5 or Rh6 was counted, and the ratios were calculated. Images of *wt* retina (A), null mutant retina (*Uzip*^{D43}) (B), and hypomorph retina (*Uzip*^{23}) (C) are shown.

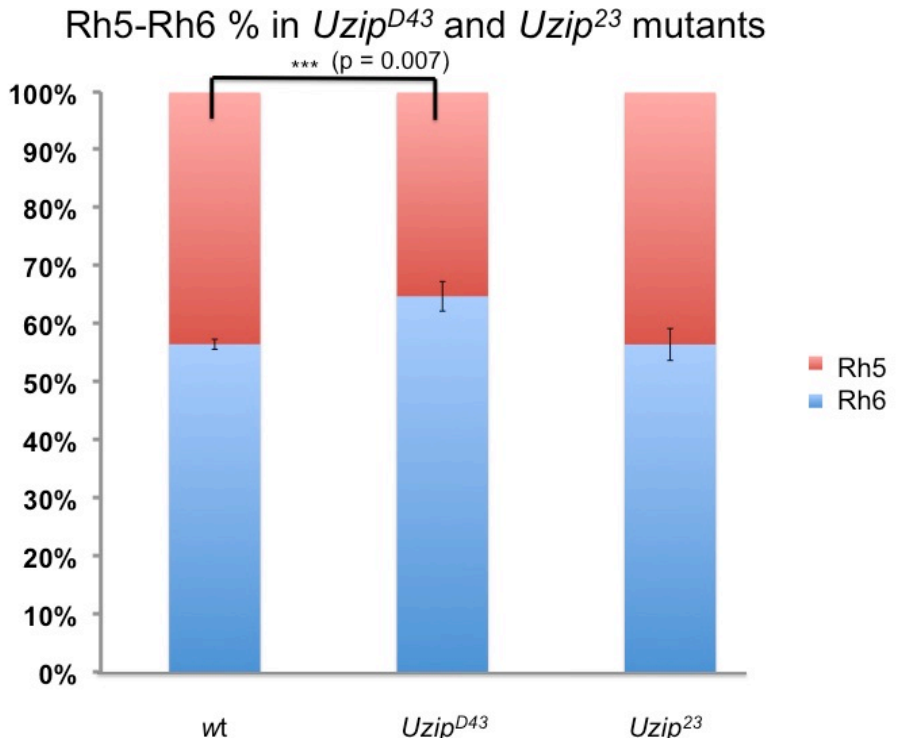

Figure 4.38. Statistical Analysis of the Rh5/Rh6 ratios in Unzipped mutant flies. The Rh5 and Rh6 ratios were calculated for Unzipped mutant flies in the PRs. From left to right in the graph: wt (n=10, N=4225), *Uzip* ^{D43} (n=15, N=6933), and *Uzip* ^{23} (n=12, N=5980). The Rh5 - Rh6 % ratio of *Uzip*^{23} is 43,5 – 56,5 %, and *Uzip* ^{D43} *is* 36 – 64 % compared to the 43 – 57 % *wt* group. Error bars SD. ($p<0.05$ Student two tailed T-Test)

We also performed a knockdown experiment by driving *UAS-Uzip-RNAi* line by the PR driver *lGMR*. From the visual inspection of the images, no significant change in Rh5/Rh6 expression was noticed and the distribution was similar to the null and hypomorph mutants, thus no effect on subtype specification was observed and the statistical analysis for the Unzipped knockdown experiments was not performed (Figure 4.39). Therefore, the statistical analysis for the Unzipped knockdown experiments was not performed.

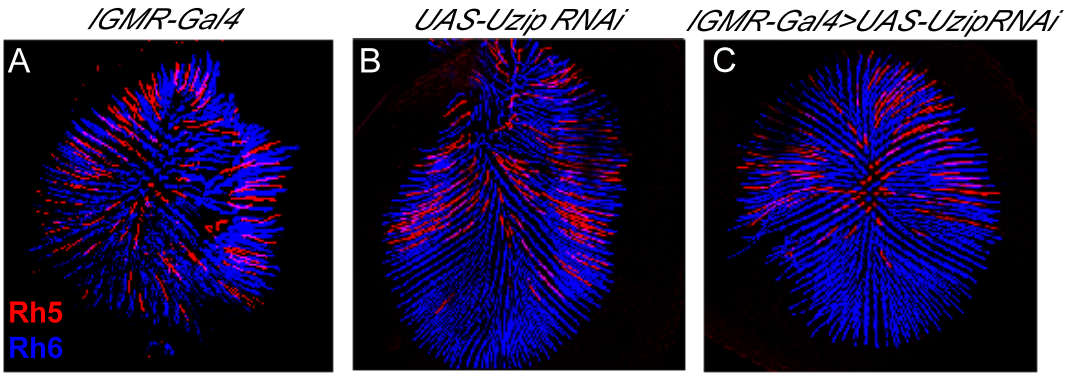

Figure 4.39. Analysis of whole-mount adult retinas after Unzipped downregulation. Retinas were stained with anti-Rh5 (red) and anti-Rh6 (blue) antibodies. Images of *lGMR-Gal4* (A), *UAS-Uzip RNAi* (B), and *lGMR-Gal4>UAS-Uzip RNAi* (C) whole-mount retina stainings.

We also tested if the misexpression of Unzipped in PR cells caused any change in the p/y subtypes. *Wt*, *lGMR-Gal4*, and *UAS-Uzip* flies were used as controls for the overexpression experiment *lGMR-Gal4>UAS-Uzip*. Adult retinas were dissected and stained with Rh5 and Rh6 (Figure 4.40).

11 retinas were analyzed and the ratio of Rh5/Rh6, thus p/y was calculated as 37/63 % in *lGMR-Gal4>UAS-Uzip* flies. This ratio is very close to the number of Rh5 and Rh6-expressing cells in the diverse controls that were used in this experiment. We thus conclude that misexpression of Unzipped in all PRs does not have an effect on subtype specification (Figure 4.41).

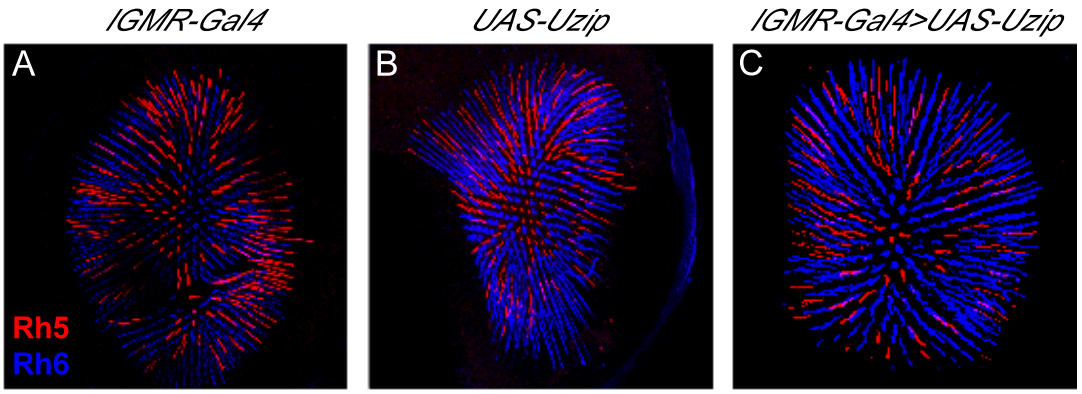

Figure 4.40. Analysis of Unzipped misexpression in the adult retina. Adult retinas were stained with anti-Rh5 (red) and anti-Rh6 (blue) antibodies. Each R8 expressing Rh5 or Rh6 was counted and the ratios were calculated. Images of *lGMR-Gal4* (A), *UAS-Unzipped* (B), and *lGMR-Gal4>UAS-Unzipped* retina (C) whole-mount stainings.

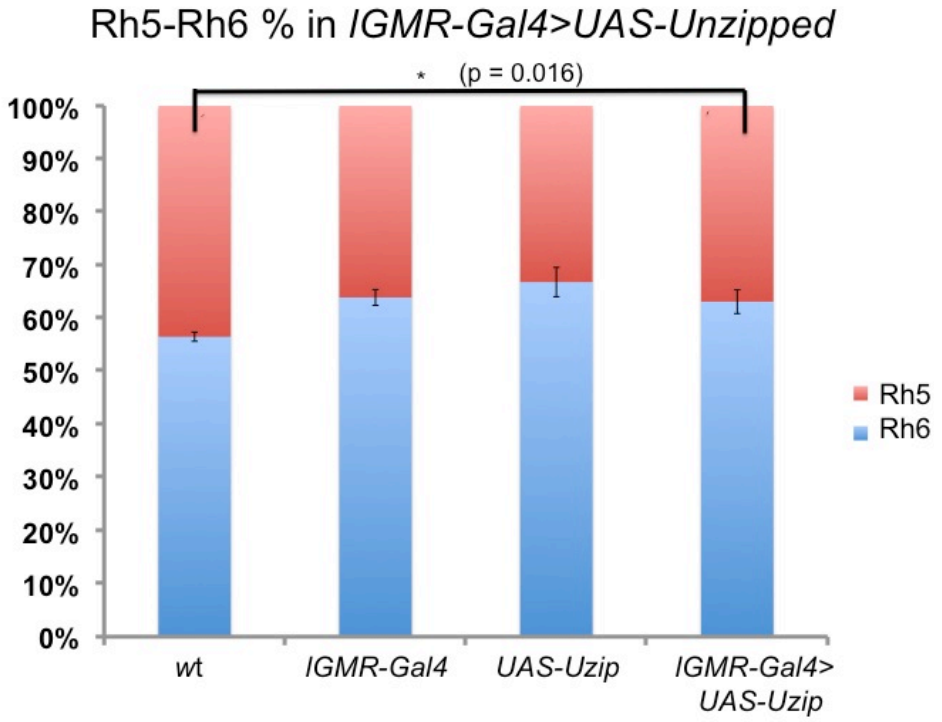

Figure 4.41. Statistical analysis of the Rh5/Rh6 ratios in *lGMR-Gal4>UAS-Uzip* flies. The Rh5 and Rh6 ratios for Unzipped misexpression in PRs from left to right: *wt* (n=10, N=4225), *lGMR-Gal4* (n=3, N=1202), *UAS-Uzip* (n=2, N=794), *lGMR-Gal4>UAS-Uzip* (n=11, N=5980). The Rh5/Rh6 ratio of *lGMR-Gal4>UAS-Uzip* is 37-63% compared to the 43-57% in the wt group. Error bars are SD. ($p<0.05$ Student two tailed T-Test)

4.5.2. Analysis of the effect of Unzipped on PR projections

Unzipped is a CAM molecule shown to be involved in CNS axonal targeting at the embryonic stage (Ding *et al.*, 2011). It is also known that CAMs are actively involved in PR targeting, making Unzipped a strong candidate for regulating axonal targeting. In order to analyze the effect of Unzipped on PR projections we analyzed axonal targeting in different Unzipped backgrounds.

4.5.2.1. Effect of Loss of Unzipped on R7 And R8 Axon Targeting to the Optic Lobe. First we analyzed Unzipped null mutants for changes in the projection pattern of R7 and R8 cells. To visualize axonal projections of PR neurons, different reporter lines were used. Rh-lacZ transgenic lines have been previously generated by fusing the promoters of Rh genes to the lacZ reporter and injecting these to embryos (Tahayato *et al*., 2003) The lacZ tag allows tracing the axons expressing the tagged Rhodopsins to their final destinations, by labeling their cytoplasm. Rh3-lacZ and Rh4-lacZ are expressed in R7 cells and thus label the pale and yellow subset axonal projections, respectively; Rh5-lacZ and Rh6-lacZ are expressed in the pale and yellow subsets in R8 cells and label their axons, respectively.

The Rh3-lacZ-Rh6-lacZ reporter lines were crossed into the respective backgrounds to allow for analysis of projections in differently perturbed Unzipped backgrounds. In case of the $Uzip^{D43}$ mutant, four lines were generated: '$Uzip^{D43}$, *Rh3-lacZ*'; '$Uzip^{D43}$, *Rh4-lacZ*'; '$Uzip^{D43}$, *Rh5-lacZ*'; and '$Uzip^{D43}$, *Rh6-lacZ*'. Homozygous null mutant flies carrying the reporter constructs were selected and their brains were dissected. Flies carrying only *Rh3-lacZ, Rh4-lacZ, Rh5-lacZ*, and *Rh6-lacZ* constructs without the null mutant were used as controls. We observed that both R7 and R8 cells projected to their proper destinations in *wt* and the *Uzip* null mutant flies (Figure 4.42). The *Rh3-lacZ* and *Rh4-lacZ* expressing R7 cells stopped at the M6 layer (Figure 4.42 A,B,C,D), while the Rh5-lacZ and Rh6-lacZ expressing R8 cells terminated in the M3 layer as expected (Figure 4.42 E,F,G,H).

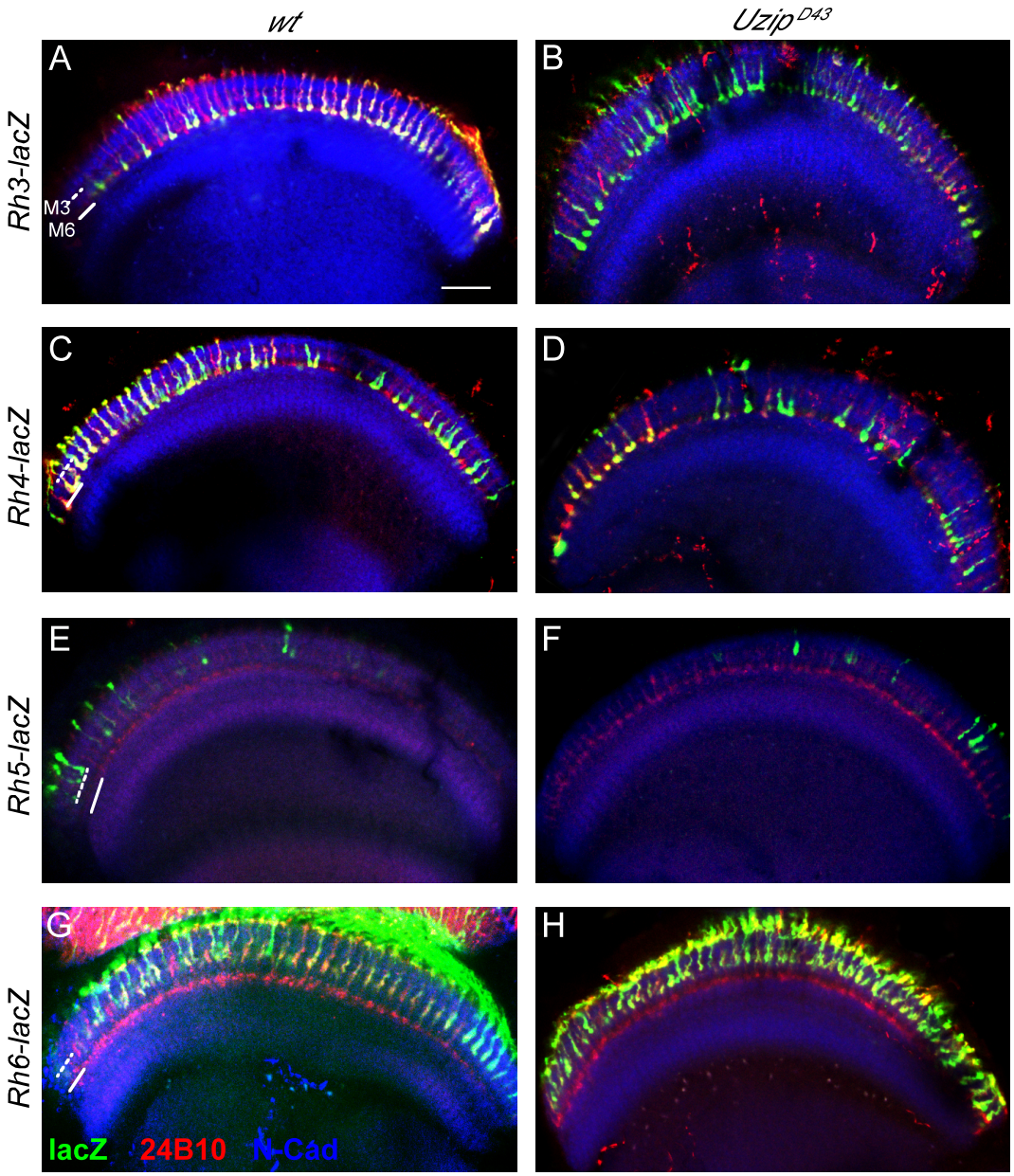

Figure 4.42. Projection analysis of R7 and R8 cells in Uzip null mutants. Adult whole-mount brains are stained with β-Gal (green), 24B10 (red), and N-Cad (blue). The dashed line is at M3, the straight line is at M6. *Rh3-lacZ* and *Rh4-lacZ*-expressing R7 cells project to the M6 layer in null mutants and wt flies (A-D). *Rh5-lacZ* and *Rh6-lacZ*-expressing R8 cells project to the M3 layer in null mutants and *wt* flies (E-H). Scalebar: 25 μm.

These results are in line with previous observations by Ding *et al*., 2011 where no significant changes in the projection pattern of neurons in the ventral nerve cord of the null

mutants was observed. Phenotypes were observed only in combination with the deletion of other molecules involved in the same pathway. We have shown that Unzipped is expressed on PR neurons as well as in glial cells in the imaginal disc and the target region, the optic lobe. Unzipped has been shown to interact homophilically. Thus, the reason why no phenotype is observed in axonal targeting might be due to the fact that Unzipped is removed from both the incoming neurons and the target area and thus no imbalance is created. In addition, redundant molecules might be replacing its function. Therefore, we chose to unravel the possible function of Unzipped by changing its levels selectively either in the outgrowing neurons or its target cells. We focused on the R8 cell as this is the major cell type where Unzipped appears to be expressed.

4.5.2.2. Effect of Specific Downregulation of Unzipped on R8 Axonal Projections. Uzip was downregulated in different groups of neuronal and glial cells separately. From the previous experiments performed to reveal the expression pattern of Unzipped, we concluded that Uzip is expressed in R8 cells as well as a subgroup of glial cells including the ones in the target area of inner PR axons. Downregulation of Unzipped in different cell types known to express it might lead to an imbalance which can not be tolerated and compensated. In that case we should observe phenotypes in axonal projection where R8 cells do not project to the expected layer or in the expected column. According to the cells in which Uzip is downregulated and the phenotype observed, we can comment on the role of Unzipped expression in neuronal and glial cells for axonal projection.

Different neuronal and glial drivers were used for driving an Unzipped RNAi line. For neuronal drivers *Elav* was used as an early and late neuronal driver, *lGMR* as a PR-specific driver, and *sens* as an R8-specific driver. A number of different drivers were used for downregulating Unzipped in glial cells. For this purpose, *gcm* was used as an early glial driver, *repo* as a later glial driver, and *moody* as a carpet-glia driver. The drivers were first tested if they are expressed in the cells as expected. Several criteria were chosen for phenotype evaluation. In addition to mistargeting these included branching of neurons in the target area, thickness of axonal ends, end-joining,where the ends of two axons join each other instead of targeting within their own columns, and bundling where a group of axons bundle together and project as a bundle in a single column instead of projecting separately to their target layers in their own columns.

In order to increase the efficiency and the penetrance of RNAi effects experimental crosses were kept at 29°C. It is known that increased temperatures increase Gal4 expression. In these experiments one out of three RNAi lines, the *UAS-Uzip-RNAi* line with the highest penetration efficiency was chosen (Çevrim Ç *et al*., *in preparation*). '*Rh5-lacZ'*; '*Uzip-RNAi, Rh5-lacZ'*; '*Rh6-lacZ'*; and '*Uzip-RNAi, Rh6-lacZ'* lines were used as controls and they were stained with β-Gal before crossing with any driver.

A few axons expressing *Rh5-lacZ* and *Rh6-lacZ* control lines mistargeted to other layers at 29°C (Figure 4.43 A,C). This number further increased when the *Uzip-RNAi* line was crossed with these reporter lines (Figure 4.43 B,D). This increase in the number of mistargeting axons was taken into account during quantification and analysis.

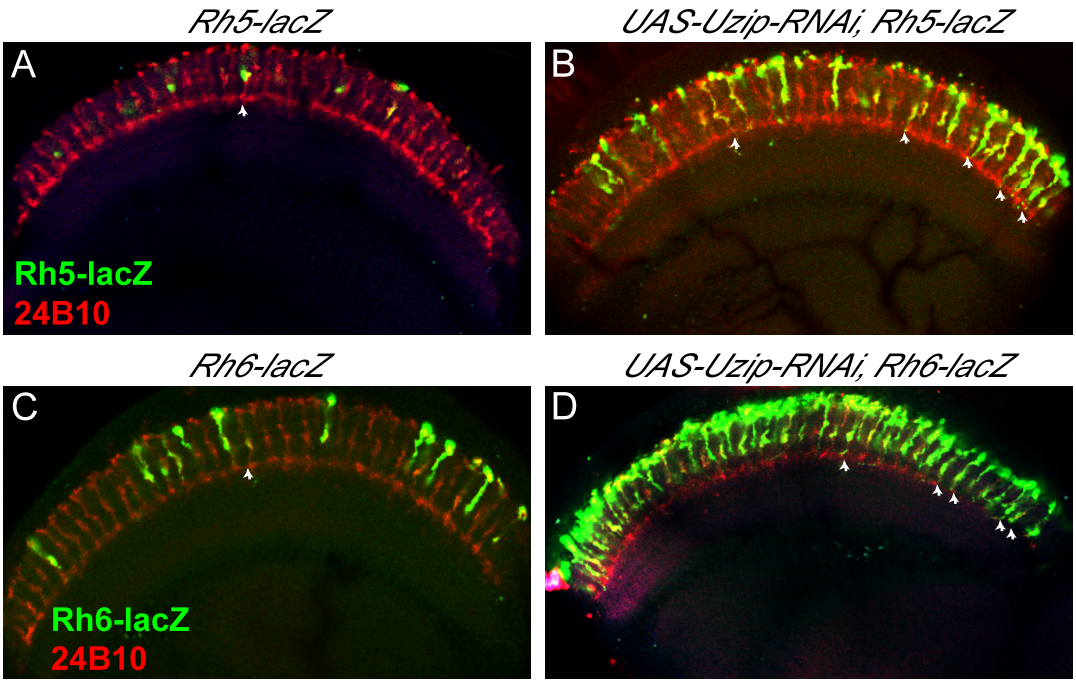

Figure 4.43. Projection of *Rh5-lacZ* and *Rh6-lacZ* expressing PRs at 29°C. *Rh5-lacZ* (A), *Rh6-lacZ* (B), *UAS-Uzip-RNAi, Rh5-lacZ* flies (C), and *UAS-Uzip-RNAi, Rh6-lacZ* flies (D) were stained with β-Gal (green) and 24B10 (red). A few the *Rh5-lacZ* and *Rh6-lacZ* expressing axons misproject at 29°C but the number of misprojecting axons increase when the flies are crossed with *UAS-Uzip-RNAi* flies (arrow heads).

Uzip was first downregulated in neuronal cells. First, the more general driver *Elav-Gal4* was used, which is expressed in all neuronal cells. The *Elav-Gal4* driver was tested and confirmed to drive the expression in the cells that are stained with the Elav antibody (Figure 4.44).

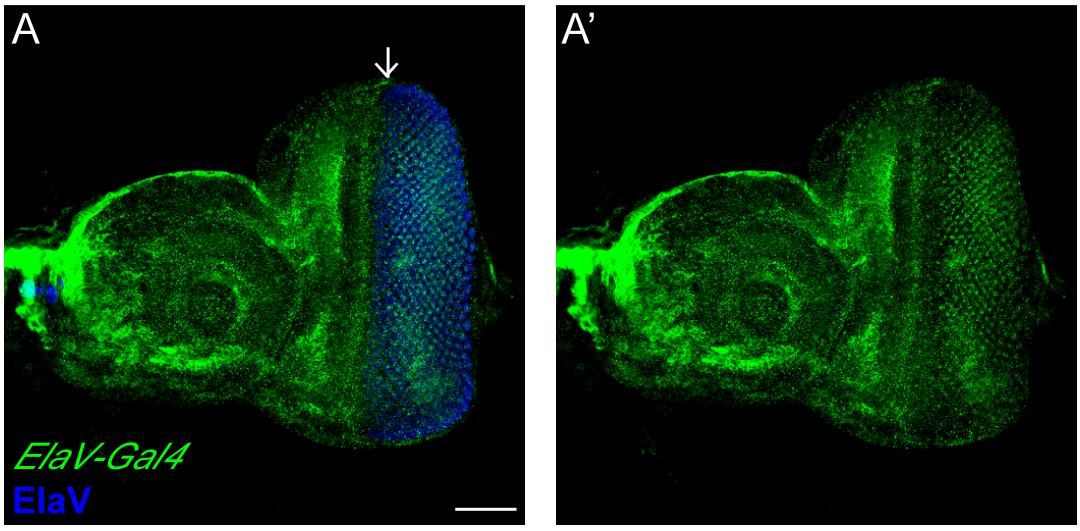

Figure 4.44. Expression pattern of the *Elav-Gal4* driver. The *Elav-Gal4* driver was tested by crossing it to the UAS-nGFP reporter. The expression at the posterior side of the MF (arrow) is similar to the staining of the Elav antibody. There is also unspecific expression at the anterior end of the eye disc (left). Scalebar: 25 μm.

Unzipped was downregulated specifically in neurons using the *Elav-Gal4* driver and its effect on the projection pattern of *Rh5-lacZ* and *Rh6-lacZ*-expressing R8 cells was analyzed. All PR neurons were visualized using an antibody against Chaoptin that labels all axons.

These experiments showed an increase in mistargeting of axons in both Rh5-lacZ and Rh6-lacZ expressing R8 cells (Figure 4.45 B,D). For the quantification of the phenotype n=321 axons expressing Rh5-lacZ and n=110 axons expressing Rh6-lacZwere analyzed. n=111/321 axons expressing Rh5-lacZ were shown to mistarget, which corresponds to 34,6% of analyzed axons, while n=40/110 axons expressing Rh6-lacZ mistargeted to the M6 layer corresponding to 36% of all axons that were analyzed.

The quantification of axonal mistargeting phenotypes showed that there was an increase in the number of axons that mistarget to the M6 layer. However there is also an increase in the mistargeting phenotype when the Rh5-lacZ and Rh6-lacZ expressing cells are crossed to the *UAS-RNAi* line. When compared to the mistargeting phenotype ratios of the control groups, which are 36,6% for Rh5-lacZ expressing axons and 32,9 % for Rh6-lacZ expressing axons, we can not suggest that there is an increase and the results are not significant (Figure 4.46). The phenotypes other than mistargeting were analyzed as well, but since they were not encountered frequently, they were not quantified.

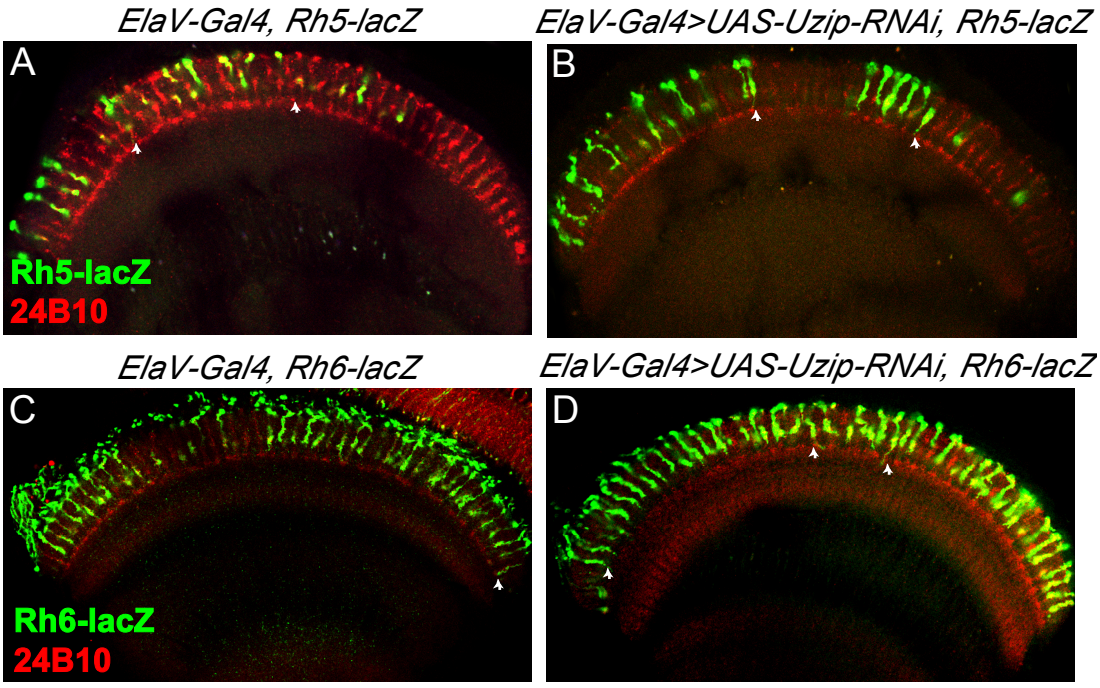

Figure 4.45. Projection analysis of R8 axons when Unzipped is downregulated *Elav-Gal4* driven cells. *Elav-Gal4, Rh5-lacZ* (A), *Elav-Gal4>UAS-Uzip-RNAi, Rh5-lacZ* (B), *Elav-Gal4, Rh5-lacZ* (C), and *Elav-Gal4>UAS-Uzip-RNAi, Rh6-lacZ* (D) flies are stained with β-Gal (green), and 24B10 (red) for PR expression. There are a few Rh5-lacZ and Rh6-lacZ expressing axons mistargeting to the wrong layer in both groups (arrowheads).

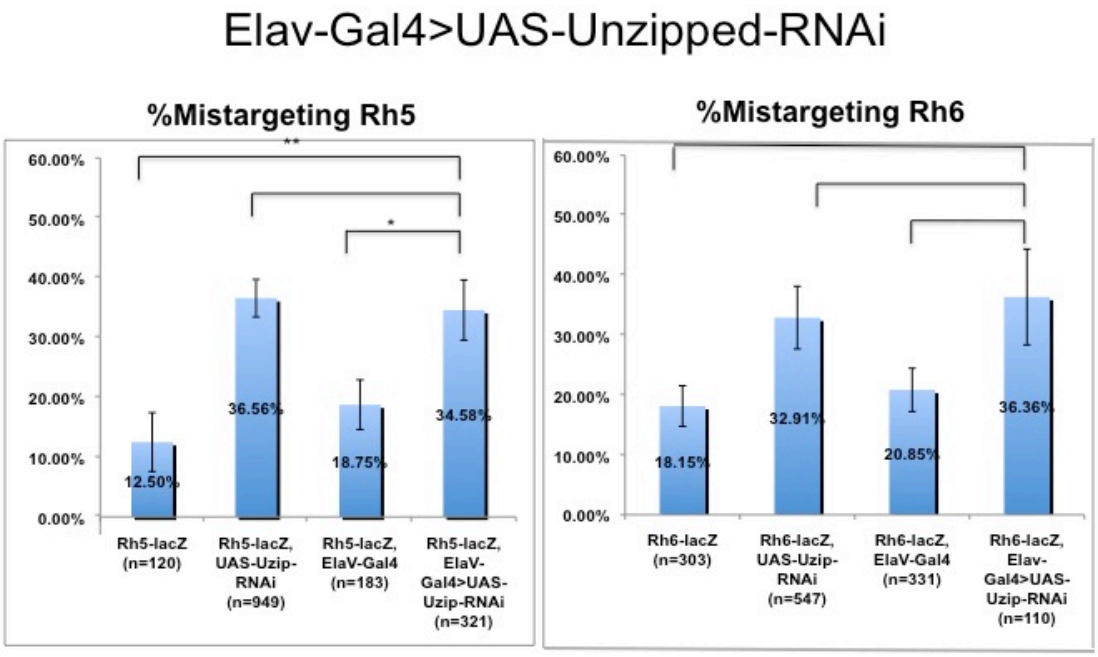

Figure 4.46. Quantification of misprojecting R8 cells in neuron-specific downregulation of Unzipped. The Rh5-lacZ and Rh6-lacZ expressing axons were counted and quantified separately. (Student two-tailed T test *p<0,05 **p<0,01 ***p<0,001) Rh5 p values= 0,007; 0,982; 0,021; Rh6 p values= 0,344: 0,808: 0,395 respectively. Y error bars represent SEM.

The next neural driver to downregulate Unzipped was *lGMR-Gal4*, which is a PR-specific driver. It is possible that downregulation in only PR cells is more effective than downregulating Unzipped in all neurons, creating a more distinct difference in expression. The *lGMR-Gal4* driver was tested and confirmed to drive expression in PR cells. Both available *lGMR-Gal4* drivers (one line on the second, and one line on the third chromosome) were tested since both drivers were used in the crosses. Both lines showed specific expression in PR cells and the Bolwig nerve (arrow in Figure 4.47). A delay of expression of *lGMR-Gal4* after the MF is a phenomenon common to all Gal4 drivers and is a result of the time that is necessary to synthesize Gal4 and for Gal4 to bind to its promoter sequence UAS and drive the expression of the reporter gene (Figure 4.47).

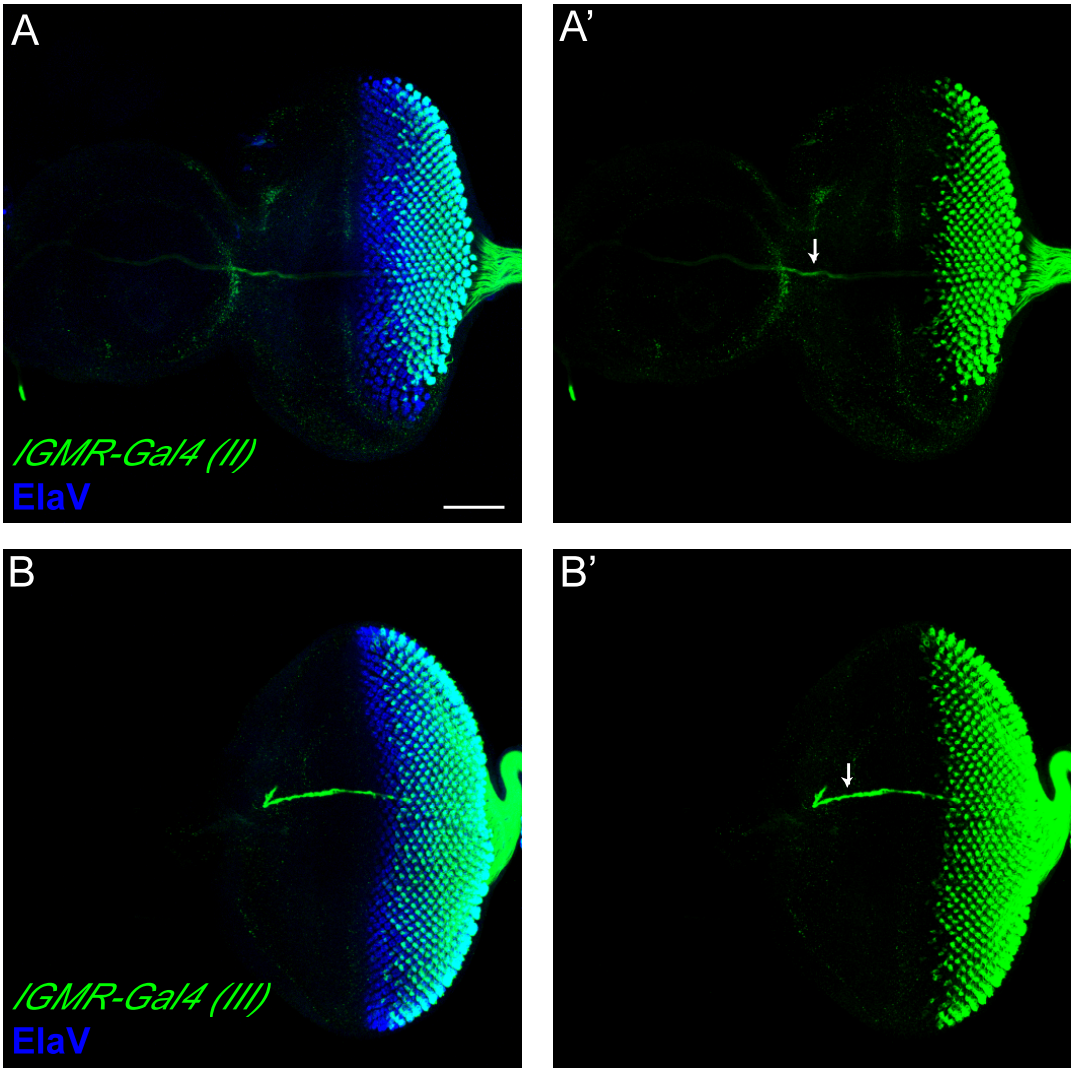

Figure 4.47. Expression pattern of the *lGMR-Gal4* driver. *lGMR-Gal4* driver was tested by crossing with UAS-CD8::GFP reporter. Both lines with lGMR on the second chromosome (A, A') and with lGMR on the third chromosome (B, B') were stained. The expression of *lGMR-Gal4* driven cells start a few rows after the MF in both lines and are expressed in PR cells. Arrow indicates the Bolwig nerve, where GMR is also expressed. Scalebar: 25 μm.

The *lGMR-Gal4* driver on the second chromosome was used to downregulate Unzipped expression specifically in PR cells and its effect on R8 cell projections was analyzed using Rh5-lacZ and Rh6-lacZ (Figure 4.48).

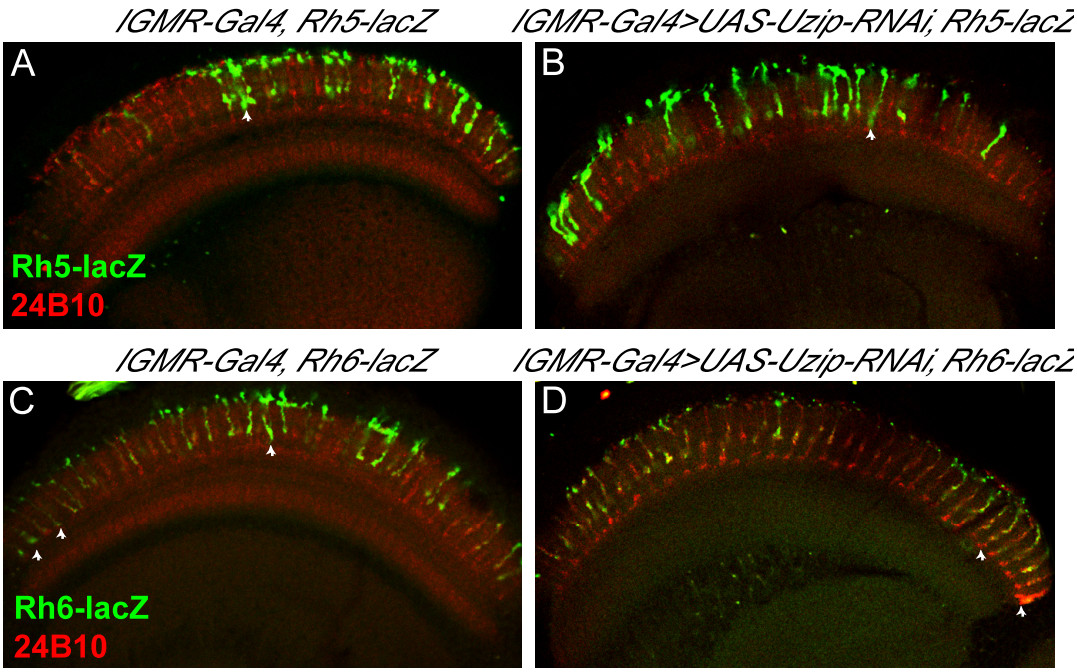

Figure 4.48. Projection analysis of R8 axons when Unzipped is downregulated *lGMR-Gal4* driven cells. *lGMR-Gal4, Rh5-lacZ* (A), *lGMR-Gal4>UAS-Uzip-RNAi, Rh5-lacZ* (B), *lGMR-Gal4, Rh6-lacZ* (C*),* and *lGMR-Gal4>UAS-Uzip-RNAi, Rh6-lacZ* (D) lines are stained with β-Gal (green), and 24B10 (red). There are a few Rh5-lacZ and Rh6-lacZ expressing axons, which mistarget to the wrong layer in both groups (arrowheads).

135 axons were counted for Rh5-lacZ expressing *lGMR-Gal4>UAS-Uzip-RNAi* flies and 548 axons were counted for Rh6-lacZ expressing ones. The percentage of mistargeting neurons in Rh5-lacZ expressing axons was 34.8% compared to 36.6% in a control group with no driver. For Rh6-lacZ expressing axons the percentage was calculated as 30,1% compared to the 32,9% in control groups without the driver. As seen from the percentages, when compared with the control groups, there is no significant increase in mistargeting axon percentages both in Rh5-lacZ and Rh6-lacZ-expressing cells (Figure 4.49). It is also important to note that as mentioned before the number of mistargeting axons in the control group increase drastically when the *UAS-Uzip-RNAi* is added to the RhX-lacZ expressing flies. Due to this reason when the samples are compared with the control groups, we take the control group with the highest mistargeting percentage into consideration. The phenotypes other than mistargeting were not sufficient for quantification.

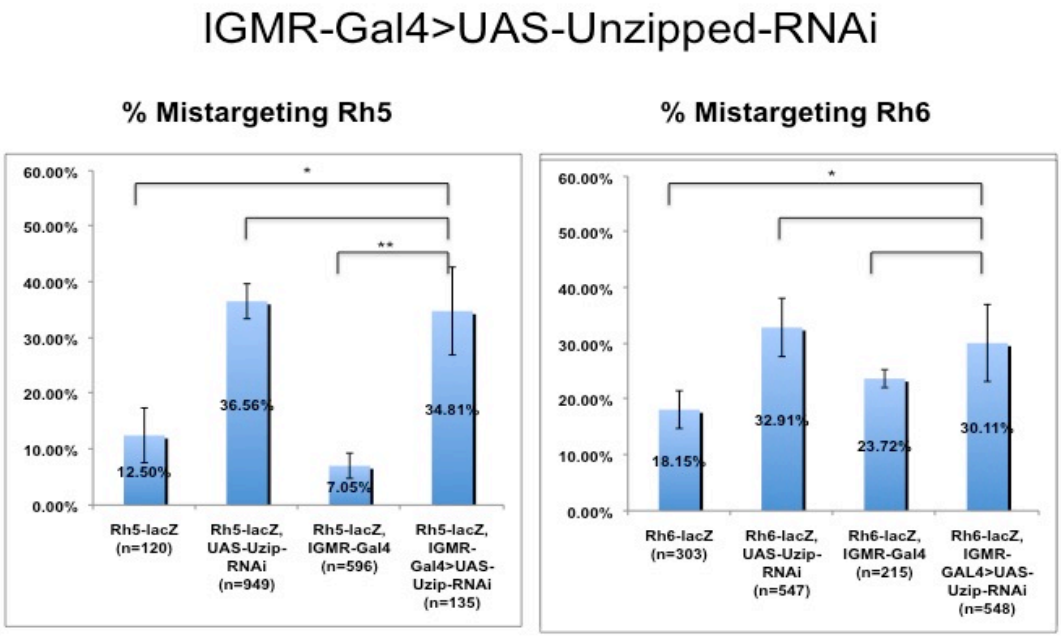

Figure 4.49. Quantification of misprojecting R8 cells when Uzip is downregulated in *lGMR-Gal4* driven cells. The Rh5-lacZ and Rh6-lacZ expressing axons were counted and quantified separately. n= number of axons counted. (Student two-tailed T test *p<0,05 **p<0,01 ***p<0,001) Rh5 p values= 0,023; 0,687; 0,009; Rh6 p values= 0,04: 0,733: 0,165 respectively. Y error bars represent SEM.

The last neural driver used for downregulation of Unzipped was *senseless-Gal4*. Uzip is expressed in R8 cells, thus, downregulating Uzip specifically in R8 cells using the *senseless-Gal4* driver might have an effect on the projection of R8 cells. In order to observe the outcome, adult whole-mount brain stainings were performed. Before setting the crosses, the *senseless-Gal4* driver was tested and its expression in R8 cells was confirmed in the 3rd instar larval eye disc (Figure 4.50).

The *sens-Gal4* driver was used to drive *Uzip-RNAi* and its effect on the projection of Rh6-lacZ was observed (Figure 4.51).

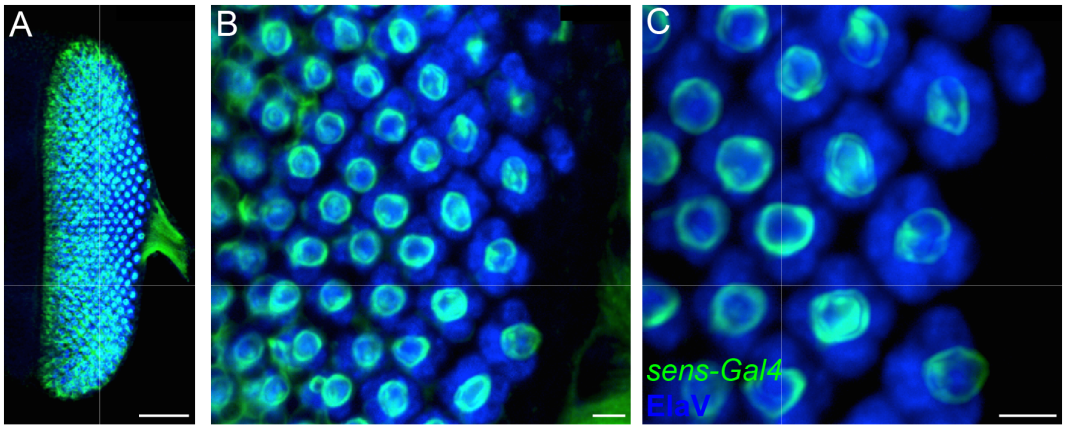

Figure 4.50. Expression pattern of the *sens-Gal4* driver. The sens-*Gal4* driver was tested by crossing with the UAS-CD8::GFP reporter. The expression of *sens-Gal4* driven cells colocalize with the differentiated PR cells at the posterior end marked by Elav. At the most posterior end, the staining of single cells R8 cells in the middle of the PR cells can be distinguished. Posterior is left side. Scalebars: 50 μm, 5 μm, and 5 μm respectively.

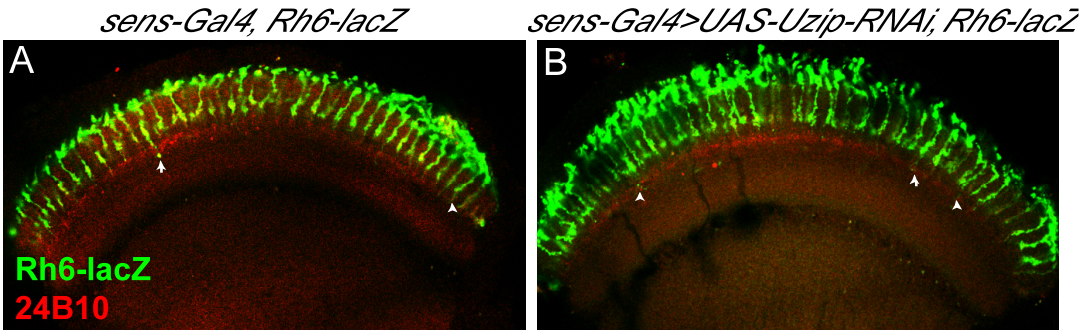

Figure 4.51. Projection analysis of Rh6-lacZ expressing R8 axons when Unzipped is downregulated in *sens-Gal4* driven cells. *sens-Gal4, Rh6-lacZ* (A) and *sens-Gal4>UAS-Uzip-RNAi, Rh6-lacZ* (B) flies are stained with β-Gal (green), and 24B10 (red). There are a few Rh6-lacZ expressing axons, which target to the wrong layer in both groups (arrowheads).

1114 axons were counted for Rh6-lacZ expressing *sens-Gal4>UAS-Uzip-RNAi* flies. The percentage of mistargeting neurons in Rh6-lacZ expressing axons was 47,3% compared to 32,9% in the control group with no driver. As seen from the percentages, when compared with the control groups, there is no significant increase in mistargeting axon percentages in Rh6-lacZ-expressing cells (Figure 4.52).

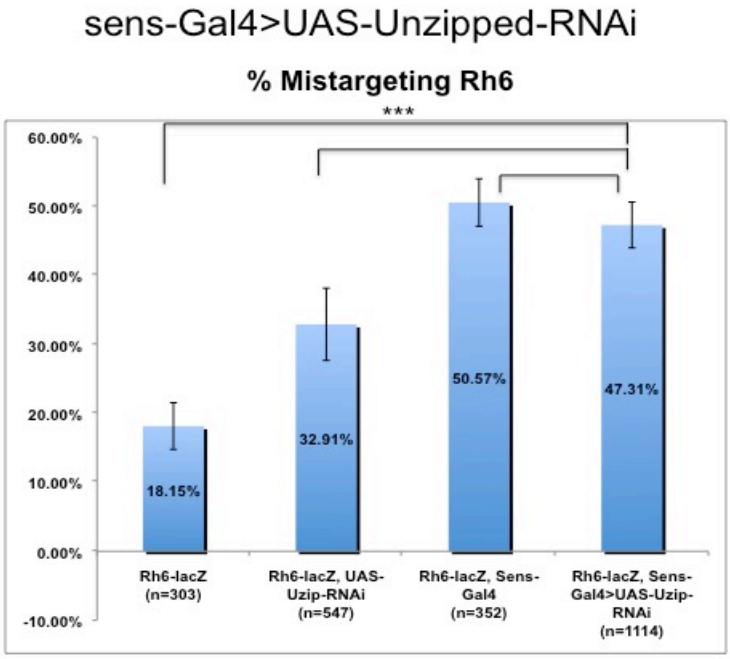

Figure 4.52. Quantification of misprojecting R8 cells when Uzip is downregulated in *sens-Gal4* driven cells. The Rh6-lacZ expressing axons were counted and quantified. n= number of axons counted. (Student two-tailed T test *p<0,05 **p<0,01 ***p<0,001) Rh6 p values= 0,000: 0,11: 0,49 respectively. Y error bars represent SEM.

From the quantifications of axonal misprojection when Uzip was downregulated in different neuronal cells, we can conclude that, neuronal downregulation of Unzipped in all neurons or more specific neurons does not affect the projection pattern of Rh5-lacZ and Rh6-lacZ-expressing R8 cells. It is also important to note that the downregulation with RNAi is not 100% so it is possible that the downregulation might be insufficient.

We showed that in addition to R8 cells, Unzipped is also expressed in a wide variety of glial cells. Thus, in another set of experiments we aimed to analyze Unzipped function by manipulating its expression in glial cells and analyzing the effect on axon guidance in R8 cells. Repo, which is the most common glial marker, was the first driver to be tested. Repo is expressed from early larval stages until the adult. Repo-Gal4 flies were crossed with the UAS-nGFP reporter to confirm that the driver is working properly. *Repo-Gal4*-positive cells were observed in a layer above the PR cells, and looking at their

distribution and expression pattern, it was concluded that *repo-Gal4* was driving the expression of glial cells as expected (Figure 4.53).

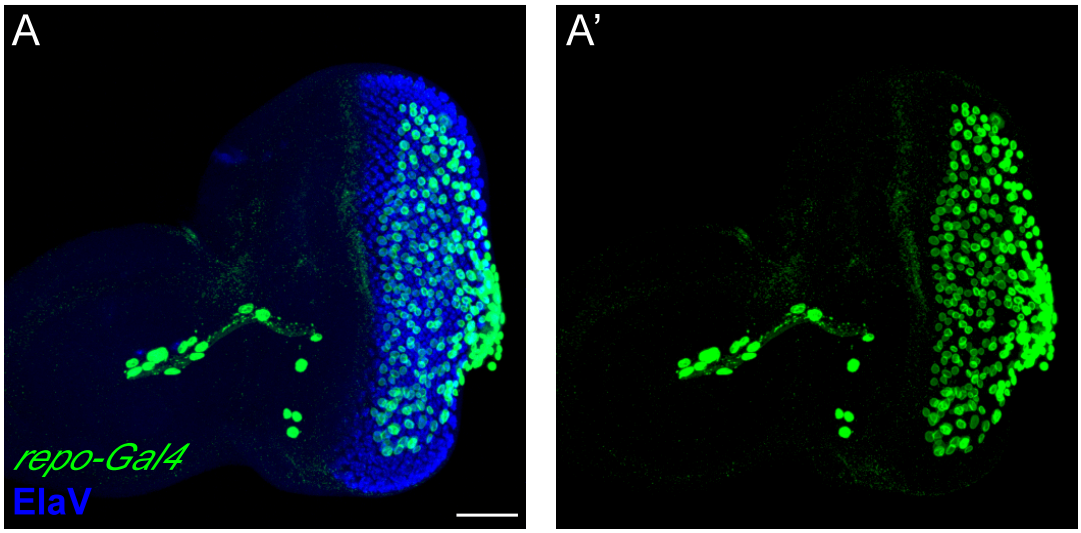

Figure 4.53. Expression pattern of the repo-Gal4 driver. The repo-Gal4 driver was tested by crossing with the UAS-nGFP reporter. The repo-Gal4 driven cells are expressed in a layer above the PR cells like glial cells and have a similar pattern to glial cell expression. Scalebar: 25 μm.

Uzip was downregulated in glial cells using *repo-Gal4*. In contrast to our results obtained after downregulation of Unzipped in neuronal cells, there was an increase in the number of mistargeting neurons both in Rh5-lacZ and Rh6-lacZ expressing R8 cells (Figure 4.54).

The increase in mistargeting axons was ~20% for Rh5-lacZ axons and ~10% for Rh6-lacZ axons compared to the control groups and these increases are significant (Figure 4.55). Such an increase is critical for axonal projections. Since there are many factors affecting the axonal targeting of PR cells; changing only one factor, which is involved in this process, does not cause major defects. Due to this reason even minor changes in phenotypes should be considered as a factor involved in the targeting pathway. By looking at the change in the mistargeting ratios, we can suggest that the expression of Uzip in *repo*-expressing glial cells might be critical for the R8 axon termination process.

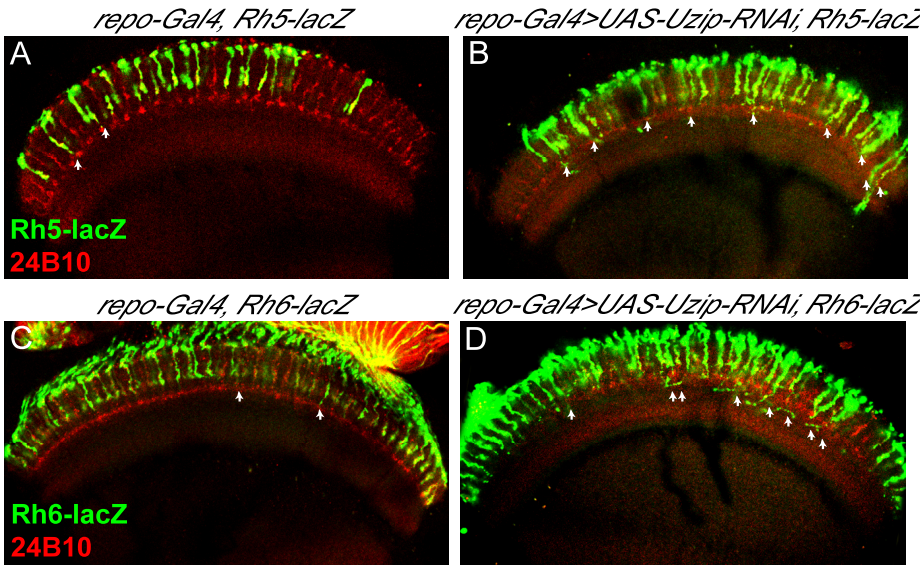

Figure 4.54. Projection analysis of R8 axons when Unzipped is downregulated *repo-Gal4* driven cells. *repo-Gal4, Rh5-lacZ* (A), *repo-Gal4>UAS-Uzip-RNAi, Rh5-lacZ* (B), *repo-Gal4, Rh6-lacZ* (C), and *repo-Gal4>UAS-Uzip-RNAi, Rh6-lacZ* (D) lines are stained with β-Gal (green), and 24B10 (red). The number and the severeness of the mistargeting phenotype increases in *repo-Gal4>UAS-Uzip-RNAi* flies (arrows)(B,D).

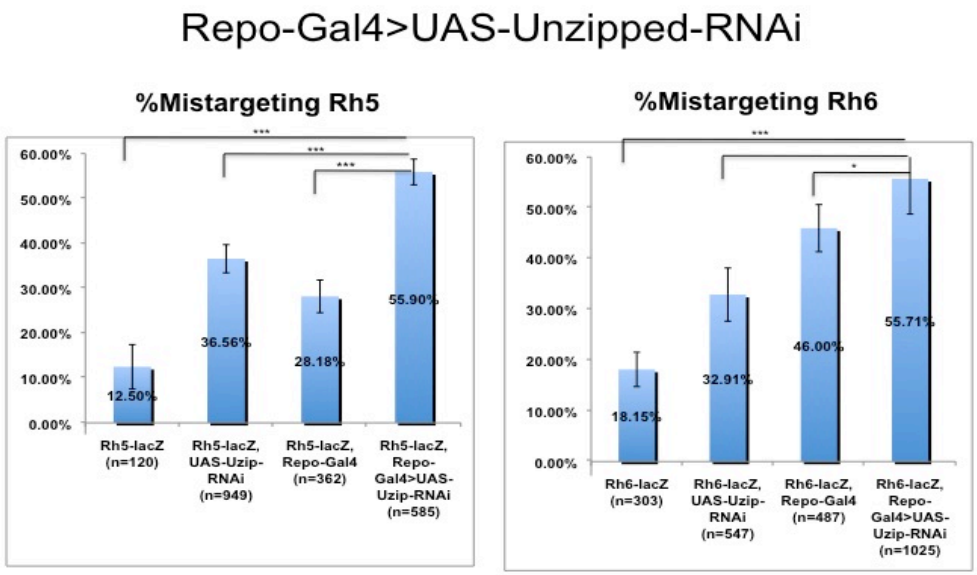

Figure 4.55. Quantification of misprojecting R8 cells when Uzip is downregulated in *repo-Gal4* driven cells. The Rh5-lacZ and Rh6-lacZ expressing R8 axons were counted and analyzed separately. n= number of axons counted. (Student two-tailed T test *p<0,05 **p<0,01 ***p<0,001) Rh5 p values= 0,000: 0,000: 0,000; Rh6 p values= 0,000: 0,06: 0,022 respectively. Y error bars represent SEM.

Then we tested if the earlier glial driver *gcm*, which is in the upstream of *repo*, had a similar effect on the projection of R8 cells. Additionally *gcm* is expressed in a different region than *repo*. It is not expressed in the eye imaginal disc in the third instar larva, but is majorly expressed in the GPC area and around in the optic lobe. Due to this reason when testing the driver, we stained the 3rd instar larva brain since there was no expression in the eye disc. The *gcm-Gal4* driver was expressed very densely in the GPC region of the optic lobe and in the glial precursor cells in the ventral nerve chord (VNC) (Yoshida *et al.*, 2005) (Figure 4.56).

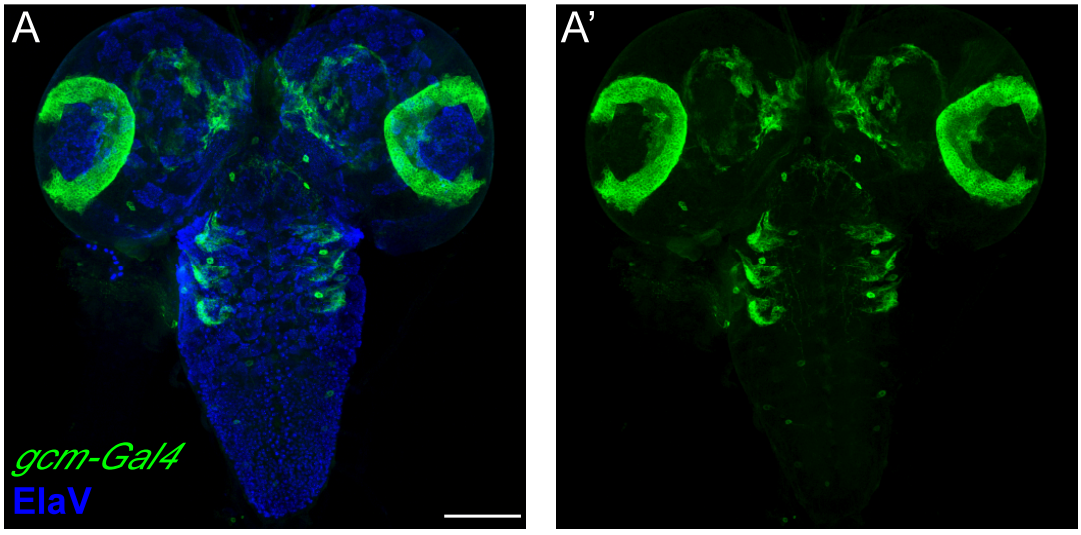

Figure 4.56. Expression pattern of the *gcm-Gal4* driver. The *gcm-Gal4* driver was tested by crossing with the UAS-CD8::GFP reporter. The *gcm-Gal4* driven cells are expressed in the GPC region in the optic lobes at the two sides of the brain, and have a button like shape at the ventral nerve chord at the region of glial precursors. There is also a faint expression in the brain. Scalebar: 75 μm.

Uzip was downregulated in *gcm* expressing cells. The '*gcm-Gal4>UAS-Uzip-RNAi, Rh5-lacZ*' flies could not be obtained due to the condition of the flies, but analyses were performed with the '*gcm-Gal4>UAS-Uzip-RNAi, Rh6-lacZ*' strain (Figure 4.57). There was an increase in the mistargeting of Rh6-lacZ in '*gcm-Gal4>UAS-Uzip-RNAi'* flies, similar to the downregulation of Uzip with the *repo* driver.

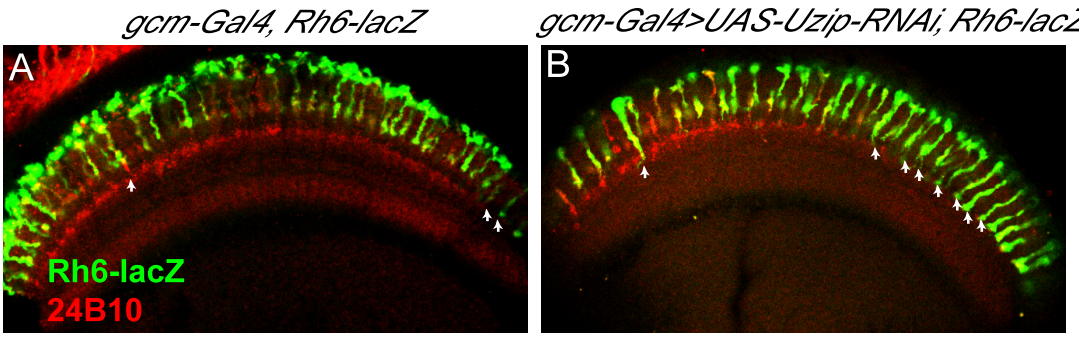

Figure 4.57. Projection analysis of Rh6-lacZ expressing R8 axons when Unzipped is downregulated in *gcm-Gal4* driven cells. *gcm-Gal4, Rh6-lacZ* (A) and *gcm-Gal4>UAS-Uzip-RNAi, Rh6-lacZ* (B) flies are stained with β-Gal (green), and 24B10 (red). Few of the Rh6-lacZ expressing axons target to the wrong layer in both groups, but the number of these mistargeting axons increase in *gcm-Gal4>UAS-Uzip-RNAi* flies. (arrows).

The misprojection increased ~20% compared to the control groups from 32,9% to 51,6% and these results are significant, suggestsing that the decrease in Uzip levels in the early glial driver *gcm* might affect the target choice of PR axons (Figure 4.58). The increase in R8 mistargeting when Unzipped is downregulated in both *repo* and *gcm* expressing cells, suggests that the expression of unzipped in glial cells might be important for proper axonal targeting of R8 cells.. The phenotypes other than mistargeting were negligible when Uzip was downregulated in both *repo* and *gcm* expressing cells, so they were not quantified.

A more specific glial driver *moody-Gal4*, which is known to be driving the expression of carpet cells in the 3rd instar larva and a subgroup of glial cells in the adult, was used to knockdown Uzip to see if the increase in the number of mistargeting cells was caused by the reduced expression of Uzip in carpet cells. The reason for chosing a carpet glia specific driver was the expression of the reporters in the carpet glia cells driven by the enhancer trap AC783. If Unzipped is expressed in carpet cells, the downregulation of Unzipped might have a role in targeting since these glia are the ones to form a ‘carpet-like’ sheet, establishing a platform for the other glia to migrate to the eye disc. The *moody-Gal4* driver was tested in the 3rd instar larva eye disc and its specific expression in the carpet cells was confirmed (Figure 4.59).

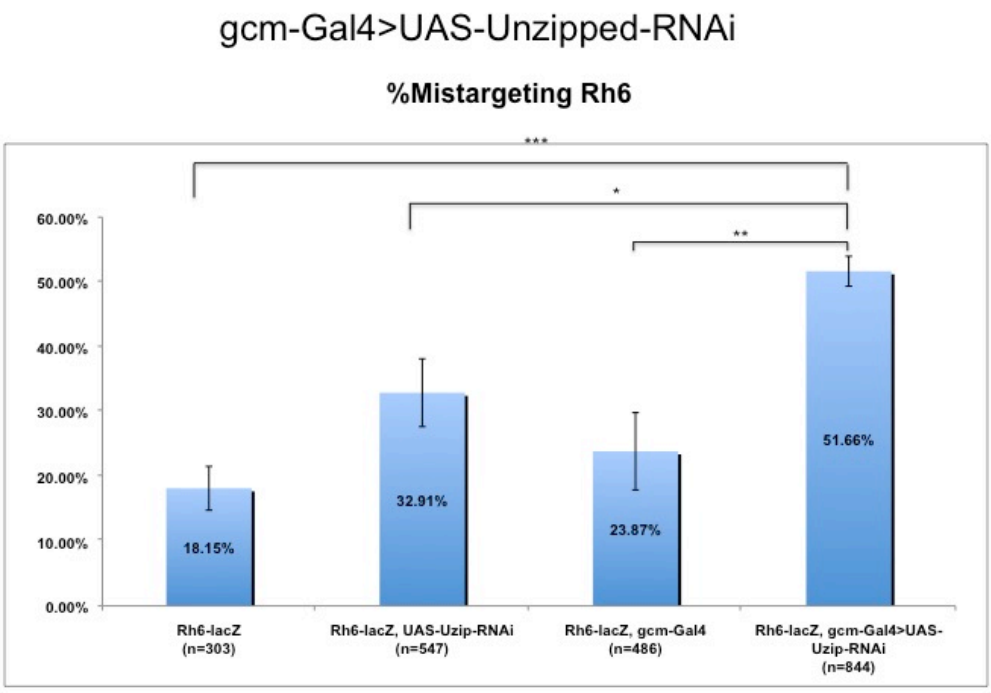

Figure 4.58. Quantification of misprojecting R8 cells when Uzip is downregulated in *gcm-Gal4* driven cells. The Rh6-lacZ expressing axons were counted and analyzed. n= number of axons counted. (Student two-tailed T test *p<0,05 **p<0,01 ***p<0,001). Rh6 p values= 0,000: 0,06: 0,001 respectively. Y error bars represent SEM.

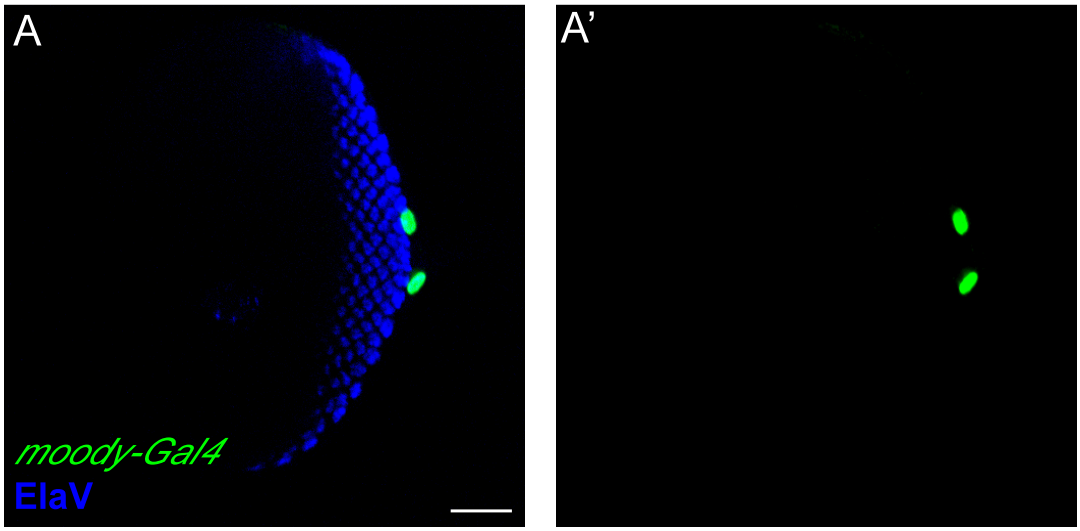

Figure 4.59. Expression pattern of the *moody-Gal4* driver. The *moody-Gal4* driver was tested by crossing with the UAS-nGFP reporter. The *moody-Gal4* driven cells are expressed in the nucleus of the two carpet cells. Scalebar 25μm.

The *moody-Gal4>UAS-Uzip-RNAi* flies were analyzed for the projections of the Rh5-lacZ and Rh6-lacZ expressing axons (Figure 4.60). Different than the other two glial cell drivers, there was not a change in the projection pattern of the R8 cells when Uzip is downregulated in *moody*-expressing cells.

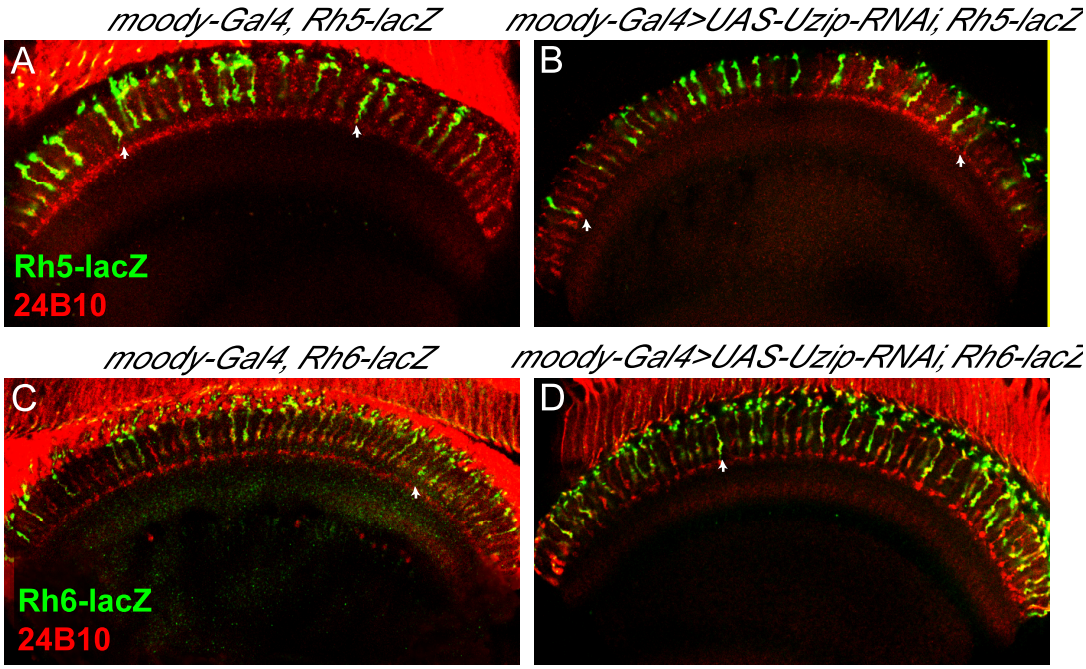

Figure 4.60. Projection analysis of R8 axons when Unzipped is downregulated *moody-Gal4* driven cells. *moody-Gal4, Rh5-lacZ* (A), *moody-Gal4>UAS-Uzip-RNAi, Rh5-lacZ* (B), *moody-Gal4, Rh6-lacZ* (C*),* and *moody-Gal4>UAS-Uzip-RNAi, Rh6-lacZ* (D) lines are stained with β-Gal (green), and 24B10 (red). There is no increase in mistargeting axons when Uzip is downregulated in moody-Gal4 expressing cells (arrows).

The percentage of mistargeting Rh5-lacZ-expressing neurons changed from 36,6% to 33% and the Rh6-lacZ expressing neurons changed from 33% to 35,8%, which are not significant statistically. These numbers suggest that the reduction of the Unzipped levels in the carpet glia is not sufficient to affect the targeting of R8 cells (Figure 4.61). It is also possible that Unzipped expressed in the carpet cells is not involved in the projection process.

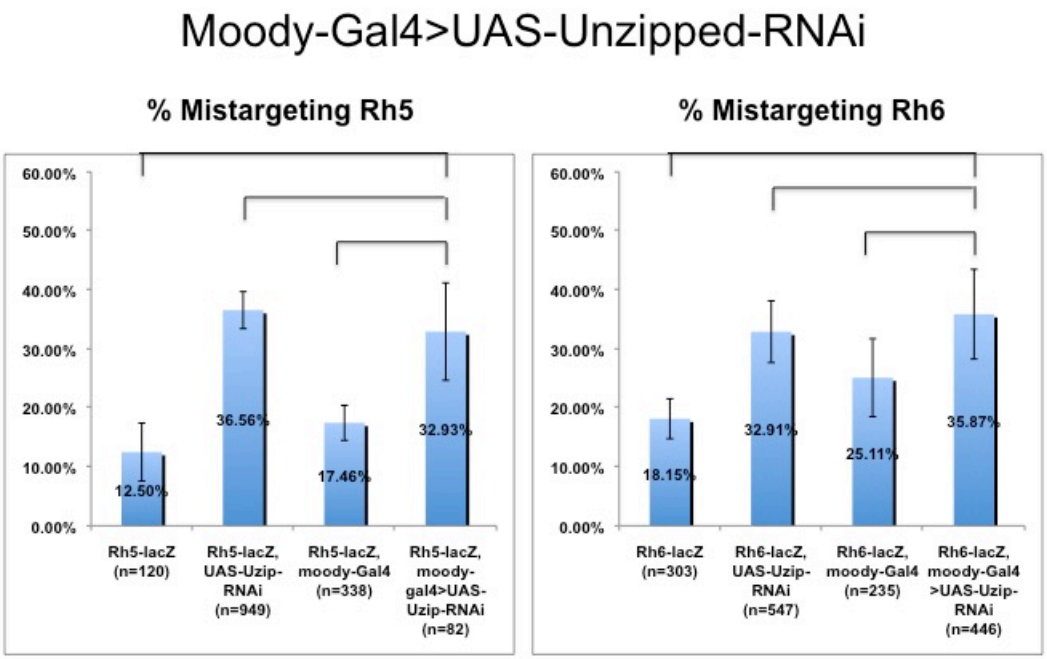

Figure 4.61. Quantification of misprojecting R8 cells when Uzip is downregulated in *moody-Gal4* driven cells. n= number of axons counted. (Student two-tailed T test *p<0,05 **p<0,01 ***p<0,001) Rh5 p values= 0,215: 0,462: 0,35; Rh6 p values= 0,09: 0,651: 0,438 respectively. Y error bars represent SEM.

From these findings we can conclude that the expression of Unzipped in glial cells is important for R8 projection and when it is downregulated in *repo* and *gcm*-expressing cells, the amount of mistargeting increases. On the other hand, the reduction of Unzipped in neuronal cells does not have a major affect on the targeting of R8 cells.

4.5.2.3. Effect of Uzip Overexpression on R8 Axonal Projections. An alternative way to manipulate Unzipped levels on selected populations on cells is the overexpression of Unzipped in particular cell types using cell-type specific drivers. Thus, in order to analyze the possible role of the misexpression of Unzipped on axonal projections Unzipped was misexpressed in different subgroups of neuronal and glial cells just as in the downregulation experiments. It is possible that overexpressing Uzip in a group of cells might lead to a different mistargeting defect. Elav and lGMR were used as neuronal drivers while repo, gcm, moody, and Mz97 were used as glial drivers. The evaluation criteria for

targeting phenotypes were the same as in downregulation experiments. The crosses were kept at 25^0C since it is the ideal temperature for fly maintenance.

'*Rh5-lacZ*'; '*UAS-Uzip, Rh5-lacZ*'; '*Rh6-lacZ*'; and '*UAS-Uzip, Rh6-lacZ*' lines were stained with β-Gal as controls. Although there were fewer axons with mistargeting defects compared with flies for RNAi downregulation that were kept at 29^0C, still some the axons terminated in the wrong layer. These defects were considered at the quantification stage (Figure 4.62).

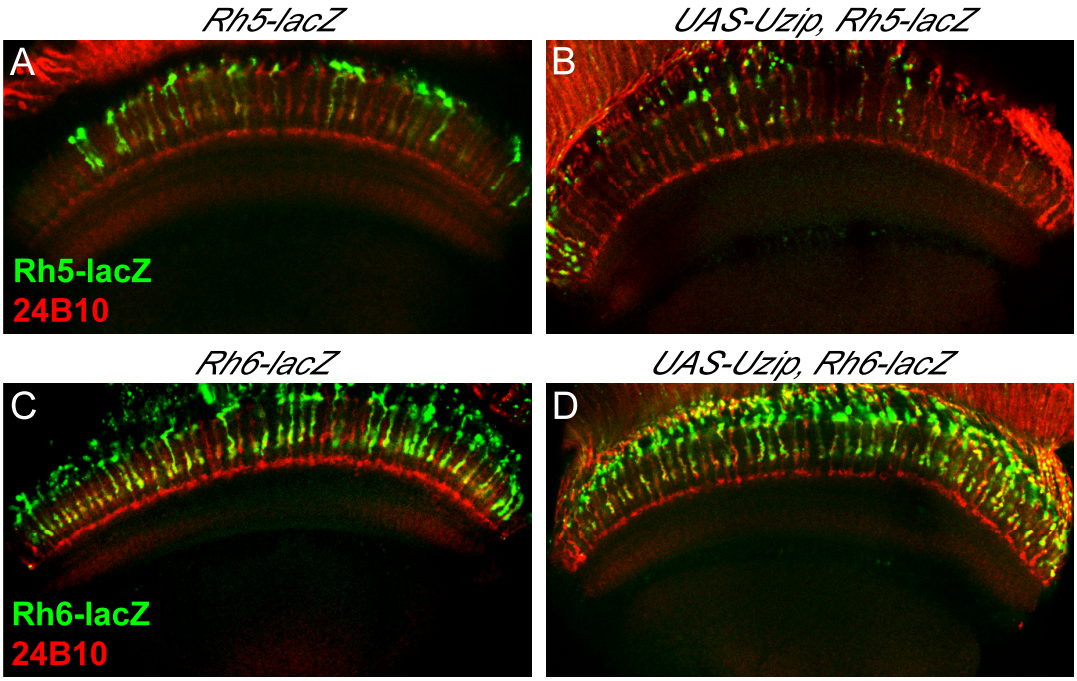

Figure 4.62. Projection of *Rh5-lacZ* expressing PRs at 25C. *Rh5-lacZ* (A), *UAS-Uzip, Rh5-lacZ* (B), *Rh6-lacZ* (C), and *UAS-Uzip, Rh6-lacZ* flies (D) are stained with β-Gal (green) and 24B10 (red). The Rh5-lacZ expressing axons terminate at the M3 layer, and the 24B10 stained PRs terminate at the M6 layer.

The first neuronal driver used was Elav-Gal4, which drives expression in all neuronal cells. The *UAS-Uzip* line was driven with the *Elav-Gal4* driver and its effect on the *Rh5-lacZ* and *Rh6-lacZ* expressing R8 cells were analyzed (Figure 4.63).

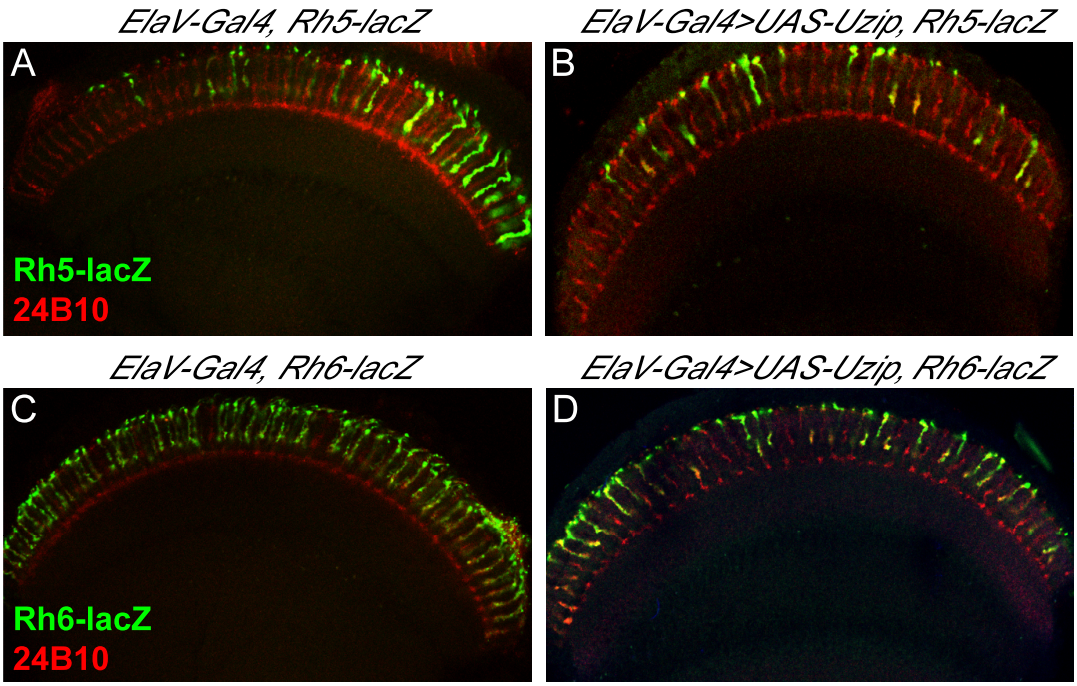

Figure 4.63. Projection analysis of R8 cells in *ElaV-Gal4>UAS-Uzip* flies. *Elav-Gal4, Rh5-lacZ* (A), *Elav-Gal4>UAS-Uzip, Rh5-lacZ* (B), *Elav-Gal4, Rh6-lacZ* (C), and *Elav-Gal4>UAS-Uzip, Rh6-lacZ* (D) flies are stained with β-Gal (green) for Rh5 and Rh6 expression, and 24B10 (red) for PR expression. *Rh5-lacZ* and Rh6-lacZ expressing axons mostly terminate at the M3 layer, and the 24B10 stained PRs terminate at the M6 layer.

158 axons were counted for Rh5-lacZ expressing Elav-Gal4>UAS-Uzip flies and 1823 axons were counted for the Rh6-lacZ expressing group. The percentages of control flies were 8,9% for '*Rh5-lacZ'* flies, 12,2% for '*Rh5-lacZ, UAS-Uzip'* flies, and 12,7% for *'Rh5-lacZ, Elav-Gal4'* flies respectively. As seen from the percentages, the change in mistargeting when UAS-Uzip or the driver is added to Rh5-lacZ is very minor, especially compared with the controls of the downregulation experiments. The percentage of mistargeting axons in '*Rh5-lacZ, Elav-Gal4>UAS-Uzip'* flies is 10,76%, which is not different from the control groups and the change is not significant.

The percentages of control flies for Rh6-lacZ expressing flies were 5,2% for '*Rh6-lacZ'*, 5,15% for '*Rh6-lacZ, UAS-Uzip'*, and 14,3% for '*Rh6-lacZ, Elav-Gal4*' respectively. The addition of the driver increases the mistargeting percentage, but the '*Rh6-lacZ, Elav-Gal4>UAS-Uzip'* flies have a similar mistargeting percentage of 14,2% and the

change is not significant, so we can conclude that misexpressing Uzip with Elav-Gal4 does not change the mistargeting of R8 axons (Figure 4.64).

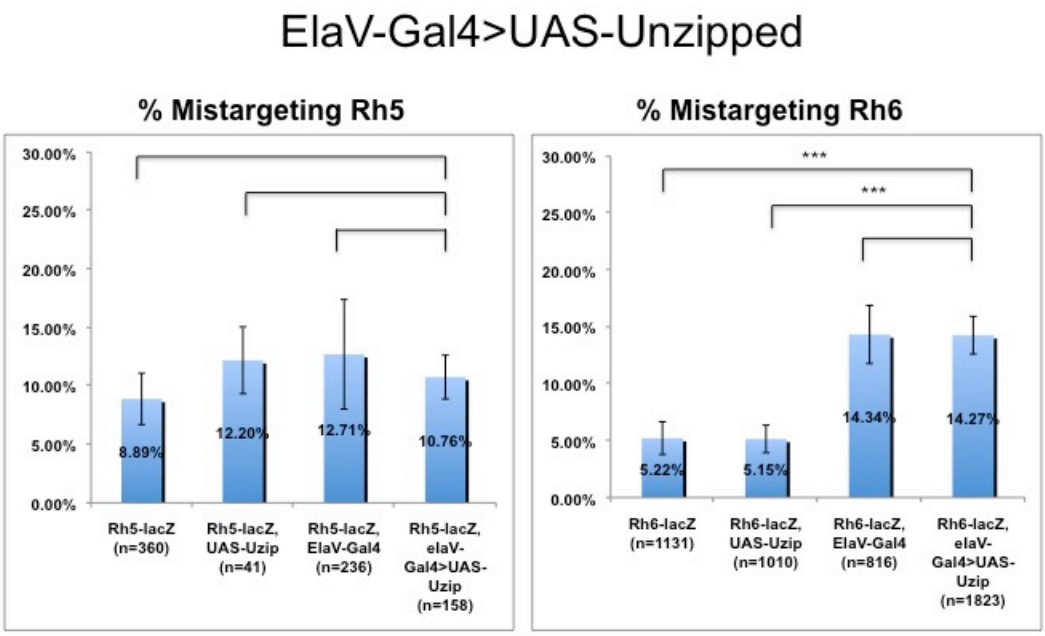

Figure 4.64. Quantification of R8 mistargeting in Elav-Gal4>UAS-Uzip flies. The Rh5-lacZ and Rh6-lacZ expressing R8 axons were counted and analyzed separately. (Student two-tailed T test *p<0,05 **p<0,01 ***p<0,001) Rh5 p values= 0,474: 0,97: 0,7; Rh6 p values= 0,000: 0,000: 0,651 respectively. Y error bars represent SEM.

In a second set of experiments, the lGMR-Gal4 driver was used to misexpress Uzip in PR cells. The Rh5-lacZ and Rh6-lacZ expressing axons were counted. *lGMR-Gal4* is a very strong driver and its existence in the second or third chromosome causes a higher number of R8 axons to mistarget, even before misexpressing Uzip. For the misexpression experiments the *lGMR-Gal4* driver on the third chromosome was used. When Uzip is misexpressed in PR cells, the number of mistargeting axons increase (Figure 4.65).

The Rh6-lacZ expressing *lGMR-Gal4>UAS-Uzip* flies increase from ~20% to ~26% compared to *lGMR-Gal4, Rh6-lacZ* expressing flies and the change is significant statistically. However, the ratio of Rh5-lacZ expressing R8 cells did not change and the mistargeting percentages were 9% for '*Rh5-lacZ'*, 12,2% for '*Rh5-lacZ, UAS-Uzip*', 14,9% for '*Rh5-lacZ, lGMR-Gal4*', and 12% for '*Rh5-lacZ, lGMR-Gal4>UAS-Uzip'* flies

respectively (Figure 4.66). Rh6 is expressed in ~70% of R8 cells while Rh5 is expressed in ~30%. When this ratio is considered, we can suggest that a mild phenotype can be seen easier in *Rh6-lacZ* expressing axons. These results indicate that misexpressing Uzip in PR cells causes a mild misprojection phenotype, and has an affect on axonal targeting. The phenotypes other than misprojection were very few in number, so they were not considered for quantification.

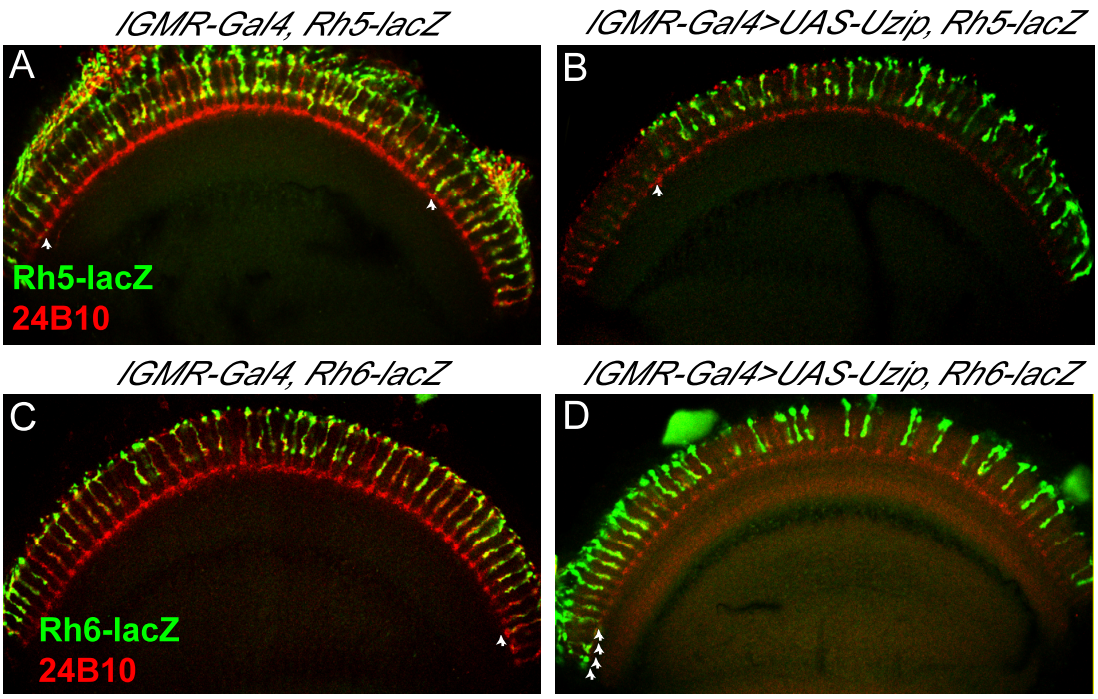

Figure 4.65. Projection analysis of R8 cells in *lGMR-Gal4>UAS-Uzip* flies. *lGMR-Gal4, Rh5-lacZ* (A), *lGMR-Gal4>UAS-Uzip, Rh5-lacZ* (B), *lGMR-Gal4, Rh6-lacZ* (C), and *lGMR-Gal4>UAS-Uzip, Rh6-lacZ* (D) flies are stained with β-Gal (green), and 24B10 (red). Some of the Rh5-lacZ expressing axons mistarget in both groups. The number of misprojecting axons increase when Uzip is misexpressed in PR cells (arrows).

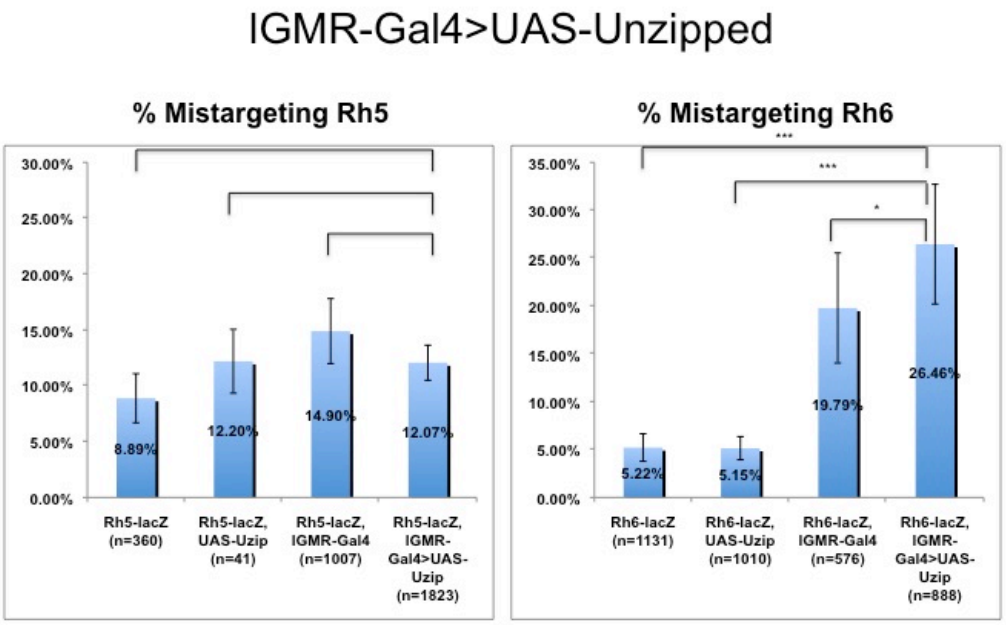

Figure 4.66. Quantification of R8 mistargeting in *lGMR-Gal4>UAS-Uzip* flies. The *Rh5-lacZ* and *Rh6-lacZ* expressing R8 axons were counted and quantified separately. n= number of axons counted. (Student two-tailed T test *p<0,05 **p<0,01 ***p<0,001) Rh5 p values= 0,622: 0,355: 0,159; Rh6 p values= 0,000: 0,000: 0,042 respectively. Y error bars represent SEM.

First the *repo-Gal4* line was used to misexpress Uzip in glial cells (Figure 4.67). The ratio of the *Rh5-lacZ* expressing flies were 9% for '*Rh5-lacZ'*, 12,2% for '*Rh5-lacZ, UAS-Uzip*', 14,9% for '*Rh5-lacZ, repo-Gal4*', and 12,4% for '*Rh5-lacZ, repo-Gal4>UAS-Uzip'* flies respectively. These ratios are very similar to the ratios of *lGMR-Gal4>UAS-Uzip* flies expressing Rh5-lacZ, thus there is not a difference between the controls and the misexpression of Unzipped in repo-Gal4 driven cells. For the *R6-lacZ* expressing R8 cells the ratios were 5,2% for '*Rh6-lacZ'* flies, 5,2% for '*Rh6-lacZ, UAS-Uzip'* flies, and 18,16% for '*Rh6-lacZ, repo-Gal4*' flies respectively. The mistargeting ratio of *'Rh6-lacz, repo-Gal4>UAS-Uzip'* flies were 15,7%, which is not a significant change and is accordance with the control group, indicating that the Rh6-lacZ expressing axons did not show an increase in the mistargeting phenotype. These results suggest that the knockdown of Uzip in *repo* expressing cells have a more severe affect on projection compared to the misexpression of Uzip (Figure 4.68).

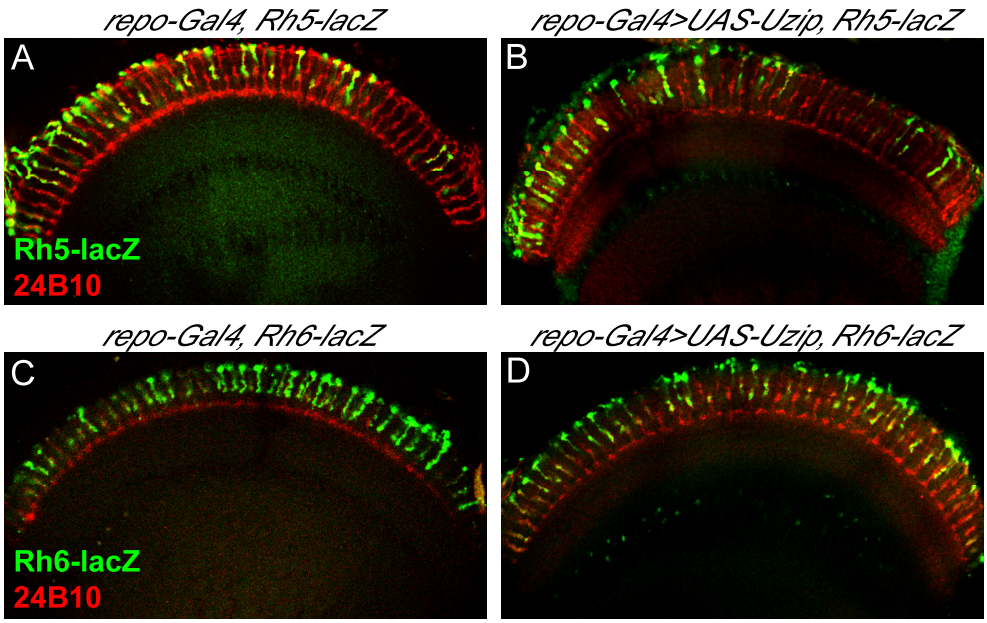

Figure 4.67. Projection analysis of R8 cells in *repo-Gal4>UAS-Uzip* flies. *repo-Gal4, Rh5-lacZ* (A), *repo-Gal4>UAS-Uzip, Rh5-lacZ* (B), *repo-Gal4, Rh6-lacZ* (C), and *repo-Gal4>UAS-Uzip, Rh6-lacZ* (D) flies are stained with β-Gal (green), and 24B10 (red). Rh5-lacZ and Rh6-lacZ-expressing axons terminate at M3, 24B10 stained PRs terminate at M6.

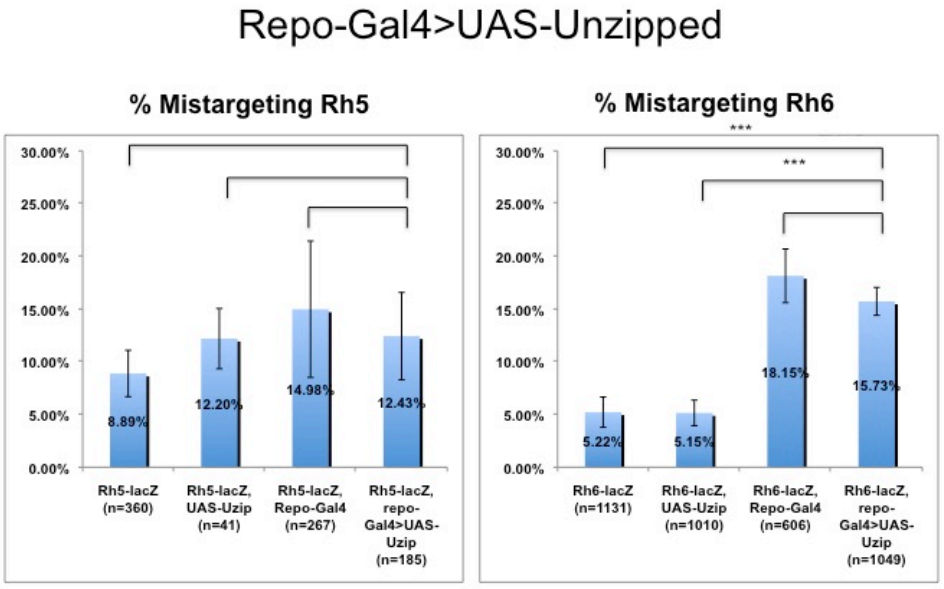

Figure 4.68. Quantification of R8 mistargeting in *repo-Gal4>UAS-Uzip* flies. The *Rh5-lacZ* and *Rh6-lacZ*-expressing R8 axons were counted and analyzed. n= number of axons counted. (Student two-tailed T test *p<0,05 **p<0,01 ***p<0,001) Rh5 p values= 0,34: 0,6: 0,845; Rh6 p values= 0,000: 0,000: 0,375 respectively. Y error bars represent SEM.

The next glial driver to be tested was *gcm-Gal4*. Uzip was misexpressed in *gcm* expressing cells and the projections were quantified (Figure 4.69). Although a change in the projection patterns of *Rh5-lacZ* expression was not observed, there was an increase in the misprojection of *Rh6-lacZ* expressing axons from ~7,5% to ~15% that was significant (Figure 4.70). A similar case where there was a mild increase in Rh6-lacZ expressing axons but not in Rh5-lacZ axons was observed in lGMR-Gal4 driven cells, suggesting that it is easier to detect the phenotype when there are more axons represented in one optic lobe. The increase in Unzipped misexpression is milder compared to the Uzip knockdown flies driven with the *gcm-Gal4* driver, but we can suggest that both misexpressing and knocking down Uzip in *gcm* expressing glial cells affect the projection pattern of R8 cells.

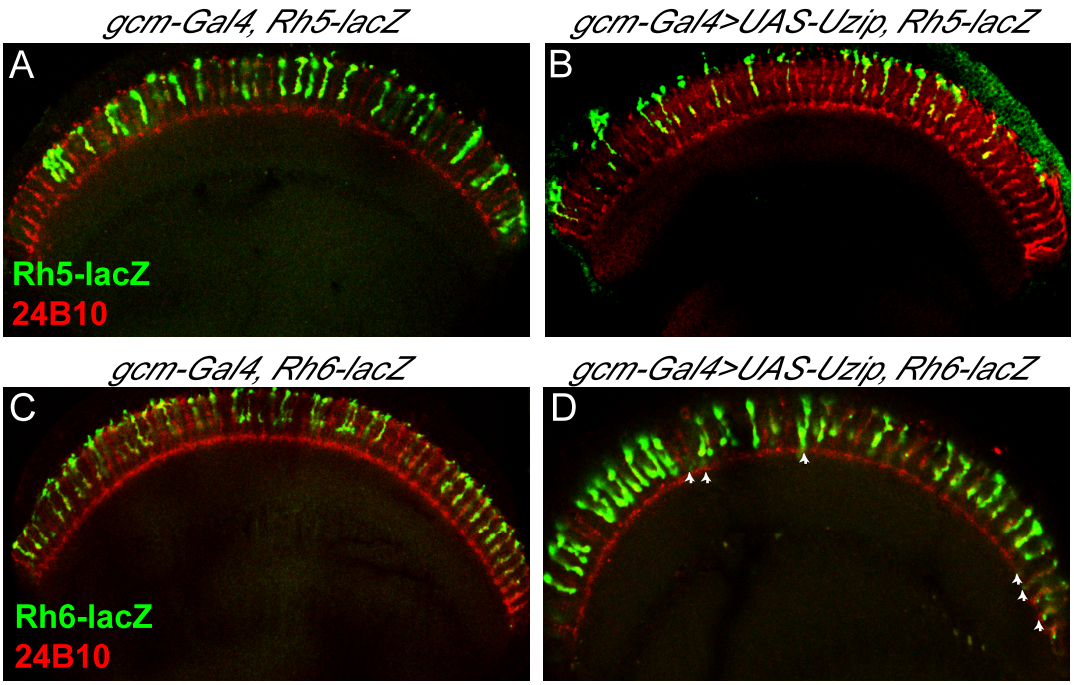

Figure 4.69. Projection analysis of R8 cells in gcm-Gal4>UAS-Uzip flies. gcm-Gal4, Rh5-lacZ (A), gcm-Gal4>UAS-Uzip, Rh5-lacZ (B), gcm-Gal4, Rh6-lacZ (C), and gcm-Gal4>UAS-Uzip, Rh6-lacZ (D) flies are stained with β-Gal (green), and 24B10 (red). Rh5-lacZ expressing axons terminate at M3, and the 24B10 stained PRs terminate at M6. The mistargeting axons increase in Rh6-lacZ expressing *gcm-Gal4>UAS-Uzip* flies (arrows).

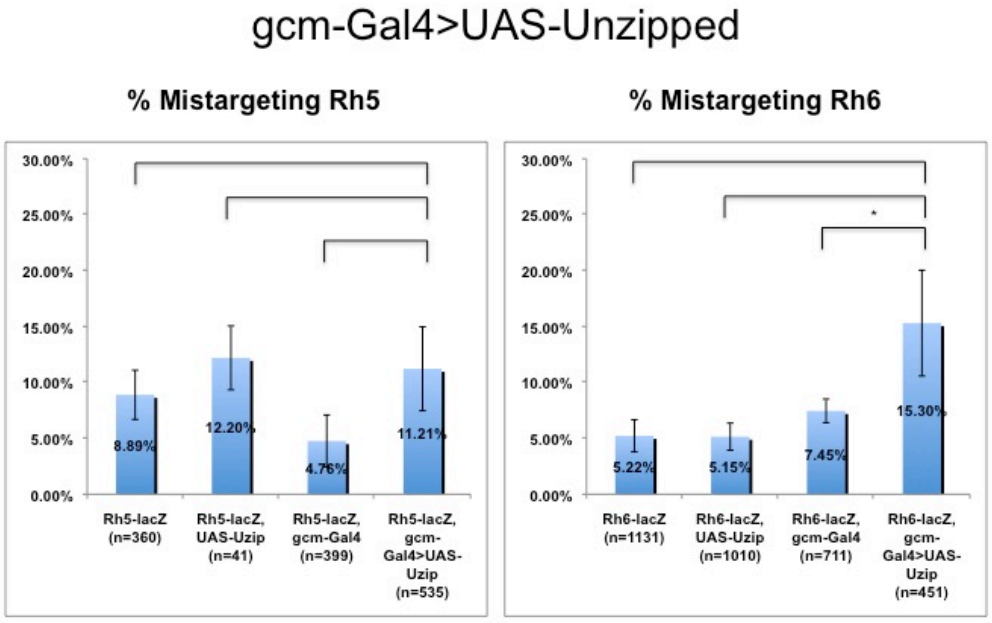

Figure 4.70. Quantification of R8 axons mistargeting in gcm-Gal4>UAS-Uzip flies. The Rh5-lacZ and Rh6-lacZ expressing R8 axons were counted and analyzed separately. (Student two-tailed T test *p<0,05 **p<0,01 ***p<0,001) Rh5 p values= 0,7: 0,964: 0,177; Rh6 p values= 0,06: 0,06: 0,048 respectively. Y error bars represent SEM.

Moody-Gal4 was the next driver, used for misexpressing Uzip in carpet glia cells and another subgroup of glial cells at the adult stage, which are not yet identified. Due to restrains in fly maintenance, the '*moody-Gal4>UAS-Uzip, Rh5-lacZ'* flies could not be generated, so the projection of the R6-lacZ expressing axons could be observed only (Figure 4.71).

The misexpression of Uzip in *moody-Gal4* driven cells did not cause a change in the projection of Rh6-lacZ expressing cells. The ratios for mistargeting are 20,33% for the 711 axons counted for '*moody-Gal4,Rh6-lacZ'* flies and 19,7% for the 451 axons counted for '*moody-Gal4>UAS-Uzip,Rh6-lacZ'* flies. The change is not significant (Figure 4.72). It is possible that the carpet cells are not involved in the projection of R8 cells and neither knocking down nor misexpressing Uzip causes a defect in the projection.

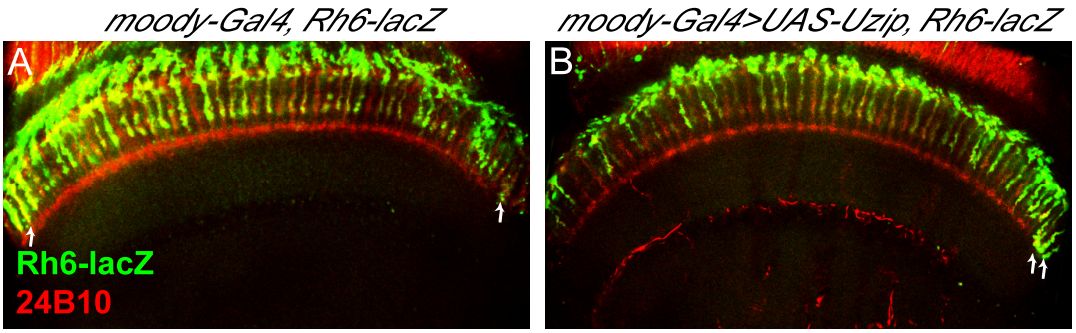

Figure 4.71. Projection analysis of Rh6-lacZ expressing R8 cells in *moody-Gal4>UAS-Uzip* flies. *moody-Gal4, Rh6-lacZ* (A) and *moody-Gal4>UAS-Uzip, Rh6-lacZ* (B) flies are stained with β-Gal (green), and 24B10 (red). With a few exceptions (arrows) the Rh6-lacZ expressing axons terminate at M3, and the 24B10 stained PR cells terminate at M6.

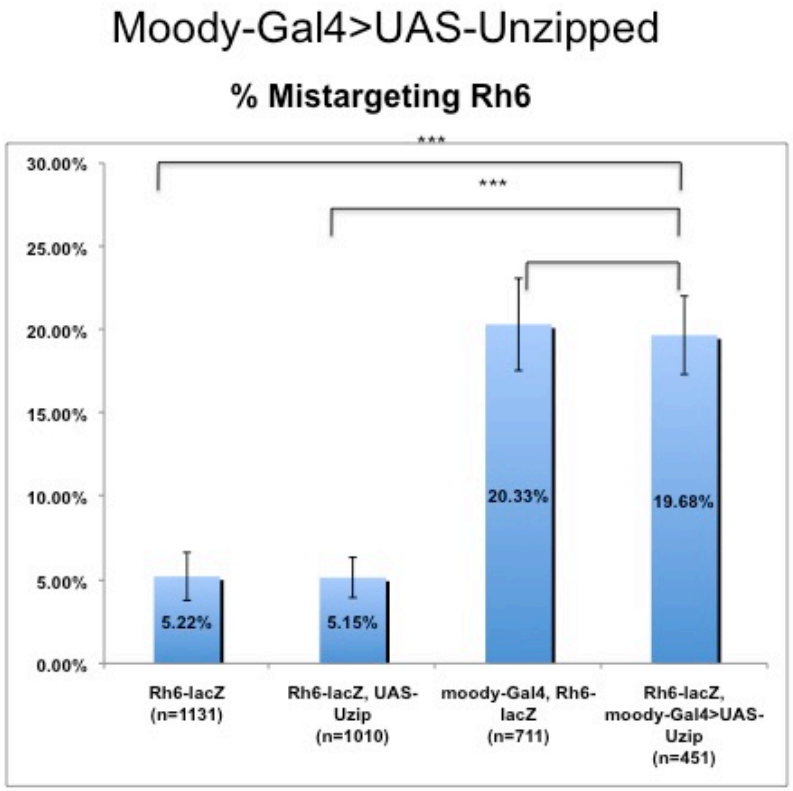

Figure 4.72. Quantification of R8 mistargeting in *moody-Gal4>UAS-Uzip* flies. The *Rh6-lacZ* expressing R8 axons were counted and quantified. (Student two-tailed T test *p<0,05 **p<0,01 ***p<0,001) Rh6 p values= 0,000: 0,000: 0,904 respectively. Y error bars represent SEM.

The last driver to be tested was *Mz97-Gal4*, which is expressed in wrapping glia. We wanted to see the affect of misexpressing Uzip in another glial subgroup. The reason why we chose wrapping glia is their role in wrapping the axons after the PRs have differentiated. First we tested the driver, and confirmed that it is expressed in a subgroup of glial cells (Figure 4.73). There is no other way of testing it since no antibody exists against wrapping glia.

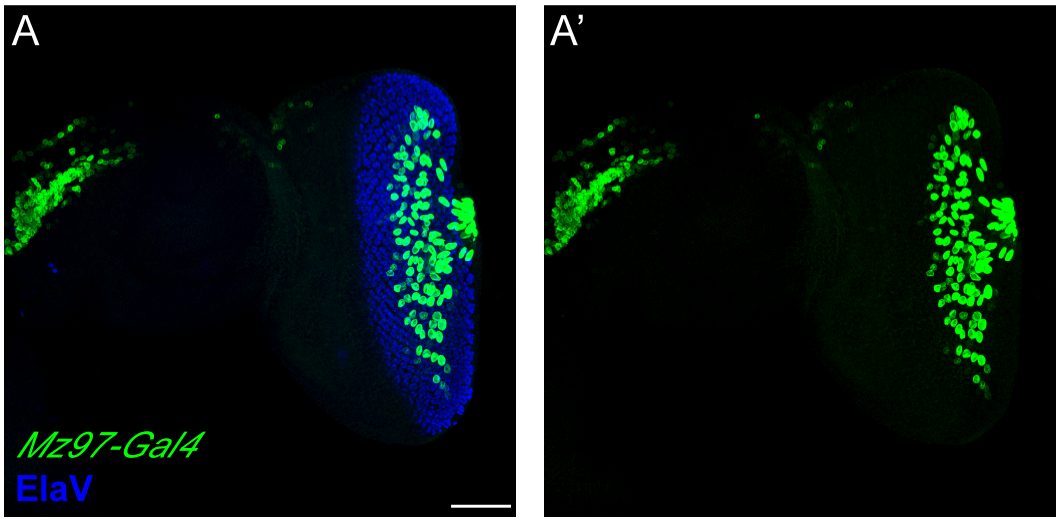

Figure 4.73. Expression pattern of the *Mz97-Gal4* driver. The *Mz97-Gal4* driver was tested by crossing with the UAS-nGFP reporter. The *Mz97-Gal4* driven cells are expressed in a layer above the PR cells like glial cells and their expression start a few rows after the MF, which is compatible with the expression of wrapping glia.

Then we misexpressed Uzip in *Mz97-Gal4* driven cells and observed the projection pattern of Rh5 and Rh6 expressing cells. The ratio in *Rh5-lacZ* expressing flies were 9% for '*Rh5-lacZ'*, 12,2% for '*Rh5-lacZ, UAS-Uzip*', 15,7% for '*Rh5-lacZ, Mz97-Gal4*', and 13,3% for '*Rh5-lacZ, Mz97-Gal4>UAS-Uzip'* flies respectively. These ratios are very close to each other, thus are not significant. For the *R6-lacZ* expressing R8 cells, the ratios were 5,2% for '*Rh6-lacZ'* flies, 5,2% for '*Rh6-lacZ, UAS-Uzip'* flies, 13,9% for '*Rh6-lacZ, Mz97-Gal4*' flies, and 11% for *'Rh6-lacz, Mz97-Gal4>UAS-Uzip'* flies. This group does not show a significant change in ratios either. In overall we can conclde that misexpressing Uzip in wrapping glia does not have an affect on R8 axonal targeting (Figure 4.74, 4.75).

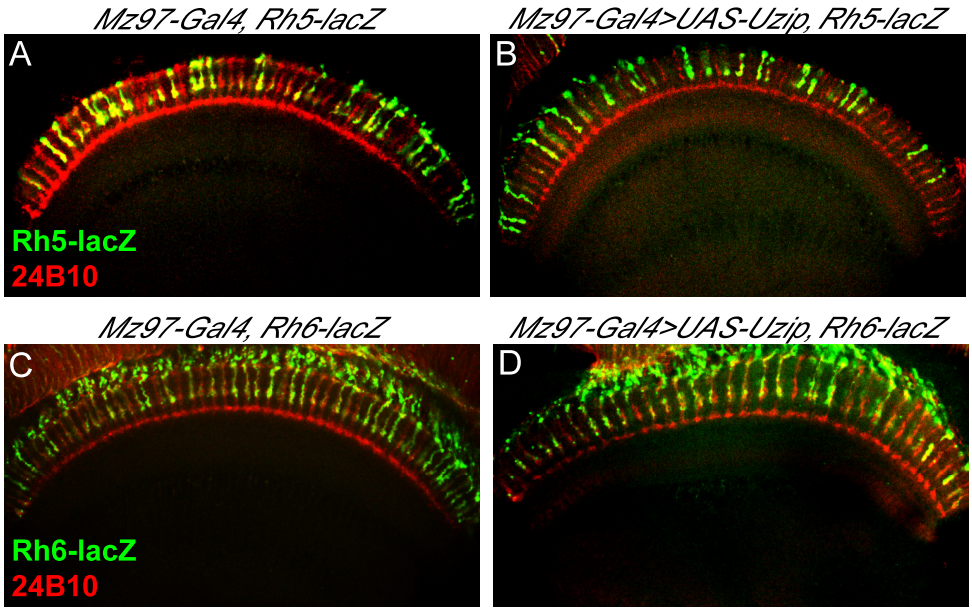

Figure 4.74. Projection analysis of R8 cells in *Mz97-Gal4>UAS-Uzip* flies. *Mz97-Gal4, Rh5-lacZ* (A), *Mz97-Gal4>UAS-Uzip, Rh5-lacZ* (B), *Mz97-Gal4, Rh6-lacZ* (C), and *Mz97-Gal4>UAS-Uzip, Rh6-lacZ* (D) flies are stained with β-Gal (green), and 24B10 (red). The Rh5-lacZ expressing axons terminate at M3, the 24B10 stained PRs terminate at M6.

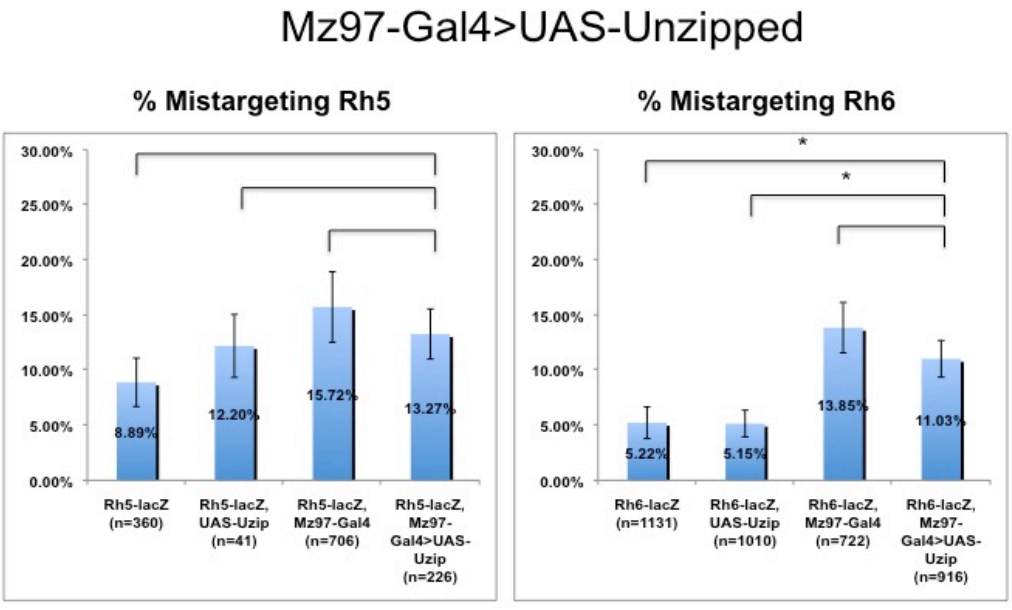

Figure 4.75. Quantification of R8 axon mistargeting in *Mz97-Gal4>UAS-Uzip* flies. The *Rh5-lacZ* and *Rh6-lacZ* expressing R8 axons were counted and analyzed separately. (Student two-tailed T test *p<0,05 **p<0,01 ***p<0,001) Rh5 p values= 0,25: 0,624: 0,29; Rh6 p values= 0,048: 0,033: 0,165 respectively. Y error bars represent SEM.

We can conclude that misexpressing Uzip in *gcm-Gal4* and *lGMR-Gal4* expressing flies lead to a mild mistargeting phenotype in Rh6-lacZ expressing axons, while there is no significant change seen when Uzip is misexpressed in other tissues. It is possible that misexpressing Uzip in PR cells which do not express Uzip and glia which are not in the target area, increases the axonal misprojection ratios, Knocking down Uzip in *gcm-Gal4* driven cells also leads to a mistargeting phenotype, suggesting that both misexpressing and downregulating Uzip in an early key glial driver which is expressed in the optic lobe is critical for R8 targeting. The misexpression of Uzip in PR cells also causes a mild targeting phenotype confirming that the PRs affect each other in the targeting process and misexpressing a CAM which is not normally expressed in all PRs can increase the adhesive force towards each other and as a result lead to misprojection. In addition downregulation of Uzip in *repo-Gal4* driven cells increases the misprojection phenotype, suggesting that *unzipped* expression in glial cells residing in the target region are critical for axonal targeting. In their absence, Unzipped can not be compensated, leading to the an increase in misprojection. The other phenotypes were counted in each group but both in the downregulation and the misexpression analysis but their numbers were insufficient for quantification so we did not analyze them further.

5. DISCUSSION

The visual system of *Drosophila melanogaster* is an excellent model for studying cell fate determination and neuronal differentiation due to its conserved molecular network in addition to its neural simplicity (Wernet and Desplan, 2004). The amount of tools generated in *Drosophila,* enables an extensive chance to study the regulatory mechanisms involved in these networks, which mostly have homologs in more complex organisms.

The compound eye of *Drosophila* is made of 800 ommatidial units, each composed of eight PRs. R1-R6 cells form the outer PRs and are responsible for motion detection and R7-R8 form the inner PRs that are responsible mainly for colour vision. The PR cells express different rhodopsins, G-protein coupled receptors that initiate phototransduction (Rister and Desplan, 2011). The outer PRs express Rh1 while the inner PRs express Rh3-Rh6. If R7 expresses Rh3, the coupled R8 expresses Rh5 forming the pale subtype. If R7 expresses Rh4, the coupled R8 expresses Rh6 forming the yellow subtype. Pale and yellow subtypes are distributed in a ratio of 30 to 70% of the ommatidia (Gao *et al.*, 2008). There is a similar organization in the vertebrate visual system where different groups of PRs are responsible for colour vision and motion detection by expressing different sets of opsins that are sensitive to different wavelengths (Cook and Desplan, 2001).

The formation of the eye starts at the embryonic stage with the eye primordium (Kumar, 2009) but the differentiation process of the PRs start at the 3rd instar larval stage. The PR cells start to differentiate with the sweeping of the MF through the eye imaginal disc and as the PR axons differentiate, their axons project to their temporal layers in the optic lobe. At the first half of the pupal stage the inner and outer PRs are distinguished from each other and the axons of the PRs move on to their second temporal layer. At the second half of the pupation period, each PR expresses a specific rhodopsin molecule, which specifies the yellow or pale subtype of each ommatidium. The PR axons also target to their final layers in the lamina and medulla, which is the lamina for outer PRs, M3 layer for R7 axons, and M6 layer for R8 axons (Wernet and Desplan, 2004; Morante *et al*., 2007; Hadjieconomou *et al*., 2010). This differentiation process requires a large network of

molecules, which are interrelated with each other. Although some pieces of this big puzzle are found, there are still many unknowns to elucidate.

Our interest was to find additional players, which are involved in the differentiation and targeting of PRs by focusing on the specification of the inner PRs, especially R8 cells. Previously an enhancer trap screen was performed to find the potential candidates. From the lines selected based on the expression pattern at the third instar stage and the localization of the enhancer trap, we chose *unzipped* in order to analyze its function in the visual system.

5.1. Unzipped: A Novel CAM

Unzipped is a novel CAM, which does not have any known functional domains or similarity to other known CAMs. It was shown to have a role in axonal targeting in the CNS at the embryonic stage (Ding *et al.*, 2011). CAMs are molecules involved in the targeting of many different types of neurons including PR axons. The R8-specific expression of an enhancer trap line inserted into its first intron made it a promising candidate to have an effect on inner PR differentiation and targeting. There are not many molecules that have an R8 specific expression, which makes Unzipped an outstanding molecule to analyze.

In order to gain a better insight to the possible function of Unzipped we did bionformatic analyses and tried to find any predicted domains that could give an idea on its function. However, no additional information other than the GPI modification site and signal peptide could be identified, which were already reported (Ding *et al.,* 2011).

Two Unzipped enhancer-trap lines were used for expression analysis at different developmental stages; both were inserted to the 5'UTR and the first intronic region of Unzipped. At the third larval instar stage both lines had R8-specific expression in addition to subsets of glial cells. We stained the AC783 line at the 48 hour pupal stage and the R8-specific expression continued at the midpupa stage. At the adult stage *AC783>UAS-nGFP* colocalized with the glial marker Repo. *AC783>UAS-CD8::GFP* projected to the same

layer in the medulla as the PRs. These results showed that Unzipped is expressed in R8 cells and a subgroup of glial cells at early stages of development, and at the adult stage it projects to the same layer in the medulla as the PR axons.

Enhancer-trap lines can give a general idea about the expression of the associated gene but they are not fully dependable for obtaining the exact expression pattern. The insertion site of the Gal4 element to the genome and its orientation are critical for the expression pattern, and there is always the possibility that the regulatory regions are far from the Gal4 element or there are multiple sites. In order to know the exact expression pattern of a gene, the endogenous expression is necessary.

The antibodies generated by the Huang group were tested in Western Blots and shown to recognize the Uzip protein. Then the antibodies were used in immunostaining experiments, however no specific staining was observed in third instar eye imaginal discs. The antibody generated against the long fragment gave no result and the antibody against the shorter fragment gave a lot of unspecific background staining. At this stage with the very low amount of antibody we had, we tested the short fragment in the adult stage. There were unspecific dot like structures, but there was also a line of projection around the M3 layer of the medulla. The structure was similar to that of the enhancer trap lines, the only difference was that it was localized at an upper layer in the medulla.

I generated an Uzip antibody against the long fragment sequence defined by Ding *et al.,* 2011. This sequence comprises the region between 174-405 aa. The antibody was tested in Western Blots against proteins isolated from wt and mutant tissue. The results were very promising as no band was detected in the mutant tissue, while a band at the correct position was detected in the protein isolated from wt flies. The antibody was then used for immunostainings in third instar larva eye discs. There was no difference between the null mutants and the wt flies. However, antibody stainings on eye imaginal discs taken from flies where Uzip was misexpressed in all PRs using the lGMR driver (*lGMR-Gal4>UAS-Uzip*) showed that the Uzip antibody was able to detect Unzipped when overexpressed. Stainings of the adult brain showed that the Uzip is expressed in the M3 layer, just like in the stainings done with the antibody of Huang group. Finally the expression pattern of the mCherry tagged BAC line generated in our lab (Kaan Mika,

2014) was analyzed. At the third instar larva stage, there was expression both in R8 cells and in the membrane of a subgroup of glial cells. At the 48 hour pupa stage, the expression the R8 cells continued. At the adult stage the mCherry was detected at the same layer to which PR cells project to, although they did not colocalize with the PR axons.

Taken together all the experiments performed towards the elucidation of Unzipped expression and localization, we conclude that Unzipped is expressed in R8 cells and a subgroup of glial cells at the 3rd instar larval stage and continues to be expressed in R8 cells at the 48 hour pupa stage. In the brain expression is observed in presumably glial cells, which send out protrusions to the M3 or M6 layer in the medulla. Using the antibody that was generated in our lab as well as the antibodies obtained from the Huang group, no specific expression could be observed either in R8 or glial cells. It is possible that the endogenous expression level is low in R8 cells. Another possibility is that since Unzipped is a CAM, probably it is not localized to the nucleus and it is hard to detect it when it is distributed along the membrane. We were able to detect expression in R8 cells and glia cells in the mCherry tagged BAC line, which might be reflecting the endogenous expression of Unzipped. Thus, it is possible that we still need to find the appropriate staining conditions in which the antibody works optimally. The protocols used in projection experiments are all similar to each other, but minor changes can sometimes affect the result of the stainings such as increasing the blocking periods, changing antibody concentrations, elongating washing steps, or trying preabsorption with higher amount of embryos. In addition, using different protocols for the purification of the antibody with NHS-activated agarose dry resin can be useful. We optimized the steps in the protocol, made some changes in the solutions, and used different columns for the purification until we got high concentrations of the Uzip antibody. Further optimization is possible with different solutions and columns. The visualization of Unzipped distribution with an Unzipped-specific antibody is crucial for elucidating its function.

5.1.1. Role of Unzipped at Early PR Differentiation Stage

Since Unzipped has an R8-specific expression at early stages of PR differentiation, we wanted to see if deleting or misexpressing Unzipped in PR cells had any affect on the

most commonly used glial and neuronal markers. We first tested if there was any change in the formation or distribution of R8 cells, which were visualized by using the anti-sens antibody at the 3rd instar larva and pupal stages. There was no change in R8 specification since only one R8 cell per ommatidium was stained with Senseless as expected. Then the R7 cells, which are the last ones to be recruited, were stained with the R7 marker Prospero both at the 3rd instar larva and pupal stages. The structure was intact and there was no change in the expression pattern or specification in the null mutants and in Uzip misexpressing flies compared to *wt* flies. Next, we tested if there was a difference in the expression of Chaoptin as a PR membrane marker to trace the projections. Chaoptin staining gives an idea on the overall projection of the PR stages, but there was no disruption in the overall pattern at the third instar stage. Finally we tested if there was any change in the expression pattern of Repo as a glial cell marker. There was no change in the structure or distribution of Repo expressing glial cells. These experiments suggest that Uzip does not play a role in the formation of R7 or R8 cells, the overall projection of the PR cells, or the distribution and specification of the glial cells.

5.1.2. Role of Unzipped in Terminal PR Differentiation and Projection

In a second set of experiments we analyzed if Unzipped plays a role in terminal PR differentiation. The major changes here involve subtype specification of PR cells and axonal projection to the medulla.

5.1.2.1. Function of Unzipped in Subtype Specification. In order to understand the role of Unzipped in subtype specification, adult retinas were stained with R8-specific Rhodopsins Rh5 and Rh6. While R8 is the first cell to be specified it is the last inner PR to terminally differentiate. The final step in terminal differentiation is the expression of specific Rhodopsin molecules. The choice of which Rh to express is made in the R7 cell and is then communicated to the R8 cell. Thus, theoretically any problem in specification in the R7 cell would also lead to a change in the Rh distribution in the R8 cell. Thus, in the subtype analyses performed here, the distribution of Rh5 and Rh6 was evaluated primarily. The adult retinas of $Uzip^{D43}$ null mutants and $Uzip^{23}$ hypomorph mutants were stained and their Rh5/Rh6 distribution were compared with wt flies. The ratios of the hypomorphs and wt

flies were very close to each other 43,5 – 56,5 % for *Uzip* ^{23} and 43 – 57 % for the *wt* group. However there was a slight change with the null mutants, which had a 36 – 64 % ratio. There has been no such mild change previously reported in the literature and in order to confirm this slight increase in the ratio, the amount of retinas stained should be increased. Additionally, the flies used as the control group were QB flies in order to omit the possible affect of the balancers in the null and hypomorph mutants. These experiments can be repeated with flies without any balancers and wt flies can be used as controls to see if the slight change in ratio remains. Similarly we analyzed the effect of overexpressing Unzipped in all PRs using *lGMR-Gal4>UAS-Uzip*. However, no significant change in the ratio of Rh5/Rh6 was encountered in these flies and the ratios were within the expected wt range as cited in the literature (Wernet *et al*., 2006).. Additionally, we analyzed the effect of specific downregulation of Uzip in PR cells rather than looking at a total knockout of Unzipped in PRs and target area. While the obtained data were not quantified for this group, no significant change in the distribution of Rh5-Rh6 expressing R8 cells was detected by simple observation. From these results we concluded that changes in the levels of Unzipped did not have a significant effect on the subtype specification of R8 cells, and also presumably R7 cells.

5.1.2.2. Function of Unzipped in Axonal Pathfinding. Since Uzip is a cell adhesion molecule and was shown to be involved in axon guidance in the CNS, we sought to analyze its possible involvement in the regulation of axonal projections of PR cells. We first checked if there was any targeting defect in the projection pattern of the inner PRs in null mutants. The adult brains of null mutants and wt flies crossed with flies carrying the reporter constructs Rh3-Rh6 lacZ, labelling R7 and R8 PRs, were analyzed for changes in axonal projections. These analyses did not reveal any phenotype in axonal targeting in Unzipped null mutants. These results are consistent with observations of Ding *et al*., where no phenotype was observed in Uzip null mutants as well. Only when Uzip was mutated together with *wnt5* or *CadN*, the severity of the phenotype of these two mutants increased (Ding *et al.,* 2011). Since CAMs mostly interact homophilically or with another CAM and compensate for each other, it is a general phenomenon that just changing the levels of one of the CAMs is not sufficient to generate a phenotype (Ding *et al*., 2011). Due to this reason we also wanted to see if the misexpression or the tissue-specific downregulation of Unzipped has an affect on the projection of inner PRs.

Uzip levels were downregulated with the neuronal drivers *Elav-Gal4*, *lGMR-Gal4*, *sens-Gal4*, and the glial drivers *repo-Gal4*, *gcm-Gal4*, and *moody-Gal4*. The projection analysis at this stage was narrowed down to R8 cells only. Except for *sens* and *gcm*, all Uzip-RNAi lines were crossed with the specific driver and both Rh5-lacZ and Rh6-lacZ lines were used to trace the projection of both Rh5 and Rh6 expressing R8 cells. The lines with the Rh5-lacZ construct could not be generated for *sens* and *gcm* because the flies were very unhealthy and could not survive at 29^0C. The major reason for using both Rh5-lacZ and Rh6-lacZ lines was the Rh5-lacZ expressing R8 cells comprise 30% and the Rh6-lacZ expressing R8 cells comprise 70% of the ommatidia. It is easier to trace single axons with Rh5-lacZ lines, but Rh6-lacZ-expressing cells would give a higher number of axons to quantify. The axonal phenotypes were evaluated according to their mistargeting. Axonal bundling, endjoining, branching, and thickness phenotypes were very low in number so those phenotypes were not evaluated.

When compared with the control groups, there was an increase in the mistargeting axons when Uzip is downregulated using the *repo-Gal4* and *gcm-Gal4* drivers. There was a ~20% increase in mistargeting axons in *repo-Gal4>UAS-Uzip-RNAi, Rh5-lacZ* flies, and a ~10% increase in mistargeting axons in *repo-Gal4>UAS-Uzip-RNAi, Rh6-lacZ* flies. As for *gcm-Gal4>UAS-Uzip-RNAi, Rh6-lacZ* flies, this ratio was ~20%. The other targeting phenotypes were very low in number. The highest phenotype after mistargeting was branching and the percentages were not more than 1% or 2%, so the other phenotypes were not considered further.

As mentioned before, CAMs do not usually give strong phenotypes when they are deleted on their own, due to their redundancy. Even minor changes in phenotypes mean that they might be involved in the targeting process because they could not be compensated. Due to this reason for some CAMs the 10% and 20% changes in the targeting when downregulated is considered as a phenotype (Sandra Müller, 2011; Bazigou *et al*., 2007). By looking at expression pattern stainings of Uzip, we had concluded that Uzip was expressed in a subgroup of glial cells starting from the third instar larval stage and it was also expressed in glial cells in the PR targeting area. It is also known that glial cells and PRs interact with each other for regulating axonal targeting. From these results we can suggest that Uzip is expressed in the glial cells, which express

the early glial marker *gcm* and its downstream target *repo*. The downregulation of Uzip in the glial cells expressing *repo* and *gcm* specifically, might have affected the Uzip expression in the glial cells residing in the target projection area of R8 axons. It was shown that Uzip functions by homophilic interactions, so it is possible that when Uzip is not expressed in the glia in the target projection area, the R8 axons cannot stop at the appropriate layer and some of them misproject. Also it is important to consider that unlike the knockout mutants, these are RNAi lines and are not fully penetrant. The RNAi lines are generated by injecting a vector, which contains the RNAi hairpin of the specific gene under the control of the UAS element, to the flies in order to generate transgenic lines. When Uzip is downregulated in a group of cells by a specific driver, the expression of Uzip is downregulated by the double hairpin but it is not fully removed. There are some methods to increase the penetrance of those lines such as increasing the temperature as we did in our RNAi experiments in order to increase the Gal4 activity, or to add other constructs such as *UAS-Dicer2*, which is also used for increasing the RNAi activity in neurons. As a summary, it is pretty normal to see partial phenotypes with the RNAi lines since Unzipped is not completely removed from the region. Some of the other CAMs also show a 10% to 20% mistargeting phenotype when they are downregulated by using specific drivers (Sandra Müller, 2011).

By looking at the other Uzip downregulation results, we can suggest that the expression of Uzip in the carpet glia did not affect R8 targeting. Also there does not seem to be any change when Uzip is downregulated in R8 cells with *senseless* or other neuronal drivers. The reason for this might be the low endogenous expression of Uzip in those cells. From the expression pattern analysis, the endogenous expression pattern suggested that Uzip is expressed at a lower level in R8 cells and it is hard to detect with Uzip antibodies. It is possible that although the Uzip level expressed in the R8 cells decreased, considering that the RNAi line is not fully penetrant and there is still some expression of Uzip after its downregulation, the amount express in the R8 cells was still sufficient for targeting while the decrease of Uzip in the glial cells causes a more major effect. In order to gain a better insight to the function of Uzip in R8 cells, the downregulation of Uzip might be enhanced by adding UAS-Dicer2, which increases RNAi penetrance in neuronal cells.

Uzip was also misexpressed in neuronal and glial tissues. *Elav-Gal4*, *lGMR-Gal4*, *repo-Gal4*, *gcm-Gal4*, *moody-Gal4,* and *Mz97-Gal4* were used as the drivers to misexpress Uzip. Only *Mz97-Gal4* the wrapping glia driver was added to the previous group, which was not used before. We wanted to see the consequences of misexpressing Uzip in the wrapping glia, which surround the axons as they differentiate and project towards the optic lobe.

There was a ~7% increase in the mistargeting phenotype of *lGMR-Gal4>UAS-Uzip, Rh6-lacZ* flies and ~7% increase in *gcm-Gal4>UAS-Uzip, Rh6-lacZ* flies. These increases were milder compared to the phenotypes obtained after downregulation of Uzip, but there was still an increase in the mistargeting phenotype. There was no change seen with the other drivers.

The phenotypes seen in the misexpressions are milder compared to the results obtained from Uzip downregulation. The mistargeting increased when Unzipped was misexpressed using the *lGMR-Gal4* and *gcm-Gal4* drivers. The reason why the phenotype increased in glia cells, which misexpress Uzip by using the *gcm-Gal4* driver but not the repo-Gal4 driver, might be the location of *gcm* expressing cells. At the third instar larva, the glia generated from the glial precursor region express *gcm*. In addition, the medulla glia residing at the GPC lining, which have unknown source and function, express *gcm*. These glial cells are at the lower region compared to the area where R8 axons project. It is possible that the glia at the region that normally do not express Uzip gain an adhesive property and cause the R8 axons to mistarget towards this adhesive signal. Other glia drivers can not drive the expression in this region (Chotard and Salecker, 2007; Chotard *et al.*, 2005; Awasaki *et al.*, 2008). As for *lGMR*, it is a very strong driver and its expression is stronger than *Elav* (Figure 4.43, 4.46). *lGMR* misexpresses Uzip in other PRs including R7. Instead of terminating at their target layer, some of the R8 axons follow the R7 axons, which express *uzip* which leads to their mistargeting. The same effect cannot be seen with *Elav* since it is weaker compared to *lGMR*.

For cell specific labelling and testing for cell-autonomous expression, mosaic analysis with a repressible cell marker (MARCM) labeling would be useful, which is a genetic mosaic system. MARCM is a method for studying both lineage and morphology. It

highlights postmitotic neurons on lineage and neuronal birth timing basis. The neurons from the same lineage are labelled together as a multicellular clone by recombination in a dividing neuroblast. It is also possible to label two-cell and single-cell clones. MARCM allows the analysis of single cell homozygous mutants in wildtype/heterozygous background, which enables to test the autonomous function of the candidate gene (Lai and Lee, 2006; Yu *et al.*, 2009). We tried generating those clones for Unzipped, but due to maintenance problems we could not obtain the appropriate fly lines. For the future studies MARCM clones could be generated in order to elucidate the role of Unzipped in single cells and to find out if the effect is cell autonomous or not.

5.1.2.3 Suggested Model for the Role of Unzipped in Axonal Targeting. In the light of our findings, we suggest a model for the role of Unzipped in axonal targeting (Figure 5.1). According to this model, Uzip expressed in R8 cells follow the adhesive signal coming from Uzip expressed by glial cells at the target region. The Uzip expressed in the glial region can be both membrane bound or secreted. It was shown previously that the membrane bound version of Uzip was active rather than the secreted version, but this might change from system to system (Ding *et al.*, 2011). We can only suggest that the Uzip expressed by the R8 cells are membrane bound, since the mCherry tagged Unzipped fusion protein, labeled at the C-terminus, are expressed in R8 cells in the 3rd instar larva and pupa stage. As we cannot make conclusions for the target region, we considered both the secreted and the membrane bound form of Unzipped in our model.

When Uzip is knocked down in the glial cells at the target region with the *repo-Gal4* and *gcm-Gal4* drivers, the adhesive signal from the glial cells in the target region is reduced and some of the R8 axons can not stop at their target region leading to a misprojection phenotype (Figure 5.2). When Uzip is misexpressed with the *gcm-Gal4* in the lower glial region, the glial cells which do not normally express Uzip express it and the adhesive signal leads some of the axons to move further from the temporal layer instead of stopping. The same effect is also seen when PR cells misexpress Uzip. When the R7 cell misexpresses Uzip together with the other PRs, this causes some of the R8 cells to follow the R7 cells and project further compared to its target layer (Figure 5.3).

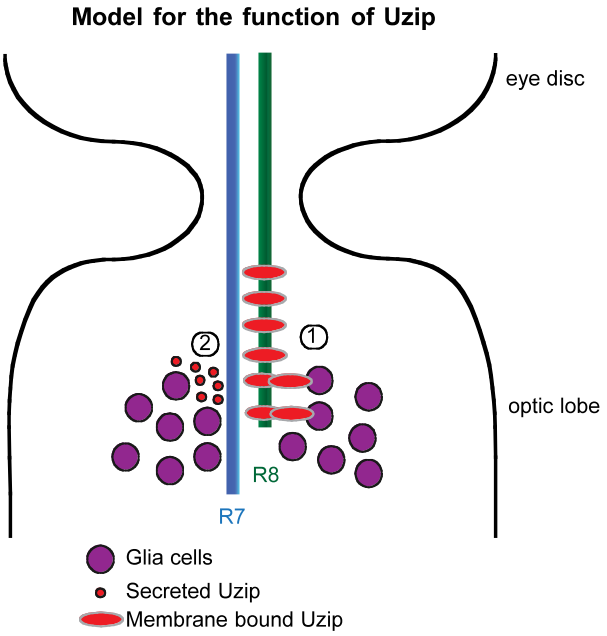

Figure 5.1. Suggested model for the function of Uzip in R8 axonal targeting. The Uzip expressed in R8 cells either bind (1) or are attracted to the secreted form (2) of Unzipped expressed by the glial cells at the target region.

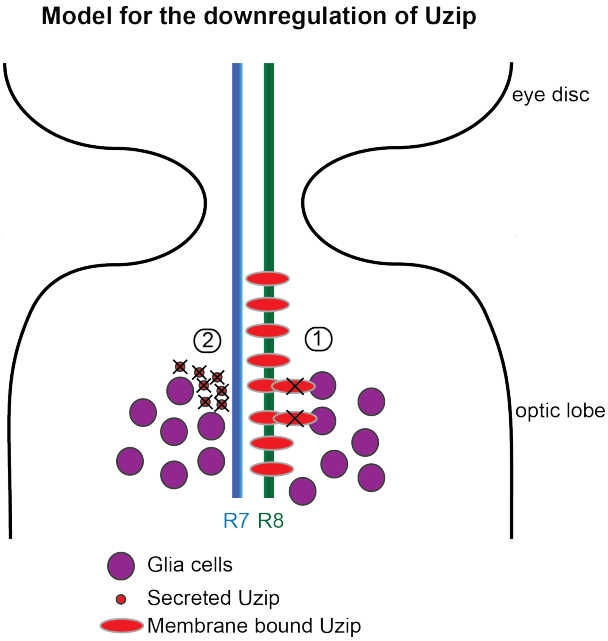

Figure 5.2. Suggested model for R8 axonal targeting when Uzip in knocked down in the glia at the target region. The Uzip expressed in R8 cells cannot bind (1) or respond to the secreted form (2) of Unzipped and misproject to layers past their target layer. Anterior up, posterior down.

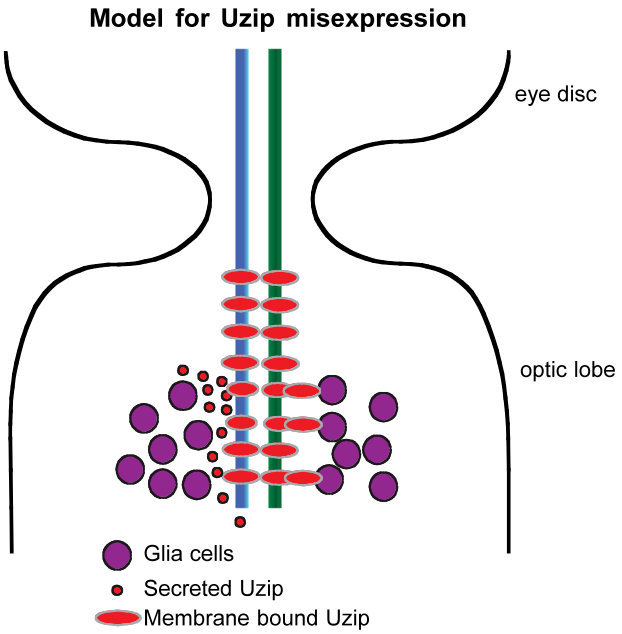

Figure 5.3. Suggested model for R8 axonal targeting when Uzip is misexpressed in the glia at the posterior regions of the optic lobe and PR cells. The Uzip expressed in R8 cells bind (1) or respond to the secreted form (2) of Unzipped misexpressed in R7 cells or glial cells residing in the posterior regions compared to the temporal projection layer. The Uzip expressing R8 cells are attracted to the cell adhesion molecules and misproject to layers past their target layer. Anterior up, posterior down.

These models are based on our findings and previous knowledge, but there are also other points to be considered. We presume here that Uzip does homophilic binding as previously shown with the aggregation assay. Since there is not much known about Uzip or its domains, it is possible that it has other interaction partners. Previously, it was shown that deleting Uzip on its own did not cause any phenotype, while it increased the severity of the phenotypes of *wnt5* and *N-Cad* mutants in the VNC when mutated together with those molecules. Although no direct interaction was found between these molecules with pulldown asays, by looking at the evidence that it increases the targeting phenotype, it is possible that Uzip has other partners of interaction.

One of the possible candidates is N-Cad, which is also a cell-adhesion molecule. Previously it was shown that the mutation of Uzip did not lead to any phenotype, but when mutated together with NCad, it increased the severity of the axonal targeting phenotype (Ding *et al.,* 2011). NCad is also involved in PR targeting, so it is highly possible that it might be interacting with Uzip (Ting *et al.*, 2005; Lee e*t al.,* 2001). Flamingo and Gogo are other two cell surface molecules, which are involved in R8 targeting. Both Gogo and Fmi are expressed in photoreceptor axons in the third instar larvae. In the optic lobe, Fmi is strongly expressed in the target region together with photoreceptor axons, while Gogo is mainly detected in photoreceptor axons (Berger-Muller and Suzuki, 2011; Lee *at al.,* 2003; Berger *et al.,* 2008; Hakeda-Suzuki *et al*., 2011; Hakeda and Suzuki, 2013; Hein *et al*., 2013; *Mann et al.*, 2012; Ohler *et al.,* 2011; Tomasi *et al.,* 2008). These two molecules interact with each other for regulating axonal targeting, it is also possible that there are other molecules which they interact with. Uzip might be one of those CAMs. Capricious, which is another transmembrane protein with leucine-rich repeats, can be another candidate. It is also one of the molecules shown to have an R8 specific expression pattern and is also expressed in several medulla layers including M3. It has been lately shown that *caps* has a mild affect on axonal targeting like *unzipped*, and there is the possibility that due to the expression pattern and functional similarities, *capricious* might be a candidate for being an interaction partner of *uzip* (Abrell and Jackle, 2001; Kohsaka and Nose, 2009; Shishido *et al.,* 1998; Taniguchi *et al.,* 2000, Berger-Muller *et al.,* 2013). Elucidating those partners and trying double mutations might give a better understanding on the function of Uzip.

Also looking at the initial stages of projection, which take place at the 3rd instar larva and first half of the pupal stage, in detail with other markers might be an important prospect. Here, axonal projections were analyzed at the larva stage by looking at null mutants and Uzip misexpressing flies, but no changes in the general projection pattern of the PRs were observed. However, since 24B10 stains all PRs, the projections of R7 axons and R8 axons could not be distinguished from each other. In order to gain a better insight it would be better to label R7 and R8 axons separately and analyze them to see if there is any change in the projection patterns. Analyzing the projection pattern at the pupal stage would also be an important step in this perspective since the final target choice takes place at this stage.

Although there are no homologues of Unzipped in the vertebrate system, considering the fact that Uzip has no similarity to any other known CAM, there might be other molecules that have an overlapping function in higher organisms but do not share a similarity in sequence. This can only be revealed when the exact role and the pathway that Unzipped is involved is elucidated, so that it can be matched with a similar interaction network can be found in more complex organisms.

6. CONCLUSION

In this study we investigated the role of Unzipped in the initial and terminal PR differentiation stages. Our results suggest that Unzipped is involved in the axonal targeting process of R8 cells. According to the expression pattern analysis, Uzip is expressed in R8 cells and in a group of glial cells at the target region of projection. From the downregulation/misexpression experiments performed for elucidating targeting defects the downregulation of Uzip in the target area and the misexpression of Uzip in the neighboring PRs and glia that are not in the target region, lead to an increase in axonal misprojection phenotypes.

For future studies it would be appropriate to look at early stages of the axonal projection process in more detail by specifically labelling and tracing the R8 cells. In addition, the search for interaction partners would be useful in both understanding the function of Unzipped and revealing the pathway that it is involved in. The elucidation of new partners and CAMs with these interaction experiments would reveal new players in axonal targeting. The changes in Unzipped expression, when its potential partners are downregulated and upregulated can also be studied, which would give important information on the networking of the molecules.

This study shows the expression and involvement of Unzipped in the visual system and axonal targeting. In addition, a working antibody was generated for performing future functional studies, which can also be used in order to find out about the function of Unzipped in other systems. Unzipped and its potential partners might reveal a new set of players in the targeting process of PR cells.

APPENDIX: PRIMER DESIGN FOR THE CANDIDATE ENHANCER TRAP INSERTION SITE

TCCTCTCTTCGAATCAGTTCTTGGTAAAACCAAACTTCAATAAACCGTTGGGTTAATGCGCGGATGT

GCGGATACTTTCAGTTAATTTTGAATTTTTCGAGGAACGGTGAAGGTCCGCGCTTGAATCAgtaagt**ccagt**

tccgagtatcacagccagatgtgagtgcttggcgccagtcgcaattaaattgactttaataaaatatct

ggcgggctccttgcgaacttttaattctggggaaacggacttgagtgattccaactaagagcaagaacacagt

tccttaaatgaagtgctacttctggcagcgttcttgagatgcgcgcagcatccttggcaatgacgtcattcgc

ctgctgaccagtttctctgtgttcgtgtgtatgtgtggcga**gagtgcgtatgcgtgtgtatgtgccg**aaatta

gagcgcaatagcgaattcaatttgcatttgcggaagaaataactgcaaacgaacagaatcgattgttgttgtc

gcgagtgctttgttaaggataagaagaagtcgcgactagttccgcaaaactctcacgttttgtctatggtttc

tcgtttccagAATCCTAAGTGAGGGACTCCGAATAGGATTCATTGGATGACAAA**CTAACGTGCAGCCAGG**

AATTATCGATTCAGgtaagccatcgtttctccttgaagcaactgggtcagacagcgataataattgcacgt

gtagttcctggttttccacaaaattgtcgtggtaagctgagccaccccatcttcccgaaaccttccagcttta

tgctgataatgaatttttaatgtgcgctgagactgctagtagaaaagaaaaaacaaacccacataaattaaac

ttgcaaaatcttcaaaggacagagaactgcgtcggtgcttccattccgctttttgggaggctgtaaattatg

aaagaccagacaagcggtagacaacaaggtttgcccgttcccaagggatcccggggcaacataatcaaaggcc

tttattactgggctggaatcggatggggcccgtccggaaaccatgccgcagacggctttcctggcccggagtc

ccgtgaca**gggcacgttcgacctaataag**catacgtcgttgagtaaatgggggccgtggaactttgcat

ttacgactcggcagagctgtaagtgcttccgggctgccccccgagggcaagaatcgattttcgatgttaa**tc**

gagttgaaaaccctgcaaactcggctgtgtttgtgtcctgttcaaaagggtgtttcacaatgaccagacatg

gaggcccttaa**ag**tcagttccaatttcgcctggtcaggatagaaaagcagatctctgtaagctctcctgcg

atcatatgtattcgttgttttatttatattagatttgctcatttgcgtggtccactcgcaaagttctcgactc

ctcctcagtccgccgtcaaaacttgttttatattcaaattttgatgcttctgcttgggttcgatttgtttgga

gatcgctcttccctctctcgtcatctacttattttcgccaatttacataatttagaccgatttatgatggca

ct**cgattgttgccgttctttctgggtgc**taatggtgtgtgatatcatcatccaaacaacacatgtttg

ctaatatatttacttcttgctttaatcacacctcgttactgcgatcttagtgacagaaatgtaatgtacatgt

gcaactcattcatgaacactttcaacagctgaatatatttacgttgcctggtaacatgattggatattaaaaa

ctctga**gaacgtcccctgcatatctgac**atttcatagcctcaagtgggccccattgaagcttggcggc

attgaaatggcgccaagttgtcgttcgctcgtttgacgcctcctctccgacctcctgctcctggggaggaaac

ctatttgacgccacacgcacacagctgagctggagggcaaaggacaccggcacgaaaacaaataaatgctcaa

ggagtagtcaaaggggaaggacgcggggcgatagcaattgtctgcgaaggcagcgaaggggataacgaaacc

ttggcttgatatcaggattcaggatatgaacaaaagttggcagttaattcgtttcgaagccgttgcccgcatt

gaggtctctctcagatcctgttgaaggtcgcaggattcgtaggaggcacgatgagtcatcagttctttagtta

at**ggcccaaaatggagagcaacagctcgg**gggaacgtcgtaaatttcccattgctagcagttgttga

ttatgaaattttattctctgcccaattaacttgcgtcgagcacgcgatggcccatatagcctcccaagctcgc
atagatatatgcataaagaccgatgttgctcagttgggtttcggattgcggtaggttgactacgattcgcttt
gtttatttgacggaatggtgcatgtaggcctggttccgggacctccaagcactctcaaaaatgaaaatcgatt
ttgtt

Figure A1. Primer design for the candidate enhancer trap insertion site. A 2500 bp region was chosen in the first intron of the *unzipped* gene. The yellow region is the site thought to be in the upstream of the enhancer trap insertion**,** the gray region is the site thought to be in the downstream of the enhancer trap insertion**,** the green region is the enhancer trap region, which is thought to be left in the genome after digesting the genome with the TaqI restriction enzyme. The first 3 red regions are the forward primers designed and the last 3 are the reverse primers designed in case the enhancer trap has inserted in a reverse orientation. The region between the bold black region is the piggyBac sequence.

REFERENCES

Awasaki, T., S.-L. Lai, K. Ito, and T. Lee, 2008, "Organization and Postembryonic Development of Glial Cells in the Adult Central Brain of Drosophila.", *The Journal of Neuroscience*, Vol. 28, No. 51, pp. 13742–13753.

Baker, N. E., and S. Y. Yu, 2001, "The EGF Receptor Defines Domains of Cell Cycle Progression and Survival to Regulate Cell Number in the Developing Drosophila Eye.", *Cell*, Vol. 104, pp. 699–708.

Baonza, A., and M. Freeman, 2002, "Control of Drosophila Eye Specification by Wingless Signalling.", *Development*, Vol. 129, pp. 5313–5322.

Bazigou, E., H. Apitz, J. Johansson, C. E. Lorén, E. M. A. Hirst, P. L. Chen, R. H. Palmer, and I. Salecker, 2007, "Anterograde Jelly Belly and Alk Receptor Tyrosine Kinase Signaling Mediates Retinal Axon Targeting in Drosophila", *Cell*, Vol. 128, pp. 961–975.

Bellen, H. J., C. Tong, and H. Tsuda, 2010, "100 Years of *Drosophila*research and Its Impact on Vertebrate Neuroscience: A History Lesson For The Future", Nature Reviews Neuroscience, Vol. 11, pp. 514-522.

Berger-Müller, S., A. Sugie, F. Takahashi, G. Tavosanis, S. Hakeda-Suzuki, and T. Suzuki, 2013, "Assessing the Role of Cell-Surface Molecules in Central Synaptogenesis in the Drosophila Visual System.", *Plos One*, Vol. 8, No. 12, p. e83732.

Bonini, N. M., Q. T. Bui, G. L. Gray-Board, and J. M. Warrick, 1997, "The Drosophila Eyes Absent Gene Directs Ectopic Eye Formation in a Pathway Conserved between Flies and Vertebrates", *Development*, Vol. 124, pp. 4819–4826.

Borst, A., 2009, "Drosophila's View on Insect Vision.", *Current Biology*, Vol. 19, No. 1, pp. R36–47.

Brand, A. H., and N. Perrimon, 1993, "Targeted Gene Expression as a Means of Altering Cell Fates and Generating Dominant Phenotypes.", *Development*, Vol. 118, No. 2, pp. 401–415.

Chen, P.-L., and T. R. Clandinin, 2008, "The Cadherin Flamingo Mediates Level-Dependent Interactions That Guide Photoreceptor Target Choice in Drosophila", *Neuron*, Vol. 58, No. 1, pp. 26–33.

Choe, K.-M., S. Prakash, A. Bright, and T. R. Clandinin, 2006, "Liprin-Alpha Is Required for Photoreceptor Target Selection in Drosophila", *Proceedings of the National Academy of Sciences of the United States of America*, Vol. 103, pp. 11601–11606.

Choi, K.-W., and S. Benzer, 1994, "Migration of Glia along Photoreceptor Axons in the Developing Drosophila Eye", *Neuron*, Vol. 12, pp. 423–431.

Chotard, C., W. Leung, and I. Salecker, 2005, "Glial Cells Missing and gcm2 Cell Autonomously Regulate Both Glial and Neuronal Development in the Visual System of Drosophila", *Neuron*, Vol. 48, No. 2, pp. 237–251.

Chotard, C., and I. Salecker, 2004, "Neurons and Glia: Team Players in Axon Guidance", *Trends in Neurosciences*, Vol. 27, No. 11, pp. 655–661.

Chotard, C., and I. Salecker, 2007, "Glial Cell Development and Function in the Drosophila Visual System.", *Neuron Glia Biology*, Vol. 3, No. 1, pp. 17–25.

Chou, W.-H., K. J. Hall, D. B. Wilson, C. L. Wideman, S. M. Townson, L. V Chadwell, and S. G. Britt, 1996, "Identification of a Novel Drosophila Opsin Reveals Specific Patterning of the R7 and R8 Photoreceptor Cells", *Neuron*, Vol. 17, No. 6, pp. 1101–1115.

Clandinin, T. R., C. H. Lee, T. Herman, R. C. Lee, a Y. Yang, S. Ovasapyan, and S. L. Zipursky, 2001, "Drosophila LAR Regulates R1-R6 and R7 Target Specificity in the Visual System", *Neuron*, Vol. 32, No. 2, pp. 237–248.

Clandinin, T. R., and S. L. Zipursky, 2000, "Afferent Growth Cone Interactions Control Synaptic Specificity in the Drosophila Visual System", *Neuron*, Vol. 28, No. 2, pp. 427–436.

Cook, T., and C. Desplan, 2001, "Photoreceptor Subtype Specification: From Flies to Humans", *Seminars in Cell and Developmental Biology*, Vol. 12, No. 6, pp. 509–518.

Cook, T., F. Pichaud, R. Sonneville, D. Papatsenko, and C. Desplan, 2003, "Distinction between Color Photoreceptor Cell Fates Is Controlled by Prospero in Drosophila", *Developmental Cell*, Vol. 4, No. 6, pp. 853–864.

Cooper, M. T., and S. J. Bray, 2000, "R7 Photoreceptor Specification Requires Notch Activity.", *Current Biology*, Vol. 10, No. 23, pp. 1507–1510.

Czerny, T., G. Halder, U. Kloter, A. Souabni, W. J. Gehring, and M. Busslinger, 1999, "Twin of Eyeless, a Second Pax-6 Gene of Drosophila, Acts Upstream of Eyeless in the Control of Eye Development", *Molecular Cell*, Vol. 3, pp. 297–307.

Dalva, M. B., A. C. McClelland, and M. S. Kayser, 2007, "Cell Adhesion Molecules: Signalling Functions at the Synapse.", *Nature Reviews Neuroscience*, Vol. 8, No. 3, pp. 206–220.

Ding, Z.-Y., Y.-H. Wang, Z.-K. Luo, H.-F. Lee, J. Hwang, C.-T. Chien, and M.-L. Huang, 2011, "Glial Cell Adhesive Molecule Unzipped Mediates Axon Guidance in Drosophila", *Developmental Dynamics*, Vol. 240, No. 1, pp. 122–34.

Domingos, P. M., S. Brown, R. Barrio, K. Ratnakumar, B. J. Frankfort, G. Mardon, H. Steller, and B. Mollereau, 2004, "Regulation of R7 and R8 Differentiation by the Spalt Genes", *Developmental Biology*, Vol. 273, No. 1, pp. 121–133.

Domingos, P. M., M. Mlodzik, C. S. Mendes, S. Brown, H. Steller, and B. Mollereau, 2004, "Spalt Transcription Factors Are Required for R3/R4 Specification and Establishment of Planar Cell Polarity in the Drosophila Eye", *Development*, Vol. 131, No. 22, pp. 5695–5702.

Domínguez, M., 1999, "Dual Role for Hedgehog in the Regulation of the Proneural Gene Atonal during Ommatidia Development", *Development*, Vol. 126, No. 11, pp. 2345–2353.

Domínguez, M., and F. Casares, 2005, "Organ Specification-Growth Control Connection: New in-Sights from the Drosophila Eye-Antennal Disc.", *Developmental Dynamics*, Vol. 232, No. 3, pp. 673–684.

Domínguez, M., and E. Hafen, 1997, "Hedgehog Directly Controls Initiation and Propagation of Retinal Differentiation in the Drosophila Eye", *Genes and Development*, Vol. 11, pp. 3254–3264.

Duffy, J. B., 2002, "GAL4 System in Drosophila: A Fly Geneticist's Swiss Army Knife", *Genesis*, Vol. 34, No. 1-2, pp. 1–15.

Earl, J. B., and S. G. Britt, 2006, "Expression of Drosophila Rhodopsins during Photoreceptor Cell Differentiation: Insights into R7 and R8 Cell Subtype Commitment", *Gene Expression Patterns*, Vol. 6, No. 7, pp. 687–694.

Edwards, T. N., A. C. Nuschke, A. Nern, and I. A. Meinertzhagen, 2012, "Organization and Metamorphosis of Glia in the Drosophila Visual System", *The Journal of Comparative Neurology*, Vol. 2085, No. 520, pp. 2067–2085.

Ferguson, K., H. Long, S. Cameron, W.-T. Chang, and Y. Rao, 2009, "The Conserved Ig Superfamily Member Turtle Mediates Axonal Tiling in Drosophila", *The Journal of Neuroscience*, Vol. 29, pp. 14151–14159.

Fischbach, K.-F., and a P. Dittrich, 1989, "The Optic Lobe of Drosophila Melanogaster. I: A. Golgi Analysis of Wild-Type Structure", *Cell Tissue Research*, Vol. 258, pp. 441–475.

Frankfort, B. J., and G. Mardon, 2002, "R8 Development in the Drosophila Eye: A Paradigm for Neural Selection and Differentiation", *Development*, Vol. 129, No. 6, pp. 1295–1306.

Frankfort, B. J., R. Nolo, Z. Zhang, H. Bellen, and G. Mardon, 2001, "Senseless Repression of Rough Is Required for R8 Photoreceptor Differentiation in the Developing Drosophila Eye", *Neuron*, Vol. 32, No. 3, pp. 403–414.

Franzdottir, S. R., D. Engelen, Y. Yuva-aydemir, I. Schmidt, A. Aho, and C. Klambt, 2009, "Switch in FGF Signalling Initiates Glial Differentiation in the Drosophila Eye", Vol. 460, No. 7356, pp. 758-761.

Freeman, M., 1996, "Reiterative Use of the EGF Receptor Triggers Differentiation of All Cell Types in the Drosophila Eye", *Cell*, Vol. 87, pp. 651–660.

Gao, S., S. ya Takemura, C. Y. Ting, S. Huang, Z. Lu, H. Luan, J. Rister, A. S. Thum, M. Yang, W. F. Odenwald, B. H. White, I. A. Meinertzhagen, C. H. Lee, 2008, "The Neural Substrate of Spectral Preference in Drosophila", *Neuron*, Vol. 60, pp. 328–342.

Gehring, W. J., 2005, "New Perspectives on Eye Development and the Evolution of Eyes and Photoreceptors", *The Journal of Heredity*, Vol. 96, No. 3, pp. 171–84.

Hacker, U., S. Nystedt, M. P. Barmchi, C. Horn, and E. a Wimmer, 2003, "piggyBac-Based Insertional Mutagenesis in the Presence of Stably Integrated P Elements in Drosophila.", *Proceedings of the National Academy of Sciences of the United States of America*, Vol. 100, No. 13, pp. 7720–7725.

Hadjieconomou, D., K. Timofeev, and I. Salecker, 2010, "A Step-by-Step Guide to Visual Circuit Assembly in Drosophila", *Current Opinion in Neurobiology*, Vol. 21, No. 1, pp. 76–84.

Hakeda-suzuki, S., and T. Suzuki, 2014, "Cell Surface Control of the Layer Specific Targeting in the Drosophila Visual System", *Genes and Genetic Systems*, Vol. 89, No. 1, pp. 9–15.

Halder, G., P. Callaerts, and W. J. Gehring, 1995, "Induction of Ectopic Eyes by Targeted Expression of the Eyeless Gene in Drosophila", *Science*, Vol. 267, pp. 1788–1792.

Halter, D. A., J. Urban, C. Rickert, S. S. Ner, K. Ito, A. A. Travers, and G. M. Technau, 1995, "The Homeobox Gene Repo Is Required for the Differentiation and Maintenance of Glia Function in the Embryonic Nervous System of Drosophila Melanogaster", *Development* , Vol. 121, pp. 317–332.

Hardie, R. C., 1979, "Electrophysiological Analysis of Fly Retina. I: Comparative Properties of R1-6 and R 7 and 8", *Journal of Comparative Physiology,* Vol. 129, No. 1, pp. 19–33.

Heberlein, U., T. Wolff, and G. M. Rubin, 1993, "The TGF?? Homolog Dpp and the Segment Polarity Gene Hedgehog Are Required for Propagation of a Morphogenetic Wave in the Drosophila Retina", *Cell*, Vol. 75, pp. 913–926.

Hofmeyer, K., and J. E. Treisman, 2009, "The Receptor Protein Tyrosine Phosphatase LAR Promotes R7 Photoreceptor Axon Targeting by a Phosphatase-Independent Signaling Mechanism.", *Proceedings of the National Academy of Sciences of the United States of America*, Vol. 106, pp. 19399–19404.

Horn, C., N. Offen, S. Nystedt, U. Häcker, and E. A. Wimmer, 2003, "piggyBac-Based Insertional Mutagenesis and Enhancer Detection as a Tool for Functional Insect Genomics", *Genetics*, Vol. 163, pp. 647–661.

Hosoya, T., K. Takizawa, and K. Nitta, 1995, "Glial Cells Missing a Binary Switch between Neuronal and Glail Determination in Drosophila", *Cell*, Vol. 82, No. 6, pp. 1025–1036.

Hosoya, T., K. Takizawa, K. Nitta, and Y. Hotta, 1995, "Glial Cells Missing: A Binary Switch between Neuronal and Glial Determination in Drosophila", *Cell*, Vol. 82, No. 6, pp. 1025–1036.

Huang, Z., and S. Kunes, 1996, "Hedgehog, Transmitted along Retinal Axons, Triggers Neurogenesis in the Developing Visual Centers of the Drosophila Brain", *Cell*, Vol. 86, pp. 411–422.

Huang, Z., and S. Kunes, 1998, "Signals Transmitted along Retinal Axons in Drosophila: Hedgehog Signal Reception and the Cell Circuitry of Lamina Cartridge Assembly", *Development*, Vol. 125, pp. 3753–3764.

Huang, Z., B.-Z. Shilo, and S. Kunes, 1998, "A Retinal Axon Fascicle Uses Spitz, an EGF Receptor Ligand, to Construct a Synaptic Cartridge in the Brain of Drosophila", *Cell*, Vol. 95, No. 5, pp. 693–703.

Hummel, T., S. Attix, D. Gunning, and S. L. Zipursky, 2002, "Temporal Control of Glial Cell Migration in the Drosophila Eye Requires Gilgamesh, Hedgehog, and Eye Specification Genes", *Neuron*, Vol. 33, No. 2, pp. 193–203.

Jang, C.-C., J.-L. Chao, N. Jones, L.-C. Yao, D. A. Bessarab, Y. M. Kuo, S. Jun, C. Desplan, S. K. Beckendorf, and Y. H. Sun, 2003, "Two Pax Genes, Eye Gone and Eyeless, Act Cooperatively in Promoting Drosophila Eye Development", *Development*, Vol. 130, pp. 2939–2951.

Jarman, A. P., E. H. Grell, L. Ackerman, L. Y. Jan, and Y. N. Jan, 1994, "Atonal Is the Proneural Gene for Drosophila Photoreceptors", *Nature*, Vol. 369, pp. 398–400.

Johnston, R. J., Y. Otake, P. Sood, N. Vogt, R. Behnia, D. Vasiliauskas, E. Mcdonald, B. Xie, S. Koenig, B Gebelein, E. Kussell, H. Nakagoshi, and C. Desplan, 2011, "Interlocked Feedforward Loops Control Cell-Type-Specific Rhodopsin Expression in the Drosophila Eye", Vol. 145, No. 6, pp. 956-968.

Jones, B. W., R. D. Fetter, G. Tear, and C. S. Goodman, 1995, "Glial Cells Missing: A Genetic Switch That Controls Glial Versus Neuronal Fate", *Cell*, Vol. 82, No. 6, pp. 1013–1023.

Jukam, D., and C. Desplan, 2009, "Binary Fate Decisions in Differentiating Neurons", *Current Opinion in Neurobiology*, Vol. 20, No. 1, pp. 6–13.

Katz, B., B. Minke, and M. Stengl, 2009, "Drosophila Photoreceptors and Signaling Mechanisms", Vol. 3, No. June, pp. 1–18.

Kenyon, K. L., S. S. Ranade, J. Curtiss, M. Mlodzik, and F. Pignoni, 2003, "Coordinating proliferation and tissue specification to promote regional identity in the Drosophila head", *Developmental Cell*, Vol. 5, No. 3, pp. 403-413.

Kirschfeld, K., and N. Franceschini, 1977, "Evidence for a Sensitising Pigment in Fly Photoreceptors.", *Nature*, Vol. 269, pp. 386–390.

Krämer, H., R. L. Cagan, and S. L. Zipursky, 1991, "Interaction of Bride of Sevenless Membrane-Bound Ligand and the Sevenless Tyrosine-Kinase Receptor.", *Nature*, Vol. 352, pp. 207–212.

Kumar, J. P., 2001, "Signalling Pathways in Drosophila and Vertebrate Retinal Development", *Nature Reviews Genetics*, Vol. 2, No. 11, pp. 846–857.

Kumar, J. P., 2009, "The Molecular Circuitry Governing Retinal Determination", *Biochimica et Biophysica Acta - Gene Regulatory Mechanisms*, Vol. 1789, No. 4, pp. 306-314.

Lai, S.-L., and T. Lee, 2006, "Genetic Mosaic with Dual Binary Transcriptional Systems in Drosophila", *Nature Neuroscience*, Vol. 9, No. 5, pp. 703–709.

Lee, C.-H., T. Herman, T. R. Clandinin, R. Lee, and S. L. Zipursky, 2001, "N-Cadherin Regulates Target Specificity in the Drosophila Visual System", *Neuron*, Vol. 30, No. 2, pp. 437–450.

Lee, R. C., T. R. Clandinin, C.-H. Lee, P.-L. Chen, I. a Meinertzhagen, and S. L. Zipursky, 2003, "The Protocadherin Flamingo Is Required for Axon Target Selection in the Drosophila Visual System", *Nature Neuroscience*, Vol. 6, No. 6, pp. 557–563.

Lopes, C. S., and F. Casares, 2010, "Hth Maintains the Pool of Eye Progenitors and Its Downregulation by Dpp and Hh Couples Retinal Fate Acquisition with Cell Cycle Exit", *Developmental Biology*, Vol. 339, pp. 78–88.

Mann, K., M. Wang, S.-H. Luu, S. Ohler, S. Hakeda-Suzuki, and T. Suzuki, 2012, "A Putative Tyrosine Phosphorylation Site of The Cell Surface Receptor Golden Goal is Involved in Synaptic Layer Selection in The Visual System", *Development*, Vol. 139, No. 4, pp. 760-771.

Mazzoni, E. O., A. Celik, M. F. Wernet, D. Vasiliauskas, R. J. Johnston, and T. A. Cook, 2008, "Iroquois Complex Genes Induce Co-Expression of Rhodopsins in Drosophila", Vol. 6, No. 4, p. e97.

Mazzoni, E. O., C. Desplan, and A. Celik, 2004, "One Receptor Rules in Sensory Neurons", *Developmental Neuroscience*, Vol. 26, No. 5-6, pp. 388–395.

Meinertzhagen, I. A., S. D. O. Neil, L. S. Centre, and N. Scotia, 1991, "Synaptic Organization of Columnar Elements in the Lamina of the Wild Type in Drosophila Melanogaster", *Journal of Comparative Neurology*, Vol. 305, No. 2, pp. 232-263.

Melnattur, K. V, and C.-H. Lee, 2011, "Visual Circuit Assembly in Drosophila", *Developmental Neurobiology*, Vol. 71, No. 12, pp. 1286–96.

Mika, K., 2014, *The Role of Unzipped in Axon Guidance and Targeting in the Olfactory System of Drosophila melanogaster*, MSc Thesis, Bogazici University.

Mikeladze-Dvali, T., M. F. Wernet, D. Pistillo, E. O. Mazzoni, A. A. Teleman, Y. W. Chen, S. Cohen, and C. Desplan, 2005, "The Growth Regulators Warts/lats and Melted Interact in a Bistable Loop to Specify Opposite Fates in Drosophila R8 Photoreceptors", *Cell*, Vol. 122, pp. 775–787.

Mlodzik, M., Y. Hiromi, U. Weber, C. S. Goodman, and G. M. Rubin, 1990, "The Drosophila Seven-up Gene, a Member of the Steroid Receptor Gene Superfamily, Controls Photoreceptor Cell Fates", *Cell*, Vol. 60, No. 2, pp. 211–224.

Mollereau, B., M. Dominguez, R. Webel, N. J. Colley, B. Keung, J. F. de Celis, and C. Desplan, 2001, "Two-Step Process for Photoreceptor Formation in Drosophila", *Nature*, Vol. 412, No. 6850, pp. 911–913.

Mollereau, B., M. F. Wernet, P. Beaufils, D. Killian, F. Pichaud, R. Kühnlein, and C. Desplan, 2000, "A Green Fluorescent Protein Enhancer Trap Screen in Drosophila Photoreceptor Cells", *Mechanisms of Development*, Vol. 93, No. 1-2, pp. 151–60.

Morante, J., and C. Desplan, 2004, "Building a Projection Map for Photoreceptor Neurons in the Drosophila Optic Lobes", *Seminars in Cell and Developmental Biology*, Vol. 15, No. 1, pp. 137–143.

Morante, J., and C. Desplan, 2008, "The Color-Vision Circuit in the Medulla of Drosophila", *Current Biology*, Vol. 18, No. 8, pp. 553–565.

Morante, J., C. Desplan, and A. Celik, 2007, "Generating Patterned Arrays of Photoreceptors", *Current Opinion in Genetics and Development*, Vol. 17, No. 4, pp. 314–319.

Morey, M., S. K. Yee, T. Herman, A. Nern, E. Blanco, and S. L. Zipursky, 2008, "Coordinate Control of Synaptic-Layer Specificity and Rhodopsins in Photoreceptor Neurons", *Nature*, Vol. 45, pp. 795–799.

Morgan, T. H., 1910, "Sex Limited Inheritance in Drosophila", *Science*, Vol. 32, pp. 120–122.

Müller, S., 2011, *Golden Goal Collaborates with Flamingo in Synaptic-Layer Targeting in the Drosophila Visual System*, MSc Thesis, Ludwig-Maximilians-Universität München.

Nern, A., L.-V. T. Nguyen, T. Herman, S. Prakash, T. R. Clandinin, and S. L. Zipursky, 2005, "An Isoform-Specific Allele of Drosophila N-Cadherin Disrupts a Late Step of R7 Targeting", *Proceedings of the National Academy of Sciences of the United States of America*, Vol. 102, No. 36, pp. 12944–12949.

Niwa, N., Y. Hiromi, and M. Okabe, 2004, "A Conserved Developmental Program for Sensory Organ Formation in Drosophila Melanogaster", *Nature Genetics*, Vol. 36, pp. 293–297.

O'Tousa, J. E., W. Baehr, R. L. Martin, J. Hirsh, W. L. Pak, and M. L. Applebury, 1985, "The Drosophila ninaE Gene Encodes an Opsin", *Cell*, Vol. 40, No. 4, pp. 839–50.

Ohler, S., S. Hakeda-suzuki, and T. Suzuki, 2011, "Hts , the Drosophila Homologue of Adducin , Physically Interacts With the Transmembrane Receptor Golden Goal to Guide Photoreceptor Axons", Vol. 240, No. 1, pp. 135–148.

Öztürk, A., 2010, *Characterization of Genes Involved in Photoreceptor Differentiation*, M.Sc. Thesis, Boğaziçi University.

Pao, S. S., I. T. Paulsen, and M. H. Saier, 1998, "Major Facilitator Superfamily", *Microbiology and Molecular Biology Reviews*, Vol. 62, pp. 1–34.

Papatsenko, D., G. Sheng, and C. Desplan, 1997, "A New Rhodopsin in R8 Photoreceptors of Drosophila: Evidence for Coordinate Expression with Rh3 in R7 Cells", *Development*, Vol. 124, pp. 1665–1673.

Pepple, K. L., M. Atkins, K. Venken, K. Wellnitz, M. Harding, B. Frankfort, and G. Mardon, 2008, "Two-Step Selection of a Single R8 Photoreceptor : A Bistable Loop between Senseless and Rough Locks in R8 Fate", *Development*, Vol. 135, No. 24, pp. 4071–4079.

Petrovic, M., and T. Hummel, 2008, "Temporal Identity in Axonal Target Layer Recognition", *Nature*, Vol. 456, No. 7223, pp. 800-803.

Pichaud, F., A. Briscoet, and C. Desplan, 1999, "Evolution of Color Vision", *Current Opinion in Neurobiology*, Vol. 9, pp. 622–627.

Poeck, B., S. Fischer, D. Gunning, S. L. Zipursky, and I. Salecker, 2001, "Glial Cells Mediate Target Layer Selection of Retinal Axons in the Developing Visual System of Drosophila", *Neuron*, Vol. 29, No. 1, pp. 99–113.

Prakash, S., J. C. Caldwell, D. F. Eberl, and T. R. Clandinin, 2005, "Drosophila N-Cadherin Mediates an Attractive Interaction between Photoreceptor Axons and Their Targets", *Nature Neuroscience*, Vol. 8, No. 4, pp. 443–450.

Quan, X., A. Ramaekers, and B. A. Hassan, 2012, "Transcriptional Control of Cell Fate Specification: Lessons from the Fly Retina", *Current Topics in Developmental Biology*, Vol. 98, pp. 259–76.

Rangarajan, R., Q. Gong, and U. Gaul, 1999, "Migration and Function of Glia in the Developing Drosophila Eye", *Development*, Vol. 126, No. 15, pp. 3285–3292.

Ready, D. F., T. E. Hanson, and S. Benzer, 1976, "Development of the Drosophila Retina, a Neurocrystalline Lattice.", *Developmental Biology*, Vol. 53, pp. 217–240.

Reddy, V. S., M. A. Shlykov, R. Castillo, E. I. Sun, and M. H. Saier, 2012, "The Major Facilitator Superfamily (MFS) Revisited", *FEBS Journal*, Vol. 279, pp. 2022–2035.

Rister, J., and C. Desplan, 2011, "The Retinal Mosaics of Opsin Expression in Invertebrates and Vertebrates", *Developmental Neurobiology*, Vol. 71, No. 12, pp. 1212–26.

Rister, J., C. Desplan, and D. Vasiliauskas, 2013, "Establishing and Maintaining Gene Expression Patterns: Insights from Sensory Receptor Patterning.", *Development*, Vol. 140, No. 3, pp. 493–503.

Roignant, Jean-Yves and Treisman, J. E., 2009, "Pattern Formation in the Drosophila Eye Disc", Vol. 53, pp. 795–804.

Ryder, E., and S. Russell, 2003, "Transposable Elements as Tools for Genomics and Genetics in Drosophila", *Briefings in Functional Genomics and Proteomics*, Vol. 2, No. 1, pp. 57–71.

Şahin, H. B., and A. Çelik, 2013, Drosophila Eye Development and Photoreceptor Specification, *eLS*, John Wiley & Sons, Ltd., pp. 1-12.

Saier, M. H., J. T. Beatty, A. Goffeau, K. T. Harley, W. H. Heijne, S. C. Huang, D. L. Jack, P. S. Jähn, K. Lew, J. Liu, S. S. Pao, I. T. Paulsen, P. S. Virk, 1999, "The Major Facilitator Superfamily", *Journal of Molecular Microbiology and Biotechnology*, Vol. 1, pp. 257–279.

Sanes, J. R., and S. L. Zipursky, 2010, "Design Principles of Insect and Vertebrate Visual Systems", *Neuron*, Vol. 66, No.1, pp. 15–36.

Sato, M., D. Umetsu, S. Murakami, T. Yasugi, and T. Tabata, 2006, "DWnt4 Regulates the Dorsoventral Specificity of Retinal Projections in the Drosophila Melanogaster Visual System", *Nature Neuroscience*, Vol. 9, pp. 67–75.

Schmitt, A., A. Vogt, K. Friedmann, R. Paulsen, and A. Huber, 2005, "Rhodopsin Patterning in Central Photoreceptor Cells of the Blowfly Calliphora Vicina: Cloning and Characterization of Calliphora Rhodopsins Rh3, Rh5 and Rh6", *The Journal Of Experimental Biology*, Vol. 208, pp. 1247–1256.

Schmucker, D., 2007, "Molecular Diversity of Dscam: Recognition of Molecular Identitiy in Neuronal Wiring", *Neuroscience*, Vol. 8, No. 12, pp. 915–920.

Senti, K.-A., T. Usui, K. Boucke, U. Greber, T. Uemura, and B. J. Dickson, 2003, "Flamingo Regulates R8 Axon-Axon and Axon-Target Interactions in the Drosophila Visual System", *Current Biology*, Vol. 13, No. 10, pp. 828–832.

Sepp, K. J., and V. J. Auld, 1999, "Conversion of lacZ Enhancer Trap Lines to GAL4 Lines Using Targeted Transposition in Drosophila Melanogaster", *Genetics*, Vol. 151, No. 3, pp. 1093–1101.

Shen, W., and G. Mardon, 1997, "Ectopic Eye Development in Drosophila Induced by Directed Dachshund Expression", *Development*, Vol. 124, pp. 45–52.

Shinza-Kameda, M., E. Takasu, K. Sakurai, S. Hayashi, and A. Nose, 2006, "Regulation of Layer-Specific Targeting by Reciprocal Expression of a Cell Adhesion Molecule, Capricious", *Neuron*, Vol. 49, pp. 205–213.

Silies, M., and C. Klambt, 2011, "Adhesion and Signaling between Neurons and Glial Cells in Drosophila", *Current Opinion in Neurobiology*, Vol. 21, No. 1, pp. 11–16.

Silies, M., Y. Yuva, D. Engelen, A. Aho, T. Stork, and C. Klämbt, 2007, "Glial Cell Migration in the Eye Disc", *The Journal of Neuroscience*, Vol. 27, No. 48, pp. 13130–13139.

Silies, M., Y. Yuva-Aydemir, S. R. Franzdóttir, and C. Klämbt, 2010, "The Eye Imaginal Disc as a Model to Study the Coordination of Neuronal and Glial Development.", *Fly*, Vol. 4, No. 1, pp. 71–79.

Silver, S. J., and I. Rebay, 2005, "Signaling Circuitries in Development: Insights from the Retinal Determination Gene Network.", *Development*, Vol. 132, No. 1, pp. 3–13.

Strutt, D., R. Johnson, K. Cooper, and S. Bray, 2002, "Asymmetric Localization of Frizzled and the Determination of Notch-Dependent Cell Fate in the Drosophila Eye", *Current Biology*, Vol. 12, No. 10, pp. 813–24.

Suh, G. S. B., B. Poeck, T. Chouard, E. Oron, D. Segal, D. A. Chamovitz, and S. L. Zipursky, 2002, "Drosophila JAB1/CSN5 Acts in Photoreceptor Cells to Induce Glial Cells", *Neuron*, Vol. 33, pp. 35–46.

Tahayato, A., R. Sonneville, F. Pichaud, M. F. Wernet, D. Papatsenko, P. Beaufils, T. Cook, and C. Desplan, 2003, "Otd/Crx, a Dual Regulator for the Specification of Ommatidia Subtypes in the Drosophila Retina.", *Developmental Cell*, Vol. 5, No. 3, pp. 391–402.

Terakita, A., 2005, "Protein Family Review The Opsins", *Genome Biology*, Vol. 6, No. 3, pp. 1–9.

Timofeev, K., W. Joly, D. Hadjieconomou, and I. Salecker, 2012, "Localized Netrins Act as Positional Cues to Control Layer-Specific Targeting of Photoreceptor Axons in Drosophila.", *Neuron*, Vol. 75, No. 1, pp. 80–93.

Ting, C.-Y., S. Yonekura, P. Chung, S.-N. Hsu, H. M. Robertson, A. Chiba, and C.-H. Lee, 2005, "Drosophila N-Cadherin Functions in the First Stage of the Two-Stage Layer-Selection Process of R7 Photoreceptor Afferents.", *Development*, Vol. 132, No. 5, pp. 953–963.

Tomasi, T., S. Hakeda-Suzuki, S. Ohler, A. Schleiffer, and T. Suzuki, 2008, "The Transmembrane Protein Golden Goal Regulates R8 Photoreceptor Axon-Axon and Axon-Target Interactions", *Neuron*, Vol. 57, pp. 691–704.

Tomlinson, A., and G. Struhl, 2001, "Delta/Notch and Boss/Sevenless Signals Act Combinatorially to Specify the Drosophila R7 Photoreceptor", *Molecular Cell*, Vol. 7, pp. 487–495.

Tsachaki, M., and S. G. Sprecher, 2012, "Genetic and Developmental Mechanisms Underlying the Formation of the Drosophila Compound Eye", *Developmental Dynamics*, Vol. 241, No. 1, pp. 40–56.

Umetsu, D., S. Murakami, M. Sato, and T. Tabata, 2006, "The Highly Ordered Assembly of Retinal Axons and Their Synaptic Partners is Regulated by Hedgehog/Single-Minded in the Drosophila Visual System.", *Development*, Vol. 133, No. 5, pp. 791–800.

Walmsley, A. R., M. P. Barrett, F. Bringaud, and G. W. Gould, 1998, "Sugar Transporters From Bacteria, Parasites and Mammals: Structure-Activity Relationships", *Trends in Biochemical Sciences*, Vol. 23, No. 12, pp. 476-481.

Wernet, M. F., and C. Desplan, 2004, "Building a Retinal Mosaic: Cell-Fate Decision in the Fly Eye", *Trends in Cell Biology*, Vol. 14, No. 10, pp. 576–584.

Wernet, M. F., T. Labhart, F. Baumann, E. O. Mazzoni, F. Pichaud, and C. Desplan, 2003, "Homothorax Switches Function of Drosophila Photoreceptors from Color to Polarized Light Sensors.", *Cell*, Vol. 115, No. 3, pp. 267–279.

Wernet, M. F., E. O. Mazzoni, A. Celik, D. M. Duncan, I. Duncan, and C. Desplan, 2006, "Stochastic Spineless Expression Creates the Retinal Mosaic for Colour Vision", *Nature*, Vol. 440, No. 7081, pp. 174–180.

Wolff, T., and D. F. Ready, 1991, "The Beginning of Pattern Formation in the Drosophila Compound Eye: The Morphogenetic Furrow and the Second Mitotic Wave", *Development* , Vol. 113, No. 3, pp. 841–850.

Xiao, M., and A. Hendrickson, 2000, "Spatial and Temporal Expression of Short, Long/Medium, or Both Opsins in Human Fetal Cones", *Journal of Comparative Neurology*, Vol. 425, No. 4, pp. 545–559.

Xie, B., M. Charlton-Perkins, E. McDonald, B. Gebelein, and T. Cook, 2007, "Senseless Functions as a Molecular Switch for Color Photoreceptor Differentiation in Drosophila.", *Development*, Vol. 134, No. 23, pp. 4243–4253.

Xiong, W. C., H. Okano, N. H. Patel, J. A. Blendy, and C. Montell, 1994, "Repo Encodes a Glial-Specific Homeo Domain Protein Required in the Drosophila Nervous System", *Genes and Development*, Vol. 8, pp. 981–994.

Yamaguchi, S., C. Desplan, and M. Heisenberg, 2010, "Contribution of Photoreceptor Subtypes to Spectral Wavelength Preference in Drosophila", *Proceedings of the National Academy of Sciences of the United States of America*, Vol. 107, pp. 5634–5639.

Yonekura, S., L. Xu, C. Y. Ting, and C. H. Lee, 2007, "Adhesive but Not Signaling Activity of Drosophila N-Cadherin is Essential for Target Selection of Photoreceptor Afferents", *Developmental Biology*, Vol. 304, pp. 759–770.

Yoshida, S., L. Soustelle, A. Giangrande, D. Umetsu, S. Murakami, T. Yasugi, T. Awasaki, K. Ito, M. Sato, and T. Tabata, 2005, "DPP Signaling Controls Development of the Lamina Glia Required for Retinal Axon Targeting in the Visual System of Drosophila.", *Development*, Vol. 132, No. 20, pp. 4587–4598.

Yu, H., C. Chen, L. Shi, Y. Huang, and T. Lee, 2009, "Twin-Spot MARCM to Reveal the Developmental Origin and Identity of Neurons", *Nature Neuroscience*, Vol. 12, No. 7, pp. 1–8.

Zhao, D., S. Cte, F. Jahnig, J. Haller, and H. Jackle, 1988, "Zipper Encodes a Putative Integral Membrane Protein Required for Normal Axon Patterning during Drosophila Neurogenesis", *The Embo Journal*, Vol. 7, No. 4, pp. 1115-1119.

Zuker, C. S., A. F. Cowman, and G. M. Rubin, 1985, "Isolation and Structure from D . Melanogaster of a Rhodopsin", *Cell*, Vol. 40, No. 4, pp. 851–858.